

Multiple freshwater mussel species of the Brazos River, Colorado River, and Guadalupe River basins

CMD 1—6233CS

Supplemental Report

August 31, 2018

Principal investigators:

Timothy H. Bonner, Texas State University, Department of Biology
Edmund L. Oborny and Bradley M. Littrell, BIO-WEST, Inc.
James A. Stoeckel, Auburn University, School of Fisheries, Aquaculture, and Aquatic Sciences
Brian S. Helms, Troy University, Department of Biology & Environmental Sciences
Kenneth G. Ostrand, USFWS San Marcos Aquatic Resources Center
Patricia L. Duncan, USFWS Uvalde National Fish Hatchery
Jeff Conway, USFWS Inks Dam National Fish Hatchery

Table of Contents

	Page
Task 2.1 – 2.3: Potential factors limiting growth, survival, reproduction.....	2
Task 2.4: Desiccation tolerances.....	99
Task 2.5: Stable isotope assessment.....	100
Task 3: Environmental flow analysis.....	134
Task 5: Captive propagation.....	191

The Texas Comptroller of Public Accounts office provided financial assistance for this study. We thank R. Gulley, M. Hope, and K. Horndeski of the Texas Comptroller of Public Accounts office for their support and coordination of our research activities. We also thank staff from Austin Ecological Field Office, Texas Parks and Wildlife, Lower Colorado River Authority, and Brazos River Authority for their assistance and coordination among our partners.

The findings and conclusions in this report presented by U.S. Fish and Wildlife Service project team members do not necessarily represent the views of the U.S. Fish and Wildlife Service.

Task 2: Potential Factors Limiting Growth, Survival, and Reproduction of Freshwater Mussel Species of Interest

Contributing authors: Austin Haney¹, Ryan Fluharty¹, Hisham Abdelrahman¹, Rebecca Tucker¹, Kaelyn Fogelman¹, Brian Helms², and James Stoeckel¹

Addresses: ¹203 Swingle Hall, School of Fisheries, Aquaculture, and Aquatic Sciences, Auburn University, Auburn, Alabama 36849

²Department of Biological & Environmental Science, Troy University, Troy, AL 36082

Principle Investigators: James Stoeckel and Brian Helms

Email: jimstoeckel@auburn.edu, helmsb@troy.edu

Task 2. Objectives: The overall objective of this study was to conduct applied research experiments on up to three mussel species of interest to investigate impacts of the following stressors: temperature, hypoxia, suspended solids, salinity, and nitrogenous compounds. Specific objectives are listed under each sub-task.

Task 2.1 Sublethal effects of thermal and hypoxia stress

Task 2.1.A. Test microplate respirometry using early stage *Ligumia subrostrata*

2.1.A. Goal: The goals of this task were to:

- 1) Use a surrogate species to develop protocols for conducting microplate respirometry on early stage (glochidia and/or juveniles) mussels.
- 2) Determine the relationship between respiration rate, regulation index, DO_{crit}, and brood viability.

Based on initial observations described in previous Final Report(s) we hypothesized that respiration rate would increase, ability to regulate oxygen consumption would decrease, and DO_{crit} would increase as brood viability decreased (Fig. 1).

2.1.A. Methods: Gravid *Ligumia subrostra* were collected from an earthen pond at the South Auburn Fisheries Research Station of Auburn University, and held in the laboratory in the same manner as mussels shipped from Texas (see subsequent sections). All females were held at a cool temperature (18°C) in order to maximize glochidia retention until used in experiments. During this time they were fed 2 mL Shellfish Diet 1800 (Reed Mariculture Inc, Campbell, CA) in the morning and 1 mL in the afternoon on a daily basis.

Prior to experimental runs, glochidia were flushed from gills of gravid mussels using a syringe and 18°C AFW into separate beakers. Viability of each brood was calculated using methodology of Fritts et al. (2014). Respiration rates of glochidia were measured using an optical microrespirometry system (Loligo Inc.). Two thousand glochidia were loaded into a single 1 ml respirometry well containing 1 ml AFW at 18°C. Three replicate wells were loaded per brood. Control wells contained no glochidia. The twenty-four well microrespirometry tray was then sealed with a silicone gasket and PVC block, placed in a waterbath, and gently rocked on a hula-type shaker table to keep water mixed within each well. Dissolved oxygen in each well was measured every 15 seconds. Glochidia remained in wells until dissolved oxygen in each well was drawn down to <0.5 mg O₂/L. Respiration rates were calculated using the following formula:

$$\text{Respiration (mg O}_2\text{ / 2,000 glochidia / hr)} = ([\text{O}_2]_{t_0} - [\text{O}_2]_{t_1}) * V / t$$

Where:

[O₂]_{t₀} = oxygen concentration at t₀ (mg O₂/liter)

[O₂]_{t₁} = oxygen concentration at t₁ ((mg O₂/liter)

V = respirometer volume (liter)

T = t₁ – t₀ (hour)

Correction for background (bacterial) oxygen demand

Chlorination, followed by rinsing, was used to reduce/eliminate bacteria in plate wells and associated tubing prior to each respiration run. However, bacteria populations tend to grow quickly and may have accounted for a significant portion of chamber oxygen demand by the end of a given run (i.e. background respiration). To account for this, we measured the respiration rates of control wells (no glochidia) during each run. The mean control oxygen demand was then divided by the mean observed respiration rate under normoxic conditions with glochidia present in order to determine the proportion of total well respiration that was due to background respiration. This proportion was referred to as the correction factor. We assumed that this proportion remained constant as dissolved oxygen declined below normoxia and corrected our respirometry data in each chamber by multiplying the observed respiration rate by 1 minus the correction factor.

Regulation indexes (RI's) were calculated using the methodology of Mueller and Seymour (2011). Corrected RMR ($\text{mgO}_2/\text{g/hr}$) values were plotted against DO (mgO_2/L) for each respirometry run. Data were fitted with the curve (3-parameter exponential rise to maximum, 2-parameter hyperbola, or 2-segment piecewise regression) that showed the lowest Akaike information criterion adjusted for small sample size (AICc: SigmaPlot 13.0). We then used the Sigma Plot area under the curve (AUC) macro to calculate AUC for 1) the observed data, 2) a horizontal line that represented perfect regulation, and 3) a linear decrease that represented perfect conformation (see Fig. 3c). RI was calculated as $(\text{Observed AUC} - \text{Conformation AUC}) / (\text{Regulation AUC} - \text{Conformation AUC})$. The RI provided a quantitative measure of the degree to which mussels were able to regulate oxygen consumption as ambient DO declined from 6 to $< 0.2 \text{ mg O}_2/\text{L}$. DO_{crit} was calculated as the dissolved oxygen

concentration showing the greatest distance between the observed RMR and the perfect conformation line (Mueller and Seymour 2011).

2.1.A. Results:

Brood viability of the 14 gravid females tested ranged from 46.5% to 94%. Contrary to our hypothesis, we found no significant linear relationship between respiration rate ($p = 0.2765$), RI ($p = 0.5583$), or DO_{crit} ($p = 0.1006$) and % viability of glochidia (Fig. 2).

2.1.A. Conclusions:

We successfully developed protocols to measure respiratory patterns of mussel glochidia. Due to the low respiration rate of an individual glochidium, the methodology required use of 2,000 glochidia per well in order to obtain usable results. We can apply this methodology to glochidia of focal species in this study, if/when they become available.

Contrary to our hypotheses, respiration rate, regulation index, and DO_{crit} did not appear to be consistently affected by brood viability of our surrogate species – *Ligumia subrostrata*. Regulation index was as high or higher than adult mussels of focal species in this study and DO_{crit} remained below 2 mg O₂/L. These results suggest that glochidia are not more sensitive to declining dissolved oxygen levels than adult mussels. Using different methodologies, Tankersley and Dimock (1993) also found no evidence that response of glochidia to reduced oxygen availability differed from adult mussels. Because respiration rates could not be measured for individual glochidia and we were not able to obtain reliable mass estimates for glochidia, we cannot directly compare mass-specific respiration rates between glochidia and adult mussels at this time.

Task 2.1.B. Collection of focal species to be used in trials

Mussels for experiments were collected by BIO-WEST, Texas State University, and Auburn University personnel during surveys (see Table 1 for species list and collection information). Mussels were placed in coolers between moist cotton towels. Sufficient ice-packs were added above and below the toweling to try to maintain a shipping temperature intermediate between collection temperature in Texas and holding temperature (18°C) at Auburn. All coolers were shipped overnight via FedEx. Upon arrival, mussels were tagged, measured (length), and placed in upwellers containing ~80 L of hard artificial freshwater (HAFW: 0.192 g NaHCO₃, 0.10 g CaSO₄*H₂O, 0.10 g CaCl₂, 0.06 g MgSO₄, and 0.008 g KCl per liter of reverse osmosis/deionized water; modified from Smith et al. 1997) at 18°C. Biofilters in each upweller were allowed to establish for > 2 weeks prior to arrival of experimental mussels. Mussels in each upweller were fed 2 mL Shellfish Diet 1800 (Reed Mariculture Inc, Campbell, CA) in the morning and 1 mL in the afternoon on a daily basis. Water quality (ammonia, nitrites, nitrates) was measured 3 times/week using either Tetra 6-in-1 and Ammonia Aquarium Test Strips or API 5 in 1 and Ammonia Test Strips. Ammonia and nitrites remained at undetectable levels (< 0.5 mg/L) throughout the study. Nitrates were consistently detected and water changes were triggered when nitrate concentrations reached or exceeded 20-40 mg/L.

Newly arrived mussels were allowed to acclimate to HAFW and laboratory holding conditions for > 2 weeks. Following the lab acclimation, mussels were randomly assigned to one of six temperature treatments (13, 17, 23, 28, 32, and 36°C). However, the lowest temperature was changed to 15°C after we found respiration rates at 13°C were too low to reliably assess metabolic patterns. Mussels were acclimated in insulated upwellers (~70 L) equipped with chillers and/or heaters with temperature control (4 mussels/species/cooler, 2 coolers per

temperature treatment). During acclimation, temperature was adjusted up or down at a rate of 1°C/day until the target temperature was reached. Mussels were then acclimated to the temperature treatment for > 1 week. During the acclimation period, mussels were fed Shellfish Diet 1800 twice daily (2 mL morning, 1 mL afternoon per ~70 L upweller) and held at a 12h light: 12h dark cycle.

Task 2.1.C1a. Thermal and hypoxia tolerance of adult *C. houstonensis* and *C. petrina*:

Effects on metabolic patterns.

2.1.C1a. Goals

Following acclimation, we used closed respirometry to estimate resting metabolic rates (RMR) of freshwater mussels at different temperatures as dissolved oxygen (DO) decreased from near 100% saturation to anoxic conditions. RMR represents the oxygen demand of organisms while at rest and approximates the metabolic rate required for basic maintenance. We then used the relationship between RMR and DO to calculate a regulation index (RI) for each mussel. The regulation index provides an assessment of the ability of an organism to maintain a constant respiration rate (i.e. meet its basic metabolic requirements) as oxygen declines. The closer the RI is to 1, the better an organism is able to continue to meet its energetic demands as DO declines (Fig. 3a,c). The closer the RI is to zero, the less an organism is able to meet its energetic demands as DO declines (Fig. 3b,c). We also used the relationship between RMR and DO to calculate critical dissolved oxygen levels (DO_{crit}). The DO_{crit} indicates the DO threshold below which an organism switches from aerobic to anaerobic respiration and thus is experiencing severe respiratory stress (Fig. 3a,b).

2.1.C1a. Methods:

Respirometry experiments were conducted in 8-chamber fiber optic respirometry systems using AutoRespTM 2.3.0 software (Loligo, Inc.). Chambers were made of acrylic and ranged in volume from ~200 – 700 mL. Each chamber was connected to two Eheim submersible 300 L/h pumps: one circulated fresh oxygenated water through the chamber during acclimation, and the other circulated water through the chamber during experiments. A fiber-optic sensor was inserted in the closed recirculation line of each chamber. Respirometry chambers and associated pumps and sensors were submerged in a ~300 L tub filled with HAFW. Temperature was controlled by means of a TECO 1/3 hp chiller/heater unit. Chambers, tubing, and gravel associated with the respirometry setup were chlorinated (5 ml bleach/gallon tap water) to reduce bacteria and then rinsed thoroughly before each trial.

We measured respiration rates of 8 randomly selected individuals per temperature for *Cyclonaias houstonensis* and *C. petrina* (4 individuals per species/run * 2 runs per temperature). Acclimated individuals were removed from temperature-controlled upwellers, scrubbed lightly with a brush to remove any algae, and weighed (gWW). Mussels were then set in PVC cups filled with gravel within the respirometry tub, and held without food for ~24 hours to prevent feeding and digestion from affecting estimates of RMR.

Following the 24 hr starvation period, mussels were assigned to an appropriately sized respirometry chamber (chamber that accommodated a mussel's shell without touching sides or lid). A PVC cup (1.5" H) half full of pea gravel was placed in each chamber to provide substrate for the mussels to burrow into. Cups had 4-mm mesh screening on the bottom to allow for water recirculation and reduce the chance of 'dead zones'. Flush pumps associated with each chamber were turned on and mussels allowed to acclimate to respirometry chambers for 5 hrs – a period

of time which equaled or exceeded the amount of time required for mussels to reach a stable RMR as determined by previous experiments (Haney and Stoeckel, unpublished data). During this time, DO levels were near 100% saturation levels. Respirometry rooms were held at a 12h light: 12h dark cycle.

Acclimation periods were always initiated in late afternoon/early evening, and respirometry initiated before midnight. Following acclimation, the flush pumps were turned off and closed pumps turned on – creating a closed system where the volume of water recirculating within each chamber and associated tubing was constant, and no new, oxygenated water entered the system. Pumps were controlled remotely using TeamViewer software to minimize any disturbance to the mussels within the respirometry rooms. Mussels were allowed to respire until dissolved oxygen levels fell below $\sim 0.2 \text{ mgO}_2/\text{L}$ in the chambers or until mussels exhibited valve closure (abrupt cessation of respiration). Valve closure rendered respiration data unusable for RI or DO_{crit} analyses. At the end of each experimental run, mussels were removed from their testing chambers and then returned to upwellers to recover. Duration of each run was temperature dependent. At the coldest temperature, it generally took $> 8 \text{ hrs}$ for DO to fall below $0.2 \text{ mgO}_2/\text{L}$ whereas at the warmest temperature, DO typically declined to $< 0.2 \text{ mgO}_2/\text{L}$ within 8 hours or less.

Correction for background (bacterial) oxygen demand

Chlorination, followed by rinsing, was used to reduce/eliminate bacteria in chambers and associated tubing prior to each respiration run. However, bacteria populations tend to grow quickly and may have accounted for a significant portion of chamber oxygen demand by the end of a given run (i.e. background respiration). To account for this, we measured background respiration rate of each chamber before and after each run, under normoxic conditions ($\text{DO} \geq 5$

mgO₂/L), for ~1.5 hrs without mussels present. The mean background oxygen demand was then divided by the mean observed respiration rate under normoxic conditions with mussels present in order to determine the proportion of total chamber respiration that was due to background respiration. This proportion was referred to as the correction factor. We assumed that this proportion remained constant as dissolved oxygen declined below normoxia and corrected our respirometry data in each chamber by multiplying the observed respiration rate by 1 minus the correction factor.

Regulation Index and DO_{crit}

Regulation indexes (RI's) were calculated using the methodology of Mueller and Seymour (2011). Corrected RMR (mgO₂/g/hr) values were plotted against DO (mgO₂/L) for each respirometry run. The upper limit of the DO range for which RI was calculated was held constant at 6 mg O₂/L to avoid bias in colder temperature runs where initial DO could be much higher than warmer runs (Mueller and Seymour 2011). Data were fitted with the curve (3-parameter exponential rise to maximum, 2-parameter hyperbola, or 2-segment piecewise regression) that showed the lowest Akaike information criterion adjusted for small sample size (AICc: SigmaPlot 13.0). We then used the Sigma Plot area under the curve (AUC) macro to calculate AUC for 1) the observed data, 2) a horizontal line that represented perfect regulation, and 3) a linear decrease that represented perfect conformation (see Fig. 3c). RI was calculated as (Observed AUC-Conformation AUC)/(Regulation AUC-Conformation AUC). The RI provided a quantitative measure of the degree to which mussels were able to regulate oxygen consumption as ambient DO declined from 6 to < 0.2 mg O₂/L. DO_{crit} was calculated as the dissolved oxygen

concentration showing the greatest distance between the observed RMR and the perfect conformation line (Mueller and Seymour 2011).

2.1.C1a: Results:

Resting metabolic rate increased linearly with increasing temperature for *Cyclonaias houstonensis* from the Colorado (RMR = $0.0007 \cdot \text{temp} - 0.0053$; $R^2 = 0.9744$, $P = 0.0002$) and Navasota rivers (RMR = $0.0004 \cdot \text{temp} - 0.0046$; $R^2 = 0.9423$, $P = 0.0013$). The regulation index did not show a significant linear relationship with temperature for *C. houstonensis* from the Colorado ($R^2 = 0.6328$, $P = 0.0584$) or Navasota ($R^2 = 0.0164$, $P = 0.8088$) rivers. Similarly, DO_{crit} did not show a significant linear relationship with temperature for *C. houstonensis* from the Colorado ($R^2 = 0.1166$, $P = 0.5078$) or Navasota ($R^2 < 0.01$, $P = 0.9922$) rivers (Fig. 4).

Cyclonaias petrina exhibited similar patterns. Resting metabolic rate increased linearly with increasing temperature for *C. petrina* from the Colorado (RMR = $0.0004 \cdot \text{temp} - 0.0038$; $R^2 = 0.9757$, $P = 0.0002$) and Guadalupe (RMR = $0.0005 \cdot \text{temp} - 0.0070$) rivers. The regulation index did not show a significant linear relationship with temperature for *C. petrina* from the Colorado ($R^2 = 0.4592$, $P = 0.2088$) or Guadalupe ($R^2 = 0.4574$, $P = 0.2100$) rivers. DO_{crit} did not show a significant linear relationship with temperature for *C. petrina* from the Colorado ($R^2 = 0.6336$, $P = 0.1072$) or Guadalupe ($R^2 = 0.5517$, $P = 0.1504$) rivers (Fig. 5).

There was no significant difference in mean RI (calculated across all temperatures) among species and locations (ANOVA, $P = 0.079$). There were significant differences in DO_{crit} among species and locations (ANOVA, $P = 0.025$) with *C. houstonensis* from the Navasota River exhibiting a significantly lower DO_{crit} than *C. houstonensis* from the Colorado River (Tukey's, $P = 0.026$). DO_{crit} of *C. petrina* did not differ between locations or from *C.*

houstonensis collected from either location (Tukey's, $P > 0.05$) (Fig. 6).

The proportion of animals exhibiting at least one episode of valve closure, as evidenced by a sudden drop of RMR to 0, increased at high temperatures. *C. petrina* tended to show higher proportions of valve closure than did *C. houstonensis* (Fig. 7).

2.1.C1a Conclusions:

Results suggest that the main impact of increasing temperatures to a maximum of 36°C is to increase metabolic demand for basic maintenance. Thus, mussels of both species require more food, and are likely to become more susceptible to food limitation, at warm temperatures. *C. houstonensis* from the Colorado River is likely the most sensitive to food limitation as its RMR increased at a faster rate with increasing temperature than did *C. houstonensis* from the Navasota River or *C. petrina* from either location. For example, we used temperature data from the San Saba gage in the Colorado River in 2009 as an example of a “warm” (maximum temperatures $\geq 36^\circ\text{C}$) temperature regime. The relationships between respiration rate and temperature for each mussel population was used to determine resting metabolic rate for each temperature measurement and the result converted to metabolic energy requirement (Joules/gWW/hr; Gnaiger 1983). Results show that under this temperature regime, maximum energy requirements of *C. houstonensis* from the Colorado River increased by 2-3x between March and July and were approximately twice as high as *C. houstonensis* from the Navasota River, or *C. petrina* from either site (Fig. 8). This result emphasizes the importance of understanding mussel food resource availability, particularly during the warm summer months, as well as differences in energetic requirements among species and subpopulations.

Valve closure results further support the potential for food limitation at high temperatures. Previous studies have shown bivalves exhibit valve closure in response to stressful temperatures (e.g. Anestis et al. 2007). In our study, all species/location combinations showed a trend of increasing episodes of valve closure as temperatures increased, with 40-87% of all mussels exhibiting at least one episode of closure when temperatures reached 36°C. Because increased frequency of valve closure would reduce feeding and aerobic respiration activities while demand for energy is increasing, mussels would become increasingly susceptible to growth limitation as temperatures approach and exceed 36°C. However, mussels appeared to exhibit tradeoffs to potentially offset this effect. *C. houstonensis* (Colorado River) exhibited the greatest increase in energy demand as temperatures increased, but kept valves open until temperatures reached 36°C. *C. petrina* exhibited a greater frequency of closed valves than *C. houstonensis* as temperatures approached 36°C, but exhibited a lower energy demand. Studies examining the effects of intermittent valve closure on mussel energy budgets at high temperatures would help determine which species is more strongly affected by food limitation at high temperatures.

Surprisingly, there was little evidence that increasing temperatures up to 36°C increased sensitivity to hypoxia for any species/location tested. Although some weak trends in RI and DO_{crit} with increasing temperature were apparent, none were significant. The ability of mussels to obtain oxygen from the water column (RI) remained fairly constant as temperatures increased, with a switch from aerobic to anaerobic respiration (DO_{crit}) only becoming apparent when DO levels fell below ~2.0 mgO₂/L. Short term tolerance of low DO, even at high temperatures, is further supported by the lack of mortality when mussels remained in respirometry chambers at 36°C at DO concentrations < 1 mgO₂/L for several hours prior to termination of trials.

Task 2.1.C1b. Thermal and hypoxia tolerance of adult *L. bracteata*: Effects on metabolic patterns and brood retention.

Forty nine adult *L. bracteata* were collected from the dewatered Llano Park Lake shoreline on November 1, 2017 and shipped to Auburn University following previously described methodology. Upon arrival mussels were placed in upwellers containing hard AFW at 18°C and fed Reed Mariculture Shellfish Diet as described previously. After several days of acclimation, mussels were examined for gender (shell morphology) and gravidity (swollen gills), revealing 25 males, 14 gravid females, and 10 non-gravid females. Because the presence of embryos was likely to affect metabolic patterns, and based on previous research (Gascho Landis et al. 2012) it was likely that females would expel broods as temperatures increased, we could not simply repeat the full suite of metabolic experiments described previously (2.1.C1a) for *C. houstonensis* and *C. petrina*. Objectives were modified accordingly.

2.1.C1b Objectives:

Objectives of this task were to

- 1) Determine the relationship between brood expulsion and temperature for gravid *L. bracteata*.
- 2) Compare metabolic patterns between males, gravid females, and non-gravid females at 28°C.
- 3) Determine relationship between temperature and metabolic patterns for male *L. bracteata*.

2.1.C1b. Methods:

After acclimating to laboratory conditions for ≥ 2 weeks at 18°C, temperature for 8 males, 7 gravid females, and 5 non-gravid females was reduced to 17°C. Temperature for an additional 8 males, 7 females, and 5 gravid females was increased by 1°C/day until temperatures reached 28°C. Temperature for the remaining 9 males was increased by 1°C/day until reaching 36°C. Mussels were subsequently held at each experimental temperature (17, 28, 36°C) for ≥ 2 weeks, after which metabolic patterns were measured for each individual following the previously described respirometry protocols (see 2.1.C1a Methods). After respirometry experiments had been conducted, temperatures for gravid females were again raised by 1°C/day to 36°C, at which time surviving females were sacrificed and gills removed in order to count # glochidia remaining in gills.

During temperature adjustment and acclimation phases, all gravid females were held in individual cups with screened sides to allow water to flow through while preventing released glochidia from leaving cups. Every 2 days, water from each cup was poured through a 105 μm sieve to retain glochidia. Glochidia were then preserved in 75% ethanol and subsequently enumerated under a compound microscope using cross-polarized lighting. Total brood size of each gravid female was calculated by summing the number of glochidia collected on each sampling date plus the number of glochidia remaining in gills when the mussel died prior to reaching 36°C, or when it was sacrificed after reaching 36°C. Proportion of brood released was subsequently calculated for each sampling day by dividing the cumulative number of glochidia released prior to that day by the total brood size calculated for that individual.

2.1.C1b. Results:

Respiration:

Resting metabolic rate (RMR) of male *L. bracteata* was significantly higher at 28 and 36 than 17°C, but there was no significant difference in RMR between 28 and 36°C (ANOVA: $F_{2,16} = 17.161$, $p < 0.001$; Tukey's $p < 0.001$, $p = 0.719$ respectively). There was no significant difference in either RI (ANOVA: $F_{2,16} = 0.288$, $p = 0.753$) or DO_{crit} (ANOVA: $F_{2,14} = 0.239$, $p = 0.791$) among temperatures (Fig. 9).

At 28°C, there was no significant difference in the ability to regulate oxygen consumption among males, non-gravid females, and gravid females (ANOVA: $F_{2,17} = 0.5$, $p = 0.615$). Similarly there was no significant difference in the DO_{crit} (ANOVA: $F_{2,17} = 1.12$, $p = 0.352$) (Fig. 10).

Resting metabolic rate (RMR) data were not normally distributed (K-S: $D = 0.09$, $P < 0.01$). Results of ANCOVA on rank-transformed data revealed a significant effect of gender/gravid status on RMR (ANCOVA: $F_{3, 3799} = 330.16$, $P < 0.0001$). As a covariate, DO showed a significant effect on RMR (ANCOVA: $F_{1, 3799} = 5079.25$, $P < 0.0001$).

Results indicated a significant interaction effect between DO and gender/gravid status (ANCOVA: $F_{2, 3799} = 10.04$, $P < 0.0001$). The homogeneity-of-slopes assumption was violated, which means regression lines for these groups had unequal slopes. The Johnson-Neyman (J-N) technique was used to determine differences among slopes within the range of DO values. At all DO values (0.5 to 7.3 ppm), RMR of males was higher than that of gravid and nongravid females. The J-N technique revealed no significant difference in RMR between gravid and nongravid females when DO values were 2.1 ppm (T-test: $t_{3799} = 2.27$, $P = 0.0602$) or lower. At DO values of 2.2 ppm (T-test: $t_{3799} = 2.43$, $P = 0.0406$) or higher –up to 7.3 ppm (T-test: $t_{3799} = 4.15$, $P = 0.0001$) - RMR of gravid females was significantly higher than that of non-gravid females (Fig. 11).

Brood expulsion: Total brood size of *L. bracteata* scored as “gravid” ranged from 825 to 105,568 glochidia/female. There was no significant difference in total brood size between females in the 17°C (Mean = 54,509, SD = 3,2081) and warming (Mean = 47,520, SD = 34,087) treatments; $t(11)=0.381$, $p = 0.355$. During the 50 day trial, there was zero mortality in the cool (17°C) treatment, whereas five of seven mussels in the warming treatment died before reaching 36°C. Each mussel that died still retained >50% of its total brood size upon death. There was no significant relationship between total brood size and day of death (Fig. 12a; linear regression, $p = 0.4533$), nor was there a significant relationship between proportion brood released and day of death (Fig. 12b; linear regression, $p = 0.2829$). On average, the proportion of brood released by surviving mussels through time was higher in the warming mussel treatment than in the cool mussel treatment (Fig. 13).

2.1.C1b. Conclusions

Similar to the *Cyclonaias* species and subpopulations tested, there was little evidence that sensitivity of *L. bracteata* to hypoxia increased with warming temperatures. RI did not decline, nor did DOcrit increase as temperatures rose from 17 to 36°C. However, energetic demands, as represented by RMR, showed a faster increase with temperature than even *C. houstonensis* from the Colorado River. This suggests that *L. bracteata* are more sensitive to food limitation at high temperatures than even the most sensitive *Cyclonaias* species/population. Interestingly, RMR of *L. bracteata* did not increase further as temperatures rose from 28 to 36°C. This leveling off of RMR with increasing temperature was not observed for any of the previously tested *Cyclonaias* species * location combinations. In fishes and some invertebrates, attainment a maximum metabolic rate, followed by metabolic depression as temperatures rise, is considered an indicator

of thermal stress (Brown 1989, Walsh et al. 1997, Anestis et al. 2007). Our results suggest temperatures between 28 and 36°C begin to cause respiratory stress in *L. bracteata* and this species is more sensitive to thermal stress than *C. houstonensis* or *C. petrina*.

Tankersley and Dimock (1993) found that gravid *Pyganodon cataracta* had reduced respiration rates relative to males, and interpreted this as an indication of stress and declining physiological condition. In our study, gravid females at 28°C had a lower respiration rate than males at DO concentrations ranging from 0.5 to 7.3 mgO₂/L. This reduction in respiration rate is presumably due to impairment of the ability of brooding females to obtain oxygen from surrounding waters and suggests that brooding *L. bracteata* may be more sensitive to thermal stress than males.

Previous studies have shown that *Ligumia subrostrata* release broods in response to rising temperatures (Gascho Landis et al. 2012). We expected *L. bracteata* to exhibit brood expulsion as temperature rose to 28°C and mussels showed signs of respiratory stress as well as increased mortality. Females exposed to warming temperatures did release more glochidia than females held at a constant, cool temperature (17°C). However, the proportion of glochidia released never exceeded 50% even when stress was high enough to result in mussel mortality, nor did mussels release >50% of their brood when temperatures were further elevated to 36°C. These results show that mussel species have different strategies regarding brood expulsion in response to severe thermal stress. Warming temperatures are less likely to cause complete brood expulsion in *L. bracteata* stress than some other species such as *L. subrostrata*. However, partial brood expulsion in response to rising temperatures is a risk for *L. bracteata*.

Task 2.1.C2. Thermal tolerance of adult mussels: Effects on respiratory enzymes.

2.1.C2. Objectives:

The electron transport system (ETS) assay measures the activity of enzymatic complexes I and III of the respiratory chain within the mitochondria. It provides excess substrate (NADH and NADPH) for the enzyme complexes to act upon and utilizes INT dye as the electron acceptor. Originally developed by Packard (1971) it has since been used as a proxy for in-situ respiration rates of marine and freshwater organisms (Owens and King 1975, Madon et al. 1998, Elderkin et al. 1998). It yields an estimate of the potential oxygen consumption rate of an organism if all enzymes function maximally by quantifying ETS activity in the presence of excess substrates (Fanslow et al. 2001). Recently, Simcic et al. (2014) showed that the relationship between ETS enzyme activity and temperature can be used to estimate optimal thermal temperatures for organisms at the cellular level. They also showed that ETS activity shows a high degree of correlation with scope for growth at the organismal level, with optimal temperatures for organism growth being a few degrees cooler than optimal temperature for ETS enzymes. We used the ETS assay to determine optimal enzymatic temperatures for acclimated and non-acclimated mussels and to compare intra and interspecific variation in optimal temperatures among species and locations.

2.1.C2. Methods:

We used two different approaches to examine the relationships between ETS activity and temperature. In the first approach, mussels were acclimated for >1 week to each of nine experimental temperatures (see *Acclimated Approach* below). ETS activity at each temperature was measured as the mean of four acclimated mussels, and tissue sampling was non-lethal. This

approach yielded a single, composite, thermal performance curve for a given species and was limited to a non-lethal temperature range because it requires acclimation of mussels to each temperature for > 1 week with minimal mortality. It also required a large number of mussels (e.g. ≥ 4 mussels/temperature \times 9 temperatures = ≥ 36 mussels).

In the second approach (non-acclimated), mussels were acclimated to only a single temperature (21°C), and tissue sampling was lethal. However, this approach required fewer mussels because the enzymes extracted from a single mussel were tested across all temperatures, yielding a separate thermal performance curve for each individual mussel. The temperature range tested could include and exceed the lethal range for mussels because only the extracted enzymes, not the mussels themselves, are exposed to each temperature. Methods for the two approaches are described in detail below.

Acclimated Mussels

Within 24 hours of respirometry measurements (see 2.1.C1), we randomly selected four mussels from each of the original six temperature treatments, gently pried their shells open, and collected two, ~10 mg tissue plugs from the foot of each mussel using a nasal biopsy tool (Karl Storz nasal biopsy tool #453733) (Fritts et al. 2015). Tissue plugs were placed in cryovials and immediately frozen at -80°C. An additional two mussels were randomly selected from each temperature, placed in a temperature-controlled upweller, and assigned to a new temperature of 20, 25, or 30°C. Temperatures were raised or lowered at a rate of 1°C/day until the target temperature was reached. Mussels were then acclimated for >1 week at the new target temperature and tissue plugs collected and stored in the same manner as described previously. Thus, we collected tissue plugs from four mussels/species acclimated for >1 week to each of 9

temperatures (15, 17, 20, 23, 25, 28, 30, 32, 36°C). After tissue collection, all mussels were cooled back down to 18°C at a rate of 1°C/day and transferred back to the original upwellers to allow them to recover.

ETS activity of acclimated mussels was measured using standard methodologies adapted from Packard (1971) and Simcic et al. (2014). Frozen tissue plugs collected from a single mussel were weighed and placed in a 5 mL vial (note: vial could actually hold up to 7 mL) (self-standing sample tube, 5 mL, Globe Scientific via VWR, number 89497-730) filled to the 4 mL mark with 1.0 mm diameter glass beads (Biospec Products, Cat. No. 11079110) and containing 4 mL of homogenization buffer (0.1 M sodium phosphate buffer pH=8.4; 75 μ M MgSO₄; 0.15% (w/v) polyvinyl pyrrolidone; 0.2% (v/v) Triton-X-100). Tissue was then homogenized with a BeadBeater (MiniBeadBeater-24; BioSpec Products, Inc., Bartlesville, OK) for 1 min and chilled for 1-2 min in a freezer. The beadbeating/chilling cycle was repeated for 3-4 cycles until tissue was thoroughly homogenized. The vial was then centrifuged for 4 min, at 10,000 rpm, at 0°C in a refrigerated centrifuge (Allegra X-30R, Beckman Coulter, Brea, CA). Homogenate generated from a given mussel was placed in a flask, diluted to 2.5 mg tissue/mL using reagent grade DI water (Ricca, cat# 9150-1), mixed with a stir bar, distributed amongst ~ 2 mL vials (Eppendorf^(R) Safe-Lock microcentrifuge tubes (MCT), polypropylene) and frozen at -80°C. Homogenate was stored for \leq 6 weeks prior to measurement of ETS activity.

To measure ETS activity, two, replicate, 0.5 mL subsamples of thawed homogenate were each incubated in 1.5 mL substrate solution (0.1M sodium phosphate buffer pH = 8.4; 1.7mM NADH; 0.25 mM NADPH; 0.2% (v/v) Triton-X-100) with 0.5 mL INT solution (2.5mM 2-(p-iodophenyl)-3-(p-nitrophenyl)-5-phenyl tetrazolium chloride) for 30 minutes, in the dark, at the temperature to which the mussel had been acclimated. The reaction was then stopped by adding

0.5 mL of stopping solution (Formalin: H₃PO₄ = 1:1). A blank for the replicate samples was made by combining 1.5 mL substrate solution with 0.5 mL INT solution, and incubated and stopped along with the samples. Following addition of stopping solution, 0.5 mL of the corresponding homogenate was added to the blank. Absorbance (490 nm) of the replicate samples was measured with a spectrophotometer (Genesys 10S UV-VIS, ThermoScientific, Waltham, MA) and corrected for absorbance of the blank. ETS activity was calculated according to the following formula (Kenner and Ahmed, 1975):

$$\text{ETS activity } (\mu\text{l O}_2 \text{ g}^{-1} \text{ WW h}^{-1}) = (\text{ABS}^{490\text{nm}} * V_h * V_r * 60) / (V_a * S * t * 1.42)$$

where $\text{ABS}^{490\text{nm}}$ is the absorption of the sample corrected for blank; V_h is the volume of the homogenate (4 mL) prior to removal of subsamples; V_r is the volume of the reaction mixture (homogenate subsample + substrate solution + INT solution + stopping solution = 3mL); V_a is the volume of the homogenate subsample (0.5 mL); S is the mass of the tissue sample (g); t is the incubation time (min); 60 is a correction factor to convert the rate to hours, and 1.42 is the factor for conversion to volume O₂.

The mean ETS activity was then calculated for each acclimation temperature (~4 mussels per temperature), graphed against temperature, and fitted with a four-parameter Gaussian curve (SigmaPlot 13.0; Systat Software, Inc., San Jose, CA). Optimal temperature was defined as the temperature which exhibited the highest ETS activity. Optimal temperature range was defined as the temperature range within which ETS activity was within 10% of the maximum value.

Non-acclimated mussels

Following respiration measurements (see 2.1.C1), two mussels were randomly selected from each of six experimental temperatures, placed in temperature controlled upwellers, and brought to 21°C at a rate of 1°C / day. All mussels were held at 21°C for at least 1 week. Following the > 1 week holding period, each mussel was sacrificed by severing the adductor mussels with a scalpel and opening the shell. Approximately 100 mg of foot tissue was immediately collected from each mussel using the nasal biopsy tool, and frozen at -80°C. Tissue from each mussel was subsequently removed from the freezer and homogenized using the previously described beadbeater technique. Homogenate generated from a given mussel was combined in a flask, diluted to 2.5 mg tissue/mL using reagent grade DI water (Ricca, cat# 9150-1), mixed with a stir bar, distributed amongst ~ 1.8 mL vials and refrozen at -80°C. ETS activity was subsequently measured following the same methodology as described above.

For each mussel, two replicate enzyme samples were incubated for 30 minutes at each temperature of interest, yielding a complete thermal performance curve (ETS activity vs temperature) for each individual. Initially, incubation temperatures were 12, 15, 17, 20, 23, 25, 28, 30, 32, and 36°C. Optimal temperatures for each individual was calculated using a four parameter Gaussian regression. Because optimal temperature data was not normally distributed, we used a Kruskal-Wallis ANOVA on rank-transformed data to test for significant differences among species/location combinations (SigmaPlot 13.0, Systat Software, Inc., San Jose, CA, USA). Pairwise comparisons were conducted using Dunn's Method (SigmaPlot 13.0).

While analyzing samples for optimal temperature, we conducted some exploratory runs at temperatures >36°C and found ETS activity did not decline symmetrically with increasing temperatures as would be described by a Gaussian curve. We hypothesized that the post-peak

decline pattern might yield additional information regarding thermal stress. We therefore added temperatures of 39, 42, 45, 48, 51, 54, and 57°C to the non-acclimated assay for remaining species and populations. We also added a cooler temperature (9°C). We then used a 5-segment piecewise regression (SigmaPlot 13.0) to characterize the relationship between ETS activity and temperature during the decline following peak activity.

2.1.C2. Results

Acclimated Mussels

Optimal temperatures for ETS enzyme activity were higher for *C. petrina* from the Colorado (35.3°C) and Guadalupe (34.6°C) rivers than for *C. houstonensis* from the Colorado (31.6°C) and Navasota (27.6°C) rivers. Optimal range estimates predicted mussels would begin to experience enzymatic thermal stress at some point >36°C for Colorado and Guadalupe River *C. petrina*, >35.8°C for Colorado River *C. houstonensis*, and > 30.6°C for Navasota River *C. houstonensis* (Fig. 14).

Because the acclimated approach generates only a single, composite, thermal performance curve for each species/location, we were not able to test for significant differences in optimal temperature between species or locations, nor were we able to assess variability in optimal temperature among individuals within the same species/location group. To address these issues, we analyzed thermal performance curves for individual mussels using the non-acclimated approach.

Non-acclimated Mussels

ETS activity was strongly correlated with temperature for individual, non-acclimated mussels, with four parameter Gaussian regressions typically yielding an $R^2 > 0.90$ (see Fig. 15 for example; full set of graphs for other species/location combinations available upon request). Summary graphs (Fig. 16) show variation in curve height and optimal temperature (temperature at which curve peaks) within and among each species/location combination. Intraspecific variation in optimal temperature was highest for *C. petrina* from the Colorado River and lowest for *L. bracteata* (Llano Lake) and *C. houstonensis* (Navasota River) (Fig. 17).

There were significant differences in mean optimal temperature among the nine species x location combinations of rare and common species tested (Kruskal-Wallis ANOVA: $H=56.422$, d.f.= 8, $P < 0.001$). Optimal temperature for *C. houstonensis* (Colorado River) and *C. petrina* (Colorado River), were significantly higher than *L. teres* (Colorado River) and *L. bracteata* (Llano Lake) (Dunn's Method, $P < 0.05$). Optimal temperature of *C. houstonensis* (Navasota River) was significantly higher than *L. teres* Colorado River) (Dunn's Method, $P = 0.018$) and marginally higher than *L. bracteata* (Llano Lake) (Dunn's Method, $P = 0.057$). Optimal temperatures of *F. mitchelli* (Guadalupe River), *C. petrina* (Guadalupe River), *A. plicata* (Colorado River) and *L. bracteata* (Llano River) were intermediate (Figure 18).

There was no evidence of intraspecific differences in thermal optima between subpopulations of three candidate species. *C. houstonensis* (Colorado River) did not significantly differ from *C. houstonensis* (Navasota River) (Dunn's Method, $P = 0.7$). *C. petrina* (Colorado River) did not significantly differ from *C. petrina* (Guadalupe River) (Dunn's Method, $P = 1.0$). *L. bracteata* (Llano River) did not significantly differ from *L. bracteata* (Llano Lake) (Dunn's Method, $P = 0.791$) (Figure 18).

There was no evidence that two common species tested had a higher thermal optima than the four candidate species. *Amblema plicata* (Colorado River) had an intermediate optimal temperature, and *Lampsilis teres* (Colorado River) had a low optimal temperature relative to the four candidate species (Figure 18).

We measured activity of ETS enzymes from non-acclimated adult mussels at temperatures expected to exceed 24-hr lethal temperature (LT_{50}) thresholds for five species (Fig. 19). As temperatures increased above the thermal optimum, ETS activity did not decline in a linear fashion. Rather, each species exhibited a “shoulder” pattern where enzyme activity initially declined, then leveled off, then declined again. In a previous study, Marshall et al. (2011) showed that a bimodal pattern of snail respiration with increasing temperature was correlated with the onset of heat shock protein production and 24-hr LT_{50} thresholds. Because ETS activity represents the maximum potential respiration rate of an organism (Fanslow 2001), it is likely that similar endpoints are correlated with ETS activity patterns. We hypothesize that the point at which the decline in ETS activity begins to level off represents the activation of heat shock proteins – signaling the onset of major thermal stress and the transition from sublethal to lethal thermal stress. Preliminary comparison of independent LT_{05} (temperature at which 5% of animals die) data from the lab of Dr. Charles Randklev (Texas A&M University) is providing support for this hypothesis. We plan to continue this line of inquiry with Dr. Randklev in 2018. The hypothesized breakpoint between sublethal and lethal effects was 38.9°C for *C. petrina* (Guadalupe River), 37.1°C for *C. houstonensis* (Navasota River), 36.0°C for *A. plicata* (Colorado River), 32.7°C for *L. bracteata* (Llano Lake), 32.6°C for *F. mitchelli* (Guadalupe River) collected in November, 31.0°C for *F. mitchelli* collected from the same site in August, and 29.4°C for *L. teres* (Colorado River) (Fig. 19). Season of collection did not appear to have a large impact on

these estimates. *F. mitchelli* collected in summer (August) and fall (November) differed by only 1.6°C in terms of estimated breakpoint between sublethal and lethal effects.

2.1.C2. Conclusions:

There were significant differences in optimal enzymatic temperatures among specific species x location combinations. However there was no evidence for differences in optimal temperatures between subpopulations within the same species. Optimal temperatures for common species were intermediate to low compared to the rare, candidate species. There was some evidence that optimal temperatures were linked to taxonomic status as *Cyclonais spp.* generally exhibited higher thermal optima than *Lampsilis spp.*

Mussels acclimated to warm temperatures generally exhibited higher optimal temperatures than non-acclimated mussels (Table 4). However, optimal temperatures of non-acclimated mussels still fell within the optimal range of acclimated mussels – usually near the lower end of the range (Fig. 20, Table 4). The primary effect of acclimation appeared to be an increase in the upper portion of the optimal range rather than shifting the entire range. This suggests that in natural populations, a given mussel species will enter its optimal thermal range at approximately the same temperature threshold regardless of previous thermal history. However, mussels subjected to rapid, flashy increases in temperature will leave their thermal optima and start to experience thermal stress at lower temperatures than mussels subjected to gradual, stable increases in temperature. Intraspecific variation in non-acclimated optimal temperature (Fig. 17) was highest for *C. petrina* from the Colorado River, suggesting they may have a greater capacity to adapt to future fluctuations in temperature than species such as *L. bracteata* (Llano River/Lake) and *C. houstonensis* (Navasota River), which exhibited relatively low variation in

optimal temperatures. A summary of the estimated optimal and stressful temperatures for ETS enzymes of acclimated and non-acclimated mussels can be found in Table 4.

While the ETS assay estimates optimal temperatures at the enzymatic level, corresponding estimates of optimal temperature measured at the more complex organismal level (e.g. optimal scope for growth) may be cooler by 2-3° C (Simcic et al. 2014). Therefore, temperature ranges that are optimal or stressful to the organism as a whole are likely to be a few degrees lower than temperatures optimal or stressful to the organism's ETS enzymes. One way to explain this is using the concept of Aerobic Scope - the difference between an organisms resting metabolism (energy required to meet basic metabolic needs) and its metabolic potential (maximum metabolic rate). The greater the aerobic scope, the more energy can be used for growth and reproduction (e.g Clark et al. 2011, Simcic et al. 2017). In the context of this project, ETS activity is an estimate of metabolic potential whereas respiration rates of mussels starved for 24 hrs provide an estimate of resting metabolic rate. As temperatures increased, metabolic potential increased, leveled off, and then declined whereas resting metabolic rate continued to increase (Fig 21A). For *C. houstonensis* (Colorado River), aerobic scope was greatest at ~28°C (Fig. 21 A,B) which suggests that the optimal temperature at the organismal level was ~ 3.6°C lower than the enzymatic optimal temperature of 31.6°C (Table 4, acclimated).

Task 2.1.D. Effect of temperature on respiration of glochidia and juveniles.

2.1.D. Objectives: The objectives of this task were to:

- 1) Refine methodology for conducting microrespirometry on early stage juveniles.
- 2) Determine the differences in metabolic rate, regulation index, and DO_{crit} between juvenile and adult mussels at one or more temperatures.

3) Determine the relationship between metabolic rate, regulation index, DO_{crit} and temperature for juveniles of one or more candidate mussel species.

2.1.D. Methods:

Approximately 150 *C. petrina* early juveniles (< 1mm length) were shipped to Auburn University from the Inks Dam hatchery. Shipping temperature upon arrival was 20.4°C. Mussels were placed in AFW, gradually brought up to 25°C and held overnight in a beaker without food. The following day they were distributed among the microrespirometry wells at 50, 20, and 10 individuals per well, with temperature remaining at 25°C. Methodology followed that previously described for glochidia (2.1.A).

After determining that ≥ 50 individuals/well were required to conduct respirometry on early (<1mm length) juveniles (see results), we obtained older, juvenile *L. cardium* from the Center for Mollusk Conservation in Frankfort, Kentucky as part of an ongoing collaborative project with W.R. Haag (USDA Forest Service). Juveniles ranged from ~6 – 12 mm in length and were shipped and acclimated in the same manner as the *C. petrina*. However, in contrast to the smaller *C. petrina* juveniles, only a single *L. cardium* individual was placed in each respirometry well. Respirometry was conducted following the same procedures as described previously.

2.1.A. Results

C. petrina early juveniles

Wells with 10-20 early juveniles were deemed insufficient to obtain reliable respiration curves due to 1) background oxygen demand comprising a large proportion of the overall respiration rates, and 2) >24 hrs required to bring oxygen down to < 0.5 mg O₂/L. However, the

well containing 50 individuals yielded usable results, showing that, on average, early juveniles were good at regulating oxygen consumption (respiration rates remained stable as dissolved oxygen declined to low levels) and DO_{crit} did not occur until oxygen had declined below 1 mg/L (Figure 22).

L. cardium juveniles

Wells containing single *L. cardium* juveniles, ranging from 6 to 12 mm in length, yielded usable respiration curves allowing us to calculate respiration rates, regulation indices, and DO_{crit} for individual mussels. There was no significant linear relationship between RMR ($p = 0.550$) or RI ($p = 0.263$) and juvenile length. However, there was a significant linear increase in DO_{crit} with increasing juvenile length ($R^2 = 0.65$, $p = 0.029$) (Fig. 23). On average, respiration rates of this size range were approximately 10x those observed for adult mussels of other species in this study (e.g. see Figures 4, 5) and in previous studies (Chen et al. 2001).

2.1.A. Conclusions

After discussion with personnel heading the propagation portion of the overall mussel project, it was decided that the demand for large numbers of early juvenile mussels (≥ 50 individuals per well) was too high to allow for thermal tolerance experiments with the focal species juveniles. Based on the *L. cardium* microrespirometry runs, we are recommending that we resume thermal tolerance experiments when focal species juveniles in the 6-12mm size range are available from the production facilities as this will greatly reduce the numbers of animals needed and also yield mass specific respiration rates (mg O₂/gWW/hr) of individuals – which are more useful than combined (mg O₂ / x individuals/hr).

Preliminary data suggests that energy demands of juvenile mussels are much higher than adults – this is supported by anecdotal evidence from hatchery managers that juveniles have much greater food requirements for good survivorship and growth than do adult mussels. Estimates of resting metabolic rates will be of great use in developing energy budgets and determining optimal temperatures for growth for early juveniles. The ability to strongly regulate oxygen consumption, and the low DO_{crit} exhibited by the early juvenile *C. petrina* suggests that they are not more sensitive to hypoxia than adults. This makes sense in that juvenile mussels typically burrow into the sediments where dissolved oxygen is lower than overlying waters. However, these are preliminary results based on a single well containing 50 individuals. Additional runs will be required to confirm these patterns. Results from the larger juvenile *L. cardium* suggest that DO_{crit} may increase as juveniles grow, making them more susceptible to low DO conditions over time. However, similar to *C. petrina*, these results are based on a small sample size and additional runs will be required to confirm patterns.

Task 2.3 Effect of turbidity/suspended solids on valve closure of adult mussels

2.3 Objectives:

Mussels must keep their shells open to obtain food and oxygen from the surrounding waters. However, they often respond to stressors by closing their shells. Electromagnetic sensors attached to each valve can be used to monitor gaping and closing behavior and set off alarms when behavior indicates the presence of stressful toxicants in the water (Manley and Davenport 1979, Kramer et al. 1989, Gnyubkin 2009). Systems such as the MosselMonitor (www.mosselmonitor.nl; Kramer et al. 1989) and the Dreissena Monitor (Envicontrol Köln Germany; Borcharding, 1994) have been used to monitor stressors in fresh and saltwater

environments in Europe. In this study, we used a MosselMonitor to determine whether mussels fully or partially close their valves in response to high turbidity/suspended solids – indicating negative impacts on feeding and respiration.

2.3. Methods:

Sediments

Sediments were obtained from a drained, 0.1 ha, earthen pond at the South Auburn Fisheries Research Station of Auburn University, Alabama. The top two inches of sediment were collected, mixed in a 5 gallon bucket, distributed into baking pans, and dried for 24 hrs at 105°C. Dried sediment was passed through a #60 (250 µm) Fisher Scientific Company sieve and stored in an air tight 5-gallon bucket. This process was repeated until we had obtained enough sieved sediments to complete all trials. Stored sediment was mixed thoroughly via rolling and shaking in a closed container to ensure even distribution of particles immediately prior to each use. Soil analysis (T. Knappenberger, Auburn University) showed the sediments were composed of 53.5% sand (63 – 2000 µm), 46.6% silt (2.0-63 µm) and 0.0% clay (< 2.0 µm).

Experimental animals

Following respirometry experiments (see previous section), mussels were allowed to recover for > 4 weeks at 18°C. Water temperature was then raised by 1°C/day to the experimental temperature of 28°C. Mussels were acclimated to this temperature for ≥ 1 week prior to initiation of experiments. During this time mussels were fed Shellfish Diet 1800 twice daily (2 mL morning, 1 mL afternoon per ~70 L upweller) and held at a 12h light: 12h dark cycle.

Experimental protocol

To monitor valve movements, mussels were held in individual, mesh bottom, plastic baskets (8 X 5 X 4 cm) screwed to the walls of a MosselMonitor (Flow through version, AquaDect B. V. Brouwershaven, Netherlands). MosselMonitor settings, data downloads, and data display were controlled via PresentIT™ 3.0 software on a connected desktop computer. The MosselMonitor was filled with HAFW and held at 28°C. One valve of each mussel was glued (Unifast Trad Methylmethacrylate two part Resin GC America Inc. Alsip IL) to the plastic basket wall parallel to the side of the MosselMonitor. This ensured the mussel remained at a fixed distance from an electromagnetic sensor in the MosselMonitor wall. A second sensor was glued directly to the other valve of the mussel. Aquarium pea gravel was then added to the basket until half of the mussel was embedded in the substrate. Throughout the subsequent experiment, mussels were fed Shellfish Diet 1800 at the same rate as during the acclimation period. The Light:Dark cycle was held constant at 12:12.

Mussels were acclimated to the system for three days, during which time the MosselMonitor monitored distance between sensors and assessed the baseline maximum and minimum valve opening exhibited by each mussel. During the subsequent portions of the experiment, distance between valves (sensors) was reported as percent gape, based on the baseline maximum and minimum distances calculated during the acclimation period. Percent gape was calculated and recorded every 10 seconds for the remainder of the experiment. The first 24 hours following acclimation (Day 4) served as a control period, during which time food, but no sediment, was added to the MosselMonitor. The experimental period began on day 5. Sediment was added to a belt feeder located above a cone tank that was connected to the

MosselMonitor. The belt feeder dropped sediment into the cone tank at a constant rate over a period of 10 hours. Sediment was suspended in the cone tank via a submersible Resun King-2 pump (1000 L/hr) and multiple air stones. A second submersible Resun King-2 pump transferred water and suspended sediments to the MosselMonitor at a constant rate of 360 L/hr. Flexible tubing returned water at the same rate to the cone tank via ambient head pressure. A LaMotte 2020we turbidimeter was used to measure turbidity in replicate 10 mL samples collected immediately after mussel attachment (0 h), at the start of the control period (72 h), every hour for the first 12 hours of the experimental period (hrs 96-108), and at the end of the experimental period (hr 120). Supplemental samples were periodically collected to quantify TSS concentrations. A ~250 mL sample was siphoned from the center of the MosselMonitor. The siphon tube was attached to the MusselMonitor prior to the experiment so that subsequent samples could be collected without disturbing mussels. Sample water was filtered through a pre-ashed (1 hr at 550°C) 1.2 µm Whatman 47 mm glass microfiber filter to collect sediments. Filters were then dried overnight at 105°C and weighed. Filter weight was subtracted from total weight and then divided by sample volume to calculate TSS in mg dry weight/liter.

This protocol resulted in an initial ~6-hour ramping period (9:00 – 15:00 hrs) on Day 5 during which suspended solid concentration in the MosselMonitor increased with time as the rate at which sediment was added to the system exceeded the rate at which sediment settled within the system. Equilibrium between sediment addition and settlement was reached within 5-6 hrs, after which time total suspended solids (TSS) concentrations remained relatively stable for the remaining four hours (15:00 – 19:00 hrs) of the run (Fig. 24 bottom panels). Mussels were exposed to one of two treatments, with two runs per treatment. Different mussels were used for each run. Within each run, sufficient sediment was added to the belt feeder to allow turbidity to

ramp up to the target level. During our first three runs, we set a high turbidity target of ~25 NTU (~70 mg TSS/L), intending to reduce turbidity in subsequent runs. However, due to the lack of obvious effects on valve closure even under high turbidity conditions (see results), we changed our subsequent runs to target excessive turbidity levels of ~70 NTU (~ 250 mg TSS/L) for the two final runs (Fig. 24).

2.3. Results

Individuals of both species exhibited highly variable relationships between percent gape and turbidity during the ramping periods when turbidity increased from 0 to 25 or 65-75 NTU's over a 6-hr period (Figs. 25-28). During the excessive turbidity ramping period, mean percent gape of all *C. petrina* combined exhibited a negative linear relationship with turbidity (Figure 29 top panel: $R^2 = 0.53$, $P < 0.0001$, mean percent gape = $59.3214 - 0.1478 \cdot \text{NTU}$). Mean percent gape during the high turbidity ramping period showed a similar negative relationship with turbidity, albeit with a steeper slope (Fig 29 top panel: $R^2 = 0.83$, $P < 0.0001$, mean percent gape = $62.7746 - 0.4654 \cdot \text{NTU}$).

During the excessive turbidity ramping period, mean percent gape of all *C. houstonensis* combined exhibited a significant positive linear relationship with turbidity, but turbidity explained very little of the variation in valve gape (Figure 29 bottom panel: $R^2 = 0.064$, $P < 0.0001$, mean percent gape = $45.8459 + 0.0451 \cdot \text{NTU}$). Mean percent gape during the high turbidity ramping period showed a significant, negative linear relationship with turbidity, but, again, turbidity explained very little of the variation in gape (Fig. 29 bottom panel: $R^2 = 0.040$, $P < 0.0001$, mean percent gape = $63.9433 - 0.1675 \cdot \text{NTU}$).

During the constant turbidity period of the high treatment (~25 NTU), there was little to no evidence that turbidity resulted in decreased gape for either species. Exposed *C. petrina* exhibited less frequent gape values exceeding 65% than control mussels but percent gape peaked at 65% in both groups. Gape of exposed *C. houstonensis* peaked at a higher value (75%) than control *C. houstonensis* (55%) (Fig. 30).

During the constant turbidity period of the excessive treatment (60-75 NTU), there was evidence that gape decreased slightly for both species. Gape peaked at 65% in exposed *C. petrina* compared to 75% for control mussels. Gape peaked at 65% in exposed and control *C. houstonensis*, but very few exposed mussels gaped more than 65% compared to control mussels (Fig. 31).

2.3. Conclusions:

Because mussels obtain food and oxygen from surrounding water, there was concern that high concentrations of suspended solids may trigger valve closure by mussels, with subsequent, negative effects on feeding and respiration. However, we found little to no evidence that exposure to suspended solids, even at high (turbidity ~25 NTU; TSS ~70 mg/L) or excessive (turbidity ~75 NTU, TSS ~250 mg/L) concentrations resulted in valve closure. As turbidity increased, *C. petrina* exhibited only a small reduction in mean percent gape. Increasing turbidity explained very little of the variation in percent gape for *C. houstonensis*. Under conditions of excessive turbidity, mussels appeared to close valves slightly, but the peak in percent gape remained high at 65% as compared to a peak of 65-75% during the preceding control period. If high suspended solids have a negative effect on mussel feeding rates or ability to obtain oxygen, the mechanism behind negative effects is not likely to be valve closure.

2.2 Sublethal effects of nitrogenous compounds and salinity on adult mussels

2.2A. Effect of Ammonia on Respiration.

2.2A. Objectives:

In 2013, the U.S.EPA updated its Aquatic Life Ambient Water Quality Criteria for Ammonia – Freshwater in order to take into account data for highly sensitive unionid mussel and non-pulmonate snail species that had not previously been tested (USEPA 2013). Because ammonia toxicity issues are fairly complex, a brief explanation is provided here.

Ammonia in surface waters is typically reported as total ammonia nitrogen (TAN). This refers to the combined concentration of nitrogen (mg/L) occurring in two co-existing forms of ammonia – ionized (NH_4^+) and un-ionized (NH_3). Un-ionized ammonia is the most toxic form. The proportion of un-ionized to ionized (NH_3 : NH_4^+) ammonia increases with increasing pH and temperature. Thus ammonia becomes more toxic with increases in temperature and/or pH even if the concentration of ammonia, measured as TAN, remains the same. The U.S.EPA 2013 ammonia benchmark is 17 mg TAN/L for acute (1 hour average) exposure and 1.9 mg TAN/L for chronic (30-d rolling average) exposure. These benchmarks are referred to as “criterion maximum concentrations” (CMC) and represent a concentration that is expected to be lethal to <50% of individuals in sensitive species. They specifically apply to a pH of 7 and a temperature of 20°C. In many Texas rivers, pH is typically ≥ 8 and temperatures rise well above 20°C during the summer months. The toxicity of 17 (acute) and 1.9 (chronic) mg TAN/L benchmark concentrations would therefore increase and may no longer be sufficiently protective of unionid mussels. The USEPA is cognizant of this issue and provides tables to adjust benchmark concentrations for specific temperature and pH values (see tables 5b, 6 in USEPA 2013).

Unionized ammonia can affect organisms such as mussels via multiple mechanisms that include increased ventilation rates (volume of water passing through gills per unit time), gill damage, and a reduction in the ability of blood (hemolymph) to carry oxygen. Thus it is reasonable to expect that metabolic and respiration patterns would be sensitive to ammonia. The objectives of this study were to determine whether ammonia affected metabolic patterns of mussels by 1) reducing their ability to regulate oxygen consumption, 2) increasing their DO_{crit} , and 3) altering their resting metabolic rate. Note that this task was completed last due to the high probability of significant sublethal and lethal effects on experimental mussels when exposed to ammonia.

2.2A. Methods:

Following turbidity assays described in previous sections, *C. petrina* and *C. houstonensis* from the Colorado River were allowed to recover for ≥ 2 weeks at 28°C prior to initiation of ammonia experiments. During this time, they were fed Shellfish Diet 1800 according to the standard feeding regime (2 mL morning, 1 mL afternoon, per 70 L upweller). Due to a limited number of mussels remaining from the original collections, we were only able to test 5-6 individuals of *C. petrina*, and 6 individuals of *C. houstonensis* per ammonia treatment, prior to preparation of this report. Each mussel was exposed to only a single ammonia treatment. Thus we tested a total of 16 *C. petrina* and 18 *C. houstonensis*.

Resting metabolic rates (RMR) were measured at 28°C using the same respirometry system described in section B of this chapter. Mussels were starved for 24 hrs prior to experiments to prevent feeding and digesting from affecting metabolism. Following the starvation period, sufficient ammonia from a stock solution (Hach ammonia standard, 1,000 mg

TAN/L) was added to the respirometry trough to bring it to the target concentration of 0.5 or 2.0 mg TAN/L. No ammonia was added to the trough for the control runs. Ammonia concentrations in the respirometry trough were measured using a YSI 9300 Photometer (YSI Inc. 2017) at the beginning and end of each experiment to ensure the target concentration had been reached and remained stable throughout the duration of each trial. The moderate concentration, (0.5 mg TAN/L) was selected to represent the average concentration that we observed in our respirometry chambers following a standard, closed respirometry experiment (section B). The higher concentration represents the 2013 USEPA CCC chronic criteria of 1.9 mg TAN / L at pH 7, 20°C. Note that in our experiments temperature was 28°C, and pH was ~8.5. Under these conditions, the recommended acute and chronic benchmarks (CMC; Tables 5b and 6 in USEPA 2013) are adjusted downward to 0.77 (acute) and 0.21 (chronic) mg TAN/L. Thus the highest TAN concentration in our study exceeded both the acute and chronic benchmarks adjusted for pH and temperature.

Mussels were acclimated to respiration chambers for ≥ 5 hrs. During this time both the flush and closed pumps were turned on to ensure oxygenated water containing the appropriate ammonia concentration circulated through chambers and tubing. Following acclimation, flush pumps were turned off, and only the closed pumps remained on - creating a closed system where the volume of water recirculating within each chamber and associated tubing was constant, and no new, oxygenated, water entered the system.

Because mussels excrete ammonia as a waste product, and this ammonia can build up in closed respirometry chambers over time, we periodically flushed chambers during a respirometry run to ensure that ammonia levels remained fairly constant during each trial. The modified respirometry protocol was as follows: After allowing closed respirometry to run for 50 minutes,

nitrogen gas was bubbled into the trough water (external to the submerged respirometry chambers) using DO-SET software (Loligo Inc.), until DO had fallen from 7 to 5 mg O₂/L. Previous closed respirometry trials at 28°C (section 2.1.C1) using the same two mussel species yielded a decrease of approximately 2 mg O₂ per hour within the respiration chambers. At 60 minutes, the flush pumps were turned on and chambers flushed for 5 minutes with ~5 mg O₂/L water from the trough in order to flush out any ammonia excreted by the mussels that would otherwise increase ammonia levels above the targeted trial concentration. Flush pumps were then turned off to once more create a closed system at the target ammonia concentration. After 50 minutes DO in the trough was reduced from 5 to 3 mg O₂/L, and ten minutes later chambers were flushed again for 5 minutes. Flush pumps were then turned off and mussels allowed to draw DO down from 3 to < 0.2 mg O₂/L at which time the trial was terminated. This technique yielded a relationship between resting metabolic rate (RMR) and dissolved oxygen (e.g. Fig. 32) that could be analyzed for regulation index and DO_{crit} using the same methodology as described in task 2.1.C1, while at the same time avoiding problems associated with accumulating ammonia in closed respiration chambers.

2.2A Results:

TAN of the respirometry water matched the nominal treatment TAN concentrations fairly well and remained stable throughout the experiment. Background levels within the control treatment ranged from 0.04 to 0.1 mg TAN / L. Respirometry water pH ranged from 8.4 to 8.6 (Table 5).

The proportion of individuals exhibiting valve closure (cessation of respiration) increased with increasing TAN for both species, and was more frequent in *C. petrina* than *C. houstonensis*

(Fig. 33). Because accurate RMR, RI, and DO_{crit} values could not be calculated for individuals that closed during respirometry, we did not have enough usable respiration curves to test for effects of TAN on these endpoints for *C. petrina*. For *C. houstonensis*, valve closure eliminated only four individuals from the experiment, yielding 4-5 replicate estimates of these endpoints for each TAN treatment. There was no significant effect of TAN on RMR (ANOVA: $F = 2.528$, $df = 2, 11$; $P = 0.125$), RI (ANOVA: $F = 1.988$; $df = 2, 11$; $P = 0.183$), or DO_{crit} (ANOVA: $F = 1.178$, $df = 2, 11$; $P = 0.344$) (Fig. 34).

2.2A Conclusions:

At a pH of 8.5 and temperature of 18 C, the USEPA ammonia benchmarks are revised downward from 17 to 0.77 mg TAN/L for acute (1 hour average) exposure and from 1.9 to 0.21 mg TAN/L for chronic (30 day rolling average) exposure (see Tables 5b and 6 in USEPA 2013). In our study, mussels were exposed to treatment TAN concentrations exceeding both of these benchmarks for ~10 hours. Results suggest that the revised benchmarks are sufficient to protect *C. houstonensis* from short term effects of ammonia on metabolic rate (RMR) and ability to extract oxygen even under low oxygen conditions (RI and DO_{crit}). However it remains to be tested whether chronic (30 day) exposure would affect metabolism. Also, the revised benchmarks may not be sufficient to protect mussels from increased frequency of valve closure (see Fig. 33) which could affect respiration, filtration, and fertilization efficiency during long term exposure. Future studies examining effects of chronic exposure to TAN concentrations matching and exceeding the revised chronic benchmarks on metabolism and valve closure are warranted.

A major challenge of working with rare species is having a sufficient sample size to be able to detect significant differences between treatments. In the case of the ammonia studies, the sample sizes were low, increasing the chances of us not finding an effect of ammonia when one existed. We performed a power analysis (G*Power 3.1.9.2; Faul et al. 2007) to determine 1) the difference between treatments that we had a $\geq 80\%$ chance of detecting with the current sample size, and 2) the minimum number of samples (mussels) required to have a $\geq 80\%$ chance of detecting a specific difference between treatments. Given our sample size of 5 individuals/treatment and the observed variance among individuals, we had a $\geq 80\%$ chance of detecting a change of 0.004 mgO₂/gWW/hr in RMR, a change of 0.15 in RI, and a change of 1.0 mg O₂/L in DO_{crit} among treatments. In future studies, if we want to double the sensitivity of our assays (i.e. reduce the detectable difference by half) and thus have a $\geq 80\%$ chance of detecting a change of 0.002 mgO₂/gWW/hr in RMR, 0.075 in RI, and 0.5 mg O₂/L in DO_{crit}, we would need sample sizes of at least 17, 10, and 18 mussels/treatment respectively. We are currently evaluating our remaining mussel stocks and may be able to conduct additional ammonia trials with *C. petrina* and *houstonensis*. If so, data will be included in a future addendum, no later than August 2018.

A legitimate concern regarding closed respirometry techniques, such as those employed in task 2.1.C1 (thermal tolerance), is that a buildup of metabolic wastes might affect respiration rates and patterns measured in the chambers. However, these potential effects are not well understood and have not been previously tested for freshwater mussels. In our closed respirometry experiments, accumulation of metabolic-waste ammonia in closed chambers rarely exceeded 0.5 mg TAN/L and never reached 2mg TAN/L. The lack of a significant effect of 0.5-2 mg TAN/L on respiration rates, RI, or DO_{crit} in of *C. houstonensis* in the current experiment

(Task 2.2A) suggests that accumulation of metabolic wastes did not affect our estimates of these parameters in the thermal tolerance experiments (Task 2.2.C1).

2.2.A2. Effects of TAN on Valve Closure

Additional respirometry trials were conducted to increase the number of replicates in each treatment for *C. houstonensis* and *C. petrina* from the Colorado River. However, >50% of these additional animals closed during control (0 mg/L TAN) respirometry, indicating that they were in poor condition. The additional runs were therefore not integrated into the existing dataset, and results are not changed from the previous report.

Because of the increased incidence of valve closure observed in the original ammonia respirometry trials, we decided to use the MosselMonitor to better quantify these effects. It should be kept in mind that all mussels had been kept in the lab for an extended period by this point and exposed to multiple stressors in previous trials. Results of the MosselMonitor ammonia trials should therefore be interpreted as effects of ammonia on animals that were likely in fair to poor condition.

2.2.A2 Methods:

To monitor valve movements, *C. houstonensis* and *C. petrina* from the Colorado River were placed in the MosselMonitor and sensors attached to their valves following the same methodology as described for the suspended solids experiment (section 2.3). Mussels were acclimated to the system for three days, during which time the MosselMonitor assessed distance between sensors and calculated the baseline maximum and minimum valve opening exhibited by each mussel. During the subsequent portions of the experiment, distance between valves (sensors) was reported as percent gape, based on the baseline maximum and minimum distances

calculated during the acclimation period. Percent gape was then recorded every 10 seconds for the subsequent 48 hrs. This protocol was repeated four times in the following treatment order: Control (0 mg TAN/L), Ammonia (2 mg TAN/L), Control, Ammonia, until all experimental animals had been run. Different individuals were used for each run. Ammonia was added from a stock solution of Nitrogen, Ammonia Standard solution (HACH Company: 1,000 mg/L as $\text{NH}_3\text{-N}$) to bring the concentration of water in the MosselMonitor and associated mixing tank to a nominal concentration of 2 mg TAN /L. Actual concentrations of TAN in the MosselMonitor were measured approximately 15 minutes after the ammonia addition using the previously described YSI 9300 Photometer. After 24 hours, TAN was again measured and sufficient stock solution added to the MosselMonitor to bring concentrations back up to 2 mg TAN/L.

2.2.A2 Results:

Mean percent gape was significantly lower in the ammonia treatment ($M = 65.1$, $SD = 16.4$) compared to the control ($M = 45.1$, $SD = 8.5$) for *C. houstonensis*; $t(14) = 3.173$, $p = 0.003$. Mean percent gape was also significantly lower in the ammonia treatment ($M = 63.1$, $SD = 14.5$) compared to the control ($M = 42.5$, $SD = 8.8$) for *C. petrina*; $t(7) = 2.652$, $p = 0.016$ (Fig. 35).

The percent of time gape exceeded 50% was significantly higher in the control ($M = 74.5$, $SD = 17.2$) compared to the ammonia treatment ($M = 52.6$, $SD = 12.3$) for *C. houstonensis*; $t(14) = 2.976$, $p = .005$. Similarly, the duration of time gape exceeded 50% was significantly higher in the control ($M = 64.2$, $SD = 16.9$) compared to the ammonia treatment ($M = 43.6$, $SD = 11.8$) for *C. houstonensis*; $t(7) = 2.161$, $p = .034$ (Fig. 36)

The percent of time gape was < 10% did not differ between control ($M = 10.0$, $SD = 6.6$) compared to the ammonia treatment ($M = 16.1$, $SD = 17.3$) for *C. houstonensis*; $t(14) = -0.881$, $p = 0.197$. Similarly, the percent of time gape was <10% did not between control ($M =$

3.2, SD = 5.5) compared to the ammonia treatment (M = 21.5, SD = 24.1) for *C. petrina*; $t(7) = -1.472$, $p = 0.092$) (Fig. 37). However the variance among individuals was much greater in the ammonia treatment compared to the control for *C. houstonensis* (300.8 vs 44.0) and *C. petrina* (578.7 vs 29.9) (Levene's test for homogeneity of time variance; $p = 0.033$ and 0.005 , respectively)

2.2A2 Conclusions:

For both species, ammonia concentrations of 2.0 mg/L caused a reduction in mean percent gape over a 48 hour period when averaged across all individuals. This was primarily caused by a reduction in the mean percentage of time the mussels remained mostly open (>50% gape) rather than an increase in the percentage of time mussels remained closed (<10% gape). Thus, exposure to 2.0 mg TAN/L ammonia may have reduced feeding and respiratory activity but was not likely to result in a complete cessation of feeding or respiration when averaged across all mussels. However, individual mussels exhibited high variance in their susceptibility to ammonia with some individuals remaining closed for >40% of the experiment duration (i.e. ≥ 19 hrs) in the TAN treatment whereas this never happened in the control treatment. This is cause for concern in that it suggests exposure to high ammonia concentrations in the natural environment would have a strong, detrimental effect on a sensitive subset of the population even though effects may not be detectable when averaged across the entire population. This is also supported by the observed increased frequency of mussels switching from aerobic to anaerobic respiration (see Fig 33) as TAN rose to 2 mg/L. Although some mussels remained open during the entire respirometry run, an increasing proportion closed their valves and periodically ceased respiring when exposed to high ammonia levels.

2.2B. Effect of salinity on adult mussel valve closure

Mussels must keep their shells open to obtain food and oxygen from the surrounding waters. However, they often respond to stressors by closing their shells. Electromagnetic sensors attached to each valve can be used to monitor gaping and closing behavior, setting off alarms when behavior indicates the presence of stressful toxicants in the water (Manley and Davenport 1979, Kramer et al. 1989, Gnyubkin 2009). Systems such as the MosselMonitor (www.mosselmonitor.nl; Kramer et al. 1989) and the Dreissena Monitor (Envicontrol Köln Germany; Borcharding, 1994) have been used to monitor stressors in fresh and saltwater environments in Europe. Valve movements have been recommended as a sublethal, behavioral endpoint for stressors such as chloride (Hartmann et al. 2016). In this experiment, we use a MosselMonitor to determine whether mussels fully or partially close their valves in response to increasing salinity – indicating negative impacts on feeding and respiration.

Experimental animals

Following respirometry experiments (see section 2.1.C1), *C. petrina* (Colorado and Guadalupe Rivers) and *C. houstonensis* (Colorado and Navasota River) were allowed to recover for > 4 weeks at 18°C. Water temperature was then raised by 1°C/day to the experimental temperature of 28°C. Mussels were acclimated to this temperature for ≥ 1 week prior to

initiation of experiments. During this time mussels were fed Shellfish Diet 1800 twice daily (2 mL morning, 1 mL afternoon per ~70 L upweller) and held at a 12h light: 12h dark cycle.

Experimental protocol

To monitor valve movements, four mussels of each species (eight mussels total) were placed in the MosselMonitor and sensors attached to their valves following the same methodology as described for the suspended solids experiment (section 2.3). Mussels were acclimated to the system for three days, during which time the MosselMonitor assessed distance between sensors and calculated the baseline maximum and minimum valve opening exhibited by each mussel. During the subsequent portions of the experiment, distance between valves (sensors) was reported as percent gape, based on the baseline maximum and minimum distances calculated during the acclimation period. Percent gape was calculated and recorded every 10 seconds for the remainder of the experiment. Valve closure was defined as percent gape $\leq 10\%$.

The first 24 hours following acclimation (Day 4) served as a control period, during which time food, but no salt, was added to the MosselMonitor. The experimental period began on Day 5. A belt feeder dropped salt (Diamond Crystal pool salt; Cargill Inc., Minneapolis, MN) into the cone tank at a constant rate of 27.3 g/hr over a period of 11 hours. Salt was mixed in the cone tank via a submersible Resun King-2 pump (1000 L/hr) and multiple air stones. A second submersible Resun King-2 pump transferred saltwater to the MosselMonitor at a constant rate of 360 L/hr. Flexible tubing returned water at the same rate to the cone tank via ambient head pressure. A PinPoint Salinity Monitor (American Marine Inc., Ridgefield, CT) was used to measure salinity at the time of attachment, start of the control period, and every hour during the beginning of the experimental period. The salinity meter's probe was held in the cone tank to

make sure the mussels were not disturbed. Previous trials determined that the salinity in the cone tank and the MosselMonitor were equivalent due to constant flow between the two units. This protocol resulted in an 11-hour ramping period (9:00 – 20:00) during which salinity rose linearly with time from a low of <1 ppt to a high of ~4ppt at a rate of ~0.3ppt/h (Fig. 38).

2.2B Results

On average, *C. petrina* from both locations exhibited a steady decline in percent gape as salinity levels increased beyond 2.0 ppt. Both subpopulation exhibited valve closure, with percent gape declining to $\leq 10\%$ at the highest salinities (Figure 39). *C. houstonensis* (Colorado River) showed a slow but steady decline in percent gape as salinity increased above 1.5 ppt whereas *C. houstonensis* (Navasota River) showed an abrupt decline as salinity increased above 2.5 ppt. Neither population exhibited valve closure with percent gape declining to only ~30% at high salinities (Figure 40). *L. bracteata* (Llano Lake) exhibited a rapid decline in percent gape as salinity increased above 3.0 ppt and exhibited valve closure at high salinities (Figure 41).

2.2B Conclusions:

Previous studies have shown that adult mussels (*Elliptio complanata*) exposed to 6 and 4 ppt exhibited 50% mortality by day 3 and 4 respectively, while mussels exposed to 2 ppt exhibited reduced metabolic rates but no mortality after 28 days (Blakeslee et al. 2013). Our results suggest that a reduction in gape and/or complete closure, and resultant reduction and/or cessation of water flowing past the gills is a likely mechanism driving reduced metabolic rates (i.e. respiration) as salinity increases. Valve closure would also be expected to interfere with

feeding and fertilization success. These sublethal impacts of salinity >2 ppt are likely greater for *C. petrina* and *L. bracteata* than *C. houstonensis* as they exhibited steeper declines in gape.

In our study, mussels were exposed to salinities ≥ 2 ppt for less than 6 hours and exhibited zero mortality during the experiment or within 7 days of being transferred back to freshwater. However, if high salinity conditions were sustained over a long period of time, lethal effects of high salinity might occur more quickly for *C. houstonensis* due to increased exposure. They did not close valves as tightly and appeared to reopen to a greater degree than *C. petrina* and *L. bracteata* as salinity approached LC₅₀ (4ppt, 7d) concentrations reported by Blakeslee et al (2013).

References

- Anestis, A., A. Lazou, H.O. Portner, and B. Michaelidis. 2007. Behavioral, metabolic, and molecular stress responses of marine bivalve *Mytilus galloprovincialis* during long-term acclimation at increasing ambient temperature. *Comparative and Evolutionary Physiology*. 293(2):R911-R921.
- Blakeslee, C.J., H.S. Galbraith, L.S. Robertson, and B. St. John White. 2013. The effects of salinity exposure on multiple life stages of a common freshwater mussel, *Elliptio complanata*. *Environmental Toxicology and Chemistry* 32(12):2849-2854.
- Brown, L.R. 1989. Temperature preferences and oxygen consumption of three species of sculpin (*Cottus*) from the Pit River drainage, California. *Environmental Biology of Fishes*. 26:223-236.
- Chen, L.Y., A.G. Heath, and R.J. Neves. 2001. Comparison of oxygen consumption in freshwater mussels (Unionidae) from different habitats during declining dissolved oxygen concentration. *Hydrobiologia* 450:209-214.
- Clark T.D., K.M. Jeffries, S.G. Hinch, and A.P. Farrell. 2011. Exceptional aerobic scope and cardiovascular performance of pink salmon (*Oncorhynchus gorbuscha*) may underlie resilience in a warming climate. *Experimental Biology* 216:2771-2782.
- Elderkin, C.L., D.W. Schneider, J.A. Stoeckel, and D.K. Padilla. 1998. A method for measuring in situ oxygen consumption rates of freshwater gastropods. *Journal of the North American Benthological Society* 17(3):338-347.
- Fanslow, D.L., T.F. Nalepa, and T.H. Johengen. 2001. Seasonal changes in the respiratory electron transport system (ETS) and respiration of the zebra mussel, *Dreissena polymorpha* in Saginaw Bay, Lake Huron. *Hydrobiologia* 448:61-70.
- Faul, F., E. Erdfelder, A.G. Lang, and A. Buchner. 2007. G*Power 3: A flexible statistical power analysis program for the social, behavioral, and biomedical sciences. *Behavior research methods* 39(2):175-191.
- Fritts, A.K., M.C. Barnhart, M. Bradley, N. Liu, W.G. Cope, E. Hammer, and R.B. Bringolf. 2014. Assessment of toxicity test endpoints for freshwater mussel larvae (glochidia). *Environmental Toxicology and Chemistry*. 33(1):199-207).
- Fritts, A.K., J.T. Peterson, P.D. Hazelton and R.B. Bringolf. 2015. Evaluation of methods for assessing physiological biomarkers of stress in freshwater mussels. *Canadian Journal of Fisheries and Aquatic Sciences* 72:1450-1459.

Gascho Landis, A.M., T.L. Mosley, W.R. Haag, and J.A. Stoeckel. 2012. Effects of temperature and photoperiod on lure display and glochidial release in a freshwater mussel. *Freshwater Science* 31(3):775-786.

Gnyubkin, V. F. 2009. An early warning system for aquatic environment state monitoring based on an analysis of mussel valve movements. *Russian Journal of Marine Biology* 35: 431-436.

Hartmann, J.T., S.B. Beggel, K. Auerswald, and B.C. Stoeckle. 2016. Establishing mussel behavior as a biomarker in ecotoxicology. *Aquatic Toxicology*. 170:279-288.

Kenner, R.A. and S.I. Ahmed. 1975. Measurements of electron transport activities in marine phytoplankton. *Marine Biology* 33:119-127.

Kramer, K. J. M., H. A. Jenner, and D. Dezwart. 1989. The Valve Movement Response of Mussels - A Tool In Biological Monitoring. *Hydrobiologia* 188: 433-443.

Madon S.P., D.W. Schneider, and J.A. Stoeckel. 1998. In situ estimation of zebra mussel metabolic rates using the electron transport system (ETS) assay. *Journal of Shellfish Research* 17(1):195-203.

Manley, A. R., and J. Davenport. 1979. Behavioral-Responses of Some Marine Bivalves to Heightened Seawater Copper Concentrations. *Bull. Environ. Contam. Toxicol.* 22: 739-744.

Marshall, D.J., Y. Dong, C.D. McQuaid, and G.A. Williams. 2011. Thermal adaptation in the intertidal snail *Echinolittorina malaccana* contradicts current theory by revealing the crucial roles of resting metabolism. *Journal of Experimental Biology* 3649-3657.

Mueller, C.A. and R.S. Seymour. 2011. The regulation index: A new method for assessing the relationship between oxygen consumption and environmental oxygen. *Physiological and Biochemical Zoology* 84(5):522-532.

Packard, T.T., M.L. Healy, and F.A. Richards. 1971. Vertical distribution of the activity of the respiratory electron transport system in marine plankton. *Limnology and Oceanography* 16(1):60-70.

Owens, T.G. and F.D. King 1975. The measurement of respiratory electron-transport-system activity in marine zooplankton. *Marine Biology* 30:27-36.

Simcic T., F. Pajk, M. Jaklic, A. Brancelj and A. Vrezec. 2014. The thermal tolerance of crayfish could be estimated from respiratory electron transport system activity. *Journal of Thermal Biology* 41:21-30.

Simcic, T., D. Jesensek, and A. Brancelj. 2017. Metabolic characteristics of early life history stages of native marble trout (*Salmo marmoratus*) and introduced brown trout (*Salmo trutta*) and their hybrids in the Soca River. *Ecology of Freshwater Fishes* 26:141-149.

Smith, M.E., J. M. Lazorchak, L.E. Herrin, S. Brewer-Swartz, and W.T. Thoeny. 1997. A reformulated, reconstituted water for testing the freshwater amphipod, *Hyalella azteca*. *Environmental Toxicology and Chemistry* 16(6):1229-1233.

Tankersley, R.A., and R.V. Dimock. 1993. The effect of larval brooding on the respiratory physiology of the freshwater unionid mussel *Pyganodon cataracta*. *The American Midland Naturalist*. 130(1):146-163.

USEPA. 2013. Aquatic Life Ambient Water Criteria for Ammonia – Freshwater. United States Environmental Protection Agency, Office of Water. EPA 822-R-13-001.

Walsh, S.J., D.C. Haney, and C.M. Timmerman. 1997. Variation in thermal tolerance and routine metabolism among spring- and stream-dwelling freshwater sculpins (Teleostei: Cottidae) of the southeastern United States. *Ecology of Freshwater Fish* 6:84-94.

Table 1. Species, collection sites, and shipping information for mussels used in thermal and hypoxia tolerance experiments at Auburn University.

Species	Drainage	Site	Collection Date	# shipped	Collection Temp. (°C)	Receiving Temp. (°C)
<i>Cyclonaias petrina</i>	Colorado River	Altair	4/28/2017	6		NT
			5/17/2017	33		16.2
		Lometa	6/1/2017	11	26.6	22.0
	Gauadalupe River	Gonzales	11/01/2017	14	18	16.9
		Gonzales	8/17/2017	32	30.9	23.5
<i>Cyclonaias houstonensis</i>	Colorado River	Altair	4/27/2017	6		NT
			5/17/2017	50		16.4
	Navasota River	Easterly	7/17/2017	50		22.6
<i>Lampsilis bracteata</i>	Llano River	Mason	5/31/2017	20	23	15.3
		Llano Park Lake	11/01/2017	50	Stranded, 13.7	15.1, 14.4
<i>Fusconaia mitchelli</i>	Guadalupe River	Gonzales	8/17/2017	6	30.9	23.5
			11/01/2017	4	18	16.9
<i>Truncilla macrodon</i>	Brazos River	Highbank	12/4/2017	7	19	NT
<i>Amblema plicata</i>	Colorado River	Altair	4/27/2017	12		NT
			8/4/2017	20	31	21.7
<i>Lampsilis teres</i>	Colorado River	Altair	11/02/2017	12	18	NT

Table 2. Optimum temperature and optimum range for acclimated ETS activity. Prior to ETS measurement, individuals were acclimated for >1 week to each of 10 temperatures from 15 – 36°C.

Species	Drainage	Optimum	Range
<i>Cyclonaias petrina</i>	Colorado River	35.3	28.2 - >36
	Gauadalupe River	34.6	26.5 - >36
<i>Cyclonaias houstonensis</i>	Colorado River	31.6	27.5 – 35.8
	Navasota River	27.6	24.8 – 30.6

Table 3. Optimal temperature data for non-acclimated mussels. Individuals were all acclimated for >1 week to 21°C. Enzymes were then extracted from foot tissue of each individual and incubated at each of 9 temperatures ranging from 12 – 36°C, generating a separate thermal performance curve for each individual (see Fig. 9). Min and max refer to the minimum and maximum optimal temperatures among all individuals within each species X drainage combination.

Species	Drainage	Mean	Min	Max	Stdev	CV	n
<i>Cyclonaias petrina</i>	Colorado River	30.2	28.6	34.8	1.7	5.7	12
	Gauadalupe River	28.5	27.6	29.5	0.7	2.6	6
<i>Cyclonaias houstonensis</i>	Colorado River	30.5	28.3	32.1	1.1	3.7	11
	Navasota River	28.8	27.7	29.8	0.6	2.0	12
<i>Lampsilis bracteata</i>	Llano River	28.4	27.6	29.1	0.6	2.1	11
	Llano Lake	<i>April 2018</i>					
<i>Fusconaia mitchelli</i>	Guadalupe River	27.8	26.5	28.8	0.9	3.3	6
<i>Amblesma plicata</i>	Colorado River	28.4	27.5	29.0	0.5	1.6	10
<i>Lampsilis teres</i>	Colorado River	27.1	27.9	26.2	0.6	2.1	12

Table 4. Summary of ETS enzyme thermal tolerance endpoints from acclimated and non-acclimated experiments. Optimal Range for acclimated mussels represents the temperature range where ETS activity was within 10% of the observed maximum rate, whereas for non-acclimated mussels it represents the range in optimal temperatures estimated for individual mussels. The upper end of the acclimated range indicates the temperature threshold above which we predict the initiation of thermal stress at the enzymatic level for at least some individuals in the population. The upper end of the non-acclimated range represents the maximum optimal temperature observed for enzymes subjected to a sudden increase in temperature. Onset of lethal effects indicates the temperature threshold beyond which we predict the onset of mortality due to thermal stress. Months indicate when we expect additional information will be available. Blank cells indicate no results due to a lack of samples and/or animals. All temperatures are °C.

Species	Drainage	Optimal Temp.	Optimal Range	Estimated onset of lethal effects	Assay Type
<i>Cyclonaias petrina</i>	Colorado River	35.3	28.2 - >36		Acclimated
		30.2	28.6-34.8		Non-acclimated
	Gauadalupe River	34.6	26.5 - >36		Acclimated mussels
		28.5	27.6-29.5	38.9	Non-acclimated
<i>Cyclonaias houstonensis</i>	Colorado River	31.6	27.5 – 35.8		Acclimated mussels
		30.5	28.3-32.1		Non-acclimated
	Navasota River	27.6	24.8 – 30.6		Acclimated mussels
		28.8	27.7-29.8	37.1	Non-acclimated
<i>Lampsilis bracteata</i>	Llano River	28.4	27.6-29.1		Non-acclimated
	Llano Lake				Acclimated mussels
					Non-acclimated
<i>Fusconaia mitchelli</i>	Guadalupe River	27.8	26.5-28.8	31.0	Non-acclimated
<i>Amblema plicata</i>	Colorado River	28.4	27.5-29.0	36.0	Non-acclimated
<i>Lampsilis teres</i>	Colorado River	27.1	26.2-27.9	29.4	Non-acclimated

Table 5. Total ammonia nitrogen (TAN) and pH measurements in respirometry water for individual runs within ammonia treatments.

<i>Run</i>	<i>Treatment</i>	TAN (mg/L)		pH	
		<i>Initial</i>	<i>Final</i>	<i>Initial</i>	<i>Final</i>
1	0	0.05	0.4	8.6	8.6
2	0	0.1	0.1	8.6	8.6
1	0.5	0.60	0.43		8.4
2	0.5	0.66	0.30	8.6	8.5
1	2.0	2.40	2.08	8.6	8.4
2	2.0	2.16	1.76	8.5	8.4

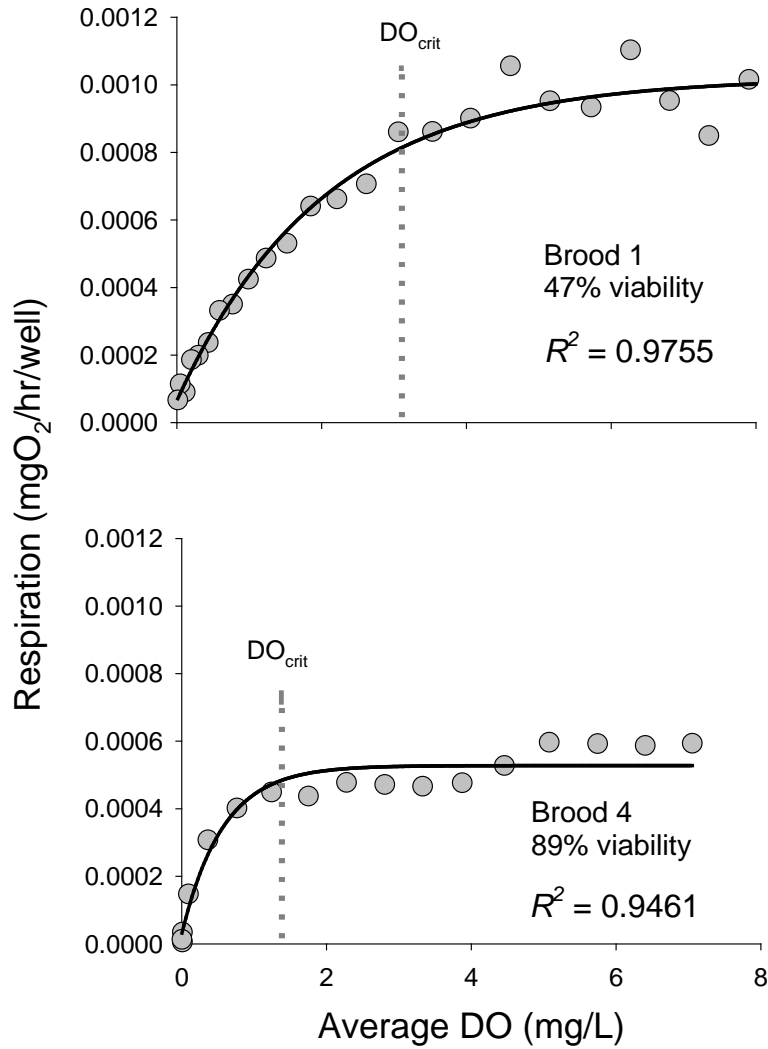


Figure 1. Example of preliminary data showing respiration patterns of *L. subrostrata* broods with low (top panel) and high (bottom panel) viability. The low viability brood had a greater respiration rate, reduced ability to regulate oxygen consumption, and increased DO_{crit} relative to the higher viability brood.

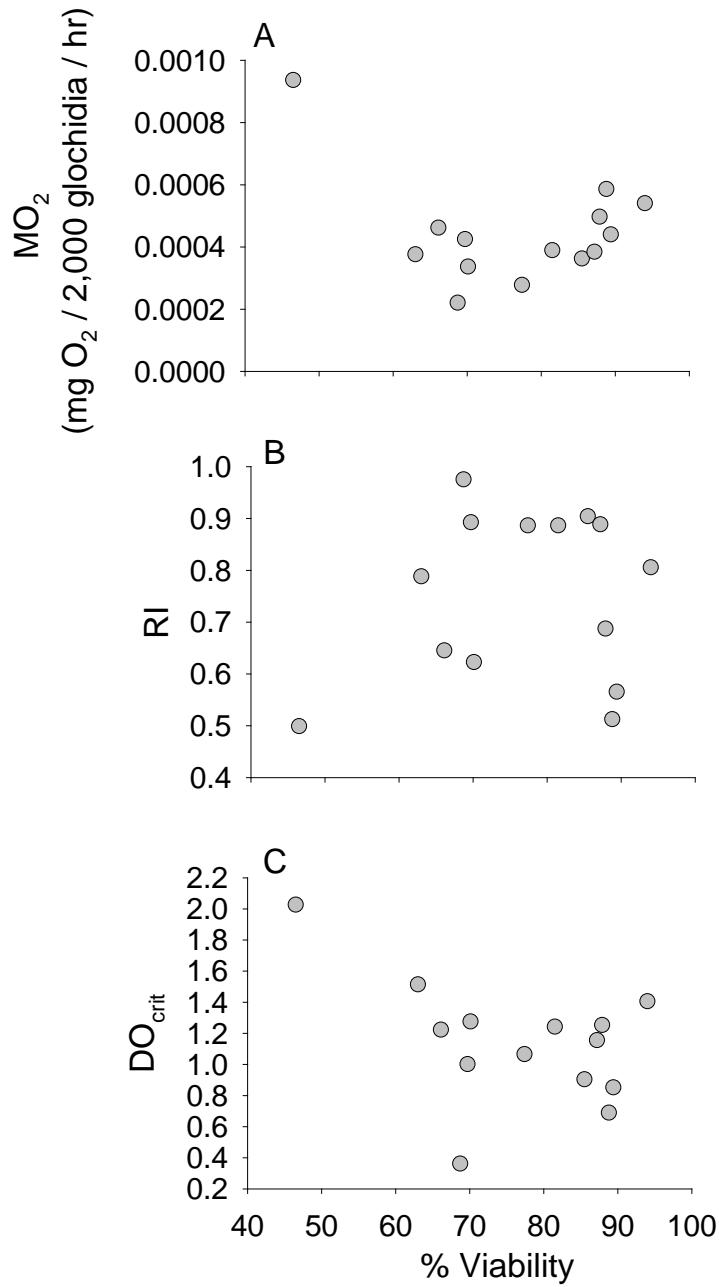


Figure 2. Relationships between (A) respiration rate (MO_2), (B) regulation index (RI), and (C) critical dissolved oxygen concentration (DO_{crit}) and % brood viability for glochidia of *L. subrostrata*. Each data point represents the mean value for 2,000 glochidia from a given brood.

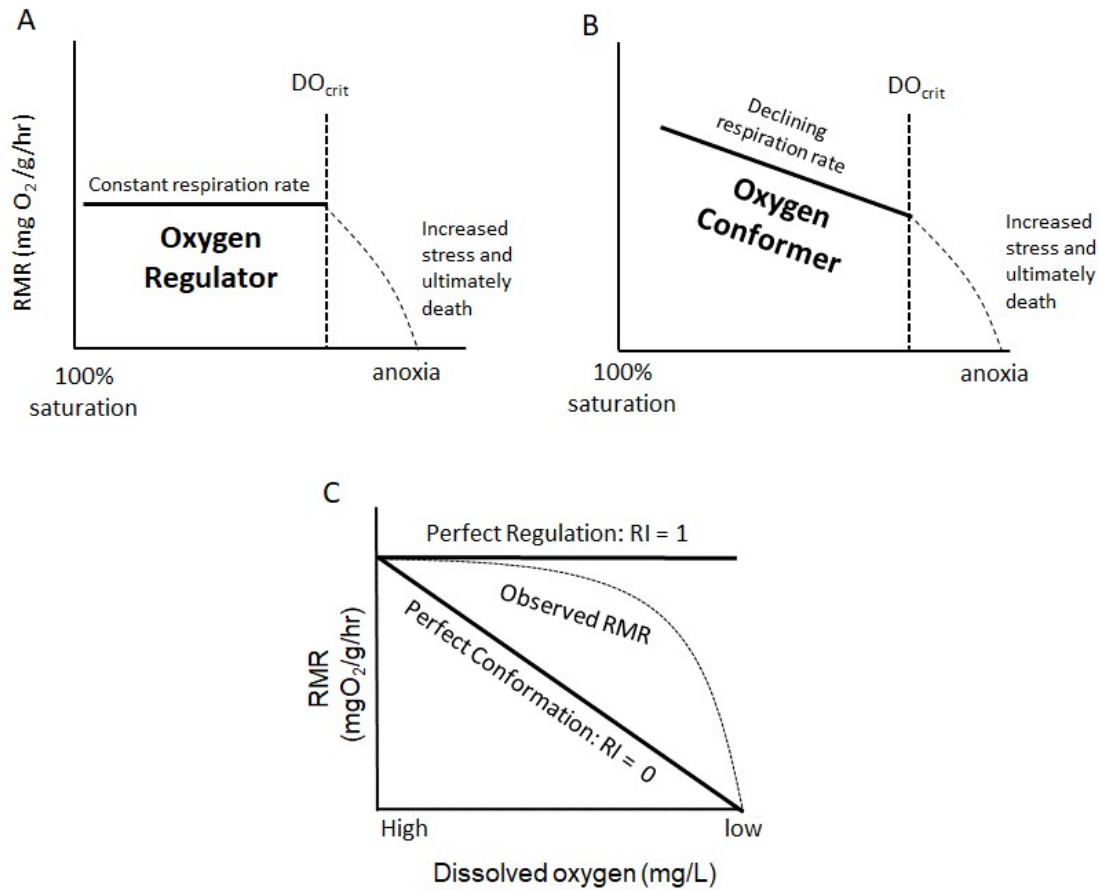


Figure 3. Resting metabolic rates (RMR) graphed as a function of declining dissolved oxygen showing A) an oxyregulator and B) an oxyconformer. DO_{crit} is the DO threshold below which respiration rates show a marked decrease or increase, indicating the switch from aerobic to anaerobic respiration. C) RMR graphed as a function of DO indicating the range of values of the Regulation Index (RI; Mueller and Seymour 2011). Solid lines indicating either perfect regulation ($\text{RI} = 1$) or perfect conformation ($\text{RI} = 0$) and dashed line indicates an intermediate, typically observed pattern that falls between perfect regulation and perfect conformation.

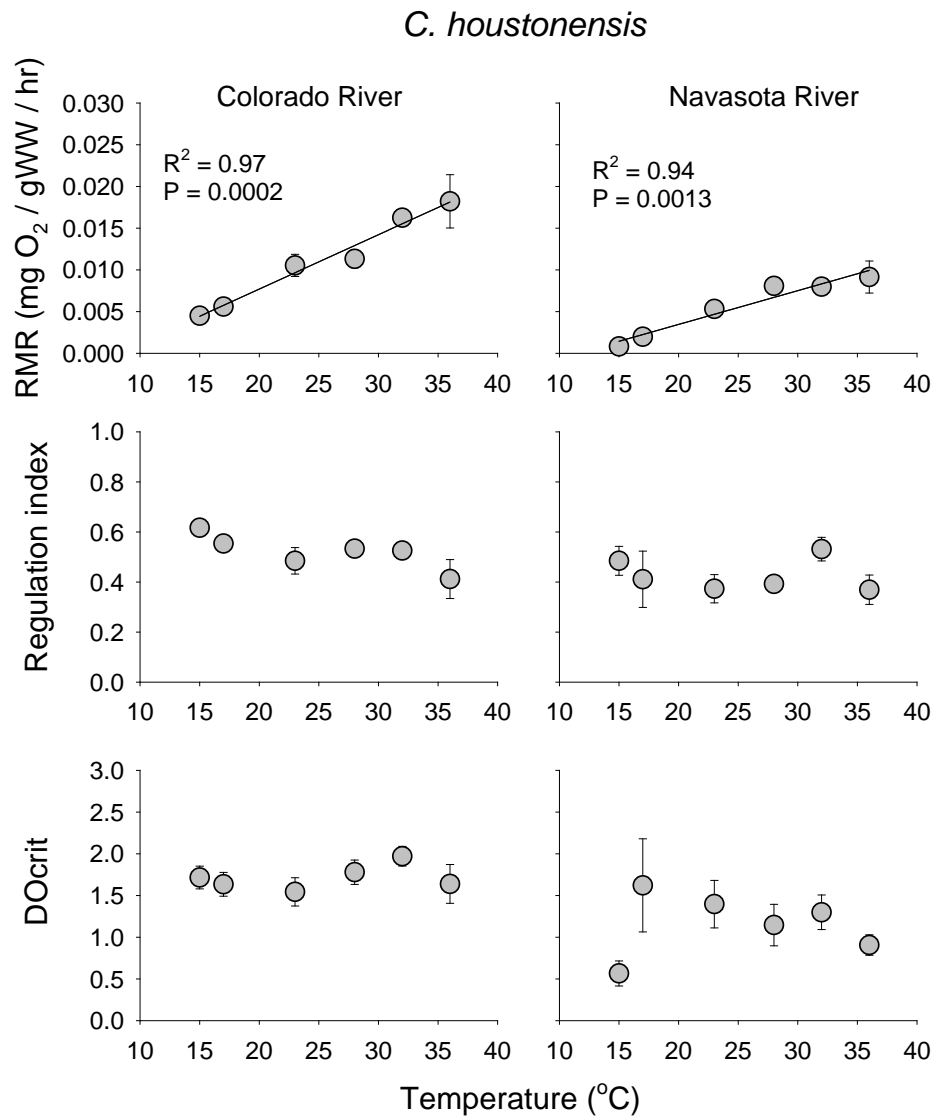


Figure 4. Relationships between resting metabolic rate (RMR), regulation index, DO_{crit} and temperature for *C. houstonensis* collected from two drainage basins. Neither regulation index nor DO_{crit} yielded a significant linear relationship with temperature. Vertical lines represent ± 1 SE.

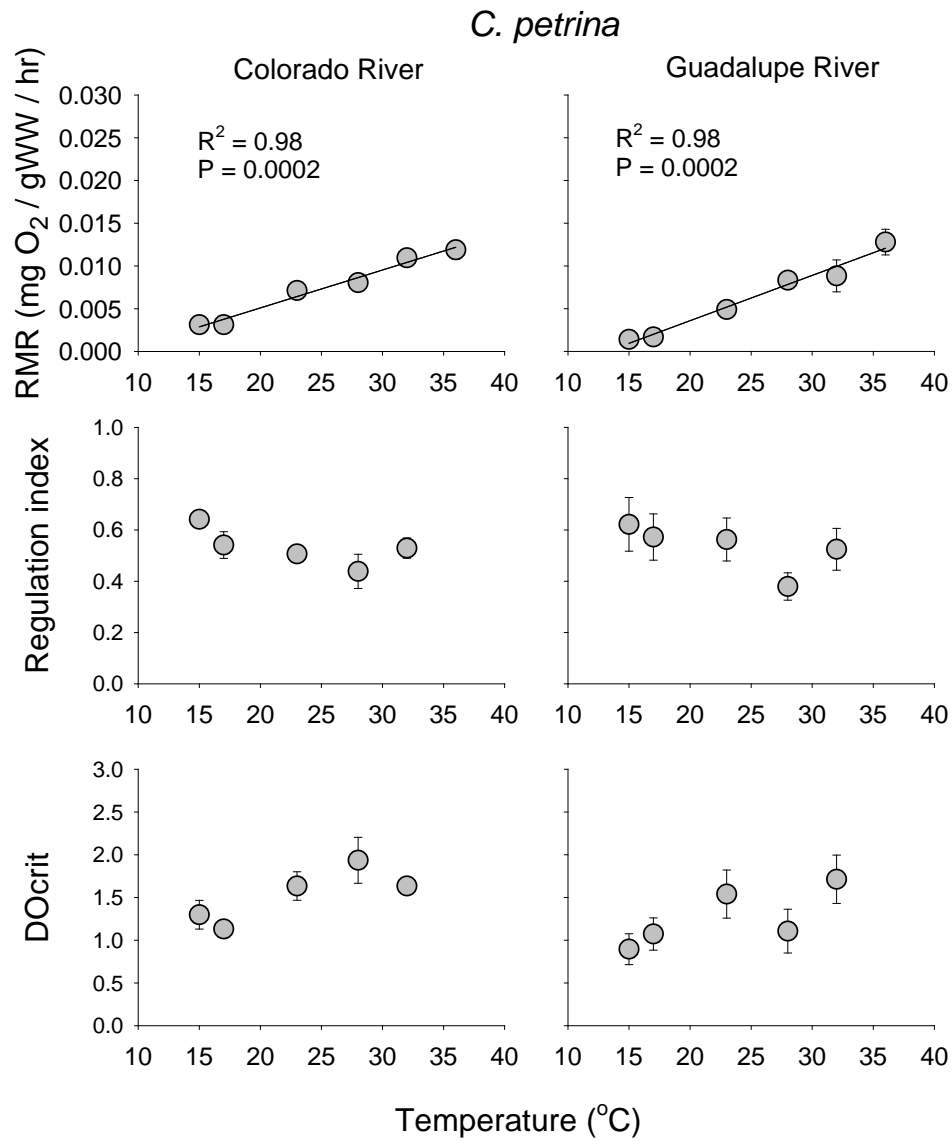


Figure 5. Relationships between resting metabolic rate (RMR), regulation index, DO_{crit} and temperature for *C. petrina* collected from two drainage basins. Neither regulation index nor DO_{crit} yielded a significant linear relationship with temperature. Vertical lines represent ± 1 SE.

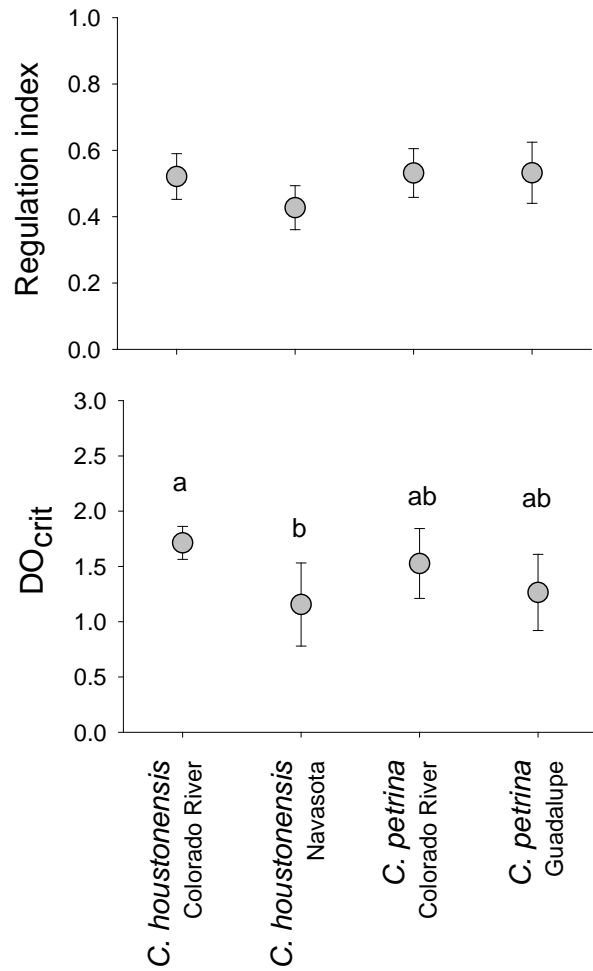


Figure 6. Mean regulation index and DO_{crit} across all temperatures for *C. houstonensis* and *C. petrina* collected from different drainage basins. No significant differences among mussel groups were found for mean regulation index. Letters indicate significant differences in DO_{crit} among mussel groups. Error bars represent ± 1 standard deviation.

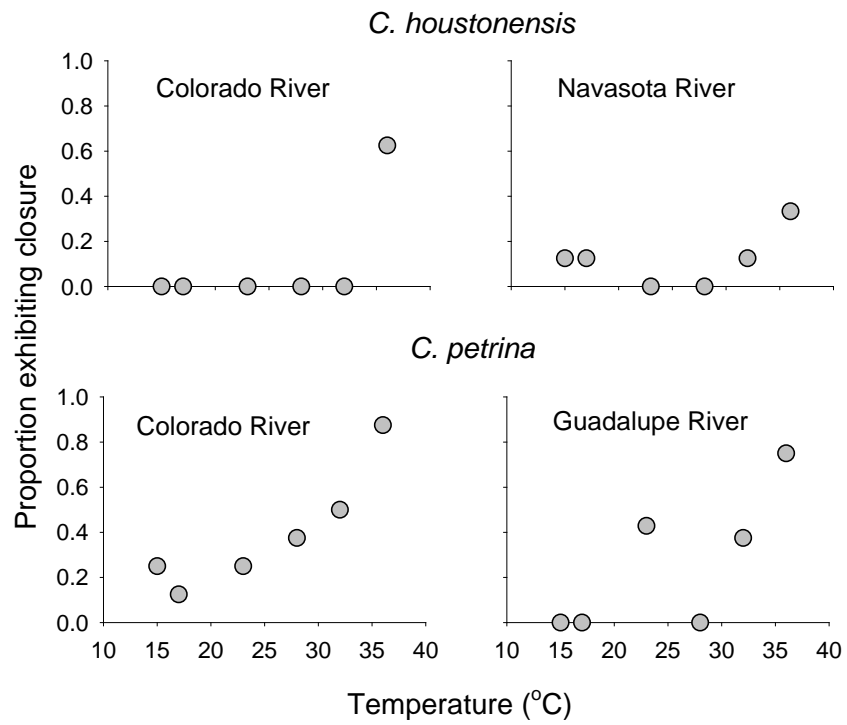


Figure 7. Proportion of individuals exhibiting at least one closure event during respirometry runs at six temperatures.

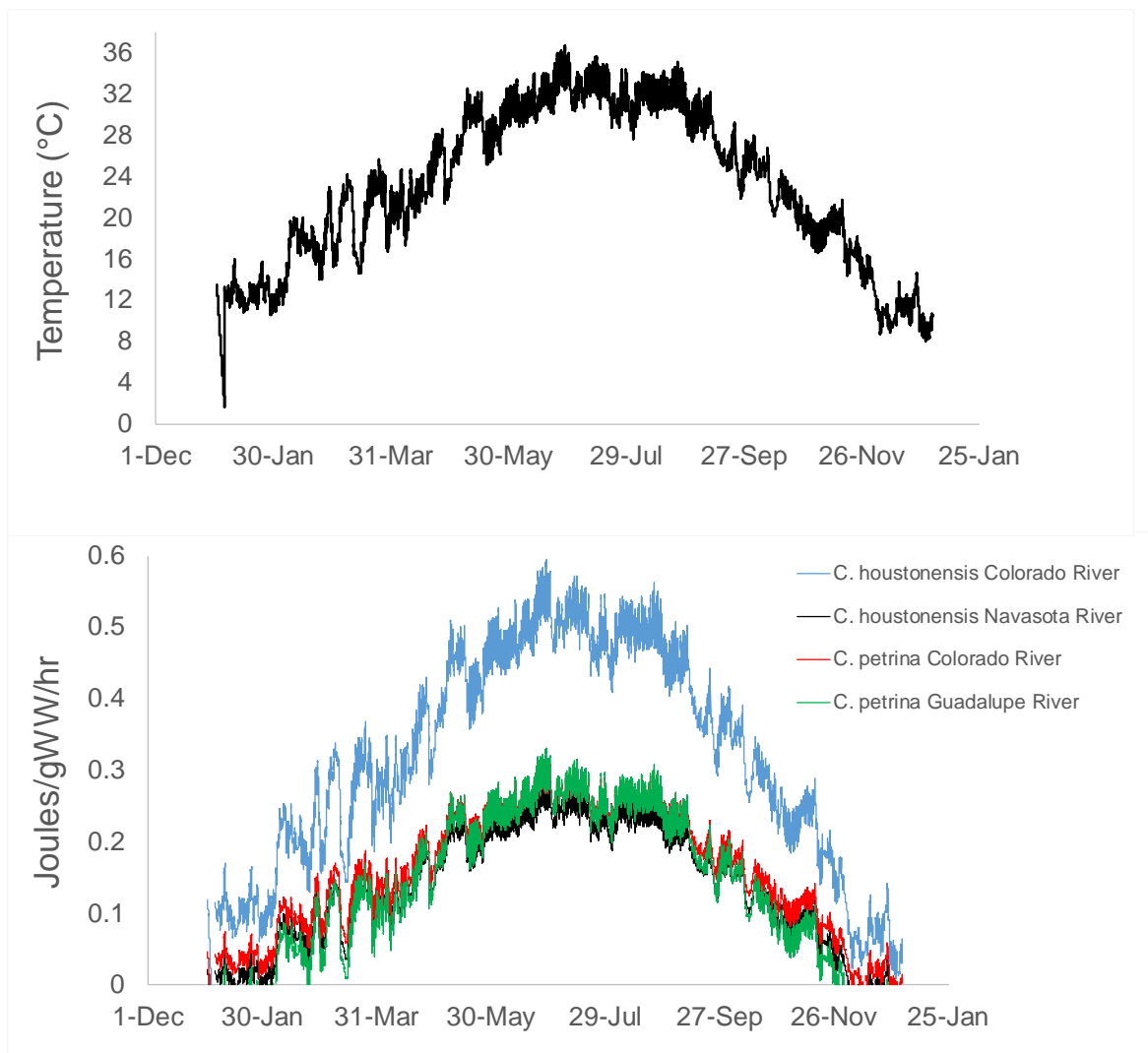


Figure 8. Comparison of estimated energy requirements to meet basic metabolic demands (Joules/gWW/hr) for 4 mussel populations if they were exposed to the same temperature regime. In this case, temperatures were obtained from the San Saba gage of the Colorado River, 2009.

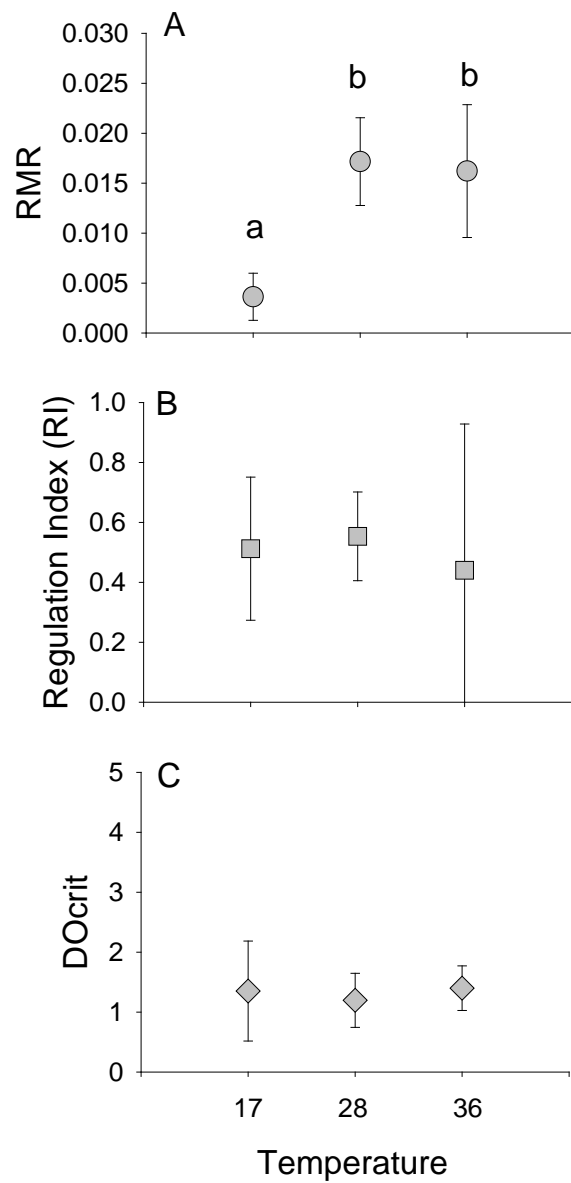


Figure 9. Relationships between (a) resting metabolic rate at 6 mg O₂/L, (b) regulation index, and (c) DO_{crit} and three temperatures for *L. bracteata* males. Vertical lines represent 95% CI. Letters above data points indicate significant differences among temperatures.

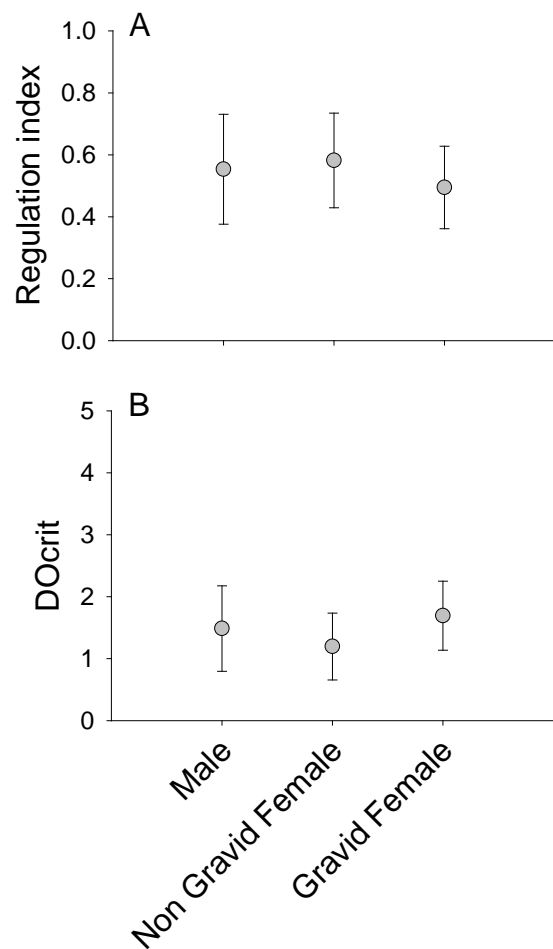


Figure 10. Mean (A) regulation index and (B) DO_{crit} estimates at 28°C for males, nongravid females, and gravid females. Vertical lines represent ± 1 standard deviation.

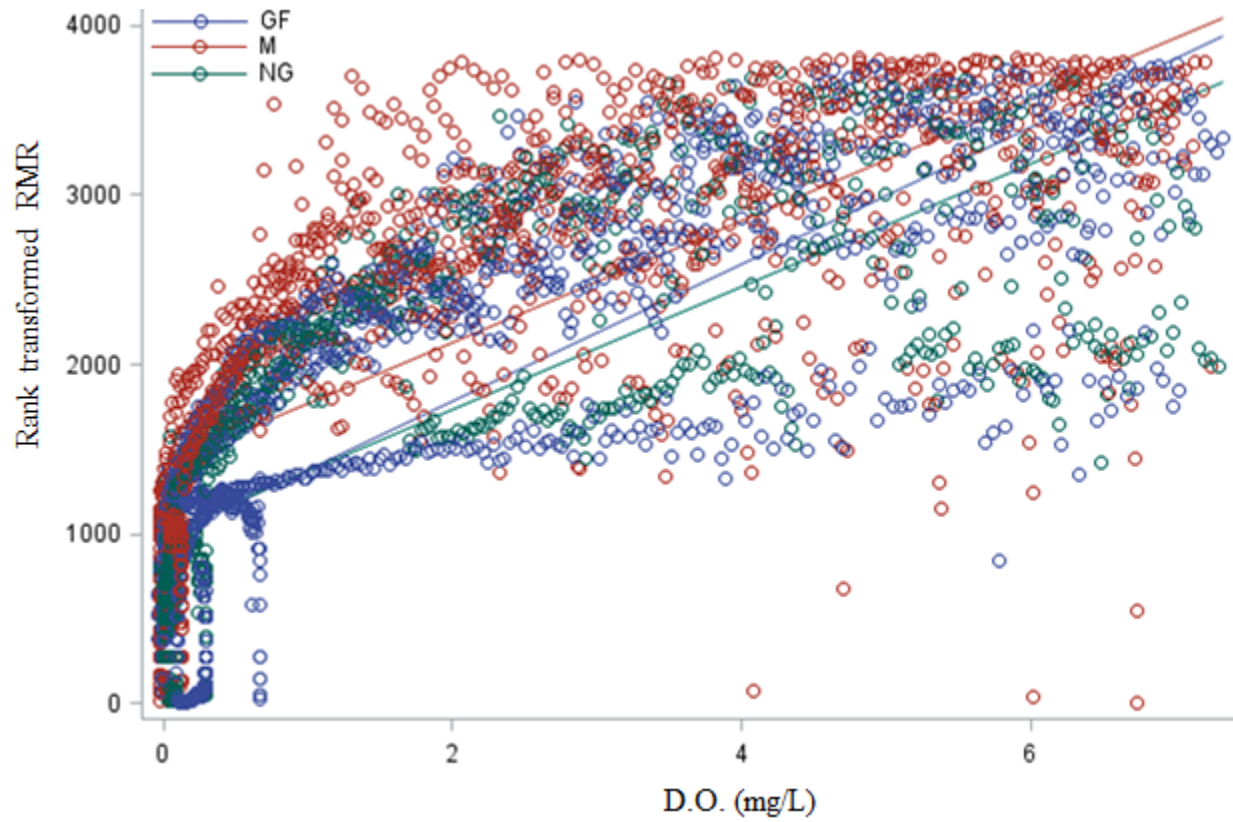


Figure 11. Relationship between resting metabolic rate (RMR) and dissolved oxygen (DO) for gravid females (GF), males (M), and nongravid females (NG) at 28°C. Each data point represents a rank-transformed respiration rate measurement for an individual mussel. All data are from *L. bracteata* collected from Llano Lake.

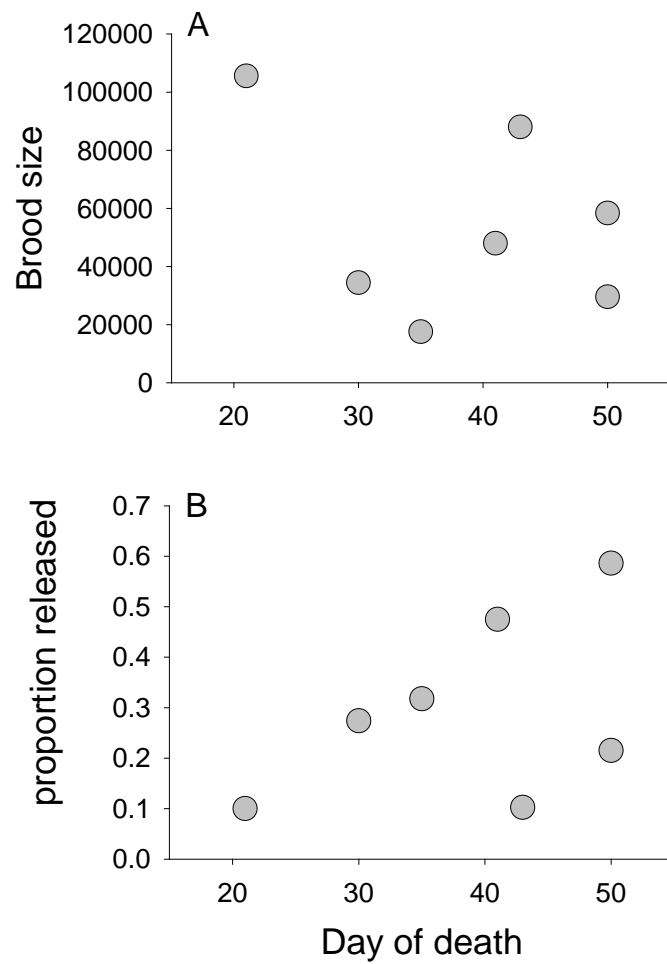


Figure 12. Relationship between (A) brood size and (B) proportion of brood released, and day of death for gravid females in the warming treatment. Each data point represents an individual mussel.

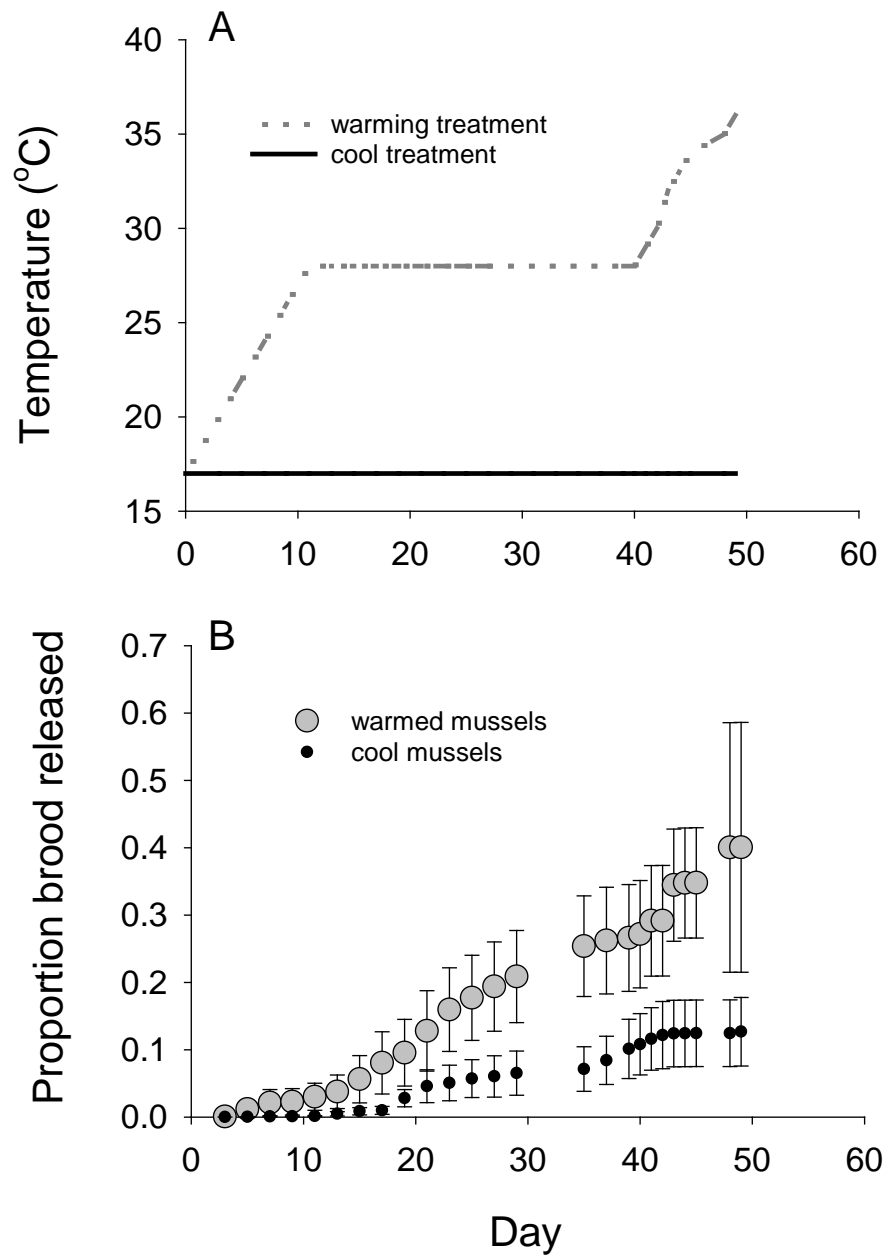


Figure 13. A. Temperature regimes for the cool (control) and warming treatments. B. Proportion of brood released over time for mussels in the cool and warming treatments. Each data point represents the mean of all surviving gravid females on that day. Vertical lines represent ± 1 standard error. Break in data indicates period when respirometry trials were conducted.

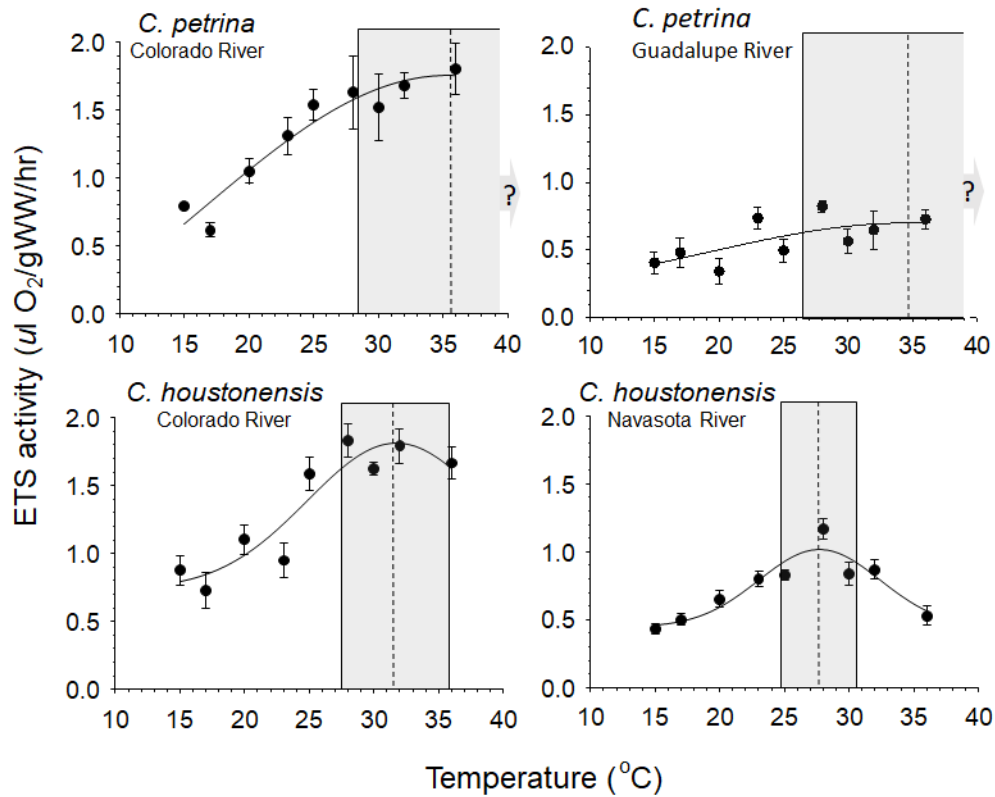


Figure 14. Relationship between ETS activity and temperature for acclimated mussels. Each data point represents the mean ETS activity of all mussels acclimated to that particular temperature. Mussel groups at each temperature were unique. ETS activity of a given mussel was measured only for the temperature to which it had been acclimated. Dashed lines indicate the optimal temperature for enzymatic activity. Grey rectangles represent the optimal temperature range within which ETS activity is within 10% of the maximum.

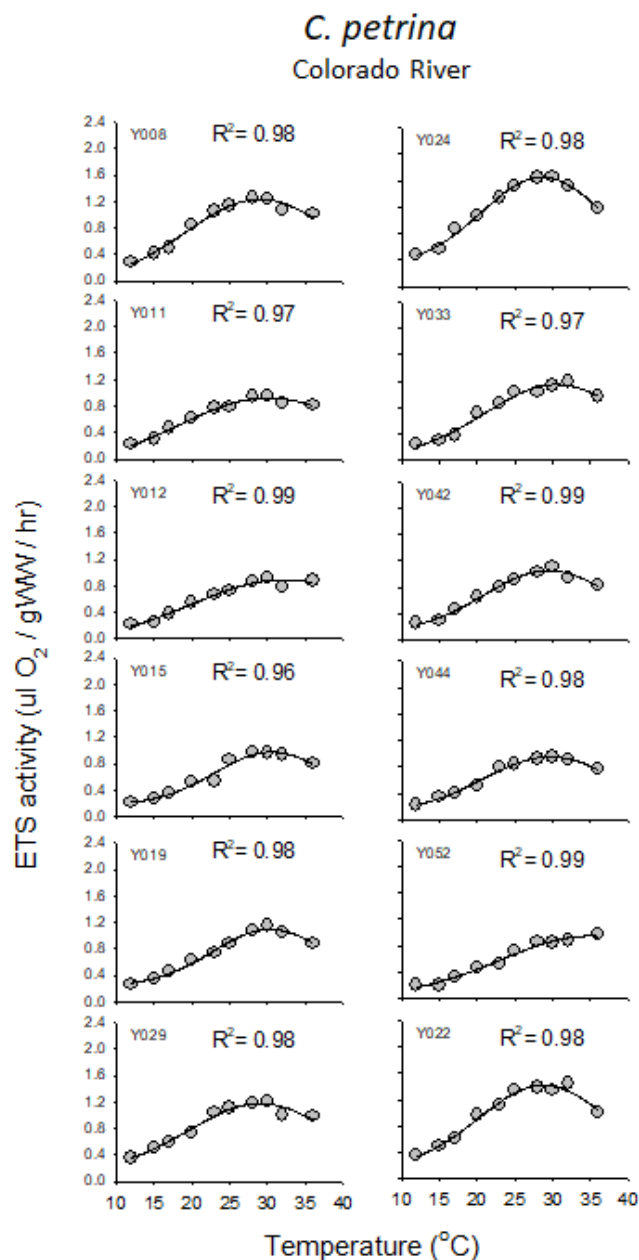


Figure 15. Relationship between ETS activity and temperature for non-acclimated *C. petrina* from the Colorado River. The tag number identifying each mussel is given in the upper left corner of each graph. Each data point represents ETS activity of enzymes collected from the same individual and incubated for 30 minutes at each temperature. Solid lines represent a four parameter Gaussian curve fitted through the data points. Optimal temperature for each individual was calculated as the temperature at the peak of each Gaussian curve.

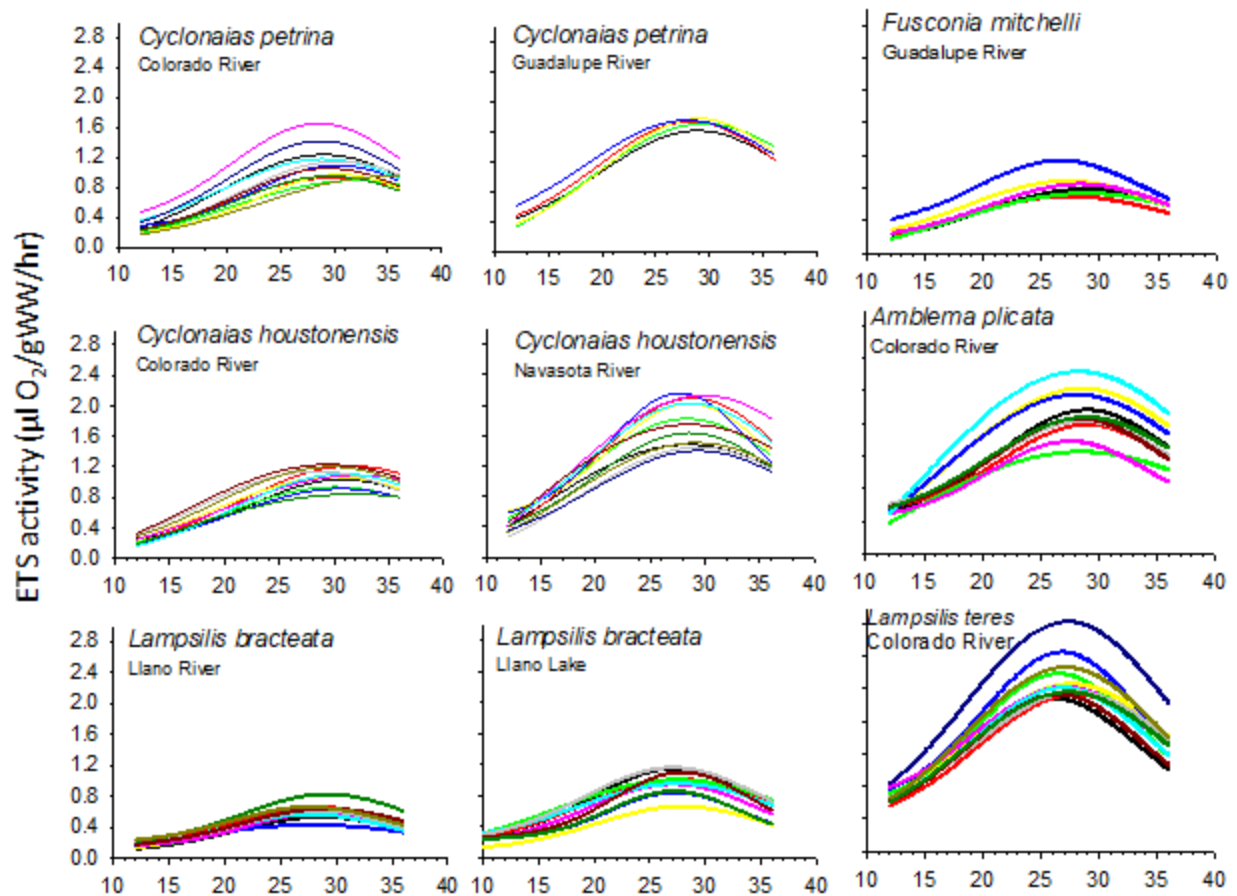


Figure 16. Summary graphs of relationship between ETS enzyme activity and temperature for non-acclimated mussels. Each curve represents a single mussel. ETS enzymes were extracted from each mussel and incubated at nine temperatures to which the mussel had not been acclimated. Colored lines represent a four parameter Gaussian curve fitted through the data for each individual mussel.

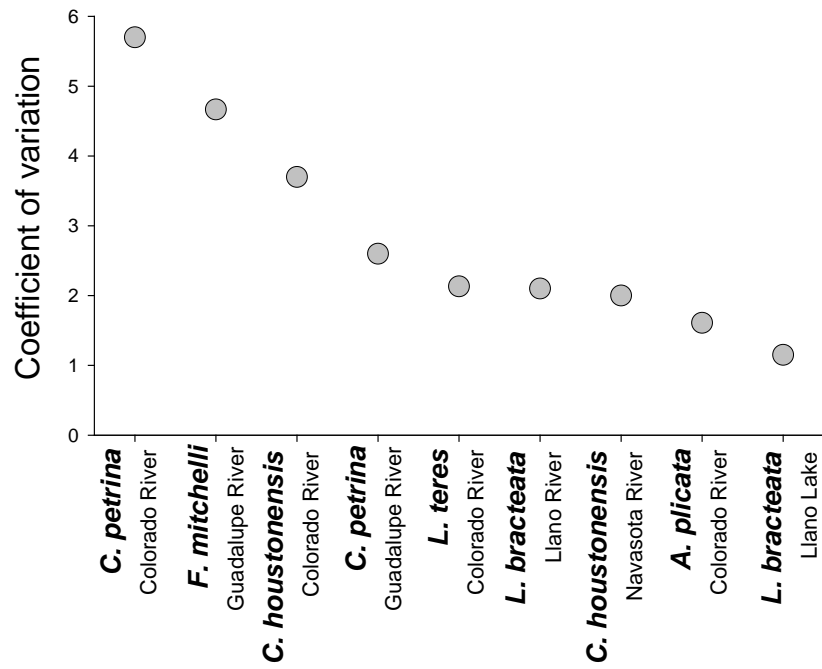


Figure 17. Coefficient of variation for optimal ETS temperatures of non-acclimated mussels from a given species and drainage, arranged in order from highest to lowest.

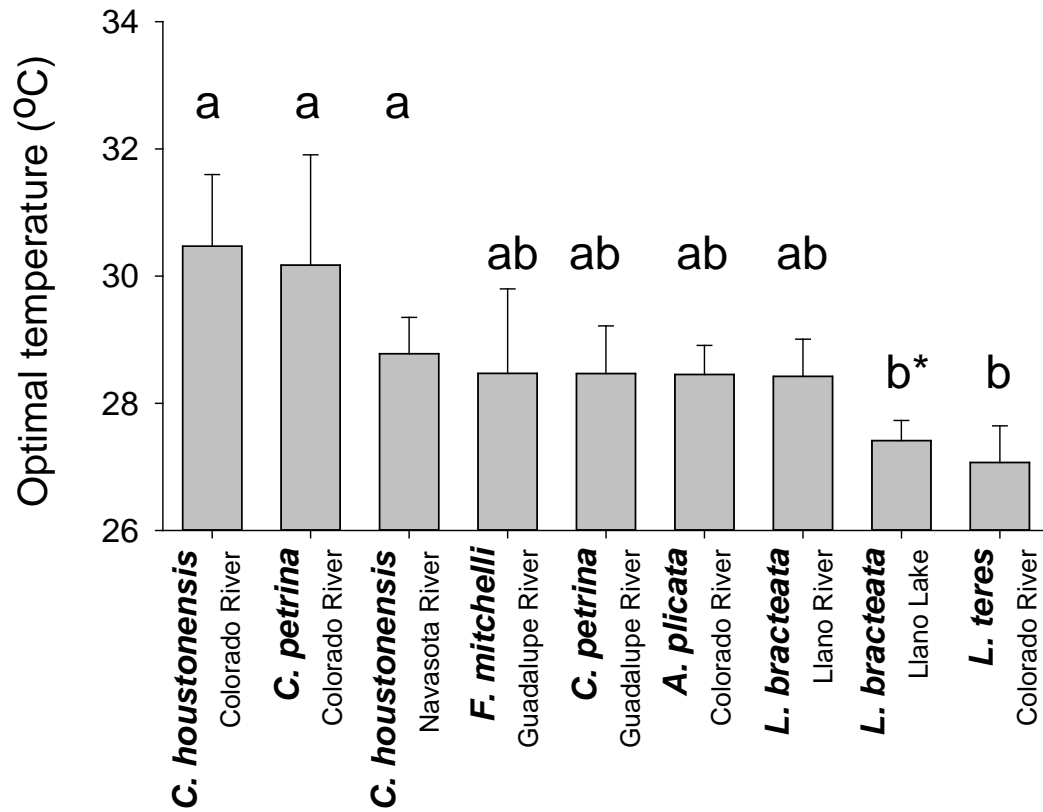


Figure 18. Mean optimal ETS temperatures of non-acclimated mussels determined from individual curves shown in Figure 2, arranged from highest to lowest. Error bars represent ± 1 SD. Letters indicate significant differences.

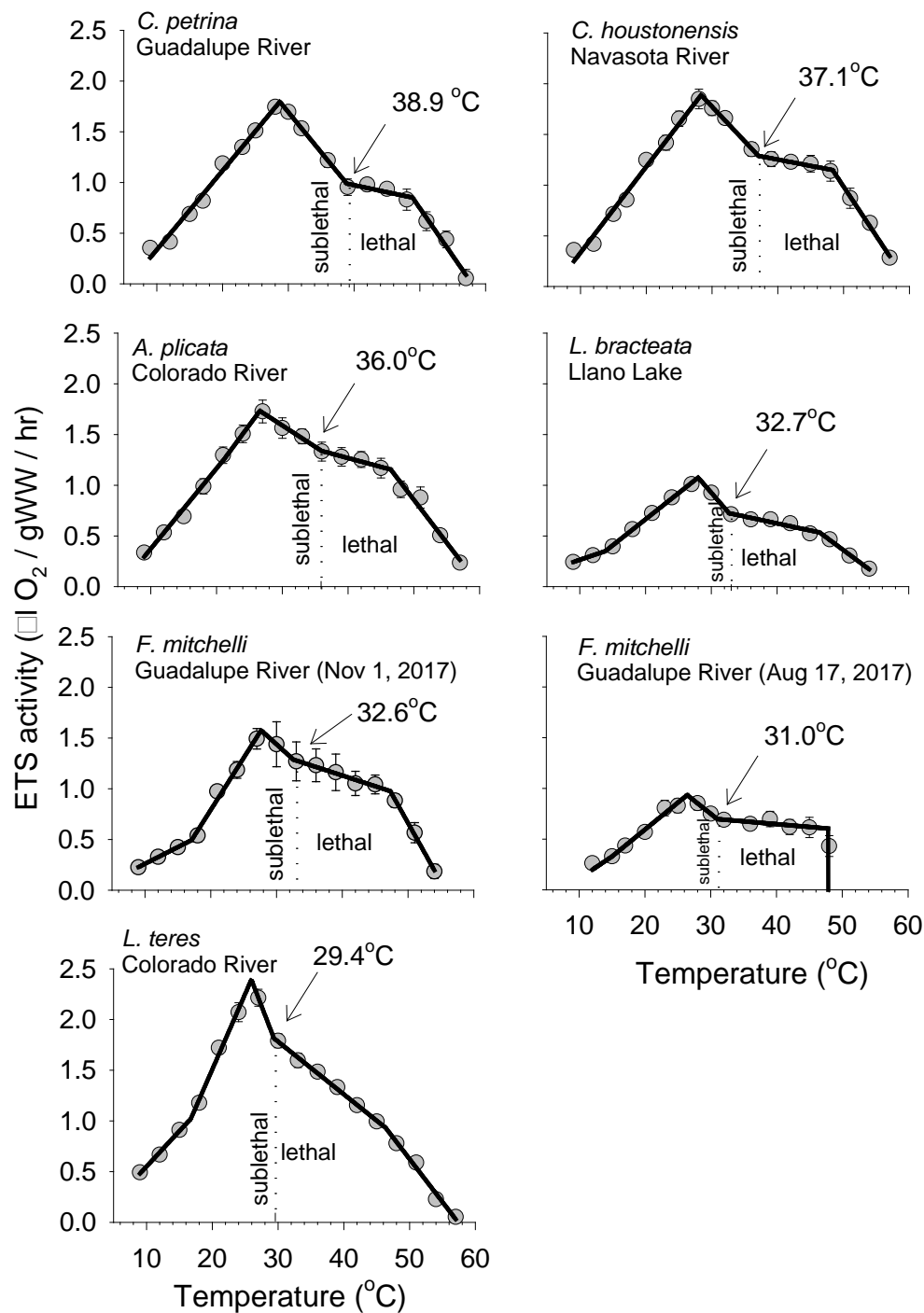


Figure 19. Relationship between ETS activity and temperature for non-acclimated mussels across the full range of experimental temperatures. Each data point within a panel represents the mean activity of enzymes extracted from the same group of mussels. Error bars represent ± 1 standard error. Solid lines represent 5-segment piecewise regressions. Dotted lines indicate temperature at which we hypothesize sublethal effects transition to lethal effects.

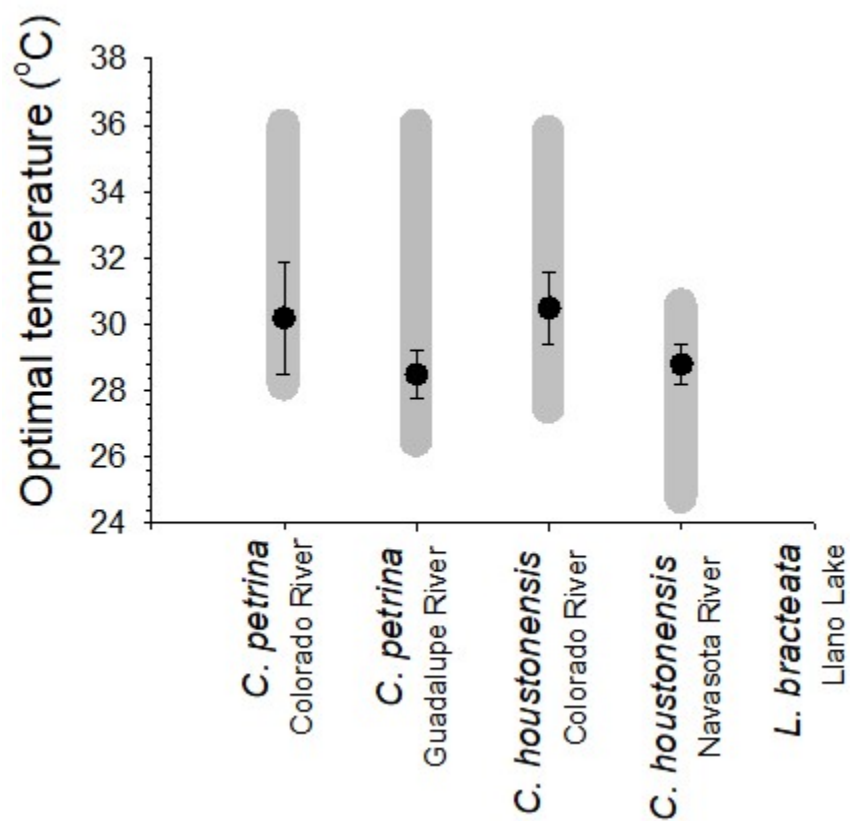


Figure 20. Comparison of optimal temperature range (grey bars) obtained from acclimated mussels and mean optimal temperature (black circles) obtained from non-acclimated mussels. Error bars represent ± 1 SD. Data for *L. bracteata* is expected to be available by May 2018.

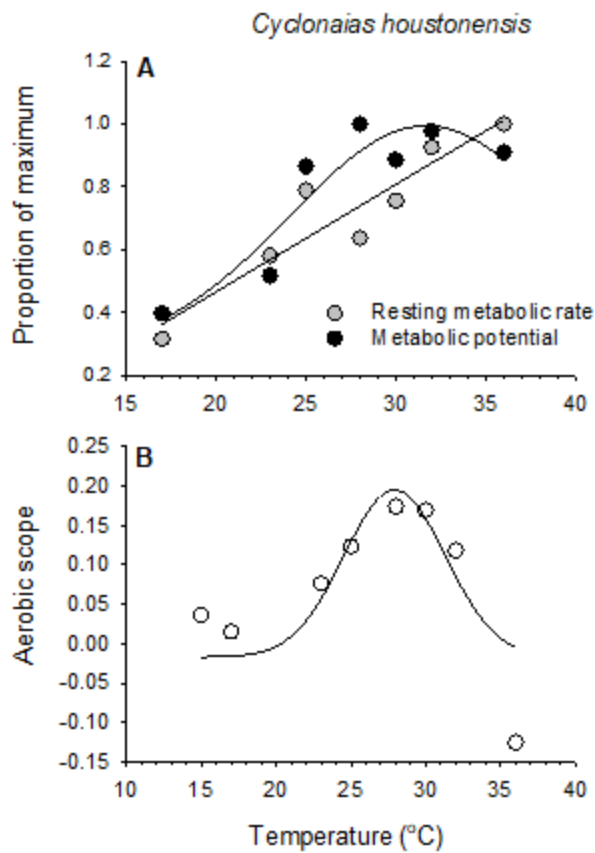


Figure 21. A) Relative changes in resting metabolic rate (RMR) and metabolic potential (ETS activity) with increasing temperature for *C. houstonensis* (Colorado River). B) Aerobic scope calculated as the difference between metabolic potential and RMR – based on this data, the optimal temperature for *C. houstonensis* would be ~28°C, which, as expected, is lower than the optimal enzymatic temperature (31.6°C, see Table 4).

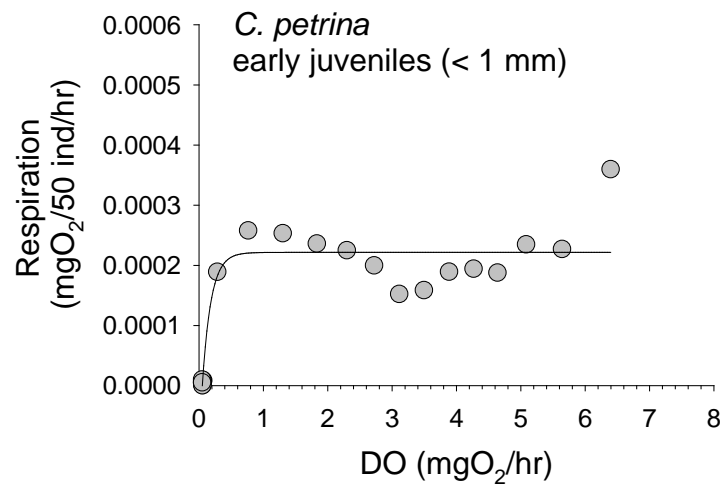


Figure 22. Relationship between respiration rate (per 50 individuals) and dissolved oxygen concentration for early juvenile *C. petrina* (3 parameter exponential rise; $R^2 = 0.8692$; $P < 0.0001$)

L. cardium juveniles

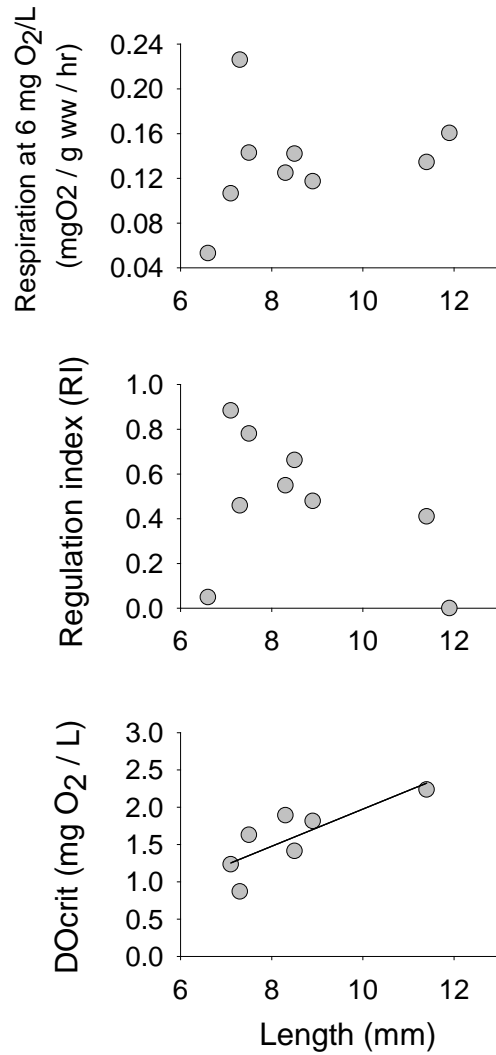


Figure 23. Relationship between respiration rate at 6 mg O₂/L and shell length for *L. cardium* juveniles. Linear regression between DOcrit and shell length was significant ($R^2 = 0.65$, $P = 0.03$).

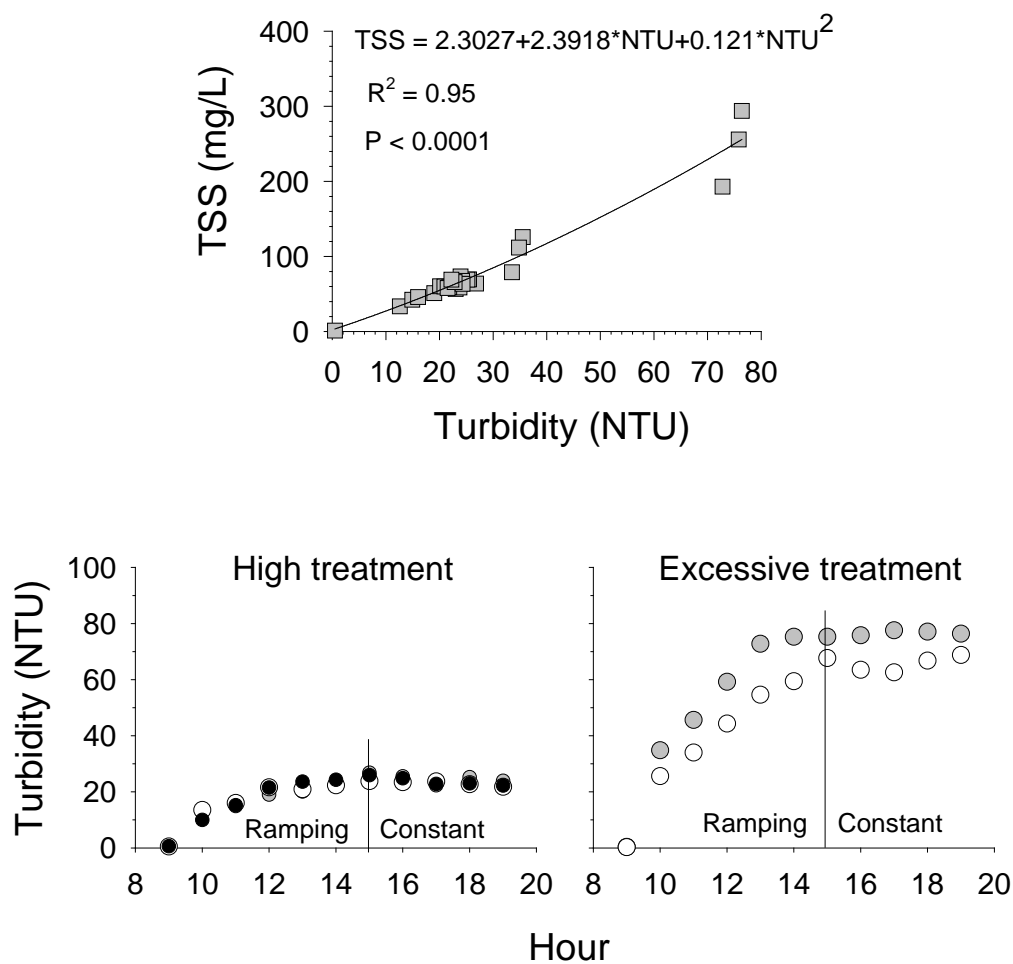


Figure 24. Top panel: Predictive relationship between turbidity (NTU) and total suspended solids (TSS mg/L). Bottom panel: Changes in turbidity through time in the High and Excessive turbidity treatments. Solid vertical line indicates the break between the ramping turbidity and the constant turbidity periods.

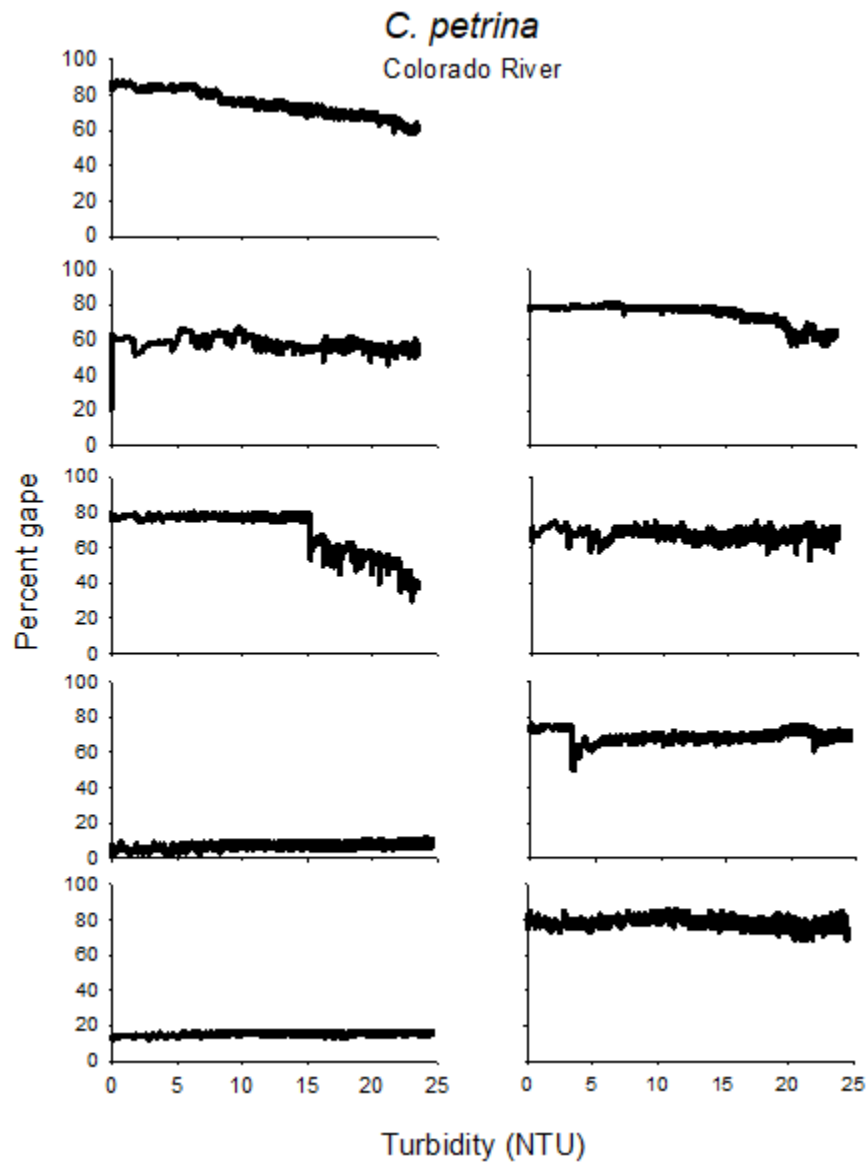


Figure 25. Percent gape for *C. petrina* from the Colorado River as turbidity increased over a ~6-hr period to a maximum of ~25 NTU. Each graph represents a unique individual.

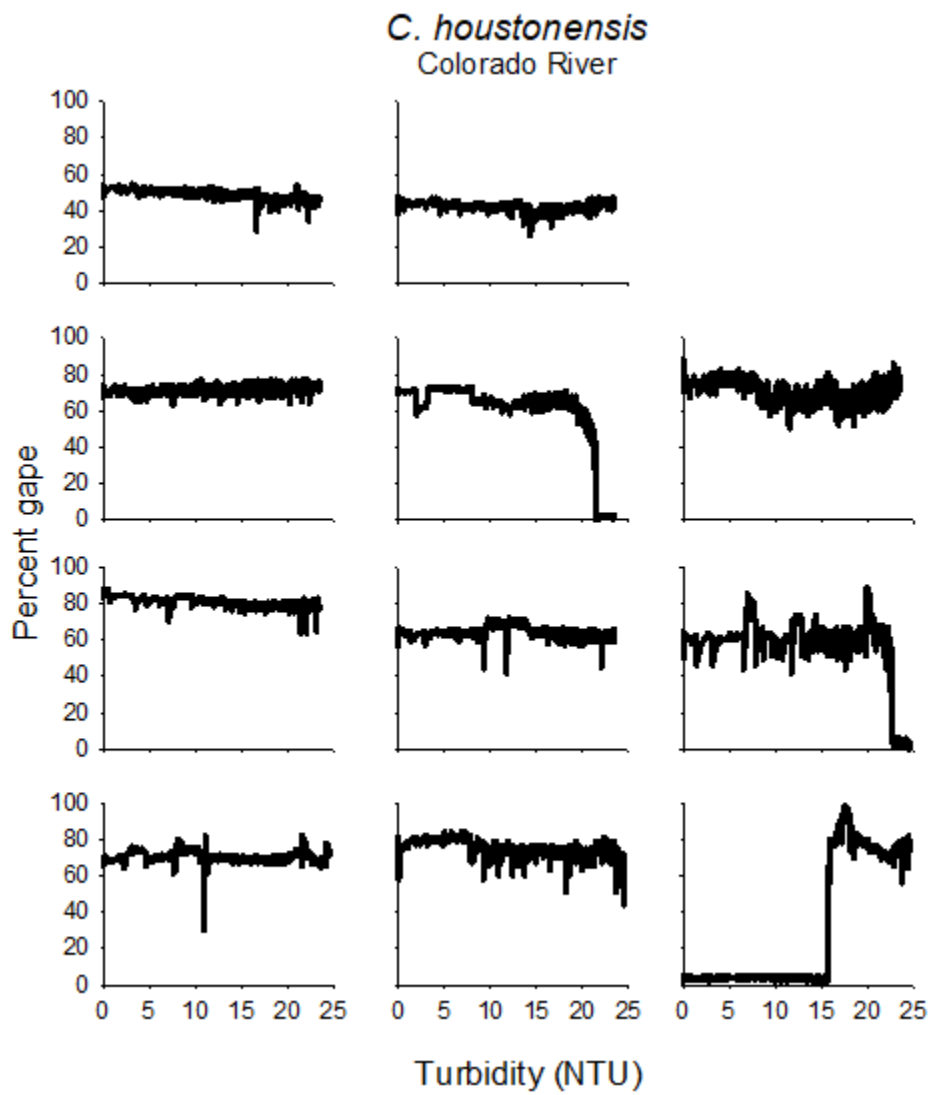


Figure 26. Percent gape for *C. houstonensis* from the Colorado River as turbidity increased over a ~6-hr period to a maximum of ~25 NTU. Each graph represents a unique individual.

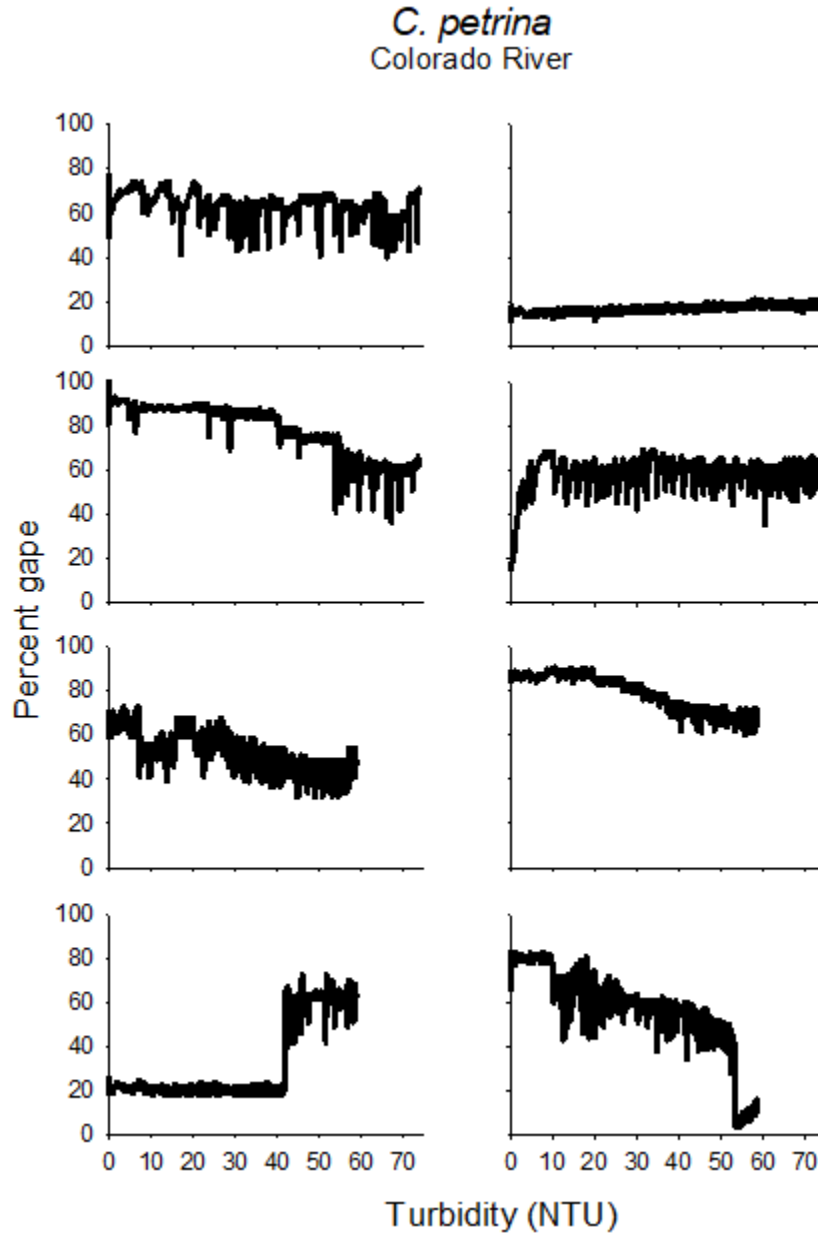


Figure 27. Percent gape for *C. petrina* from the Colorado River as turbidity increased over a ~6-hr period to a maximum of 60-75 NTU. Each graph represents a unique individual.

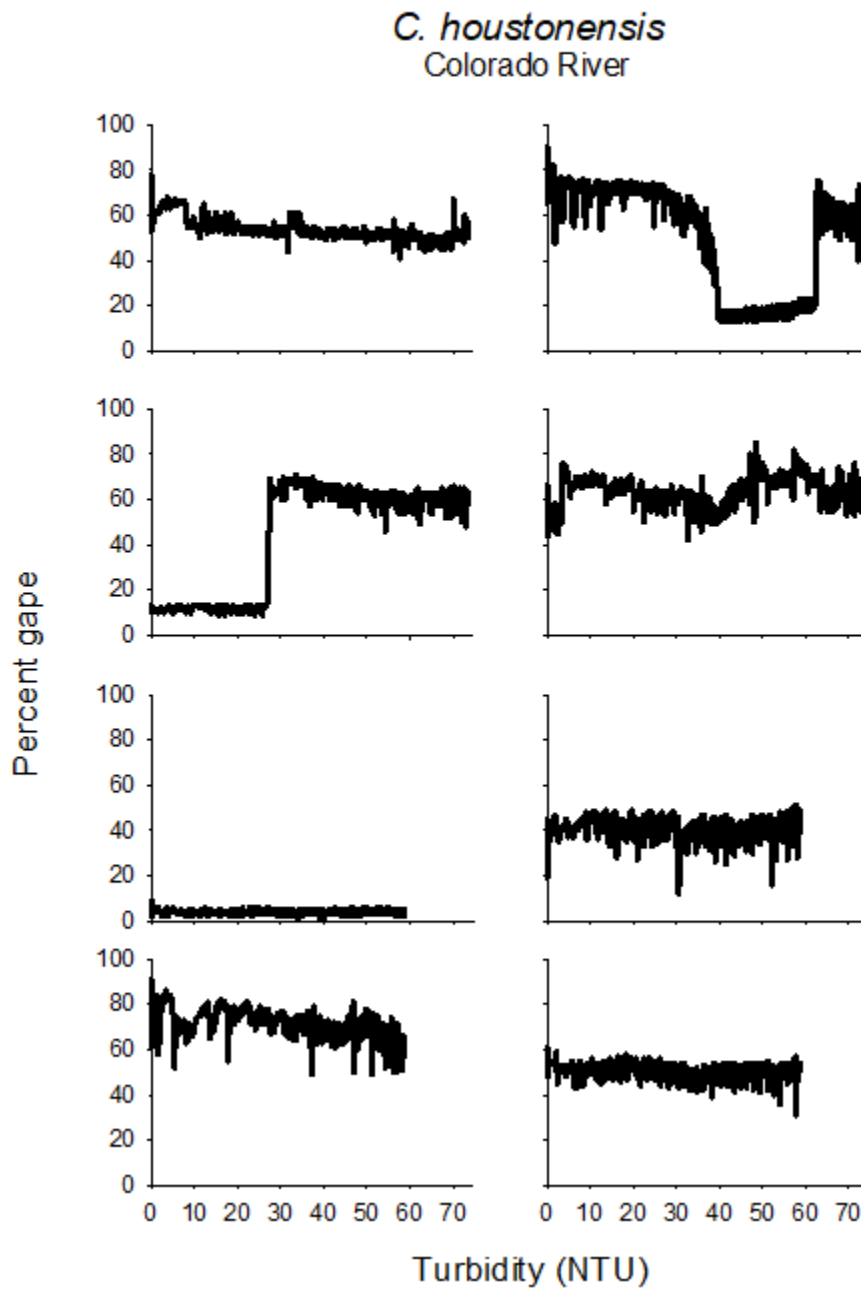


Figure 28. Mean percent gape for *C. houstonensis* from the Colorado River as turbidity increased over a ~6-hr period to a maximum of 60-75 NTU. Each graph represents a unique individual.

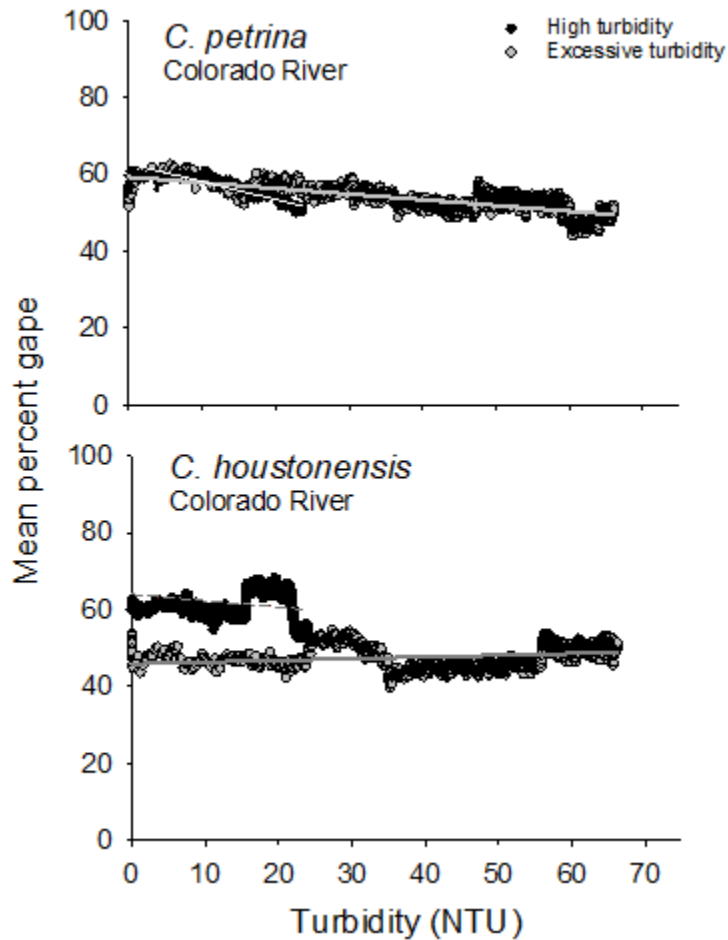


Figure 29. Mean percent gape for all individuals within each species as turbidity increased over a ~6-hr period to a high (25 NTU) or excessive (60-75 NTU) turbidity level. Solid grey lines represent linear regressions through the excessive turbidity dataset. Solid white line and dashed grey line represent linear regressions through the high turbidity datasets for top and bottom panels respectively.

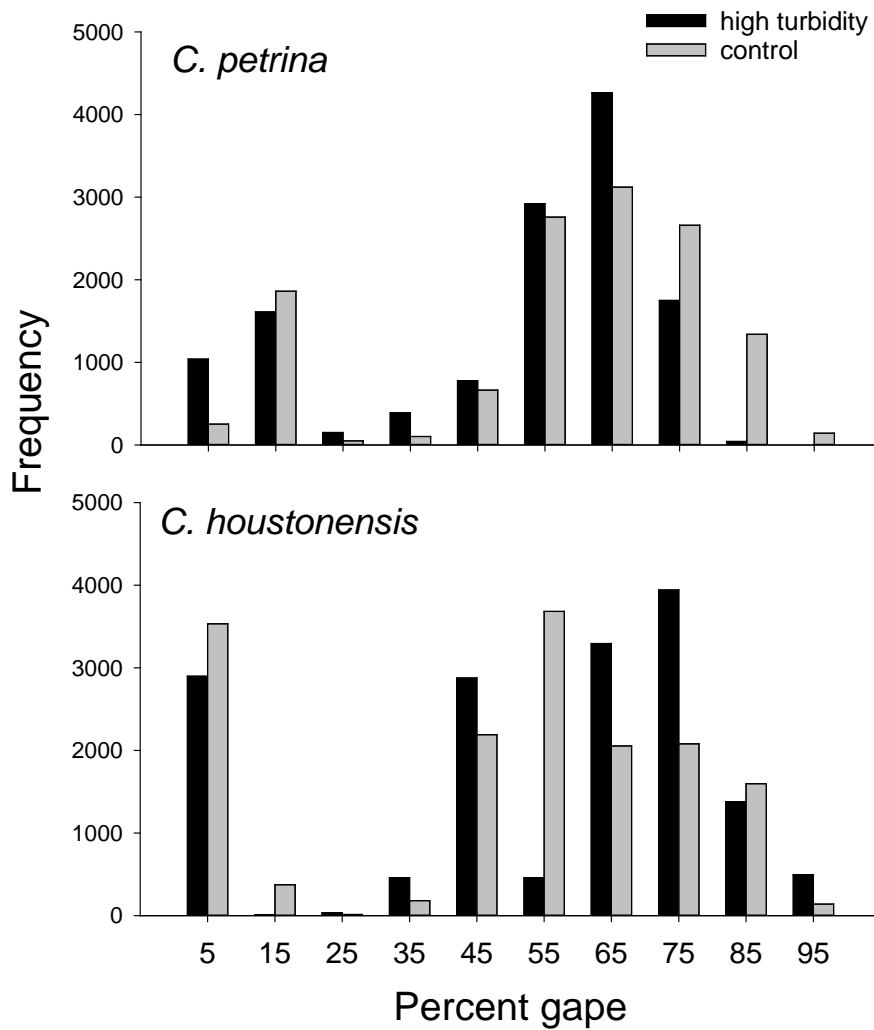


Figure 30. Frequency (# of occurrences) of a range of percent gape measurements for mussels during an initial, pre-exposure period (control: < 1 NTU) and subsequent constant turbidity period (treatment: High ~25 NTU). Only data from the same time frame (15:00 – 19:00 h) were compared between control and constant periods.

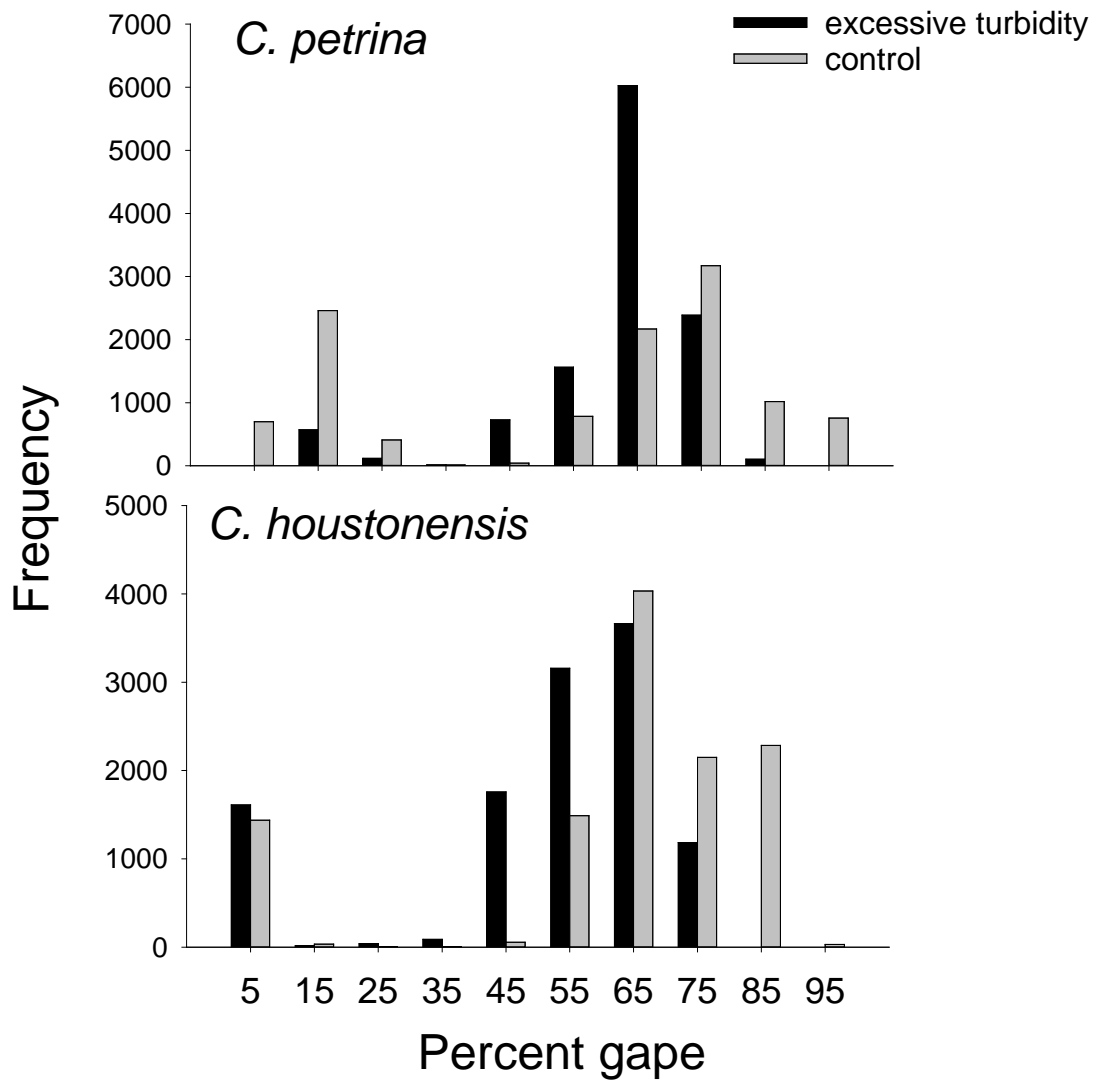


Figure 31. Frequency (# of occurrences) of a range of percent gape measurements for mussels during an initial, pre-exposure, control period (< 1 NTU) and subsequent constant turbidity period (Treatment: excessive 60-75 NTU). Only data from the same time frame (15:00 – 19:00 hrs) were compared between control and constant periods.

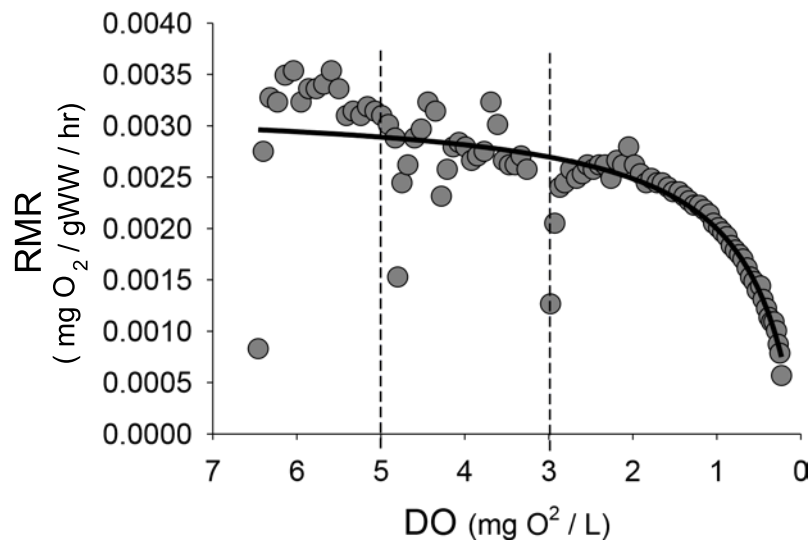


Figure 32. Typical pattern of RMR changing with declining DO when using periodic flushes to prevent excreted ammonia from accumulating in chambers. Dotted lines show when flushing occurred.

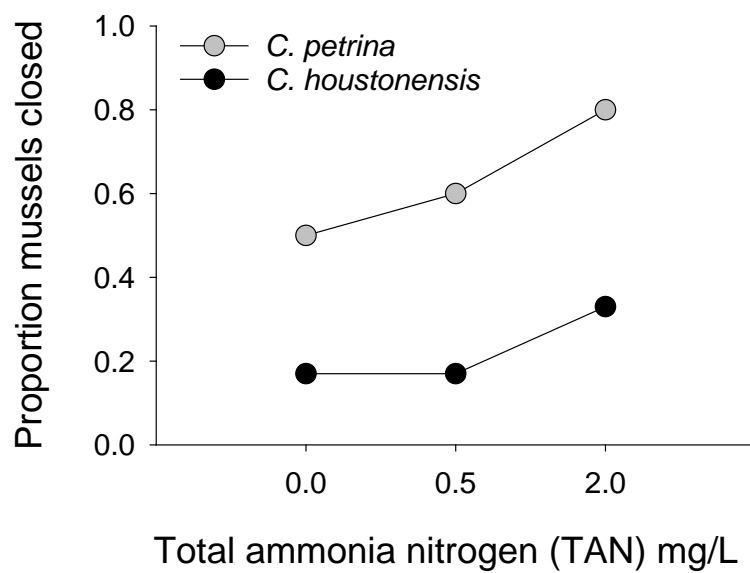


Figure 33. Proportion of mussels that exhibited at least one valve closure during respirometry at each of three TAN concentrations.

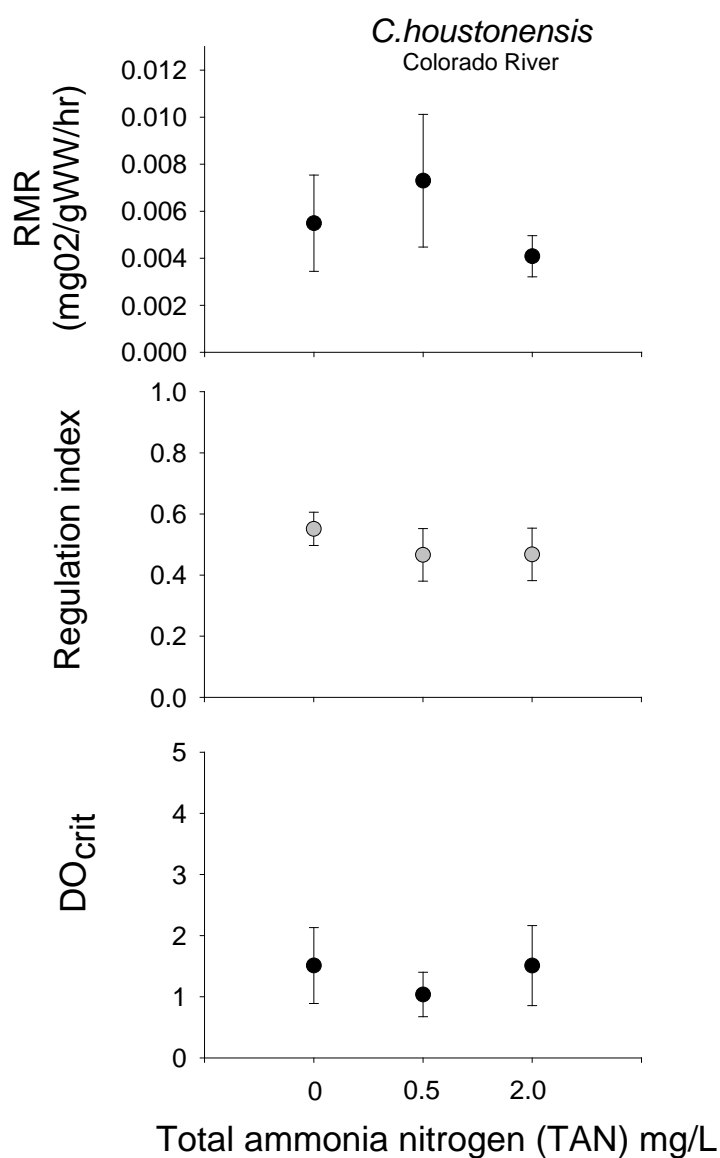


Figure 34. Mean resting metabolic rate (RMR), regulation index, and critical oxygen concentration (DO_{crit}) at three total ammonia nitrogen (TAN) concentrations. No significant differences in any response variable was found among different TAN concentrations.

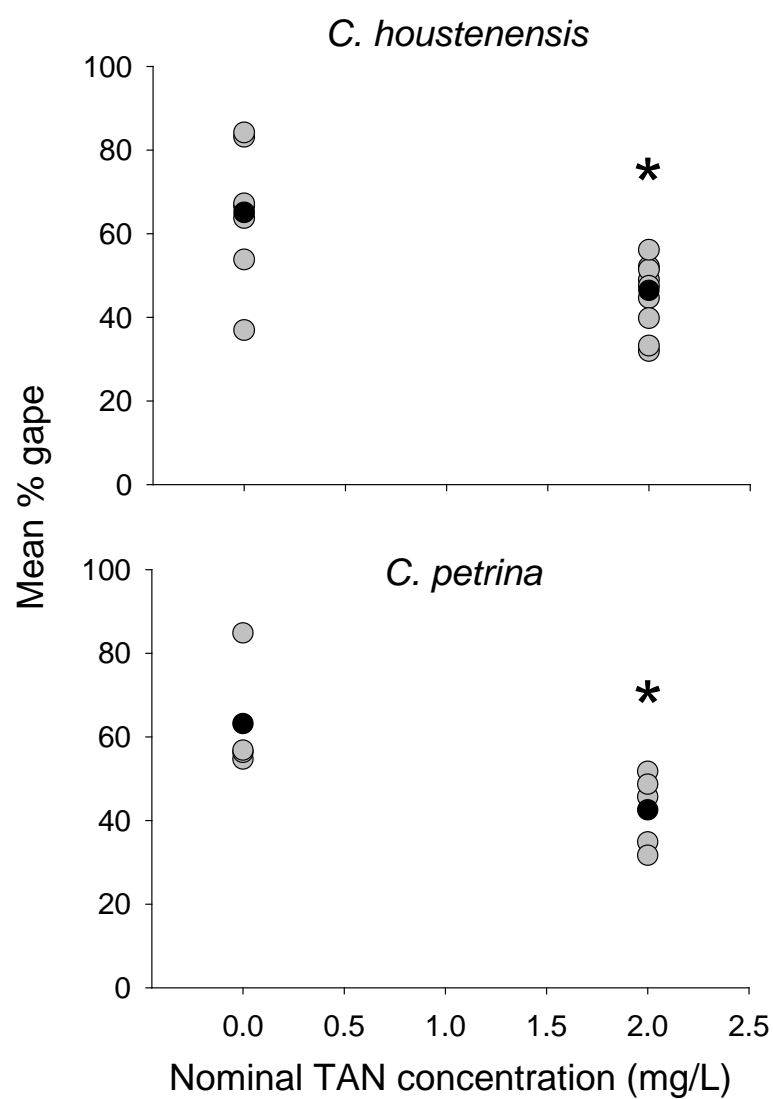


Figure 35. Mean percent gape of *C. houstonensis* and *C. petrina* during 48 hr exposure to 0.0 and 2.0 mg TAN/L. Grey circles indicate mean % gape of individual mussels. Black circles indicate mean % gape of all mussels within that group. Asterix indicates significant difference between control and treatment

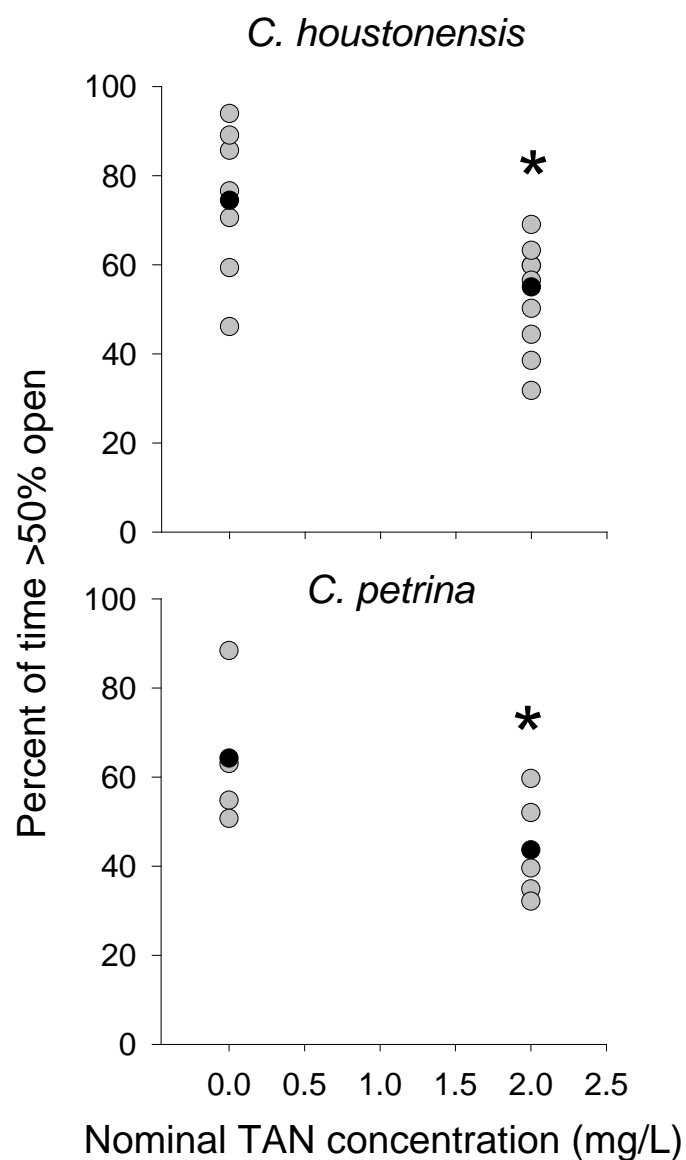


Figure 36. Percent of time mussel gape was >50% under control (0.0 mg TAN/L) and exposed (2.0 mg TAN/L) conditions over 48 hrs. Grey circles indicate percent time for individual mussels. Black circles indicate mean percent time of all mussels within that group. Asterix indicates significant difference between control and treatment.

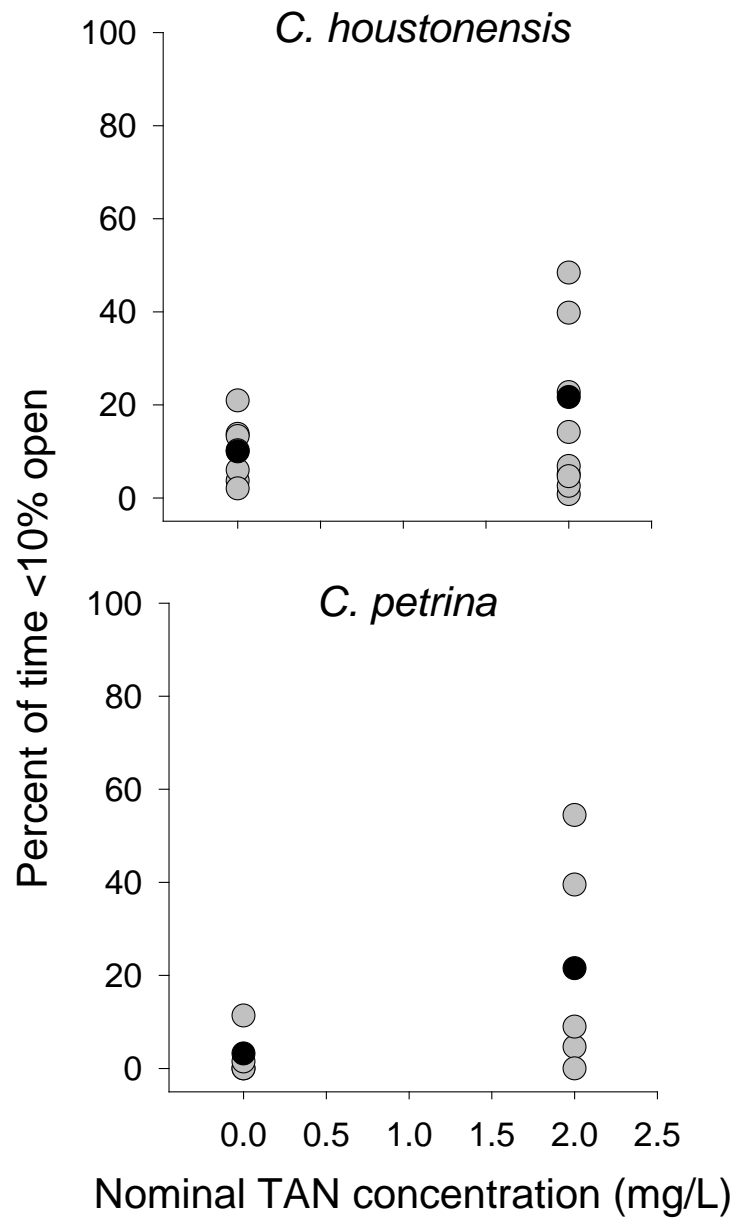


Figure 37. Percent of time mussel gape was less than 10% under control (0.0 mg TAN/L) and exposed (2.0 mg TAN/L) conditions over 48 hrs. Grey circles indicate percent time for individual mussels. Black circles indicate mean percent time of all mussels within that group. There was no significant difference between control and treatment for either species.

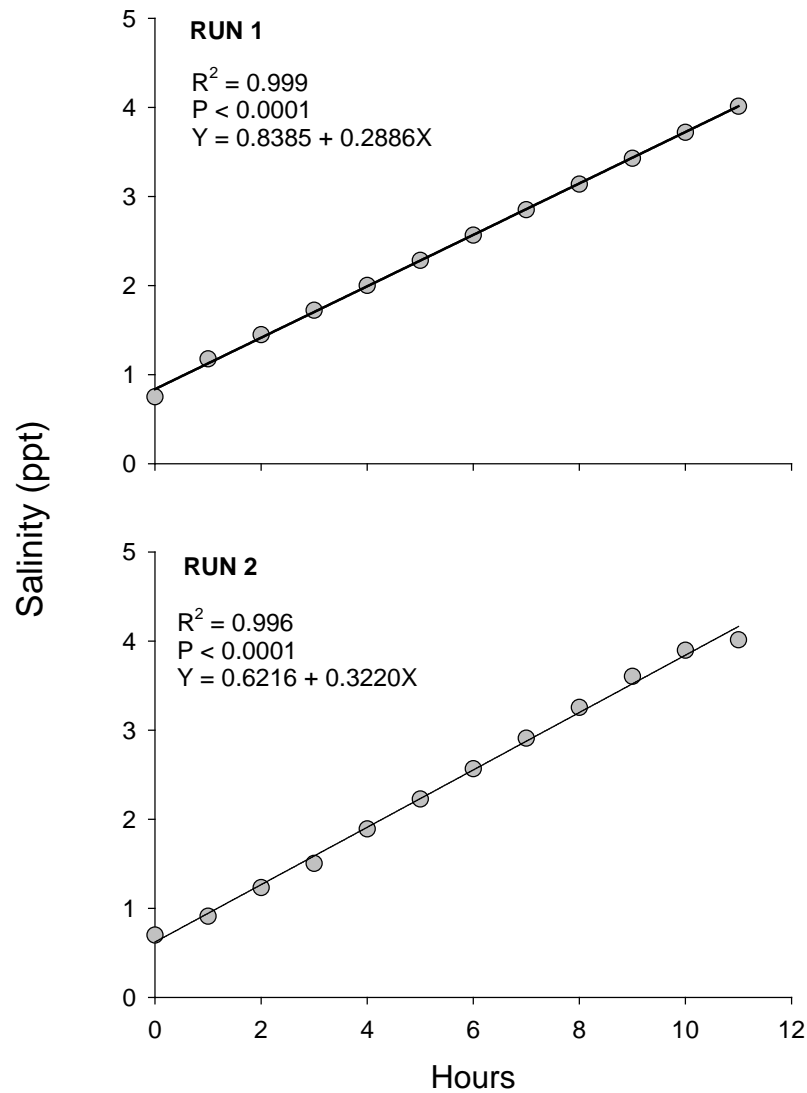


Figure 38. Increase in salinity over time for runs 1,2 of salinity experiments for *C. petrina* and *C. houstonensis* as an example of the rate of increase of salinity over time and the replicability of salinity application among runs.

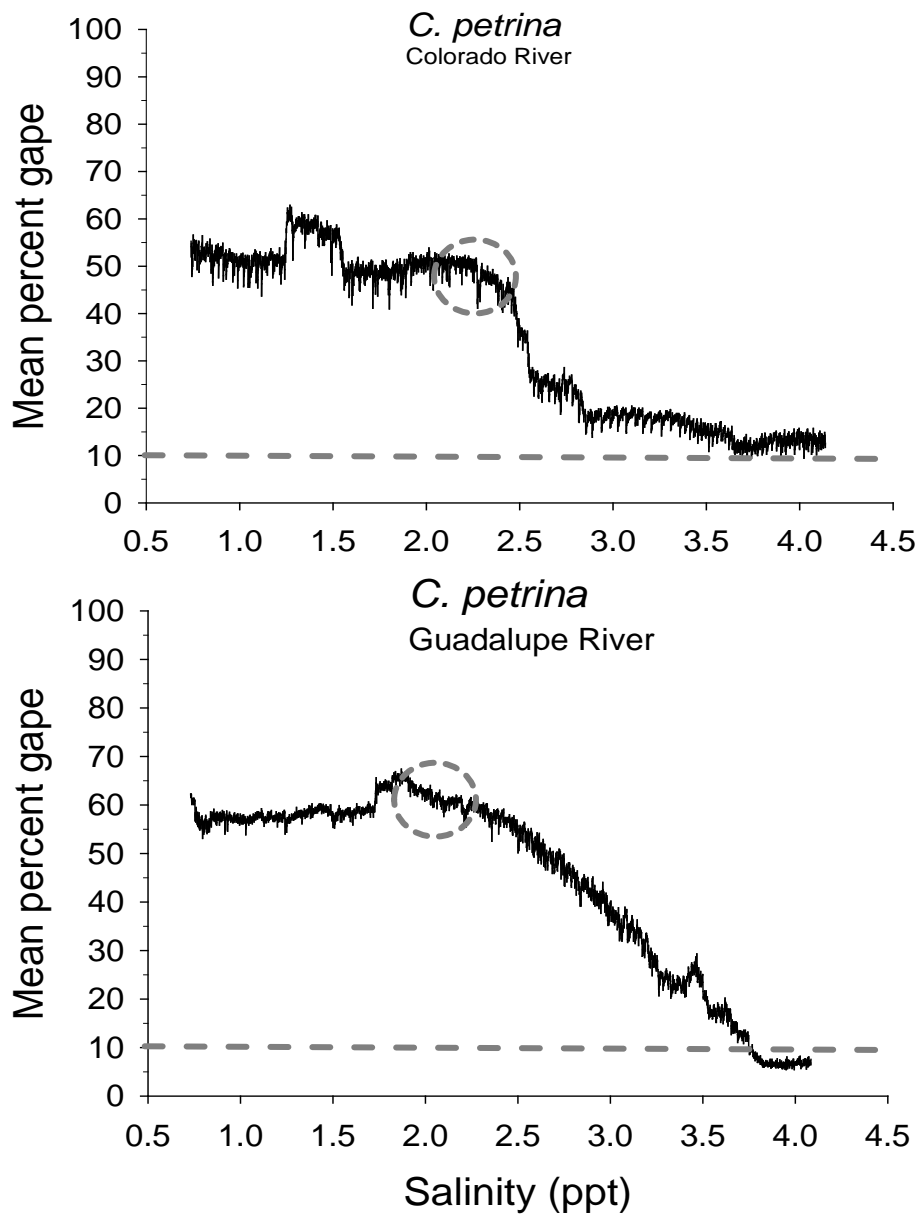


Figure 39. Change in percent gape with increasing salinity for *C. petrina* collected from the Colorado and Guadalupe Rivers. Dotted line represents the threshold for valve closure ($\leq 10\%$ gape). Dotted circle indicates the approximate salinity where percent gape begins to decrease.

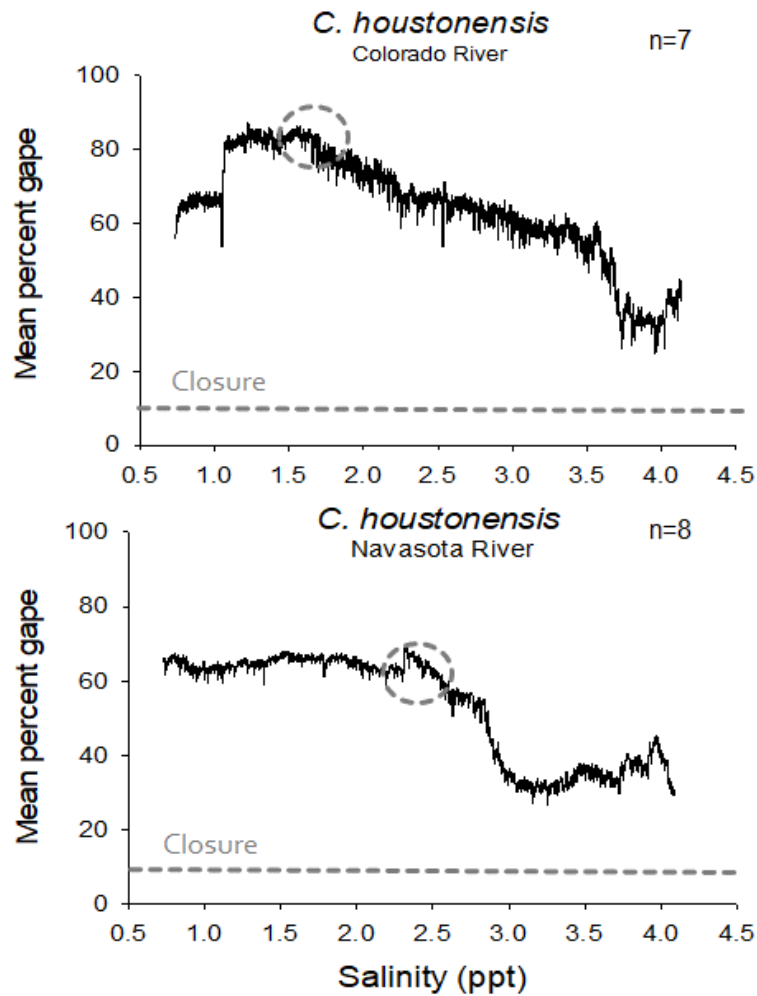


Figure 40. Change in percent gape with increasing salinity for *C. houstonensis* collected from the Colorado and Navasota Rivers. Dotted line represents the threshold for valve closure ($\leq 10\%$ gape). Dotted circle indicates the approximate salinity where percent gape begins to decrease.

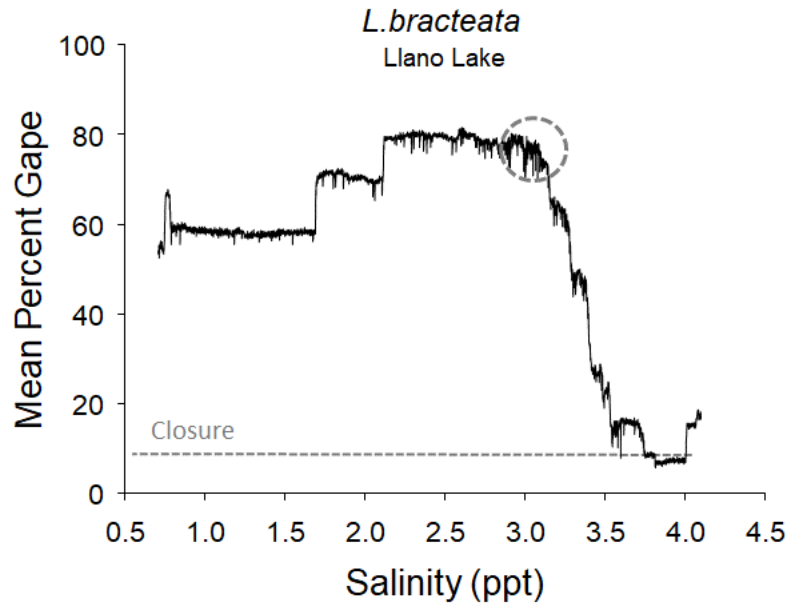


Figure 41. Change in percent gape with increasing salinity for *L. bracteata* collected from Llano Lake. Dotted line represents the threshold for valve closure ($\leq 10\%$ gape). Dotted circle indicates the approximate salinity where percent gape begins to decrease.

Task 2.4: Desiccation Tolerances and Behavioral Responses to Dewatering of Central Texas Endemic Mussels

Contributing authors: Joshua Abel, Jennifer Morton, Randy Gibson, Kenneth Ostrand

Addresses:

U.S. Fish and Wildlife Service, San Marcos Aquatic Resources Center, 500 E. McCarty Lane, San Marcos TX 78666.

Principal Investigators: Kenneth Ostrand

Email: Kenneth.Ostrand@fws.gov

During 2017, SMARC conducted desiccation studies on Texas fatmucket, *L. bracteata*, Smooth pimpleback, *C. houstonensis*, and Texas pimpleback, *C. petrina* and dewatering trials for Texas fatmucket and Texas pimpleback. During 2018, no trials were run for Texas fawnsfoot, *P. macrodon*, or false spike *F. mitchelli* due to unsuitable numbers of these rare species encountered during surveys. Surveys for adequate numbers are ongoing to complete the task.

Task 2.5. Stable isotope analysis to determine relative mussel food sources

Contributing authors: Brian Helms, Kaelyn Fogelman, Jim Stoeckel

Addresses: Department of Biological & Environmental Science, Troy University
Troy, AL 36082 (BH)

School of Fisheries, Aquaculture, and Aquatic Sciences, Auburn University, Auburn, AL 36804
(KF, JS)

Principal Investigators: Brian Helms, Jim Stoeckel

Email: helmsb@troy.edu, kjf0021@tigermail.auburn.edu, jimstoeckel@auburn.edu,

Mussels have long been considered to be suspension feeders (i.e., feeding on material suspended in the water column), with a diet comprised of phytoplankton, protozoans, detritus, bacteria, and dissolved organic carbon (Strayer et al. 2008). Suspended particulate organic matter (SPOM) in aquatic systems is a composite matrix, and previous studies using biochemical markers such as stable isotope and fatty acid analysis have elucidated prevalent components of SPOM that mussels use for food. Particularly, bacteria (Nichols & Garling 2000; Christian & Smith 2004), algae and phytoplankton (Weber et al. 2017; Raikow and Hamilton 2001) have been identified as important contributors to the freshwater mussel diet. While individual components of the mussel diet have become clearer, what they are actually assimilating from their food resources is poorly understood. Although mussels are largely considered suspension feeders, burrowing habits and associated pedal feeding (sweeping of ciliated foot through sediments) allow access to benthic food sources such as sediment-based organisms, detritus, and associated biofilms (Yeager et al. 1994; Nichols et al. 2005; Raikow and Hamilton 2001). While evidence shows that juveniles can consume benthic organic matter (Yeager et al. 1994; Haag 2012), the extent to which adult mussels utilize non-suspended food sources through pedal feeding is not fully understood.

A highly efficient method of determining mussel feeding relationships is stable isotope analysis, which compares the heavy-to-light isotopic elemental ratios of consumers to those of their potential food sources. This approach is effective in inferring both ultimate energy sources and trophic position in organisms and can help elucidate the relative assimilation of suspended or benthic food sources (Cabana and Rasmussen 1996; Raikow and Hamilton 2001; Post 2002; Christian et al. 2004; Vuorio et al. 2007; Vaughn et al. 2008; Weber et al. 2017).. Although ^{13}C of many primary producers vary, the stable C isotope ratios of consumers are similar to that of their food, reflecting the ultimate carbon source (DeNiro and Epstein 1978). However, the N pools of animals are enriched with ^{15}N relative to their food and this enrichment is on average $+3.4\text{‰}$, i.e. 3.4‰ difference in trophic levels (Deniro and Epstein 1981, Minagawa and Wada 1984). Thus ultimate energy source is estimated through carbon stable isotope ratios ($^{13}\text{C}/^{12}\text{C}$, or $\delta^{13}\text{C}$) and trophic position is estimated through nitrogen stable isotope signatures ($^{15}\text{N}/^{14}\text{N}$, or $\delta^{15}\text{N}$) (Cabana & Rasmussen 1996; Vuorio et al. 2008; Newton et al. 2013). Sulfur ($^{34}\text{S}/^{32}\text{S}$) stable isotope ratios have also been useful in marine bivalve food web studies, and can potentially separate producers when stable C and N cannot (Connolly et al. 2004). Analysis of the stable isotope signatures of potential food resources for freshwater mussels in an aquatic system, including suspended organic matter, benthic sediment containing detritus, algae, bacteria and fungi mixed with sand, detritus (decaying organic leaf material), and primary producing plants, can ultimately identify the major contributors to the mussel diet in a specific system or season.

Several drivers for population decline of endemic mussels in Texas include habitat loss and destruction through impoundments, sedimentation, dewatering, and pollution (Howells et al. 1996; Randklev et al. 2013a; Randklev et al. 2013b). The status of three Texas endemics, *Cyclonaias petrina*, *Cyclonaias houstonensis* and *Lampsilis bracteata* is currently being assessed to identify conservation needs and inform management efforts. Incomplete knowledge of mussel

food resources can inhibit successful conservation and a better understanding of mussel feeding relationships and requirements can help elucidate causes of their imperilment and inform management efforts such as propagation and relocation. Thus the objectives of this study are to 1) determine the potential food resources of focal taxa through stable isotope analysis and, 2) assess spatial and temporal variations in feeding.

Methodology

Study Sites

Study sites were chosen from previously identified sites containing beds of target mussel species (*C. houstonensis*, *C. petrina* and *L. bracteata*). Sites in the Colorado River watershed were located on the lower Colorado (LC; 29.556197N, -96.402160W) near Altair, Texas and on the Llano River, a tributary of the middle Colorado River (MC; 30.39267N, -99.19214W), located near Mason, Texas. The Guadalupe River drainage was sampled on the upper Guadalupe (UG; 29.93953N, -98.94846W) in Comfort, Texas and the Brazos River was sampled on the Navasota River, a tributary of the Lower Brazos (LB, 31.15155N, -96.19501W), near Easterly, Texas.

Mussel Sampling

Each mussel species (and its respective potential food resources) was sampled from two different basins each in spring (April 2017), summer (July 2017) and fall (October 2017). *C. petrina* was sampled in the lower Colorado and upper Guadalupe Rivers, *C. houstonensis* was sampled in the lower Colorado and Navasota Rivers and *L. bracteata* was sampled in the upper Guadalupe and Llano Rivers. Ten individuals were collected per species at the site by snorkeling and searching benthic sediments by hand. Individual mussels were collected and measured for length, width, height and

weight. Mussels were opened using reverse action pliers and two sublethal tissue samples were taken from the foot using a 1.5 x 4.5 mm biopsy punch (Karl Storz 453733) (Fritts et al. 2015). Mussels were subsequently returned to the streambed where they were collected. Tissue samples were transported on ice from the field and subsequently frozen and transported to Auburn University. Tissue samples were dried at 80°C to a constant mass, ground using a mortar and pestle, weighed (nearest 10⁻⁵ g) and placed in 4 x 6 mm tin capsules and sent to Washington State University (WSU) Stable Isotope Core Laboratory for $\delta^{13}\text{C}$, $\delta^{15}\text{N}$, and $\delta^{34}\text{S}$ stable isotope analysis (see below).

Potential Food Source Sampling

Hypothesized food sources were suspended particulate organic matter (SPOM), fine particulate organic matter associated with benthic sediments (FPOM), and coarse particulate organic matter (CPOM). These sources were collected in spring (April 2017, May 2018), summer (July 2017) and fall (October 2017) at all four sites. To isolate the particulate organic matter (primarily phytoplankton and detritus) in the water column that mussels could utilize as a food source, 1-2 L of sample water was passed through 55 μm mesh to remove larger particles, as mussels utilize items <55 μm for food (Newton et al. 2013). The filtered water was then filtered again through a precombusted 47 cm Whatman GF/F filter (nominal pore size = 0.7 μm) using vacuum filtration. This procedure isolates suspended solids between 55 and 0.7 μm , which reflects the size fraction of identified potential food sources for mussels (Christian et al. 2004; Post 2002; Newton et al. 2013). Filters were then frozen for transportation back to Auburn University where they were dried at 80°C to a constant mass. The filters were fumigated in 3N H₃PO₄ for 8 hours to remove carbonates (Harris et al. 2000). Whole filters were sent to WSU Stable Isotope Core for analysis of stable C, N and S (see below).

Ten mid-channel benthic sediment samples for FPOM (which includes detritus, algae, bacteria and fungi mixed with sand) were collected in spring and summer in the same habitats where mussels were collected to reflect the available food resources mussels could access through pedal feeding. Five mid-channel, five bank and five bedrock surface sediment samples were taken from each site during fall sampling to further differentiate between benthic food sources being utilized. Sediment FPOM samples were prefiltered through an 80 and 55 μm sieve to remove gravel and debris larger than the previously established size fraction for potential mussel food resources. Samples were filtered through Whatman GF/F filters using vacuum filtration, frozen and transported to Auburn University as above with the SPOM filters. Samples were dried to a constant mass at 80°C and the sediment layer was then removed from the filter. Sediment was fumigated in 3N H_3PO_4 for 8 hours to remove carbonates and was then ground to a fine powder using a mortar and pestle, weighed (nearest 10^{-5} g) and encapsulated in 4 x 6 mm tin capsules and sent to WSU Stable Isotope Core for analysis of $\delta^{13}\text{C}$, $\delta^{15}\text{N}$, and $\delta^{34}\text{S}$ (see below).

Coarse particulate organic matter (CPOM, a mixture of decaying terrestrial leaf litter and organic aquatic material, i.e. “detritus”) was collected from each site seasonally. Previous studies confirm that mussels produce the necessary enzymes to digest detrital food resources (Christian et al. 2004; Newton et al. 2013), and CPOM may be an important carbon source for bacteria production (Besemer et al. 2009). Additionally, filamentous algae and representative emergent (*Justicia*), submerged (*Myriophyllum*, *Alternanthera* and *Elodea*), and riparian (“grass”) vascular plants were collected when present as further potential basal food resources and to provide primary producer context. Vascular algae and vascular plant samples were identified and separated in the field and all samples were frozen for transportation to Auburn University. Additionally, the microbial biofilm associated with detritus was sampled in fall 2017 from the Middle Colorado and Lower Brazos sites. In spring 2018 periphyton, epiphyton and biofilm associated with detritus was sampled. After removing the biofilm from

the associated substrate, the samples were filtered through Whatman GF/F filters using vacuum filtration. Samples were dried at 80°C to a constant dry mass, ground to a fine powder using a mortar and pestle, weighed (nearest 10⁻⁵ g) and placed in 4 x 6 mm tin capsules and sent for analysis of stable $\delta^{13}\text{C}$, $\delta^{15}\text{N}$, and $\delta^{34}\text{S}$. Water temperature, conductivity and pH were measured and discharge from the nearest USGS gauge was recorded at the time of sample collection for each site to inform any potential patterns identified in feeding ecology.

Stable Isotope Analysis

Stable carbon, nitrogen and sulfur isotopic analyses were conducted at Washington State University Stable Isotope Core Laboratory. Samples for carbon and nitrogen isotopic analysis are converted to N₂ and CO₂ with an elemental analyzer (ECS 4010, Costech Analytical) and the two gases are separated with a 3m GC column and analyzed with a continuous flow isotope ratio mass spectrometer (Delta PlusXP, Thermofinnigan, Bremen). Isotopic reference materials are interspersed with samples for calibration. Isotope ratios are reported in parts per thousand (‰) relative to standards (Vienna Peedee belemnite (VPDB) for carbon, atmospheric N for nitrogen and Vienna-Canyon Diablo Troilite (VCDT) for sulfur), defined in delta notation as:

$$\delta^{13}\text{C} \text{ or } \delta^{15}\text{N} \text{ or } \delta^{34}\text{S} = (R_{\text{sample}} / R_{\text{standard}} - 1) \times 10^3$$

where $R = {}^{13}\text{C} / {}^{12}\text{C}$ or ${}^{15}\text{N} / {}^{14}\text{N}$ or ${}^{34}\text{S} / {}^{32}\text{S}$ (Craig 1957, Jepsen and Winemiller 2002).

Statistical Analysis

Size data for species collected were averaged across all three seasons and compared across basins (Tables 1-3). Mean (\bar{X}) and standard deviation (σ) were calculated for each species across all seasons. Two-tailed t -tests were performed to compare length, width, height and length

of species across basins. $\delta^{13}\text{C}$ and $\delta^{15}\text{N}$ data was averaged for each species for all seasons across basins and a two-tailed t -test was performed to determine within species variation between seasons. We compared mussel length and stable isotope ratios with Pearson Product-Moment correlations.

To estimate feeding patterns, data initially were visually inspected using biplots. We then applied linear mixing models (IsoSource, Phillips and Greg 2003) to model the contribution of potential source materials to mussels. Since isotopic ratios of baseline resources are often different across systems, we analyzed each basin independently. We only used potential sources that were represented across all basins in IsoSource models for comparative purposes. These sources were SPOM, CPOM, FPOM and biofilm. Due to difficulties in the laboratory analysis of $\delta^{34}\text{S}$ and as a conservative measure, we constrained modeling to $\delta^{13}\text{C}$ for this report. Thus a 3 or 4 source single-isotope model was run for each mussel species for each site with a source increment set at 1% and tolerance initially set at 0.1‰ and increased incrementally (up to 2‰) until a solution was obtained. This model effectively assesses the relative contribution of CPOM, SPOM, FPOM, and biofilm to the basal carbon source(s) of mussel diet (i.e., this model may or may not reflect *direct* feeding). Reflecting this approach, and as a conservative measure, we did not correct consumer $\delta^{13}\text{C}$ in these models due to lack of information on the true trophic position of these species.

Results

Mussel Size

C. petrina was significantly larger in length, width, height and weight in the lower Colorado River compared to the upper Guadalupe River with mean length difference of 17.78 mm, width difference of 19.03 mm, height difference of 14.63 mm and weight difference of

70.31 g (two-tailed t -test; $p < 0.001$ for length, $p < 0.001$ for width, $p < 0.001$ for height, $p < 0.001$ for weight) (Table 1).

C. houstonensis was significantly longer and wider in the lower Colorado River compared to the lower Brazos River basin. Mean length difference was 6.12 mm and mean width difference was 5.88 mm (two-tailed t -test; $p = 0.00094$ for length; $p = 0.00034$ for width). There was no difference found in height and weight across basins (two-tailed t -test; $p = 0.79$ for height, $p = 0.16$ for weight) (Table 2).

L. bracteata was significantly larger in length, width, height and weight in the upper Guadalupe compared to the middle Colorado River basin with mean length difference of 5.11 mm, width difference of 2.46 mm, height difference of 1.46 mm and weight difference of 2.77 g (two-tailed t -test; $p = 0.0047$ for length, $p = 0.019$ for width, $p = 0.018$ for height, $p = 0.022$ for weight) (Table 3).

Environmental Sampling

The upper Guadalupe consistently had lower water temperatures, likely due to it being a stenothermal, spring-fed system whereas the other sites are not directly under spring influence. pH had low variability across all sites and seasons. Conductivity and discharge were highest in the lower Colorado River and lowest in the lower Brazos River basin during all seasons sampled (Table 4).

Stable Isotope Analysis

Stable isotope $\delta^{13}\text{C}$ and $\delta^{15}\text{N}$ analysis was completed for mussel foot tissue, SPOM, FPOM, CPOM and primary producing plants for samples collected in spring, summer, and fall 2017. Stable isotope $\delta^{13}\text{C}$ and $\delta^{15}\text{N}$ analysis was completed for SPOM, FPOM, CPOM, and biofilm

samples collected in May 2018 (i.e., no mussels were sampled in May 2018). Laboratory analysis of $\delta^{34}\text{S}$ from all environmental samples was unsuccessful due to low sample volume causing sulfur detachment. Presumably due to the impacts of Hurricane Harvey on the lower Colorado River, only three *C. petrina* and four *C. houstonensis* were located for fall sampling, compared to the standard sampling protocol for this study of 10 individuals per species per site.

Average isotopic signatures (\pm SE) and C:N ratios for all sampled sources and potential resources are presented (Table 5). In general, mussels exhibited $\delta^{15}\text{N}$ enrichment and $\delta^{13}\text{C}$ depletion relative to their respective environments with minimal intraspecific variation in both $\delta^{13}\text{C}$ and $\delta^{15}\text{N}$ (Table 6, Figures 1-4). Despite this, mussel size and $\delta^{13}\text{C}$ were positively correlated for mussels in the Upper Guadalupe and Lower Colorado and $\delta^{15}\text{N}$ and size was positively correlated for *C. houstonensis* in the Upper Guadalupe (Table 7, Figure 5-7). An enrichment of $\delta^{13}\text{C}$ as mussels increase in size may reflect ontogenetic feeding shifts. For the spring, average $\delta^{13}\text{C}$ signatures for mussels ranged from -29.91‰ – -26.63‰ and average $\delta^{15}\text{N}$ ranged from 7.38‰ – 13.41‰ (Table 6). For the summer, average $\delta^{13}\text{C}$ signatures for mussels ranged from -26.45‰ – -28.83‰ and average $\delta^{15}\text{N}$ ranged from 7.28‰ – 13.38‰ (Table 6). Across seasons, mussels were more $\delta^{13}\text{C}$ enriched in the Middle Colorado basin and more $\delta^{15}\text{N}$ enriched in the Lower Colorado (Table 6). Also, where multiple species were sampled at a given site (Upper Guadalupe and Lower Colorado), all mussels had nearly identical isotopic signatures for both $\delta^{13}\text{C}$ and $\delta^{15}\text{N}$ (Table 6, Figure 1 and 2).

We observed seasonal changes in mussel isotopic signature, indicative of potential shifts in feeding and/or assimilation. There were significant changes in $\delta^{13}\text{C}$ signatures of *C. petrina* between spring and summer with a mean enrichment of 0.90 ‰ from spring to summer in the upper Guadalupe (two-tailed *t*-test; *p* = 0.0015) and a mean enrichment of 1.18‰ in the lower

Colorado (two-tailed t -test; $p < 0.001$). *C. houstonensis* also had significant changes of $\delta^{13}\text{C}$ between spring and summer with a mean enrichment of 1.54 ‰ in the lower Colorado (two-tailed t -test; $p = 0.0021$) and a mean enrichment of 0.84 ‰ in the lower Brazos basin (two-tailed t -test; $p = 0.0021$). There were no seasonal differences in $\delta^{13}\text{C}$ of *L. bracteata* in the Upper Guadalupe (two-tailed t -test; $p = 0.58$) or in the middle Colorado basin (two-tailed t -test; $p = 0.35$). There were no seasonal differences in the $\delta^{15}\text{N}$ signatures of any species in any basin (two-tailed t -test; $p > 0.05$).

Linear Mixing Models

Linear mixing models revealed that food resources are comprised primarily of materials with a carbon base of CPOM (i.e., benthic detritus) and attached biofilm, and to a lesser extent SPOM (i.e., seston) and FPOM (i.e., sediment deposits). All mussels and all seasons had high proportions of CPOM contributions, with the exception of *L. bracteata* in the Middle Colorado basin during spring 2017. In general, there was little seasonal variation in dietary contributions of basal C resources, with the exception of *C. houstonensis* in the Lower Brazos basin, which showed a decreased reliance on CPOM in the summer, and *L. bracteata* in the Middle Colorado, which showed a shift from SPOM to CPOM contributions (Table 8, Figure 8). It should be noted that mussel stable isotope ratios remained largely consistent throughout seasons within a given system, but basal resource signatures were often variable between seasons. Thus linear mixing models likely reflect less of a feeding shift in mussels and more of a changing food base offering insight on the timing of assimilation. Also, several models were only attainable after increasing tolerance above reliable levels (up to 2‰). These included *C. petrina* in the Upper Guadalupe during the summer and *L. bracteata* in the Upper Guadalupe in the spring and summer. These

seasonal models should be interpreted with caution. Other models had tolerance levels set at 0.1‰.

For *C. houstonensis*, the mean dietary contribution of CPOM ranged from a low of 36.8% in the Lower Brazos basin during the Fall to 96% in the Lower Colorado basin during the summer (Table 8). FPOM-based and SPOM-based food sources represented slightly higher proportions of total during the summer in the Lower Brazos. Further, biofilms appear to be an important C source during the Fall, representing 36% of dietary contribution (although it should be noted that these sources were not sampled in the spring and summer). In the Lower Colorado, *C. houstonensis* had somewhat higher contributions of SPOM than FPOM in the spring and summer, but this was still <5% on average of total dietary contribution (Table 8, Figure 8). Biofilm was less than 10% total dietary contribution in spring 2018.

For *C. petrina*, the mean dietary contribution of CPOM ranged from a low of 93% during the spring 2018 in the Lower Colorado to 99% in the Upper Guadalupe, in spring 2017 (Table 8). FPOM-based food sources contributed near 1% in the Lower Colorado in all seasons and less than 1% in the Upper Guadalupe in all seasons. In the Lower Colorado, SPOM contributed on average 3 - 4.9% to total *C. petrina* diet and only 1 – 5.5% to total diet in the Upper Guadalupe (Table 8, Figure 8). Biofilm contributed 2.1% in the Lower Colorado and 6.3% in the Upper Guadalupe.

The contribution of CPOM based carbon for *L. bracteata* was more variable than for the other mussel species, with a high of 100% in the Upper Guadalupe in the summer to 2% in the Middle Colorado basin during spring 2017. The contribution of FPOM was similarly low for *L. bracteata* in all seasons and both systems, with averages ranging from 0 in the Upper Guadalupe to 9.9% in the Middle Colorado basin during the fall. The dietary contribution of SPOM based sources ranged from 0 in the Upper Guadalupe in the summer to 97.8% in the Middle Colorado

basin during the spring (Table 8, Figure 8). The dietary contribution of biofilm was 37% during the fall in the Middle Colorado but only 6.9% during spring 2018.

Brief Interpretation

These data reflect samples from spring 2017, summer 2017, fall 2017, and spring 2018 ($\delta^{13}\text{C}$ and $\delta^{15}\text{N}$, no sulfur). Sulfur results were unreliable for interpretation due to the low sulfur background levels in these systems. Several conclusions can be drawn from these data. First, all three species appear to feed similarly. This is evidenced by the consistent stable C and N signatures across systems, and particularly the nearly identical signatures of *L. bracteata* and *C. petrina* in the Upper Guadalupe, and *C. petrina* and *C. houstonensis* in the Lower Colorado. The only deviation from this similarity is *L. bracteata* in the Middle Colorado, which displayed a relatively less-enriched $\delta^{15}\text{N}$ pattern. This characterization was from the Llano River, and whether this reflects differential feeding or simply is a system artifact is unclear at this point. Also, all three species showed a general trend to become carbon-enriched with increasing body size. This could reflect the inherent shift in diet from the parasitic glochidial stage thru adulthood. However, these trends were found in mussels in the Upper Guadalupe and Lower Colorado, but not the Middle Colorado basin and Lower Brazos basin, so that, again, is a system artifact cannot be ruled.

From the data presented, with the exception of *L. bracteata* in the Middle Colorado basin during the summer, a major interpretation is that a majority of the carbon assimilated by all species is derived from CPOM. Whether this is direct feeding on CPOM particles or associated bacteria and fungi is not clear. The contribution of biofilms, which is typically low but can be as high as 1/3 dietary carbon, as well as the generally elevated $\delta^{15}\text{N}$ signature of mussels, further suggests a significant role of bacteria and fungi in assimilated tissue. Further, the role of SPOM

(i.e, suspended producers and other associated organics) and FPOM (benthic diatoms, algae, and organic matter associated with sediment) seem to play a much more minor role in contribution to dietary C as compared to CPOM and biofilm. This could be interpreted as a reduced dietary reliance on filter-feeding phytoplankton and pedal feeding in sediments. However, it should be noted that mussels in general showed minimal (albeit statistically significant) seasonal variation, while food sources often showed considerable variation. Although it cannot be ruled out that we failed to fully capture the true C sources for mussel food, our data indicates these species assimilate food resources that are produced seasonally and that generally are derived from a carbon source corresponding to CPOM.

References

- Besemer, K, I Hodl, G Singer, and TJ Battin. 2009. Architectural differentiation reflects bacterial community structure in stream biofilms. *The ISME Journal* 3: 1318-1324
- Cabana, G, and JB Rasmussen. 1996. Comparison of aquatic food chains using nitrogen isotopes. *Proceedings of the National Academy of Science*. 93: 10844-10847.
- Christian, AD, BN Smith, DJ Berg, JC Smoot, and RH Findlay. 2004. Trophic position and potential food sources of 2 species of unionid bivalves (Mollusca:Unionidae) in 2 small Ohio streams. *Journal of the North American Benthological Society*. 23(1): 101-113.
- Craig, H. 1957. Isotopic Standards for Carbon and Oxygen and Correction Factors for MassSpectrometric Analysis of Carbon Dioxide. *Geochimica et Cosmochimica Acta*. 12: 133-149.
- Connolly, RM, MA Guest, AJ Melville, and JM Oakes. 2004. Sulfur stable isotopes separate producers in marine food-web analysis. *Oecologia*. 138(2): 161-167.
- DeNiro, MJ, and S Epstein. 1978. Influence of diet on the distribution of carbon isotopes in animals. *Geochimica et Cosmochimica Acta*. 42: 495-506.
- Deniro, MJ, and S Epstein. 1981. Influence of diet on the distribution of nitrogen isotopes in animals. *Geochimica et Cosmochimica Acta*. 45: 341-351.
- Fritts, AK, JT Peterson, PD Hazelton, and RB Bringolf. 2015. Evaluation of methods for assessing physiological biomarkers of stress in freshwater mussels. *Canadian Journal of Fisheries and Aquatic Sciences*. 72(10): 1450-1459.
- Gangloff, MM, and JW Feminella. 2007. Stream channel geomorphology influences mussel abundance in southern Appalachian streams, USA. *Freshwater Biology*. 52: 64-74.
- Haag, WR. 2012. *North American Freshwater Mussels*. New York, NY: Cambridge University Press.

- Harris, D, RH Williams, and C van Kessel. 2000. Acid fumigation of soils to remove carbonates prior to total organic carbon or CARBON-13 isotopic analysis. *Soil Science of America Journal*. 65(6): 1853-1856.
- Howard, JK, and KM Cuffey. 2006. The functional role of native freshwater mussels in the fluvial benthic environment. *Freshwater Biology*. 51: 460-474.
- Howells, RG, RW Neck, and HD Murray. 1996. *Freshwater mussels of Texas*. Austin, TX: Texas Parks and Wildlife Press.
- Jepsen, DB, and KO Winemiller. 2002. Structure of tropical river food webs revealed by stable isotope ratios. *Oikos*. 96: 46-55.
- Minagawa, M, and E Wada. 1984. Stepwise enrichment of ^{15}N along food chains: Further evidence and the relation between $\delta^{15}\text{N}$ and animal age. *Geochimica et Cosmochimica Acta*. 48: 1135-1140.
- Nichols, SJ, and D Garling. 2000. Food-web dynamics and trophic-level interactions in a multi-species community of freshwater unionids. *Canadian Journal of Zoology*. 78: 871-882.
- Nichols, SJ, H Silverman, TH Dietz, JW Lynn, and DL Garling. 2005. Pathways of food uptake in native (Unionidae) and introduced (Corbiculidae and Dreissenidae) freshwater bivalves. *Journal of Great Lakes Research*. 31: 87-96.
- Newton, TJ, CC Vaughn, DE Spooner, J Nichols, and MT Arts. 2013. Profiles of Biochemical Tracers in Unionid Mussels Across a Broad Geographical Range. *Journal of Shellfish Research*. 32(2): 497-507.
- Phillips, DL, and JW Gregg. 2003. Source partitioning using stable isotopes: coping with too many sources. *Oecologia*. 136: 261-269.

- Post, DM. 2002. Using stable isotopes to estimate trophic position: models, methods and assumptions. *Ecology*. 83(3): 703-718.
- Raikow, DF, and SK Hamilton. 2001. Bivalve diets in a Midwestern U.S. stream: A stable isotope enrichment study. *Limnology and Oceanography*. 46(3): 514-522.
- Randklev, CR, MS Johnson, ET Tsakiris, J Groce, and N Wilkins. 2013a. Status of the freshwater mussel (Unionidae) communities of the mainstem of the Leon River, Texas. *Aquatic Conservation: Marine and Freshwater Ecosystems*. 23: 390-404.
- Randklev, CR, ET Tsakiris, MS Johnson, JA Skorupski, LE Burlakova, J Groce, and N Wilkins. 2013b. Is False spike, *Quadrula mitchelli* (Bivalvia: Unionidae), extinct? First account of a very recently deceased individual in over thirty years. *Southwestern Naturalist*. 58(2): 247-249.
- Silverman, H, SJ Nichols, JS Cherry, E Archberger, JW Lynn, and TH Dietz, 1997. Clearance of laboratory-cultured bacteria by freshwater bivalves: differences between lentic and lotic unionids. *Canadian Journal of Zoology*. 75: 1857-1866.
- Strayer, DL. 2008. *Freshwater Mussel Ecology*. Berkeley, CA: University of California Press.
- Strayer, DL, NF Caraco, JJ Cole, S Findley, and ML Pace. 1999. Transformation of freshwater ecosystems by bivalves. *BioScience*. 49: 19-27.
- Strayer, DL, JA Downing, WR Haag, TL King, JB Layzer, TJ Newton, and S Nichols. 2004. Changing perspectives on pearly mussels, North America's most imperiled animals. *BioScience*. 54: 429-439.
- Spooner, DE, and CC Vaughn. 2006. Context-dependent effects of freshwater mussels on the benthic community. *Freshwater Biology*. 51: 1016-1024.
- Vaughn, CC, KB Gido, and DE Spooner. 2004. Ecosystem processes performed by unionid mussels in stream mecosystems: species roles and effects of abundance.

- Hydrobiologia. 527: 35-47.
- Vaughn, CC and CC Hakenkamp. 2001. The functional role of burrowing bivalves in freshwater ecosystems. *Freshwater Biology*. 46: 1431-1446.
- Vaughn, CC, SJ Nichols, and DE Spooner. 2008. Community and foodweb ecology of freshwater mussels. *Journal of the North American Benthological Society*. 27(2): 409-423.
- Vuorio, K, M Tarvainen, and J Sarvala. 2008. Unionid mussels as stable isotope baseline indicators for long-lived secondary consumers in pelagic food web comparisons. *Fundamental and Applied Limnology*. 169(3): 237-245.
- Weber, AM, JE Bauer, and GT Watter. 2017. Assessment of nutritional subsidies to freshwater mussels using a multiple natural abundance isotope approach. *Freshwater Biology*. 62: 615-629.
- Williams, JD, AE Bogan, JT Garner. 2008. *Freshwater Mussels of Alabama & the Mobile Basin*. Tuscaloosa, AL: University of Alabama Press.
- Winemiller, K, NK Lujan, RN Wilkins, RT Snelgrove, AM Dube, KL Skow, and AG Snelgrove. 2010. *Status of Freshwater Mussels in Texas*. College Station, TX: Texas A&M Department of Wildlife and Fisheries Sciences and Texas A&M Institute of Renewable Natural Resources.
- Yeager, MM, DS Cherry, and RJ Neves. 1994. Burrowing behaviors of juvenile rainbow mussels, *Villosa iris* (Bivalvia: Unionidae). *Journal of the North American Benthological Society*. 13(2): 217-222.

Table 1. Size data for *C. petrina* sampled in the upper Guadalupe River and the lower Colorado River. Note significant p-values in bold (two-tailed t-test with unequal variance).

	Upper Guadalupe		Lower Colorado		
<i>C. petrina</i>	\bar{X}	σ	\bar{X}	σ	p
Length (mm)	48.12	5.19	65.90	10.12	<0.001
Width (mm)	33.46	4.55	52.49	7.41	<0.001
Height (mm)	18.83	2.75	33.46	4.84	<0.001
Weight (g)	18.40	7.02	88.71	41.61	<0.001

Table 2. Size data for *C. houstonensis* sampled in the lower Colorado River and the lower Brazos River basin. Note significant p-values in bold (two-tailed t-test with unequal variance).

<i>C. houstonensis</i>	Lower Colorado		Lower Brazos		<i>p</i>
	\bar{X}	σ	\bar{X}	σ	
Length (mm)	50.34	7.07	44.22	4.97	<0.001
Width (mm)	44.46	5.88	38.58	5.14	<0.001
Height (mm)	28.10	3.54	27.83	3.86	0.79
Weight (g)	44.61	18.9	37.52	14.16	0.16

Table 3. Size data for *L. bracteata* sampled in the upper Guadalupe River and the middle Colorado River basin. Note significant p-values in bold (two-tailed t-test with unequal variance).

	Upper Guadalupe		Middle Colorado		
<i>L. bracteata</i>	\bar{X}	σ	\bar{X}	σ	p
Length (mm)	50.69	4.53	45.58	8.39	0.0047
Width (mm)	32.13	3.21	29.67	4.50	0.019
Height (mm)	19.26	1.83	17.80	2.70	0.018
Weight (g)	15.12	4.40	12.33	4.56	0.022

Table 4. Seasonal environmental data collected at sites in spring, summer and fall of 2017 and spring 2018 during mussel and food source sampling.

Season	Site	Water Temp (°C)	pH	Conductivity (μs/cm)	Discharge (cfs)
Upper Guadalupe	Spring '17	22.6	8.3	471	125
	Summer '17	26.5	8.4	497	55
	Fall '17	16	8.7	510	56
	Spring '18	24.5	8.4	454	52.2
Lower Colorado	Spring '17	24.5	8.5	500	1310
	Summer '17	32.7	9.2	584	1225
	Fall '17	20.6	8.4	765	1230
	Spring '18	29.4	8.9	549	1148
Middle Colorado	Spring '17	24.1	7.9	329	138
	Summer '17	31.5	8.7	354	88.7
	Fall '17	19.7	8.5	388	60
	Spring '18	25.2	8.2	198	68.7
Lower Brazos	Spring '17	21.7	7.5	340	38
	Summer '17	27.7	7.9	283	23
	Fall '17	12.7	8.3	248	11
	Spring '18	27.6	7.9	20	15

Table 5. Stable isotope values for all consumers and potential food source samples. Dashes represent unsampled sources at a given location, often due to its absence in the sampling area. Sources are defined in text.

Basin	Source	Spring 2017			Summer 2017			Fall 2017			Spring 2018		
		$\delta^{13}\text{C} \pm \text{SE}$	$\delta^{15}\text{N} \pm \text{SE}$	C:N	$\delta^{13}\text{C} \pm \text{SE}$	$\delta^{15}\text{N} \pm \text{SE}$	C:N	$\delta^{13}\text{C} \pm \text{SE}$	$\delta^{15}\text{N} \pm \text{SE}$	C:N	$\delta^{13}\text{C} \pm \text{SE}$	$\delta^{15}\text{N} \pm \text{SE}$	C:N
Upper Guadalupe	<i>C. petrina</i>	-29.21 \pm 0.18	11.15 \pm 0.17	3.76	-28.31 \pm 0.11	10.96 \pm 0.05	3.66	-28.27 \pm 0.18	11.14 \pm 0.07	3.79	-	-	-
	<i>L. bracteata</i>	-28.95 \pm 0.22	11.06 \pm 0.13	3.89	-28.78 \pm 0.19	10.75 \pm 0.19	7.81	-28.04 \pm 0.16	11.12 \pm 0.11	3.55	-	-	-
	SPOM	-24.84 \pm 0.29	2.75	8.94	-17.30 \pm 0.15	6.34 \pm 1.42	14.71	-15.17 \pm 0.61	3.80 \pm 2.87	20.52	-16.85 \pm 0.24	8.76 \pm 1.41	14.86
	CPOM	-29.26 \pm 0.31	1.85 \pm 0.85	42.99	-28.14	3.00	15.33	-27.91	3.23	36.48	-29.00 \pm 0.42	5.74 \pm 0.57	24.50
	FPOM	-9.53 \pm 0.19	4.86 \pm 0.09	38.01	-10.86 \pm 0.16	8.48 \pm 0.11	33.17	-10.40 \pm 0.08	8.02 \pm 0.07	34.25	-11.31 \pm 0.11	8.63 \pm 0.09	29.63
	Biofilm	-	-	-	-	-	-	-	-	0.05	-18.24 \pm 1.87	7.31 \pm 0.44	22.08
	Periphyton	-	-	-	-	-	-	-	-	-	-11.41 \pm 0.03	9.17 \pm 0.13	26.60
	Epiphyton	-	-	-	-	-	-	-	-	-	-14.86 \pm 0.22	8.81 \pm 0.21	19.37
	Grass	-	-	-	-30.36	5.47	25.48	-	-	-	-	-	-
	<i>Justicia</i>	-25.79 \pm 0.26	8.41 \pm 0.32	11.05	-26.26	8.32	14.40	-29.22	12.6	10.31	-	-	-
Lower Colorado	<i>Myriophyllum</i>	-29.16 \pm 0.15	10.29 \pm 0.47	16.47	-	-	-	-27.21	10.01	19.07	-	-	-
	<i>C. petrina</i>	-29.86 \pm 0.12	13.41 \pm 0.14	3.91	-28.68 \pm 0.14	13.38 \pm 0.29	9.77	-30.34 \pm 0.33	11.82 \pm 0.56	4.01	-	-	-
	<i>C. houstonensis</i>	-29.91 \pm 0.25	13.10 \pm 0.28	3.97	-28.83 \pm 0.12	12.71 \pm 0.13	8.61	-30.01 \pm 0.34	12.33 \pm 0.59	3.92	-	-	-
	SPOM	-24.49 \pm 1.11	2.35 \pm 0.26	9.56	-22.30 \pm 0.13	8.47 \pm 0.22	8.15	-23.37 \pm 0.94	8.23 \pm 0.49	1.09	-20.81 \pm 0.39	5.67 \pm 0.99	7.77
	CPOM	-29.58 \pm 0.48	4.70 \pm 0.89	29.57	-29.10	10.97	16.16	-28.54	6.81	34.57	-27.54 \pm 0.13	4.58 \pm 0.63	22.41
	FPOM	-12.63 \pm 0.24	3.86 \pm 0.18	21.51	-13.95 \pm 0.11	7.79 \pm 0.17	29.51	-13.95 \pm 0.83	5.83 \pm 0.24	17.06	-12.59 \pm 0.25	6.65 \pm 0.19	21.47
	Biofilm	-	-	-	-	-	-	-	-	14.52	-16.45 \pm 0.75	7.78 \pm 0.43	13.27
	Periphyton	-	-	-	-	-	-	-	-	-	-13.16 \pm 0.24	8.08 \pm 0.42	15.03
	Epiphyton	-	-	-	-	-	-	-	-	-	-16.65 \pm 0.29	6.83 \pm 0.47	12.60
	Grass	-30.54 \pm 0.04	10.92 \pm 0.16	20.16	-13.78	8.68	9.82	-29.17	9.73	18.99	-	-	-
	<i>Justicia</i>	-	-	-	-	-	-	-	-	-	-	-	-
	<i>Myriophyllum</i>	-	-	-	-27.97 \pm 2.04	10.25 \pm 3.14	12.16	-	-	-	-	-	-
	<i>Alternanthera</i>	-	-	-	-	-	-	-28.41	12.88	15.04	-	-	-
	<i>Elodea</i>	-	-	-	-	-	-	-15.09	9.38	32.04	-	-	-
	Algae	-	-	-	-19.70	2.17	21.75	-24.6	9.55	8.16	-	-	-

Table 5. (continued)

Basin	Source	Spring 2017			Summer 2017			Fall 2017			Spring 2018		
		$\delta^{13}\text{C} \pm \text{SE}$	$\delta^{15}\text{N} \pm \text{SE}$	C:N	$\delta^{13}\text{C} \pm \text{SE}$	$\delta^{15}\text{N} \pm \text{SE}$	C:N	$\delta^{13}\text{C} \pm \text{SE}$	$\delta^{15}\text{N} \pm \text{SE}$	C:N	$\delta^{13}\text{C} \pm \text{SE}$	$\delta^{15}\text{N} \pm \text{SE}$	C:N
Middle Colorado	<i>L. bracteata</i>	-26.63 \pm 0.16	7.38 \pm 0.16	3.75	-26.45 \pm 0.11	7.28 \pm 0.08	9.47	-25.60 \pm 0.16	7.18 \pm 0.11	3.72	-	-	-
	SPOM	-22.92 \pm 0.44	0.24 \pm 0.52	10.26	-19.02 \pm 0.32	2.88 \pm 0.67	15.26	-18.09 \pm 0.40	0.56 \pm 3.08	19.62	-18.61 \pm 0.41	2.47 \pm 1.44	15.84
	CPOM	-20.85 \pm 1.73	5.67 \pm 1.20	23.61	-28.26	0.48	16.16	-30.09	3.13	61.37	-26.52 \pm 2.26	1.754 \pm 1.08	34.89
	FPOM	-11.11 \pm 0.05	3.34 \pm 0.12	36.43	-11.01 \pm 0.08	5.30 \pm 0.10	38.75	-11.40 \pm 0.27	4.46 \pm 0.11	34.28	-10.01 \pm 0.12	4.74 \pm 0.04	42.47
	Biofilm	-	-	-	-	-	-	-27.96	3.23	31.08	-16.10 \pm 1.15	4.93 \pm 0.17	24.23
	Periphyton	-	-	-	-	-	-	-	-	-	-11.39 \pm 0.36	5.25 \pm 0.31	27.08
	Epiphyton	-	-	-	-	-	-	-	-	-	-12.28 \pm 0.69	5.32 \pm 0.19	27.38
	Grass	-28.81 \pm 0.34	4.97 \pm 0.18	22.10	-26.50	1.17	9.77	-22.86	5.63	21.13	-	-	-
	<i>Justicia</i>	-15.74 \pm 0.34	6.06 \pm 0.16	22.13	-22.97	5.57	8.71	-13.98	3.37	22.37	-	-	-
	<i>Myriophyllum</i>	-25.00 \pm 0.38	3.40 \pm 0.27	16.10	-18.89 \pm 4.60	2.68 \pm 2.92	11.19	-13.89	-0.95	25	-	-	-
Lower Brazos	Algae	-	-	-	-17.68	10.10	9.09	-17.17	3.62	20.81	-	-	-
	<i>C. houstonensis</i>	-28.37 \pm 0.05	11.81 \pm 0.13	3.76	-27.99 \pm 0.06	12.22 \pm 0.16	10.63	-27.88 \pm 0.06	11.74 \pm 0.12	3.62	-	-	-
	SPOM	-22.30 \pm 1.01	2.76 \pm 0.11	9.09	-25.89 \pm 0.10	4.06 \pm 0.58	9.59	-26.28 \pm 0.72	3.43 \pm 1.42	11.58	-27.26 \pm 0.04	7.45 \pm 0.17	10.81
	CPOM	-29.16 \pm 0.86	5.36 \pm 0.58	33.70	-29.97	3.98	30.46	-28.47	5.46	28.91	-28.67 \pm 0.74	5.64 \pm 1.22	27.52
	FPOM	-23.08 \pm 0.20	3.02 \pm 0.15	9.14	-22.85 \pm 0.28	-0.76 \pm 1.19	10.37	-23.79 \pm 0.66	4.49 \pm 0.32	8.55	-24.14 \pm 0.21	5.06 \pm 0.22	10.34
	Biofilm	-	-	-	-	-	-	-29.09	6.46	15.09	-27.07 \pm 0.34	8.26 \pm 0.41	9.03
	Periphyton	-	-	-	-	-	-	-	-	-	-25.64 \pm 0.31	7.83 \pm 0.46	7.14
	Epiphyton	-	-	-	-	-	-	-	-	-	-25.74 \pm 0.09	11.29 \pm 0.20	5.26
	Grass	-30.38 \pm 0.04	9.56 \pm 0.13	14.42	-	-	-	-30.79	11.23	17.17	-	-	-
	<i>Justicia</i>	-	-	-	-31.75	9.98	14.42	-32.6	11.49	17.56	-	-	-
	<i>Myriophyllum</i>	-	-	-	-32.37	7.35	17.67	-	-	-	-	-	-
	Algae	-	-	-	-	-	-	-26.48	9.58	11.07	-	-	-

Table 6. Mean $\delta^{13}\text{C}$ and $\delta^{15}\text{N}$ signatures of tissue from focal taxa in spring, summer, and fall 2017.

Species	Basin	Season	<i>n</i>	$\delta^{13}\text{C}$	$\delta^{15}\text{N}$
<i>C. petrina</i>	Upper Guadalupe	Spring	7	-29.21	11.15
		Summer	11	-28.31	10.4
		Fall	3	-28.27	11.14
	Lower Colorado	Spring	10	-29.86	13.41
		Summer	10	-28.68	13.38
		Fall	3	-30.34	11.82
<i>C. houstonensis</i>	Lower Colorado	Spring	10	-29.91	13.1
		Summer	10	-28.83	12.71
		Fall	4	-30.01	12.33
	Lower Brazos	Spring	12	-28.37	11.81
		Summer	10	-27.99	12.21
		Fall	10	-27.88	11.74
<i>L. bracteata</i>	Upper Guadalupe	Spring	6	-28.95	11.06
		Summer	13	-28.78	10.75
		Fall	7	-28.04	11.12
	Middle Colorado	Spring	12	-26.38	7.38
		Summer	10	-26.45	7.23
		Fall	9	-25.6	7.18

Table 7. Pearson product-moment coefficients and associated p-values for correlations between mussel size and $\delta^{13}\text{C}$ and mussel size and $\delta^{15}\text{N}$. Data were pooled across seasons for each species and each site. Bold values are statistically significant.

<i>Site</i>	<i>Species</i>	$\delta^{13}\text{C}$		$\delta^{15}\text{N}$	
		<i>r</i>	<i>p</i>	<i>r</i>	<i>p</i>
Upper Guadalupe	<i>C. petrina</i>	0.47	0.05	0.01	0.98
	<i>L. bracteata</i>	0.46	0.05	0.45	0.06
Lower Colorado	<i>C. houstonensis</i>	0.58	0.01	0.48	0.03
	<i>C. petrina</i>	0.57	0.01	0.22	0.36
Middle Colorado basin	<i>L. bracteata</i>	0.36	0.10	0.34	0.12
Lower Brazos basin	<i>C. houstonensis</i>	0.26	0.24	0.39	0.08

Table 8. IsoSource model estimates for the 3 mussel species. CPOM is coarse particulate organic matter, FPOM is fine particulate organic matter, SPOM is suspended particulate organic matter, Biofilm is scrubbed CPOM and plants, and values are mean, minimum, maximum, estimated proportional composition of each C source.

Species	Site	C:N	C source	Spring 2017			Summer 2017			Fall 2017		
				Mean	Min	Max	Mean	Min	Max	Mean	Min	Max
<i>C. houstonensis</i>	LB	3.62	CPOM	0.876	0.87	0.88	0.625	0.53	0.72	0.368	0	0.89
			FPOM	0.074	0.03	0.13	0.145	0.02	0.27	0.093	0	0.24
			SPOM	0.05	0	0.09	0.23	0.01	0.45	0.174	0	0.46
			Biofilm	-	-	-	-	-	-	0.364	0	0.79
	LC	3.89	CPOM	0.943	0.87	1	0.96	0.94	0.98	0.955	0.9	1
			FPOM	0.01	0	0.03	0.01	0	0.02	0.036	0	0.1
			SPOM	0.047	0	0.13	0.03	0	0.06	0.009	0	0.03
			Biofilm	-	-	-	-	-	-			
<i>C. petrina</i>	LC	3.86	CPOM	0.939	0.86	1	0.96	0.94	0.98	0.985	0.97	1
			FPOM	0.012	0	0.04	0.01	0	0.02	0.012	0	0.03
			SPOM	0.049	0	0.14	0.03	0	0.06	0.003	0	0.01
			Biofilm	-	-	-	-	-	-			
	UG	3.79	CPOM	0.99	0.99	0.99	0.974	0.95	1	0.984	0.97	1
			FPOM	0	0	0	0.009	0	0.03	0.006	0	0.02
			SPOM	0.01	0.01	0.01	0.017	0	0.05	0.01	0	0.03
			Biofilm	-	-	-	-	-	-			

Table 8. cont.

Species	Site	C:N	C source	Spring 2017			Summer 2017			Fall 2017		
				Mean	Min	Max	Mean	Min	Max	Mean	Min	Max
<i>L. bracteata</i>	MC	3.82	CPOM	0.02	0	0.05	0.85	0.8	0.9	0.373	0	0.76
			FPOM	0.003	0	0.01	0.054	0	0.11	0.099	0	0.24
			SPOM	0.978	0.95	1	0.096	0	0.2	0.153	0	0.38
			Biofilm	-	-	-	-	-	-	0.374	0	0.86
	UG	3.83	CPOM	0.93	0.93	0.93	1	1	1	0.975	0.96	1
			FPOM	0	0	0	0	0	0	0.01	0	0.03
			SPOM	0.07	0.07	0.07	0	0	0	0.015	0	0.04
			Biofilm	-	-	-	-	-	-	-	-	-

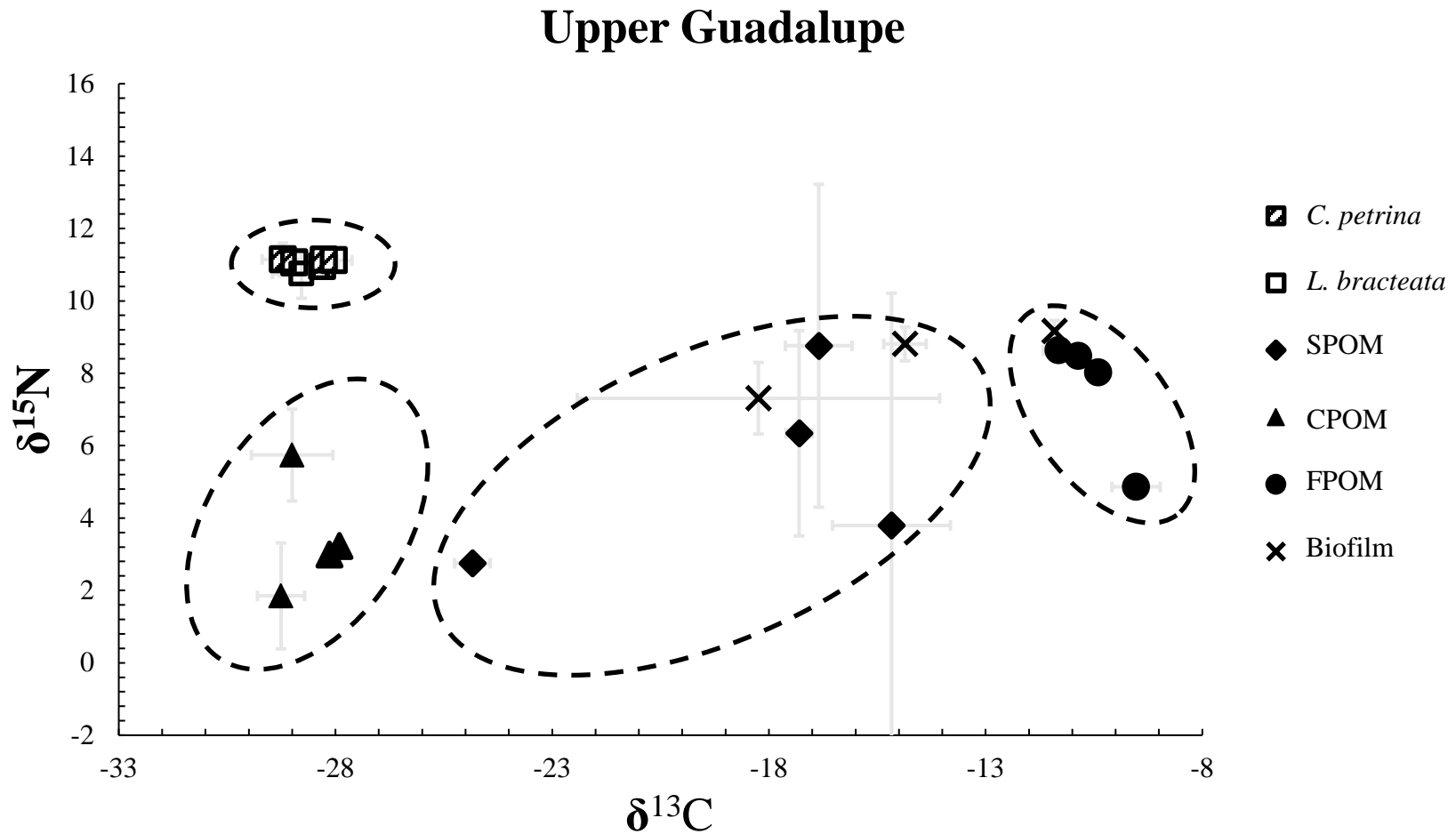


Figure 1. Stable CN isotope biplots for the Upper Guadalupe River site in April (Spring), July (Summer) and October (Fall) 2017 and May (Spring) 2018. Each point is a season average and associated SD. CPOM is coarse particulate organic matter (benthic detritus), FPOM is fine particulate organic matter from benthic sediments, SPOM is suspended particulate organic matter. Biofilm is attached periphyton.

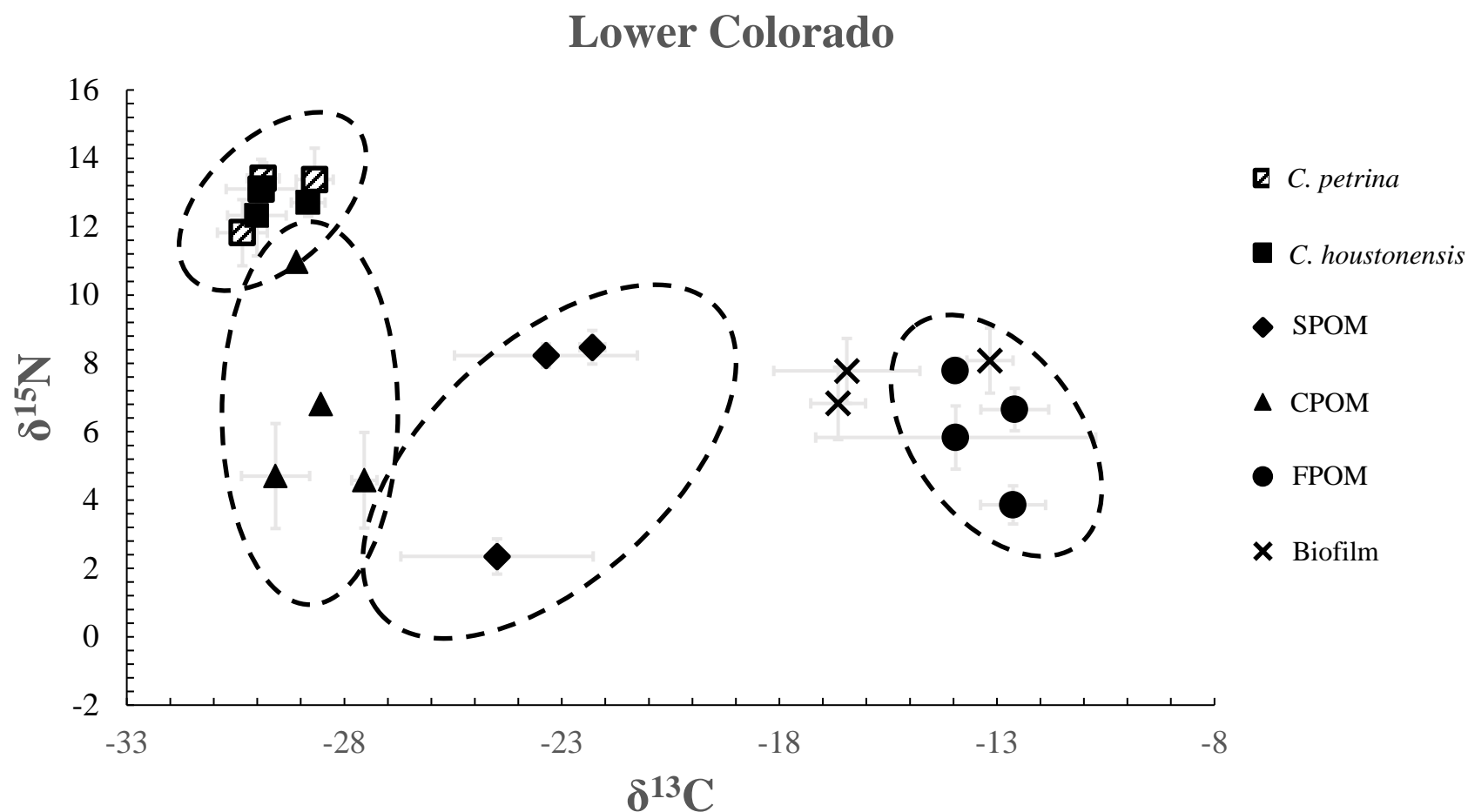


Figure 2. Stable CN isotope biplots for the Lower Colorado River site in April (Spring), July (Summer) and October (Fall) 2017 and May (Spring) 2018. Each point is a season average and associated SD. CPOM is coarse particulate organic matter (benthic detritus), FPOM is fine particulate organic matter from benthic sediments, SPOM is suspended particulate organic matter (seston). Biofilm is attached periphyton.

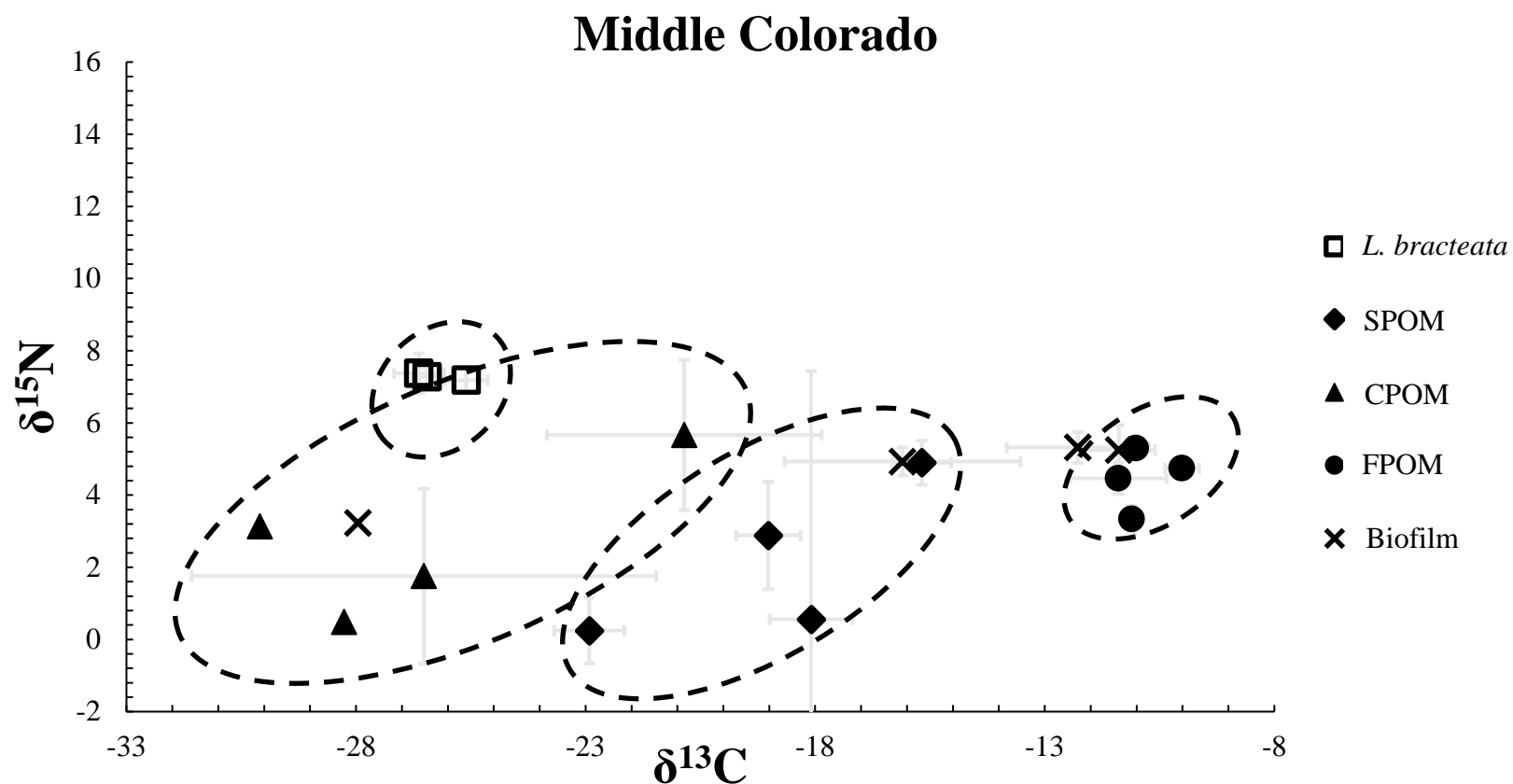


Figure 3. Stable CN isotope biplots for the Middle Colorado River basin site in April (Spring), July (Summer) and October (Fall) 2017 and May (Spring) 2018. Each point is a season average and associated SD. CPOM is coarse particulate organic matter (benthic detritus), FPOM is fine particulate organic matter from benthic sediments, SPOM is suspended particulate organic matter (seston). Biofilm is attached periphyton.

Lower Brazos

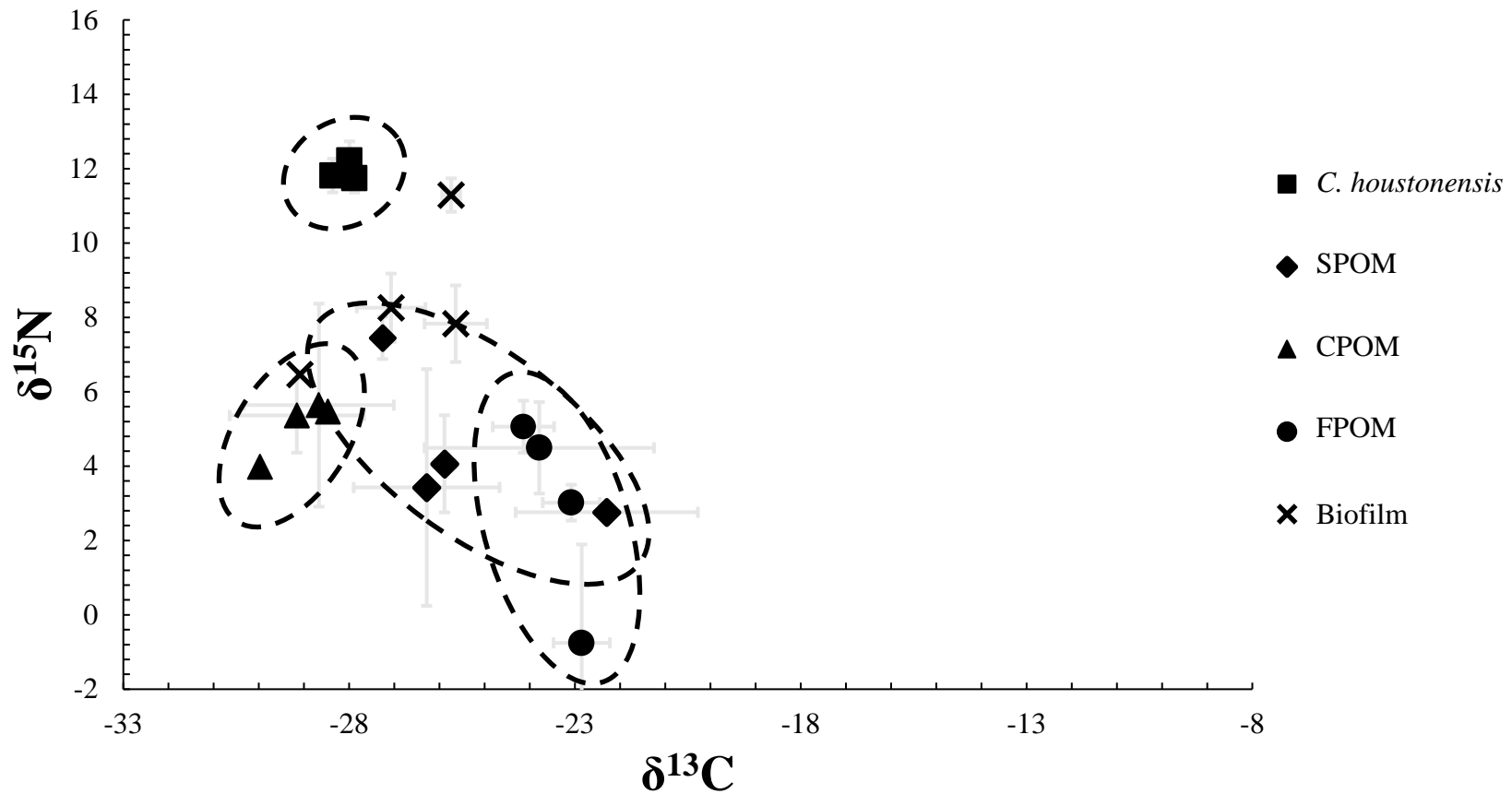


Figure 4. Stable CN isotope biplots for the Lower Brazos River basin site in April (Spring), July (Summer) and October (Fall) 2017 and May (Spring) 2018. Each point is a season average and associated SD. CPOM is coarse particulate organic matter (benthic detritus), FPOM is fine particulate organic matter from benthic sediments, SPOM is suspended particulate organic matter (seston). Biofilm is attached periphyton.

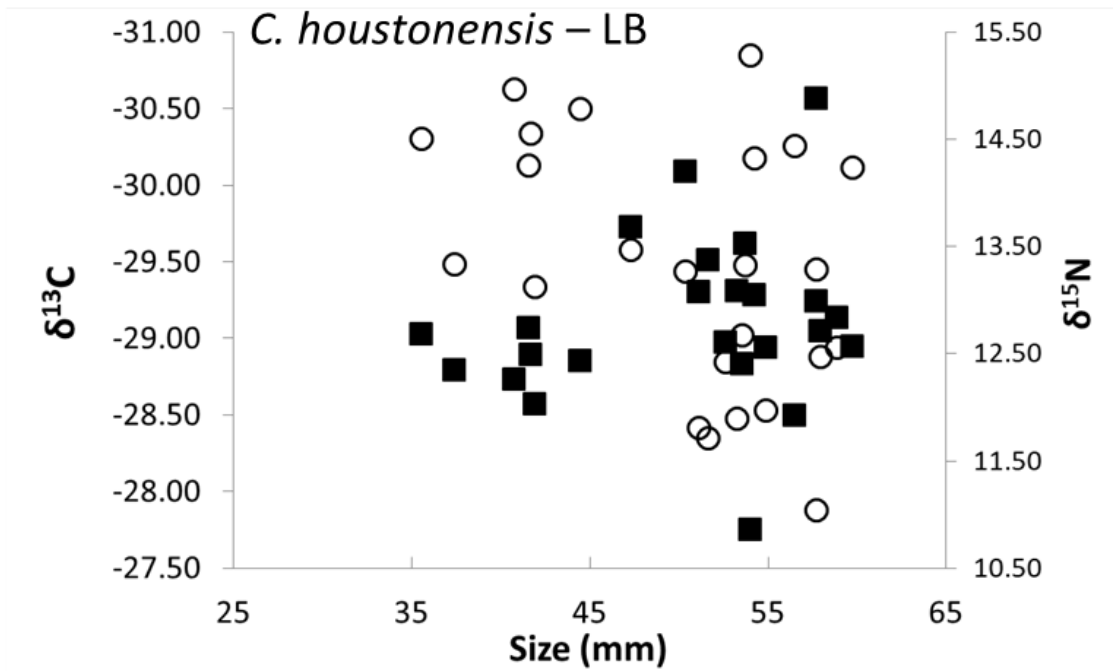
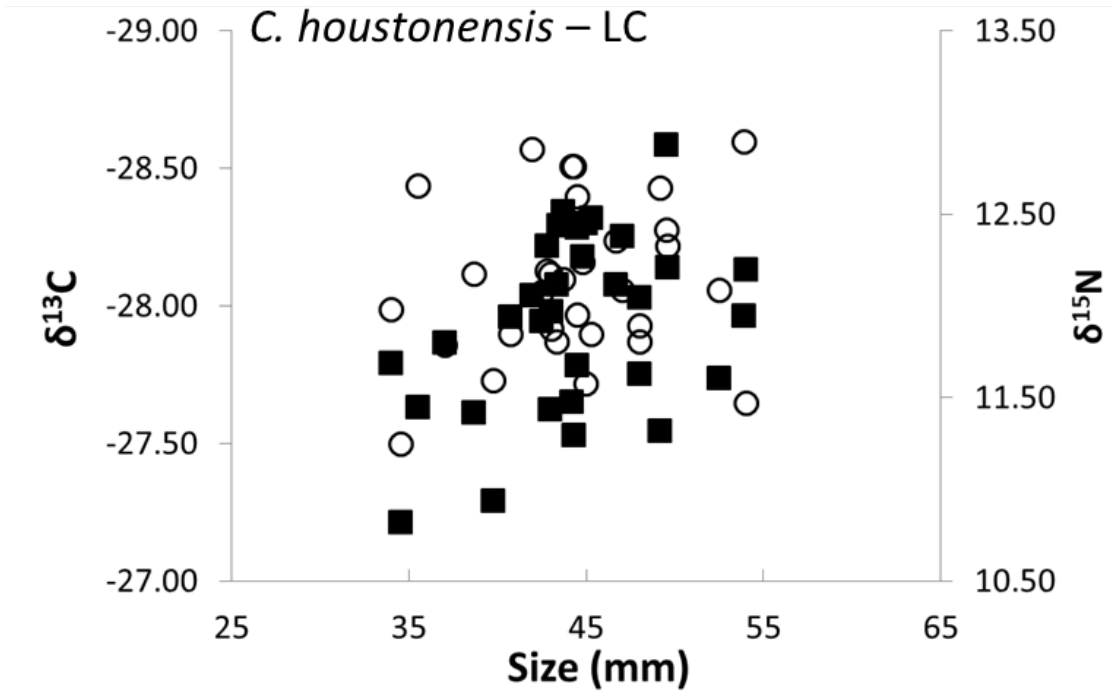


Figure 5. Relationships between stable isotope ratios ($\delta^{13}\text{C}$ and $\delta^{15}\text{N}$) and *C. houstonensis* size (length) in the Lower Colorado (LC) and Lower Brazos basin (LB). Open circles are $\delta^{13}\text{C}$ and filled squares are $\delta^{15}\text{N}$. Note $\delta^{13}\text{C}$ axis is inverted. See Table 7 for statistics.

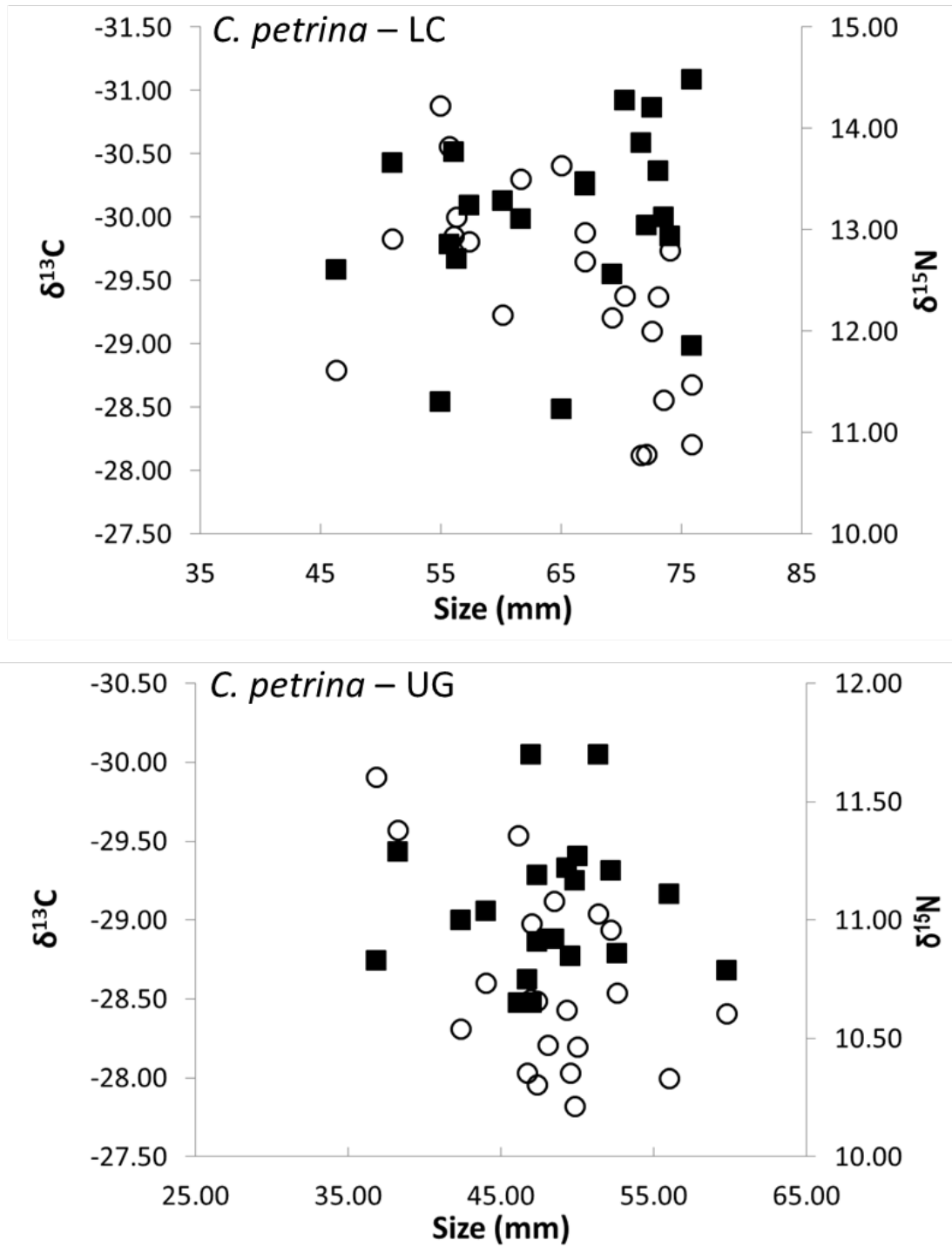


Figure 6. Relationships between stable isotope ratios ($\delta^{13}\text{C}$ and $\delta^{15}\text{N}$) and *C. petrina* size (length) in the Lower Colorado basin (LC) and Upper Guadalupe (UG). Open circles are $\delta^{13}\text{C}$ and filled squares are $\delta^{15}\text{N}$. Note $\delta^{13}\text{C}$ axis is inverted. See Table 7 for statistics.

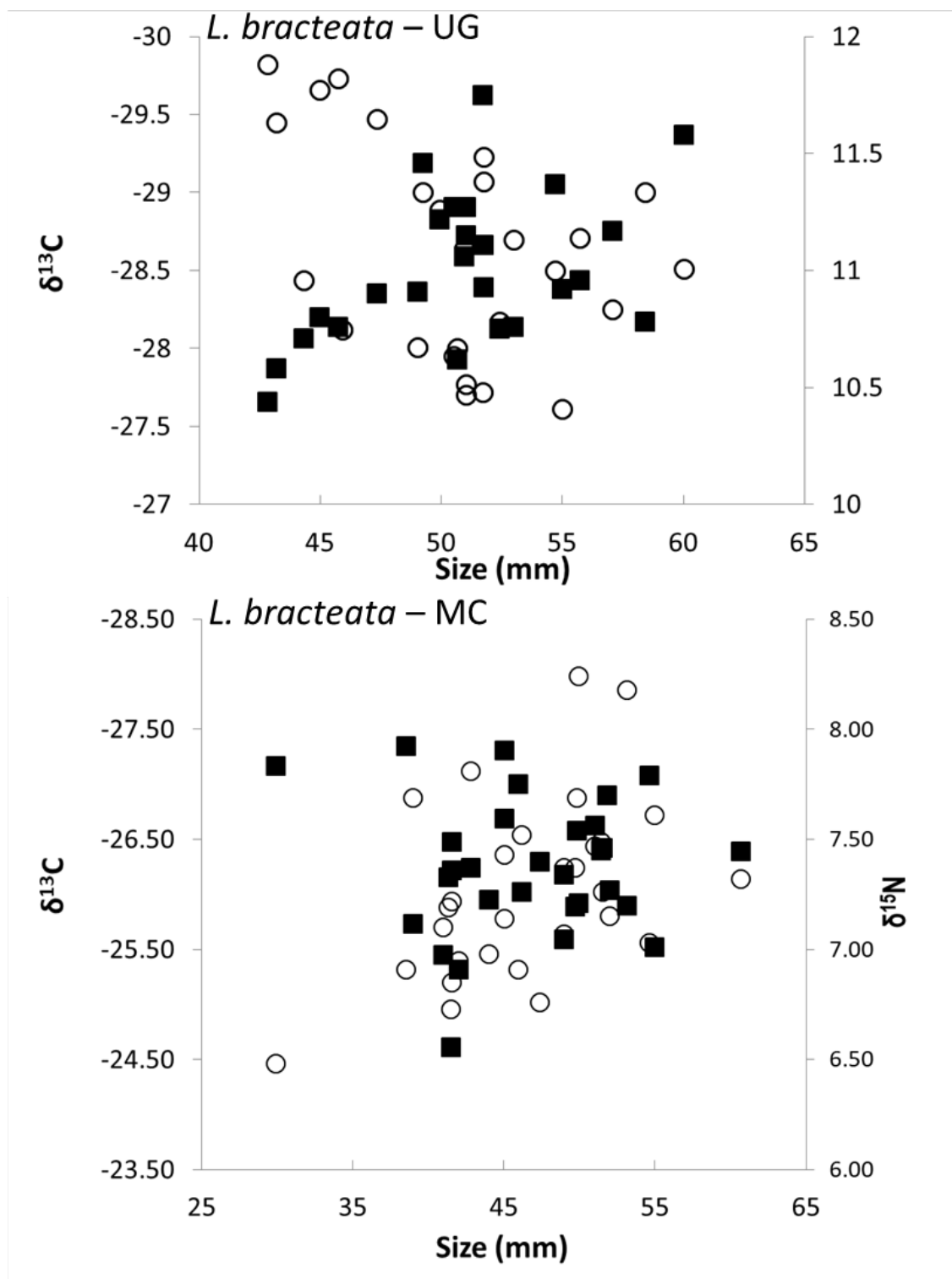


Figure 7. Relationships between stable isotope ratios ($\delta^{13}\text{C}$ and $\delta^{15}\text{N}$) and *L. bracteata* size (length) in the Upper Guadalupe (UG) and Middle Colorado basin (MC). Open circles are $\delta^{13}\text{C}$ and filled squares are $\delta^{15}\text{N}$. Note $\delta^{13}\text{C}$ axis is inverted. See Table 7 for statistics.

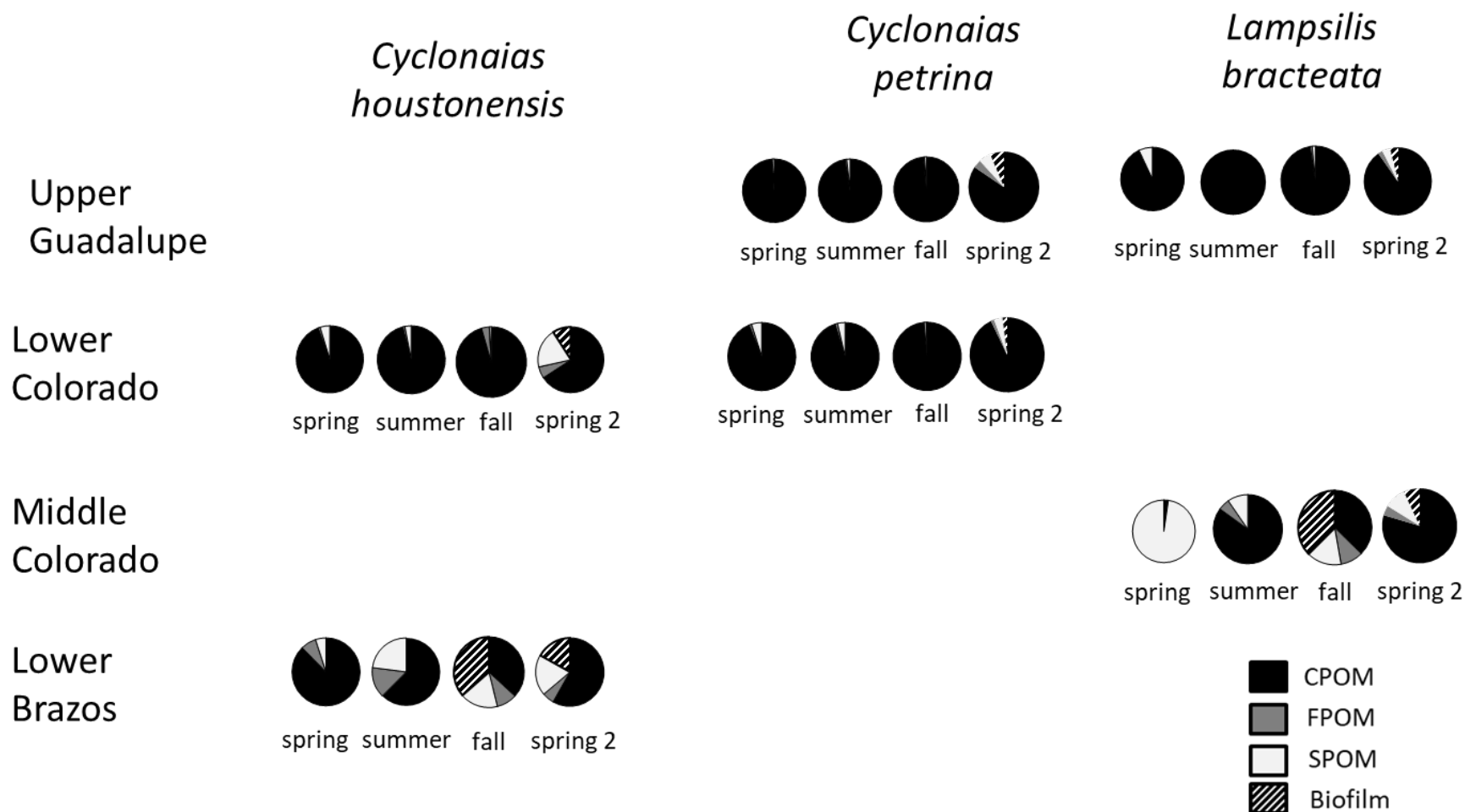


Figure 8. Estimated carbon source of *C. houstonensis*, *C. petrina*, and *L. bracteata* across the Upper Guadalupe, Lower Colorado, Middle Colorado, and Lower Brazos basin. Charts reflect mean estimate values of potential C sources from linear mixing models derived from IsoSource. Biofilm was only sampled from the Middle Colorado and Lower Brazos in the fall and was not estimated for other seasons and basin.

Task 3 Environmental Flow Analysis

Contributing Authors: Brad Littrell, Kyle Sullivan, Ed Oborny

Address: BIO-WEST, Inc. San Marcos, Texas 78666 (BL, KS, EO)

Principal Investigators: Brad Littrell and Ed Oborny

Email: blittrell@bio-west.com, eoborny@bio-west.com

Introduction and Objectives

Traditional instream flow studies model changes in simple hydraulic parameters such as depth and velocity under varying stream discharge levels and how they influence habitat availability for target organisms, usually fishes (BIO-WEST 2008). The underlying assumptions are that target organisms select their habitat based on these parameters, and that they have the ability to move to new habitats when discharge conditions change. Freshwater mussels challenge these assumptions due to their slow locomotion and sessile nature (Schwalb & Pusch 2007; Gough et al. 2012; Newton et al. 2015). Compared to fishes, mussels tend to move little and occupy small habitat patches for long periods. Therefore, for a mussel to persist at a specific location, suitable habitat must occur across a range of flow conditions. As a result, some have suggested that modeling based on habitat utilization data using simple hydraulic variables such as depth and velocity are of little use in determining conservation flows for mussels, but that complex hydraulic parameters such as shear stress modeled over a range of flow conditions to identify “persistent habitat” are better predictors of mussel abundance (Layzer and Madison 1995, Maloney et al. 2012). However, some of the same authors recognized that mussels did show a preference for particular hydraulic conditions and that depth and velocity were important factors limiting their distribution under base flow conditions (Layzer and Madison 1995). This study uses a combined approach of first evaluating shear stress across a range of flow conditions

to identify persistent habitat patches, followed by modeling with traditional habitat suitability criteria based on hydraulic parameters (i.e., depth, velocity, Froude number, Reynolds number) within those patches at base flow levels. This integrated approach accounts for the requirement of persistent habitat across a broad range of flow conditions, while simultaneously accounting for habitat selectivity of mussels under base flow conditions.

Previous environmental flow studies conducted on the lower Colorado River as part of the Lower Colorado River Authority (LCRA) – San Antonio Water System (SAWS) Water Project (LSWP) established 10 intensive study sites with detailed hydraulic models (Figure 1) (BIO-WEST 2008). These models were used to generate instream flow recommendations for the lower Colorado River based on fish habitat modeling and other flow dependent ecological variables. However, freshwater mussels were not considered as part of this previous instream flow assessment. Therefore, the overall goal of the current study was to evaluate availability and persistence of freshwater mussel habitat under various flow conditions within the lower Colorado River using a variety of both traditional (depth, velocity) and complex (Reynolds number, Froude number, shear stress) hydraulic variables at existing hydraulic model sites used previously for fish habitat modeling.

To do this, the first specific objective of Task 3 was to conduct mussel surveys at previously established hydraulic model sites on the lower Colorado River to determine which sites support significant mussel populations. These sites were included in Task 1 survey work to assess the occurrence and abundance of freshwater mussels at each location. Based on the results of these surveys, two previously-established hydraulic model sites were chosen to focus additional habitat modeling efforts, as described in the results below.

The second specific objective was to develop habitat suitability criteria for freshwater mussels within the lower Colorado River. Detailed habitat information collected as part of Task 1 survey work was summarized and used to develop Habitat Suitability Criteria (HSC). These HSC describe the habitat utilized by freshwater mussels under base flow conditions. Similar criteria were also developed using data from the Little River drainage in the Brazos basin to investigate basin-specific differences in HSC.

The third specific objective of this task was to collect additional physical and hydraulic data to validate and/or update existing hydraulic models. Initially, it appeared that hydraulic model sites had changed little since development of the models and only some minor validation data would be necessary. However, a large flood event occurred in the lower Colorado River following heavy rains from Hurricane Harvey in August 2017. A visit to one of the selected model sites shortly afterwards revealed extensive changes to channel bathymetry. Therefore, additional bathymetric and hydraulic data was collected in 2018 to update existing models to incorporate these changes. Bed topography from updated models were then compared to previous models to investigate changes in river bathymetry between modeling events.

The fourth objective was to incorporate habitat suitability information with revised model output to evaluate the effects of varying flows on freshwater mussel habitat within the selected study sites, and thus inform environmental flow recommendations in the lower Colorado River. Results of this habitat modeling are presented below, along with a discussion of results in the context of current Texas Commission on Environmental Quality (TCEQ) instream flow standards.

Finally, although no hydraulic modeling was done in the Brazos River basin, a desktop analysis of freshwater mussel environmental flow needs in the Brazos basin was conducted based on observations from this study and other available data.

Methods

Study Site Selection

Freshwater mussel data was collected using the methodology described in detail under Task 1 surveys of the previous report (Bonner et al. 2018). Surveys were conducted at several of the previously established hydraulic model sites to evaluate the mussel communities present and choose sites for further habitat modeling. Data was collected to allow for calculation of catch-per-unit-effort (CPUE; mussels/person-hour) at each study site.

Habitat Suitability Criteria

Habitat utilization data from Task 1 surveys on the lower Colorado River were used to develop Habitat Suitability Criteria (HSC) for all freshwater mussels in aggregate, as well as for each of the candidate species inhabiting the lower Colorado River (i.e., *Cyclonaias houstonensis*, *Cyclonaias petrina*, and *Truncilla macrodon*). This data was collected in spring and summer of 2017 at daily average discharges ranging from 507 – 1,870 cfs. Additionally, suitability criteria were developed for all mussels and for *C. houstonensis* from the Little River drainage in the Brazos basin to allow for between-basin comparisons. For each species or combination of species, HSC were developed for depth, mean column velocity, Froude number, Reynolds number, mean substrate compaction, FST hemisphere number, minimum bottom shear stress (MBSS; inferred from FSTs using Statzner et al. 1991), and dominant substrate. Data for depth, mean column velocity, mean substrate compaction, FST hemisphere number, and MBSS were measured during surveys as described in the Task 1 methods from the previous report (Bonner et

al. 2018). Percent substrate composition taken from survey data was converted to dominant substrate for development of suitability criteria. Froude number and Reynolds number are hydraulic parameters used to evaluate turbulence. Froude number represents a ratio of inertial to gravitational forces. Reynolds number represents a ratio of inertial force to viscous force. These parameters were calculated from survey data using the following equations:

Reynolds number (Re): $Re = Ud/\nu$

where U = benthic velocity (m/s), d = water depth (m), ν = kinematic viscosity of water ($1.0 \times 10^{-6} \text{ m}^2/\text{s}$)

Froude number (Fn): $Fn = U/\sqrt{gd}$

where U = benthic velocity (m/s), g = acceleration of gravity (9.8 m/s^2), d = water depth (m)

Suitability criteria for continuous variables were created using nonparametric tolerance limits (NPTL) (Bovee 1986). The tolerance limits representing the central 50% of the data were used to represent the highest utilization and given a suitability value of 1.0. The tolerance limits for the central 75% were assigned a suitability of 0.5. The tolerance limits for the central 90% of the data were given a suitability of 0.2. Lastly, the tolerance limits representing the central 95% of the data were given a suitability value of 0.1. Anything outside of the central 95% tolerance limit was considered unsuitable and given a suitability value of 0.0. For the categorical variable of dominant substrate, suitability values were established using the Strauss Linear Index (Strauss 1979, Persinger et al. 2010). Values of this index range from -1 to 1, with larger positive values indicating selection and negative values indicating avoidance. Significant positive values were given a suitability of 1.0, non-significant positive values were given a suitability of 0.5, non-

significant negative values were given a suitability of 0.2, and significant negative values were assigned a suitability of 0.0.

Hydraulic Model Updates

In February and March 2018, target hydraulic model study sites were resurveyed to account for changes in bathymetry following Hurricane Harvey high flow events. Most bathymetric data within the wetted channel was collected using a Son-Tek M9 River Surveyor Acoustic Doppler Current Profiler (ADCP) mounted to a small john boat. This unit simultaneously collects data on water column depth, velocity, and instrument position multiple times per second. By maneuvering the boat in a grid-like fashion across the study sites, a detailed georeferenced depth dataset was generated. This dataset was supplemented by point depth measurements taken with the aid of an incremental wading rod and Trimble GPS unit in wetted areas too shallow for the boat to operate. Additionally, elevation data in dry areas of the river bed was collected with a Trimble R10 VRS rover and data collector. The resulting georeferenced depth data was integrated with water surface elevations collected on the same dates to generate a dataset of georeferenced bed elevation points within each study site for import into River2D hydraulic modeling software (Steffler & Blackburn 2002).

To monitor changes in water surface elevation at the study site over an extended period, and thus generate stage-discharge relationships, water level data loggers (Onset HOBO U20L or Solinst Levellogger Model 3001) were installed at the upstream and downstream boundary of each site. Associated barometric pressure loggers were deployed above-water to account for changes in barometric pressure during the deployment period. On-site water surface elevation data was also collected using a Trimble R10 VRS rover and data collector under multiple flow rates.

Hydraulic modeling was conducted with River2D (Steffler & Blackburn 2002), the same program used in previous modeling efforts as part of the LSWP study. This program predicts water depth and velocity based on several measured inputs including discharge, water surface elevation, and bathymetry. Topographic/bathymetric data were entered into River2D Bed for editing. Based on this data, a triangular finite-element mesh with 5-meter spacing between nodes was generated using River2D Mesh. This mesh represented the final bathymetric input into River2D. Hydraulic data (discharge and water surface elevation) were then entered to generate first-cut models for each site at multiple flow rates. These first-cut models were then calibrated by adjusting model inputs until predictions of water surface elevation, depth, and velocity matched closely with field observations. Bed roughness was the main input adjusted during the calibration process, although minor adjustments to bathymetry and downstream water surface elevation were made sparingly. Final roughness values ranged from 0.1 m to 1.0 m, and were based on substrate conditions, with areas of smooth substrates (silt, sand) receiving lower values, gravel and cobble receiving intermediate values, and overbank areas receiving the highest roughness due to presence of riparian vegetation. To calibrate each modeled flow tier, the observed upstream and downstream water surface elevation from water level loggers or field measurements were compared to model predictions. Calibration within mid-reaches were also performed at flow tiers where water surface elevation data were available. At flow tiers where observed water surface elevation data was not available (extremely low flows), the Depth-Unit Discharge Relationship function in River 2D was used, which does not require the input of a downstream water surface elevation (Steffler & Blackburn 2002).

Habitat Modeling

First, persistent habitat was identified by evaluating shear stress across all modeled flow rates. Shear stress was calculated at each node across all modeled flow rates using the following equation:

Shear stress (τ):

$$\tau = U/5.75 \log_{10} \left(\frac{12d}{ks} \right)$$

where U = modeled current velocity (cm/s), d = modeled water depth (cm), and

ks = an estimate of bed roughness (cm) based on substrate maps (See Table 2).

Estimates of shear stress from this equation have shown to correspond with field measurements of shear stress from FST hemispheres (Randklev et al. 2014). To evaluate persistent habitat, shear stress HSC were used to identify a maximum shear stress cutoff for mussel occurrence (5.0 dyn/cm²) which was then applied to model results. Model nodes which exhibited shear stress less than the cutoff for all modeled flow rates were considered “persistent” habitat. If a given model node exhibited a shear stress higher than the cutoff at any modeled flow rate it was labeled “non-persistent”. Areas identified as persistent were considered to be potential mussel habitat, and HSC for hydraulic parameters were then applied within these areas, as described below.

Within persistent areas, base flow habitat suitability was evaluated for all unionid mussels in aggregate, as well as for *C. houstonensis*, and *C. petrina*, specifically. To do this, habitat suitability values for depth, velocity, substrate, Froude number, and Reynolds number were calculated for each node in the updated hydraulic model output. Individual habitat suitability values for each category were then combined into a Composite Suitability Index (CSI) for that node. The CSI was calculated by computing the geometric mean of the individual depth

(Depth_{SI}), velocity (Velocity_{SI}), substrate (Substrates_{SI}), Froude number (Froudes_{SI}), and Reynolds number (Reynolds_{SI}) suitability, as follows:

$$CSI = (\text{Depth}_{SI} * \text{Velocity}_{SI} * \text{Substrates}_{SI} * \text{Froudes}_{SI} * \text{Reynolds}_{SI})^{1/5}$$

The CSI was then multiplied by the area of each hydraulic model node to generate a Weighted Usable Area (WUA), and these values were summed within persistent habitat to generate a total Persistent Weighted Usable Area (PWUA) for each modeled base/subsistence flow rate. By compiling total PWUA for each mussel category at each flow rate, PWUA to discharge relationships for base and subsistence flow conditions were evaluated.

Habitat Model Validation

Current site-specific mussel distribution and abundance data were collected in summer 2018 to validate habitat modelling results. To do this, mussel survey transects were conducted at random sampling points generated within the model boundaries. Each random sampling point represented the upstream end of a 25-meter lead-core rope transect stretched parallel to streamflow. On each end of the transect the lead-core rope was secured to a cinder block with an attached buoy for easy surface location. Two biologists surveyed each transect with each surveyor maintaining contact with the rope for navigation and surveying one-meter on each side. This resulted in a total survey area of 50 m² per transect. Surveyors were equipped with mask and snorkel or surface-supplied-air from a Brownie's Third Lung Hookah System, depending on water depth. All mussels were placed in mesh bags and identified to species, measured, and enumerated following transect completion. Survey time was recorded at each transect and used to calculate CPUE. For each transect, CPUE was calculated for all mussels in aggregate, as well as for *C. houstonensis*, and *C. petrina*, specifically. A total of 85 random points was surveyed at Altair, and 70 random points were surveyed at La Grange.

Using GIS software, transect data were then overlaid with habitat modeling results. Mean CPU for all three categories was compared between non-persistent habitats with low suitability ($CSI < 0.5$), non-persistent habitats with high suitability ($CSI > 0.5$), persistent habitats with low suitability, and persistent habitats with high suitability to provide model validation.

Results

Study Site Selection

A total of 85 person-hours (p-h) of search time was conducted at the 10 intensive model sites during Task 1 surveys, resulting in collection of 862 mussels for an overall catch-per-unit-effort (CPUE) of 10.1 mussel/p-h (Table 1; Bonner et al. 2018). Site-specific CPUE ranged from 0.0 – 2.5 mussels/p-h at sites between Longhorn Dam and Smithville, and from 3.2 – 47.6 mussels/p-h from La Grange downstream to Lane City. Maximum site-specific CPUE (47.6 mussels/p-h) was observed at the Altair intensive study site. Candidate species were present from La Grange downstream, with all three candidate species being present at the Altair and Wharton study sites (Table 1).

Based on the data above, the Altair and La Grange study sites were chosen as the focus for additional data collection and modeling. Based on the high relative abundance observed and the presence of all three-candidate species, Altair was chosen to represent high-quality habitat conditions within the lower Colorado River. The La Grange study site was the upstream-most site that contained a candidate species (*C. houstonensis*), and exhibited a lower relative abundance compared to Altair, ranking third in overall CPUE. Understanding differences in hydraulic and habitat conditions between these two sites may elucidate patterns in freshwater mussel occurrence and abundance within the lower Colorado River.

Habitat Suitability Criteria

Habitat Suitability Criteria generated from survey data for all lower Colorado River unionids in aggregate demonstrated highest habitat suitability at depths of 0.6 – 0.9 meters (m), mean column velocity below 0.2 m/s, Froude number below 0.05, and Reynolds numbers below 50,000 (Figure 2). Mussels were most commonly found in habitats with mean substrate compaction less than 0.075 kg/cm² and showed highest suitability when MBSS < 2 dyn/cm² and in silt and boulder substrates (Figure 3).

For lower Colorado River *C. houstonensis*, suitability was highest at depths of 0.9 – 1.2 m, mean column velocities of 0.1 – 0.2 m/s, Froude numbers near 0.05, and Reynolds numbers of approximately 50,000 (Figure 4). They were most frequently found in habitats with mean substrate compaction from 0.025 – 0.05 kg/cm², in habitats with MBSS < 2 dyn/cm², and exhibited highest suitability in boulder substrates (Figure 5).

For lower Colorado River *C. petrina*, suitability was highest at depths from 0.6 – 0.9 m, mean column velocities below 0.2 m/s, Froude numbers below 0.05, and at Reynolds numbers below 150,000 (Figure 6). They were most commonly found where mean substrate compaction ranged from 0.025 - 0.075 kg/cm², at MBSS < 2 dyn/cm², and showed moderate suitability (0.5) in sand, boulder, and bedrock substrates (Figure 7).

Due to insufficient sample size (n = 9), HSC were not generated for lower Colorado River *T. macrodon*. However, data suggests highest utilization in depths of 0.6 – 0.9 m, in relatively low velocities, and in habitats with relatively low Froude and Reynolds numbers (Figure 8). They were most commonly found where substrate compaction and MBSS were relatively low, and Strauss Linear Index values for substrate were highest in silt (0.25), clay (0.09), and boulder (0.08) (Figure 9).

For Little River unionids in aggregate, HSC demonstrated highest habitat suitability at depths of 0.6 – 1.2 m, mean column velocity below 0.4 m/s, Froude number below 0.05, and Reynolds numbers below 100,000 (Figure 10). Mussels were most commonly found in habitats with mean substrate compaction less than 0.05 kg/cm² and showed highest suitability at an MBSS of 1.0 – 1.5 dyn/cm² and in silt substrates (Figure 11).

For Little River *C. houstonensis*, suitability was highest at depths of 0.9 – 2.7 m, mean column velocities of less than 0.4 m/s, Froude numbers less than 0.05, and Reynolds numbers below 600,000 (Figure 12). They were most commonly found in habitats with mean substrate compaction less than 0.05 kg/cm², in habitats with MBSS between 1.0 – 1.5 dyn/cm² and exhibited highest suitability in silt substrates (Figure 13).

Analysis of Bathymetric Change

Updated bathymetric data at each site allowed for analysis of changes in bed elevation between modeling periods. At Altair, comparisons of bed files between the two models showed that approximately 71% of overlapping areas exhibited an elevation change of 0.4 m or less (Figure 14). Maximum deposition of approximately 1.4 m was observed, with areas of considerable deposition occurring near the upstream boundary and near the downstream boundary of the site (Figure 15-16). Scour of over 6.4 m was observed due to the lateral erosion of a high cut bank near the downstream end of the site (Figure 15-16).

At La Grange, approximately 82% of overlapping area exhibited an elevation change of 0.4 m or less (Figure 17). Maximum deposition of 1.6 m was observed, with areas of maximum deposition occurring along the bank on the outside bend (Figure 18-19). Scour was noted along each side of a mid-channel gravel shoal/island near the downstream end of the site (Figure 18-19).

Hydraulic Model Updates

In total across both sites, 14 hydraulic model runs were conducted at flow tiers ranging from 50 cfs to 8,610 cfs (Table 3). For model runs in which field data were available for calibration ($n = 9$), 82% of the predicted water surface elevations matched observations within 5 cm (2 in) (Table 3). Only 3 upstream water surface elevation predictions were greater than 7 cm (~3 in) from observed water surface elevations (Table 3). For each model, differences between total inflow and total outflow was 0.2% or less.

Habitat Modeling Results

At Altair, node-specific calculations of shear stress ranged from 0 – 102 dyn/cm². Although shear stress generally increased with increasing flow rates, some areas experienced maximum shear stress under the lowest flow conditions. Habitat Suitability Criteria from this study suggest that mussels rarely inhabit areas with a shear stress over 5.0 dyn/cm² (Figure 3-13). Mussel HSC from the lower Brazos River show a similar trend of low to zero suitability at shear stress values over 5.0 dyn/cm² (Randklev 2014). Therefore, nodes with a shear stress of less than 5.0 dyn/cm² across all flow rates were labeled “persistent”. Much of the Altair study site was labeled as persistent, except for steeper high-energy areas along the eastern edge of the bedrock riffle and an area of constriction around a gravel bar at the downstream end (Figure 20).

At Altair, patterns in PWUA to discharge relationships for all three categories evaluated (aggregate unionids, *C. houstonensis*, *C. petrina*) were relatively consistent. For *C. petrina* and aggregate unionids, maximum PWUA was at the 287 cfs model run, with slight decreases at higher and lower flows (Table 4, Figure 21). PWUA for *C. houstonensis* peaked at the 981 cfs model run. To compare patterns across categories, PWUA was normalized to the percent of maximum in each category (Figure 22). At the lowest modeled flow of 100 cfs, 75-76% of

maximum habitat was available in all categories. Modeled habitat for all categories was greater than 98% of maximum at 287 and decreased to 80% of maximum for all categories at 525 cfs. Increases in PWUA were observed between 525 and 981 cfs, with 93-100% of maximum in each category at 981 cfs. Modeled habitat then dropped sharply to 45-46% of maximum at 1,459 cfs and dipped to 39-41% of maximum by 1,849 cfs.

At La Grange, node-specific calculations of shear stress ranged from 0 – 109 dyn/cm². As described above, nodes with a shear stress of less than 5.0 dyn/cm² across all flow rates were labeled “persistent”. Compared to Altair, persistent habitat was much more limited at La Grange, presumably due to the shallower depths and steeper longitudinal slope at this site. At La Grange, persistent habitat was limited mainly to bank areas and only extended across the channel in a pool below a steep bedrock riffle (Figure 23).

At La Grange, as at Altair, overall patterns in PWUA to discharge for all three categories evaluated (aggregate unionids, *C. houstonensis*, *C. petrina*) were relatively consistent. Model-predicted habitat availability peaked at the 100 cfs model run (Table 5, Figure 24) for all categories, and dropped to 92-99% of maximum at the 50 cfs model run (Figure 25). At the 250 cfs model run PWUA ranged from 93-95% of maximum for all categories. Predicted habitat then dropped to 63-71% of maximum by 738 cfs and reached lows of 49-57% at 2,000 cfs.

Habitat Model Validation

At Altair, CPUE ranged from 0.00-107.14 mussels/p-h (mean CPUE: 7.41 mussels/p-h) for aggregate mussels, 0.00-44.00 mussels/p-h (mean CPUE: 2.17 mussels/p-h) for *C. houstonensis*, and 0.00-3.53 mussels/p-h (mean CPUE: 0.36 mussels/p-h) for *C. petrina*. Model predictions of habitat at 287 cfs compared well to mean CPUE from validation sampling efforts for both *C. houstonensis* and aggregate mussels. For *C. houstonensis*, mean CPUE ranged from

0.18-0.51 mussels/p-h in non-persistent habitat and ranged from 1.22-3.35 mussels/p-h in persistent habitat, with the maximum CPUE observed in high-quality persistent habitat (Figure 26). For aggregate mussels, mean CPUE ranged from 2.64-3.30 mussels/p-h in non-persistent habitat and ranged from 2.01-10.63 in persistent habitat, with the maximum CPUE observed in high-quality persistent habitat. For *C. petrina*, trends in CPUE did not match as well with modeled habitat predictions. Mean CPUE for *C. petrina* ranged from 0.00-1.30 and was actually highest in low-quality non-persistent habitat. Broader HSC for *C. petrina* resulted in large expanses of predicted high-quality habitat in persistent areas and the species was not documented at many of the sites within these areas. Maps demonstrating predicted habitat for all three categories at 287 cfs and CPUE from mussel validation sampling are provided in Figures 27-29.

At La Grange, CPUE ranged from 0.00-18.75 mussels/person-hr (mean CPUE: 0.38 mussels/person-hr) for aggregate mussels and 0.00-17.50 mussels/person-hr (mean CPUE: 0.28 mussels/person-hr) for *C. houstonensis*. Model predictions of habitat at 100 cfs compared well to mean CPUE from validation sampling efforts for all aggregate mussels, as well as for *C. houstonensis*. Only one mussel was collected in non-persistent habitat (mean CPUE range: 0.00-0.06), mean CPUE ranged from 0.00-0.46 mussels/p-h in low-quality persistent habitat, and mean CPUE was highest in high-quality persistent habitat for all aggregate mussels and *C. houstonensis* (mean CPUE range: 2.47-2.61 mussels/p-h) (Figure 30). Maps of predicted habitat at 100 cfs and CPUE from mussel validation sampling are provided in Figures 31-32. Despite considerable predicted habitat, no *C. petrina* were collected from the La Grange site.

Discussion

Habitat Suitability Criteria

Habitat suitability criteria developed from survey data suggest that freshwater mussels in the lower Colorado River are most commonly utilizing moderate-depth low-energy habitats with silt and boulder substrates. Compared to all mussels in aggregate, *C. houstonensis* showed lower suitability in areas with 0 velocity, 0 turbulence, and 0 substrate compaction. *Cyclonaias petrina* showed broader curves for mean column velocity, Froude number, Reynolds number, and MBSS, suggesting increased utilization of high-energy environments compared to all mussels in aggregate.

Bathymetric Changes

As quantified above, substantial bathymetric changes to each of the selected hydraulic model sites were noted between development of the original models in 2008 and the updated models in 2018. Based on observations of the study team, the majority of these changes were due to a large high-flow event following Hurricane Harvey in August-September 2017 in which discharge at the USGS gauge at Columbus (#08161000) peaked at approximately 160,000 cfs. Data from an ongoing mark-recapture study (Bonner et al. 2018) demonstrated that this event impacted mussel densities at the Altair study site. Within the mark-recapture study site, a 300-m² area located within the hydraulic model, scouring was observed from about 0.15 m (0.5 ft) to greater than 0.3 m (1 ft) (Figure 15). Post-hurricane monitoring revealed a sharp decrease in overall unionid taxa richness and density within this area (Bonner et al. 2018). These results suggest that unionids resistance to high flows may be related to the magnitude of sediment erosion that occurs within a patch of occupied habitat. However, mussel validation data collected in summer 2018 demonstrates that freshwater mussels (including candidate species)

persist at the hydraulic model site, in high abundance at some locations. Additionally, because this high-flow event likely displaced mussels inhabiting “marginal” habitats, mussel CPUE data from summer 2018 likely represents a good snapshot of high-quality persistent habitat for use in model validation.

Model Validation

Validation data presented above demonstrate that model predictions of persistent habitat were useful in predicting areas of potential mussel habitat and that HSC based on hydraulic parameters were useful in identifying areas of high-quality habitat within these patches. At Altair, areas of highest mussel CPUE occurred within or in close proximity to persistent areas predicted to be highly suitable. However, multiple areas of zero CPUE also occurred in predicted habitats suggesting that criteria could potentially be further refined or that factors other than habitat availability may be important in structuring mussel assemblages at this site. At La Grange, the persistent habitat layer did a better job of excluding poor habitat, and few areas of zero CPUE occurred in persistent habitat patches. Many sites of zero CPUE occurred in mid-channel areas that experience high shear stress under higher flow conditions. Additionally, areas of high mussel CPUE were most-often found in predicted high quality habitat within persistent patches.

The less-predictive persistent habitat layer at Altair may be due to the abundance of deep pool habitats at the Altair site. These deeper areas qualify as persistent habitat due to low shear stress under all flow scenarios modeled. It should also be noted that modeling of higher flow scenarios could result in a decrease in persistent habitat availability at Altair. The 8,297 cfs flow rate modeled at Altair represents approximately the 90th percentile flow at this site. Although sporadic, even higher flows are important in structuring the mussel assemblage, as noted during

the mark-recapture study at this site following the 160,000 cfs event (Bonner et al. 2018).

Regardless, validation results support that the combination of defining persistent habitat and calculating habitat suitability under base flow conditions within these areas is useful in modeling mussel habitat availability.

Environmental Flow Considerations - Altair

For the habitat modeling analysis above to be useful in evaluating environmental flow recommendations, results must be put in context of existing TCEQ Environmental Flow Standards for the lower Colorado River (TCEQ 2012). For the Altair site, the nearest gauge with an environmental flow standard is the Colorado River at Columbus (USGS gauge #08161000). Depending on season and hydrologic condition, subsistence standards at this gauge range from 190-534 cfs, and base flows range from 310-1,440 cfs (Table 6). Freshwater mussel habitat modeling at Altair shows that at 190 cfs, freshwater mussel PWUA for all categories is maintained at approximately 85-90% of maximum, suggesting that from a strictly habitat standpoint, this subsistence recommendation is protective. It should be noted that under subsistence flow conditions water quality considerations such as temperature and dissolved oxygen may influence mussel communities. Although considerable data on the influence of sub-lethal water quality stressors on these candidate mussel species was produced during Task 2 of this study (Bonner et al. 2018), no water quality modeling was conducted as part of this study.

At base flow levels of 310-1,440 cfs mussel PWUA is variable. At flows from 310-981 cfs mussel PWUA is maintained at greater than or equal to 80% of maximum for all categories. However, at flows between 1,000 cfs and 1,440 cfs, PWUA drops sharply, to 45-46% of maximum at 1,459 cfs. In the Columbus environmental flow standards, base flow levels exceed 1,000 cfs on three occasions – in March under Average conditions (1,020 cfs), in May under

Average conditions (1,316 cfs) and in June under Average conditions (1,440 cfs). This analysis suggests that current base flow standards for Average conditions in May and June at Columbus may temporarily limit mussel habitat availability.

Environmental Flow Considerations – La Grange

For the La Grange site, the nearest upstream gauge with an environmental flow standard is the Colorado River at Bastrop. Depending on season and hydrologic condition, subsistence flow standards at this gauge range from 123-275 cfs, and base flow standards range from 194-824 cfs (Table 6). Freshwater mussel habitat modeling at La Grange demonstrates that PWUA peaks at the 100 cfs flow rate for all categories modeled, maintaining greater than 92% of maximum for all categories from 50-250 cfs. This suggests that from a strictly-habitat-availability perspective, subsistence flow recommendations are protective of mussel habitat.

In the base flow range of 194-824 cfs, mussel habitat availability ranges from approximately 60-70% of maximum on the high end to greater than 95% of maximum at the low end. As at Altair, lower base flow standards maximize model predictions of freshwater mussel PWUA, whereas higher base flow recommendations result in more limited habitat predictions. However, at La Grange, even under the maximum base flow recommendations in the standards, mussel PWUA stays above 60% of maximum.

Pulse Flows and Freshwater Mussels

From a pulse flow perspective, higher flows limit habitat availability for mussels and larger pulses may result in downstream displacement when shear stress becomes too high for mussel persistence. However, these same pulses are important from an ecological perspective by increasing inputs of nutrients and organic matter that are key to mussel diets (Bonner et al. 2018,

Task 2.5) and maintaining habitat heterogeneity (Poff et al. 1997). Pulse flows also provide a variety of ecological services to fish, riparian, and wildlife communities (Poff et al. 1997).

Further research is needed to elucidate relationships between mussel ecology and pulse flow events, and therefore, no analysis of pulse flow standards relative to mussels is presented herein.

Environmental Flow Considerations – Brazos Desktop Analysis

For most parameters (depth, velocity, Froude number, Reynolds number, substrate compaction, and shear stress) Little River unionids showed similar HSC to lower Colorado River unionids. However, substrate criteria were quite different due to differences in available habitat between the two systems. No boulder or bedrock substrates were encountered during surveys in the Little River basin, whereas these substrates showed high suitability in the lower Colorado River. Additionally, large differences in *C. houstonensis* HSC were apparent between systems. Species-specific HSC are based on smaller sample sizes than aggregate HSC, and therefore, are inherently more variable. Habitat modeling results presented above demonstrate that in the lower Colorado River, species-specific HSC for candidate mussels reacted similarly to aggregate HSC, and therefore, use of more consistent and statistically-robust aggregate HSC is likely sufficient for future studies.

Lower Colorado River mussel habitat modeling presented above demonstrates that mussel habitat availability peaks at flows lower than most fish habitat guilds used in previous instream modeling work in this basin (BIO-WEST 2008). Given this, and the observation that aggregate mussel HSC show similar utilization of most hydraulic variables between systems, similar results may be expected in the Brazos system, although additional site-specific modeling would be needed to confirm. A recent instream flow study conducted on the middle and lower Brazos River by the Texas Instream Flow Program (TIFP) included evaluation of mussel HSC

and persistent habitat (TIFP 2018). However, mussel habitat availability did not appear to be a major factor in setting instream flow recommendations during this study. In contrast, mussel thermal tolerance data was used to inform subsistence and base flow recommendations.

Conclusions

In conclusion, the two-step modeling approach presented above was successful in predicting mussel occurrence and abundance with mean CPUE data generally being higher in predicted high-quality habitat than in low-quality or non-persistent habitats. The approach of evaluating persistent habitat in combination with more traditional analysis of HSC and resulting WUA calculations provides a good method of accounting for persistent habitat across a wide-range of flow conditions while still recognizing selective habitat utilization of freshwater mussels. Species-specific criteria reacted similarly to aggregate criteria but were more variable and therefore less predictive. This suggests that aggregate mussel criteria based on more robust datasets may be sufficient for use in future studies, particularly when dealing with rare species and small sample sizes. The methods applied herein and the subsequent modeling results for the lower Colorado River will no doubt be useful in validating and refining instream flow standards in this basin, and potentially others, in the future.

It should be recognized that instream flow recommendations based solely on the mussel habitat modeling conducted above would result in lower base flow and potentially lower subsistence flow recommendations. However, a holistic approach is necessary when setting instream flow recommendations. While mussel habitat availability is an important consideration, it is only one component of many to be analyzed when developing ecologically-protective environmental flow recommendations. Mussel survival and recruitment could potentially be limited by water quality conditions under low flow situations. Applied research laboratory

studies conducted as a component of Task 2 of this study (Bonner et al. 2018) have provided crucial information regarding sublethal influences of water quality stressors on candidate species in the Colorado River basin. However, since this data became available, no water quality modeling studies have been conducted to integrate this new information with water quality data from the lower Colorado River.

Additionally, habitat availability for all organisms must be evaluated when setting instream flow recommendations. Previous studies have shown that habitat availability for most fish habitat guilds peak at higher flows than those for mussels presented above (BIO-WEST 2008). For the state-threatened Blue Sucker *Cycleptus elongatus*, habitat availability peaked at 2,000-2,500 cfs at the La Grange and Altair model sites (BIO-WEST 2008). High pulse flows, although they may potentially impact mussel persistence, are important for water availability and ecosystem disturbance within the riparian community (Stromberg et al. 2007). When setting instream flow recommendations, the mussel habitat modeling results presented above should be integrated with existing information for fish and riparian communities and should also include evaluation of sediment transport and other important physical components of a healthy riverine system. The above analysis fills a critical data gap in this process by providing information on mussel habitat availability in the lower Colorado River, and provides a new method for modeling mussel habitat in riverine systems.

Tables

Table 1. Results of mussel surveys at ten previously established LSWP intensive study sites on the Lower Colorado River. ^a*C. houstonensis*, ^b*C. petrina*, ^c*T. macrodon*

LSWP Site	Search Time (person-hours)	Mussel Abundance	CPUE (mussels/p-h)	Number of Candidate Species Present
Longhorn Dam	6	0	0.0	0
Uteley	11	28	2.5	0
Bastrop	6	0	0.0	0
Smithville - US	6	0	0.0	0
Smithville - DS	6	0	0.0	0
La Grange ^a	11	74	6.7	1
Columbus ^{a,b}	10	88	8.8	2
Altair ^{a,b,c}	13	619	47.6	3
Wharton ^{a,b,c}	11	35	3.2	3
Lane City ^{b,c}	5	18	3.6	2
	85	862	10.1	

Table 2. Bed roughness values (k_s ; cm) for each substrate type used in estimating shear stress. Values approximate median particle size for each substrate type from the Wentworth scale, except for bedrock. Values for bedrock were estimated based on perceived roughness of local bedrock material in comparison to other classes.

Substrate Class	k_s (cm)
Clay	0.0002
Silt	0.0016
Sand	0.05
Gravel	1.6
Cobble	6.4
Boulder	25
Bedrock	2

Table 3. Hydraulic model runs and associated water surface elevation calibration results.

Site	Discharge		Upstream			Mid-reach			Downstream		
	cms	cfs	Observed (m)	Predicted (m)	Δ (cm)	Observed (m)	Predicted (m)	Δ (cm)	Observed (m)	Predicted (m)	Δ (cm)
La Grange	1.42	50	NA	67.67	NA	NA	NA	NA	NA	66.11	NA
	2.83	100	NA	67.73	NA	NA	NA	NA	NA	66.21	NA
	7.08	250	NA	67.83	NA	NA	NA	NA	NA	66.34	NA
	12.74	450	67.97	67.93	4	66.61	66.57	4	66.61	66.60	1
						67.21	67.20	1			
	20.90	738	68.10	68.03	7	NA	NA	NA	66.60	66.62	-2
	56.63	2000	68.39	68.37	2	NA	NA	NA	67.01	67.02	-1
	243.81	8610	69.47	69.54	-7	NA	NA	NA	68.58	68.62	-2
Altair	2.83	100	NA	41.97	NA	NA	NA	NA	NA	38.53	NA
	9.81	287	42.40	42.33	7	NA	NA	NA	42.23	42.22	1
	14.87	525	42.43	42.46	-3	42.20	42.24	-4	42.24	42.24	0
						42.31	42.35	-4			
	27.78	981	42.74	42.69	5	NA	NA	NA	42.32	42.32	0
	41.39	1459	42.91	42.86	5	NA	NA	NA	42.36	42.36	0
	52.36	1849	43.00	42.98	2	NA	NA	NA	42.40	42.40	0
	234.95	8297	44.34	44.1	24	NA	NA	NA	42.77	42.77	0

Table 4. Model-predicted Persistent Weighted Usable Area (PWUA) from base flow rates at the Altair site.

Modeled Discharge (cms)	Modeled Discharge (cfs)	Aggregate Unionids		<i>C. houstonensis</i>		<i>C. petrina</i>	
		PWUA (m ²)	PWUA (% max)	PWUA (m ²)	PWUA (% max)	PWUA (m ²)	PWUA (% max)
2.83	100	50,336	76	42,781	75	65,024	76
8.13	287	66,072	100	55,987	98	85,116	100
14.87	525	52,626	80	45,718	80	67,994	80
27.78	981	62,113	94	57,345	100	79,301	93
41.39	1459	30,634	46	26,064	45	37,975	45
52.36	1879	27,138	41	22,824	40	32,920	39

Table 5. Model-predicted Persistent Weighted Usable Area (PWUA) from base flow rates at the La Grange site.

Modeled Discharge (cms)	Modeled Discharge (cfs)	Aggregate Unionids		<i>C. houstonensis</i>		<i>C. petrina</i>	
		PWUA (m ²)	PWUA (% max)	PWUA (m ²)	PWUA (% max)	PWUA (m ²)	PWUA (% max)
1.42	50	16,106	99	13,256	92	19,842	95
2.83	100	16,303	100	14,392	100	20,985	100
7.08	250	15,261	94	13,365	93	19,932	95
12.74	450	12,821	79	10,905	76	17,344	83
20.9	738	11,066	68	9,105	63	14,996	71
56.63	2000	8,872	54	6,986	49	12,032	57

Table 6. Ranges of TCEQ environmental flow standards for the lower Colorado River at Bastrop and Columbus. Specific subsistence and base flow standards vary depending on season and hydrologic condition.

Measurement Site	Environmental Flow Standards (cfs)				
	Subsistence	Base	2 per season	1 per 18 months	1 per 2 years
Bastrop	123-275	194-824	3000	8000	NA
Columbus	190-534	310-1440	3000	8000	27000

Figures

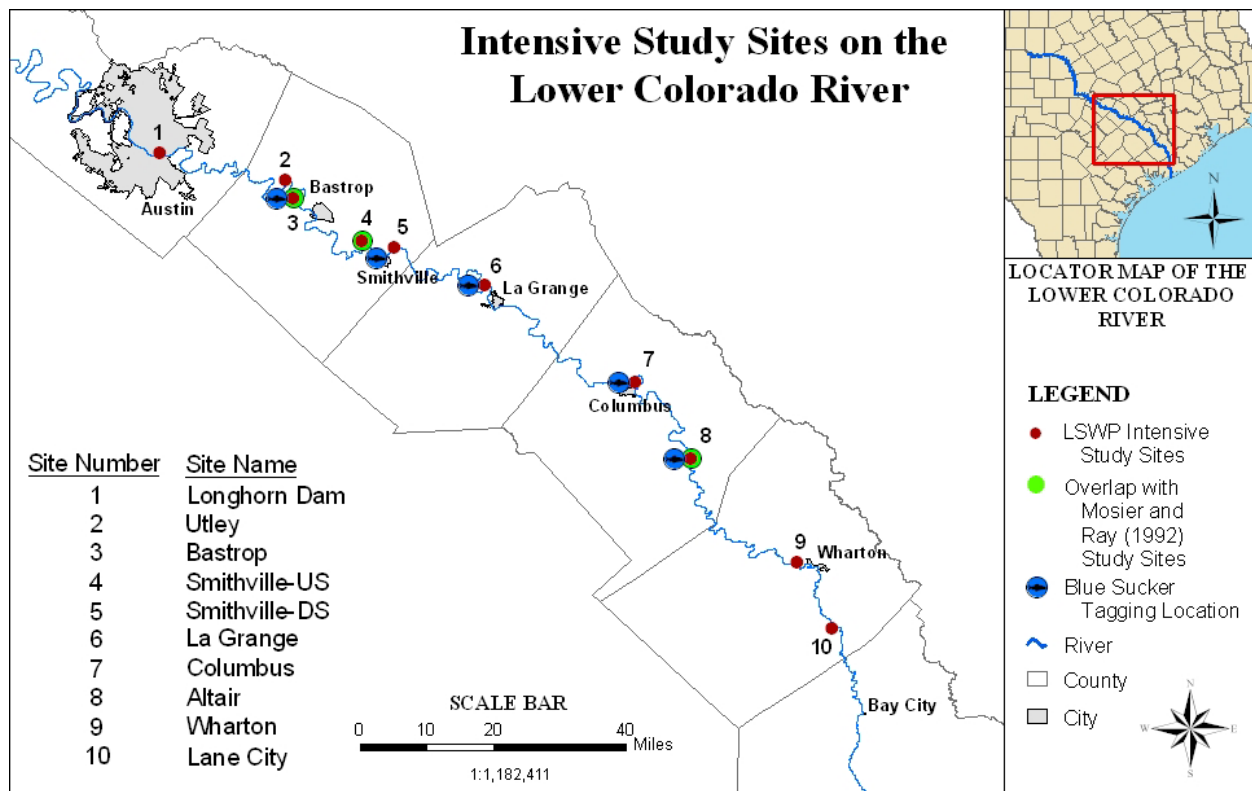


Figure 1. LSWP intensive study sites with existing hydraulic models.

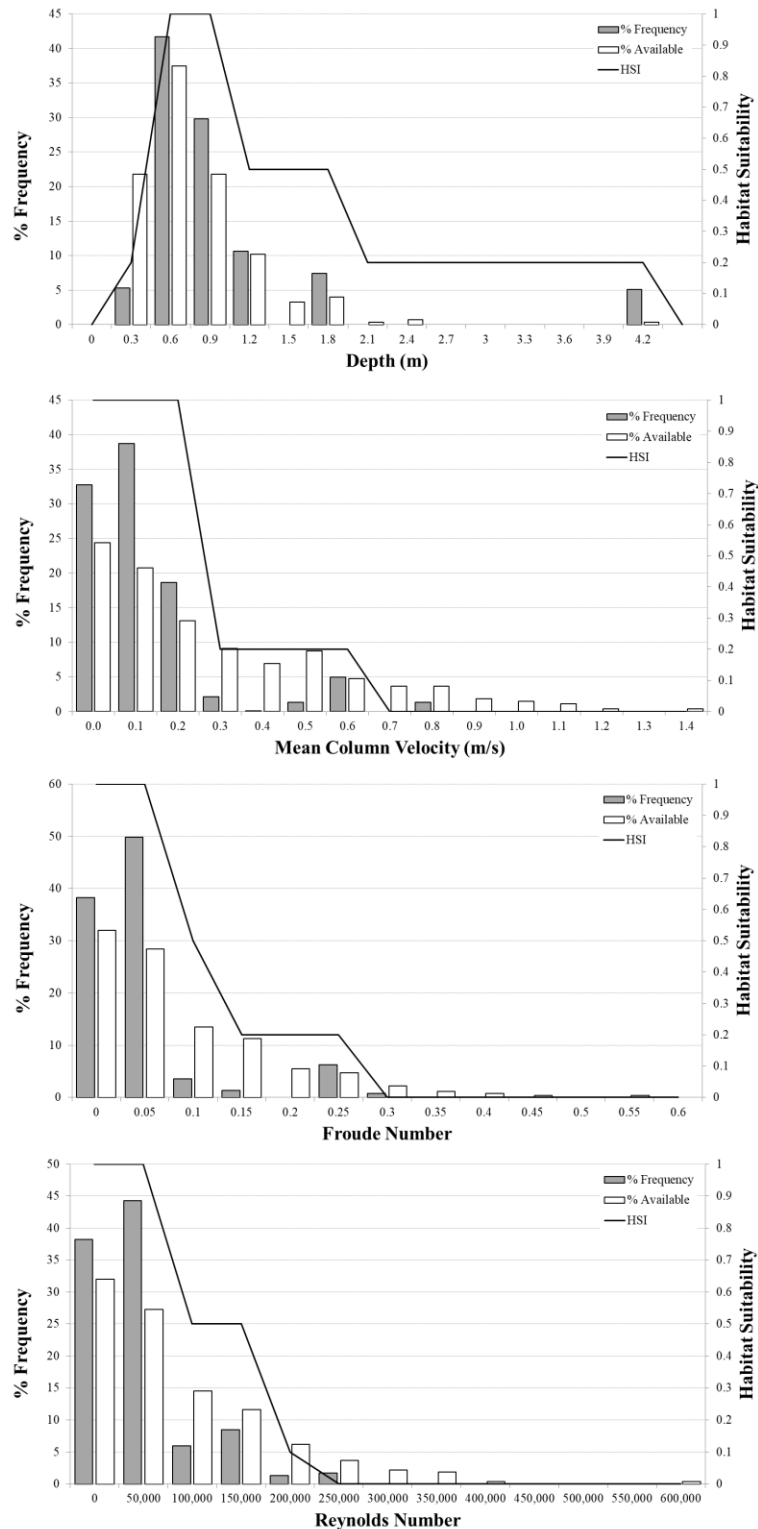


Figure 2. Percent frequency of occurrence (gray bars), percent frequency of habitats sampled (white bars), and habitat suitability values (black line) for lower Colorado River unionids ($n = 2327$) in relation to depth (m), mean column velocity (m/s), Froude number, and Reynolds number.

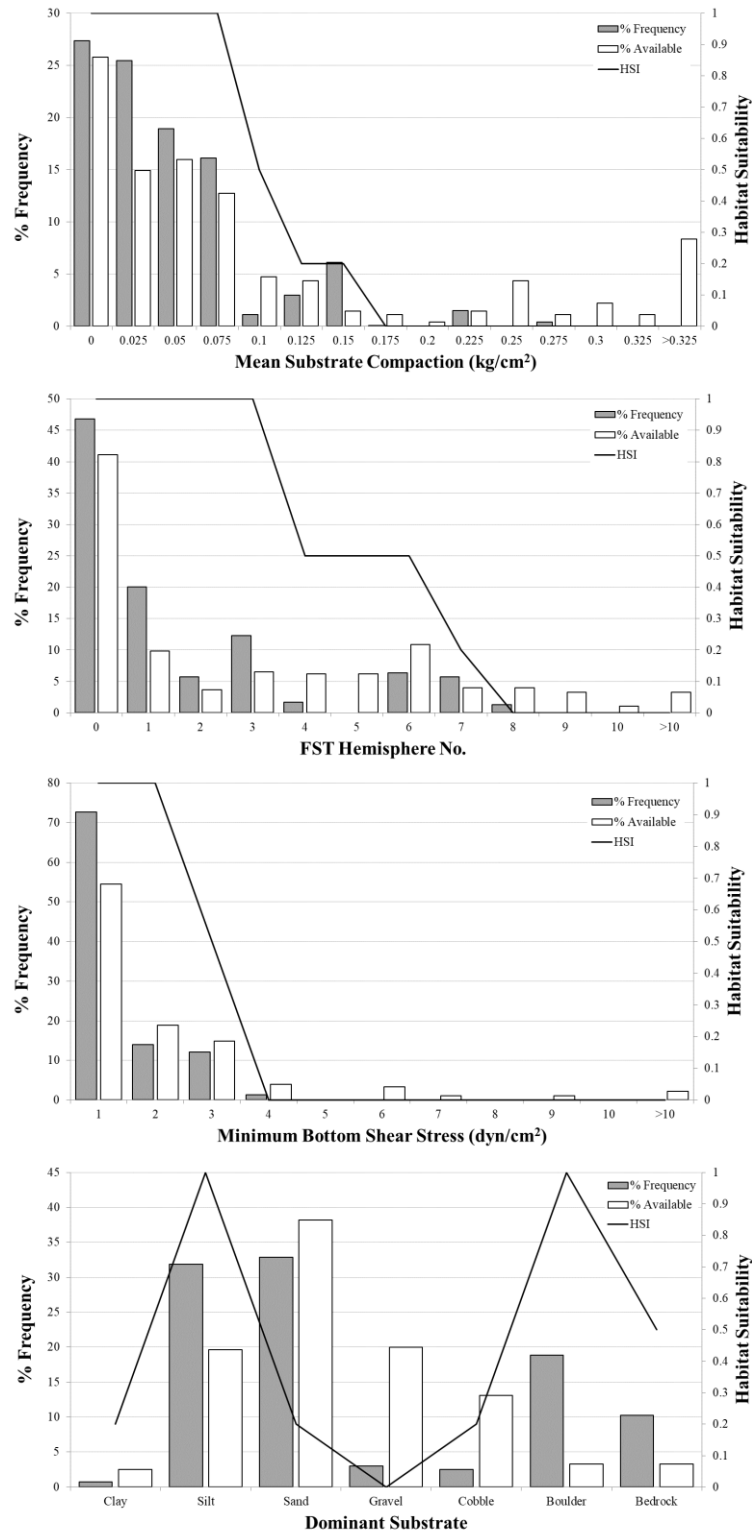


Figure 3. Percent frequency of occurrence (gray bars), percent frequency of habitats sampled (white bars), and habitat suitability values (black line) for lower Colorado River unionids ($n = 2327$) in relation to mean substrate compaction (kg/cm^2), FST hemisphere number, minimum bottom shear stress (dyn/cm^2), and dominant substrate.

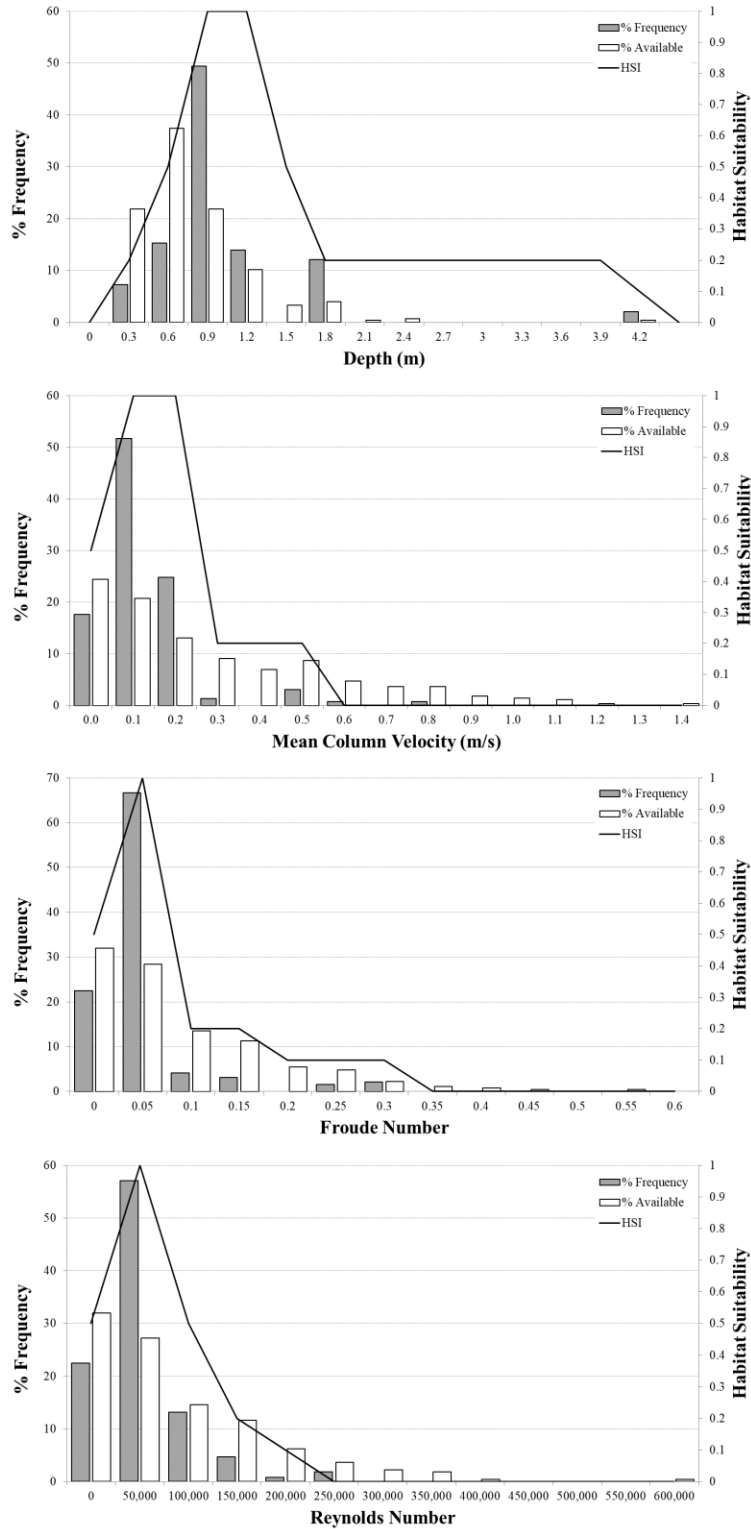


Figure 4. Percent frequency of occurrence (gray bars), percent frequency of habitats sampled (white bars), and habitat suitability values (black line) for lower Colorado River *C. houstonensis* (n = 387) in relation to depth (m), mean column velocity (m/s), Froude number, and Reynolds number.

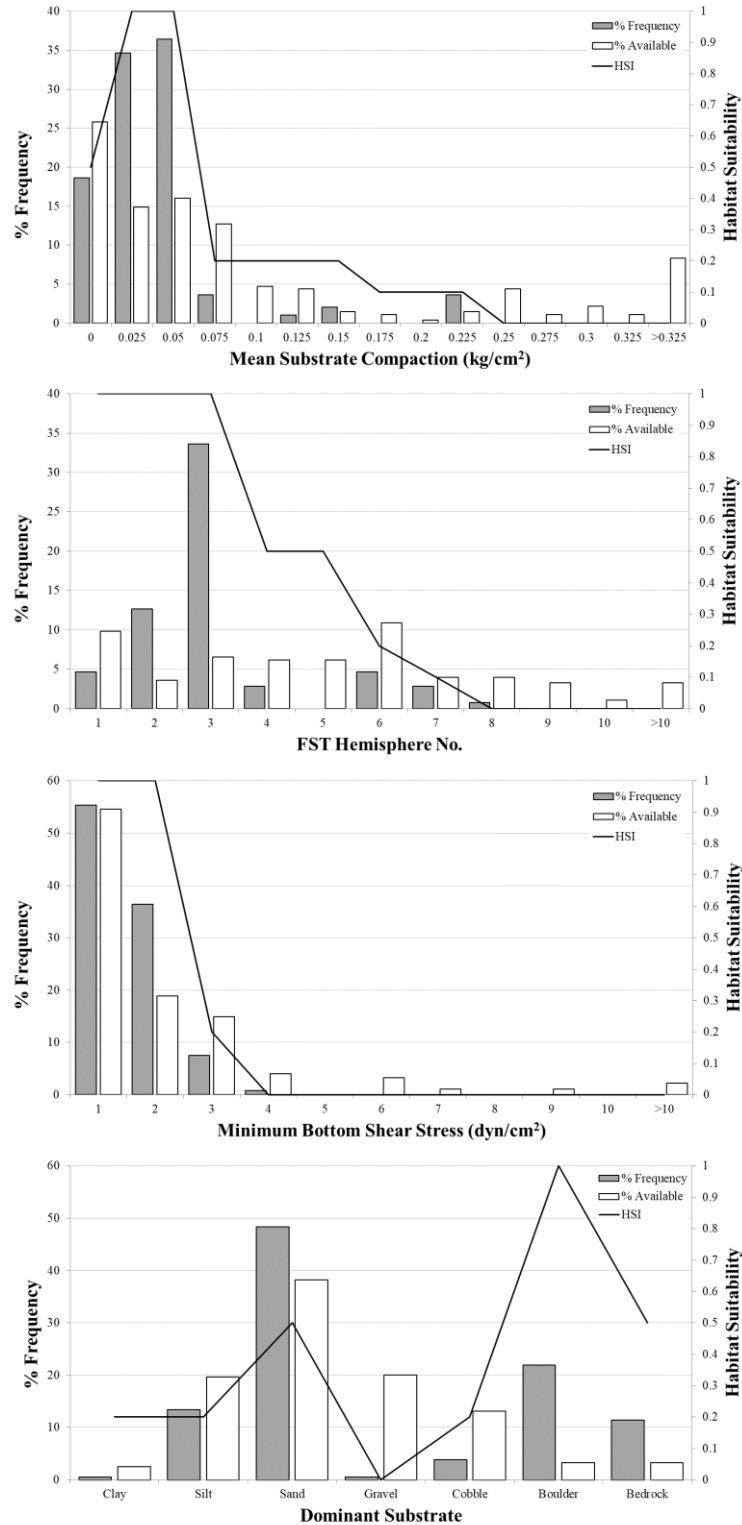


Figure 5. Percent frequency of occurrence (gray bars), percent frequency of habitats sampled (white bars), and habitat suitability values (black line) for lower Colorado River *C. houstonensis* (n = 387) in relation to mean substrate compaction (kg/cm²), FST hemisphere number, minimum bottom shear stress (dyn/cm²), and dominant substrate.

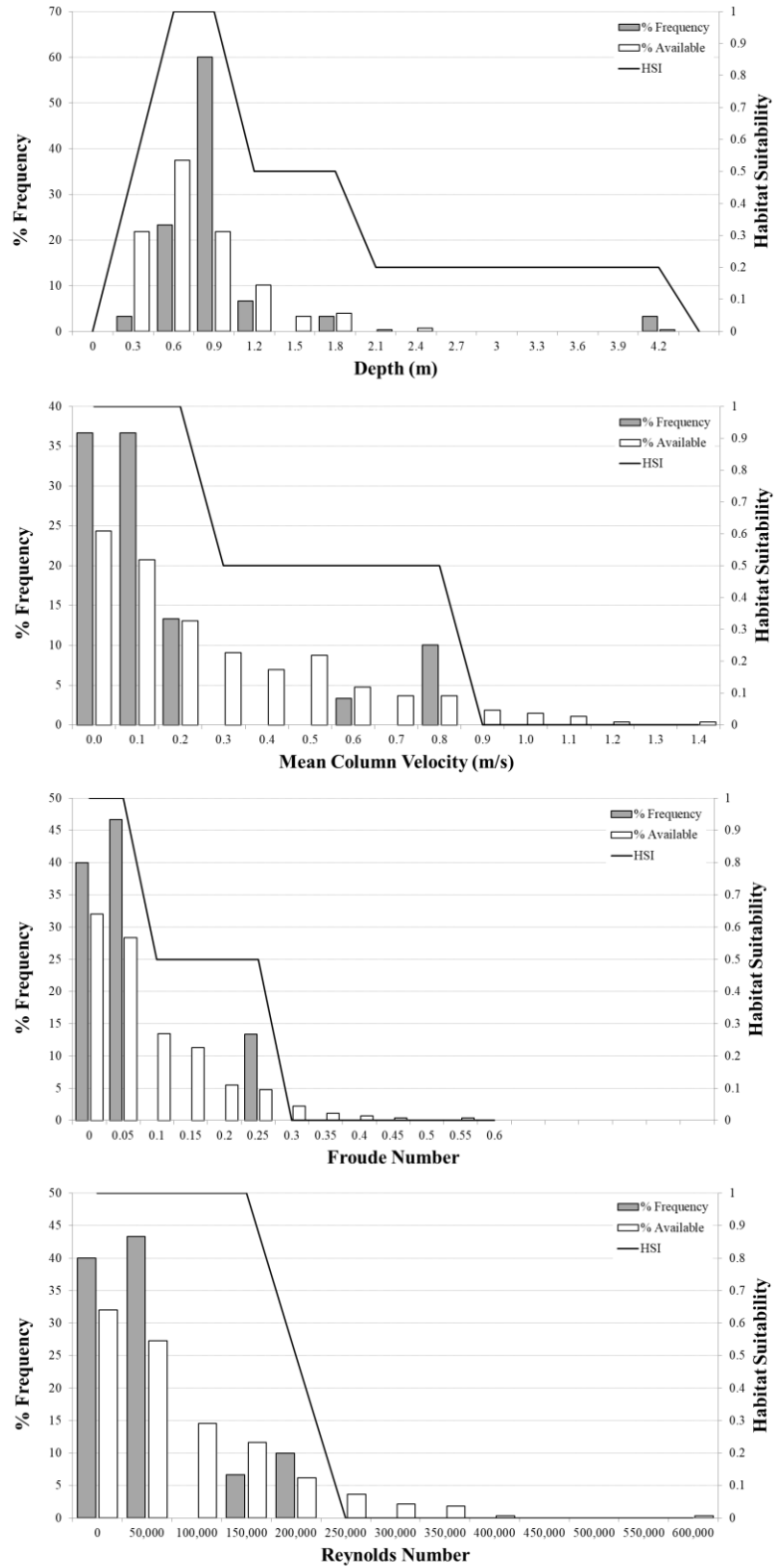


Figure 6. Percent frequency of occurrence (gray bars), percent frequency of habitats sampled (white bars), and habitat suitability values (black line) for lower Colorado River *C. petrina* (n = 30) in relation to depth (m), mean column velocity (m/s), Froude number, and Reynolds number.

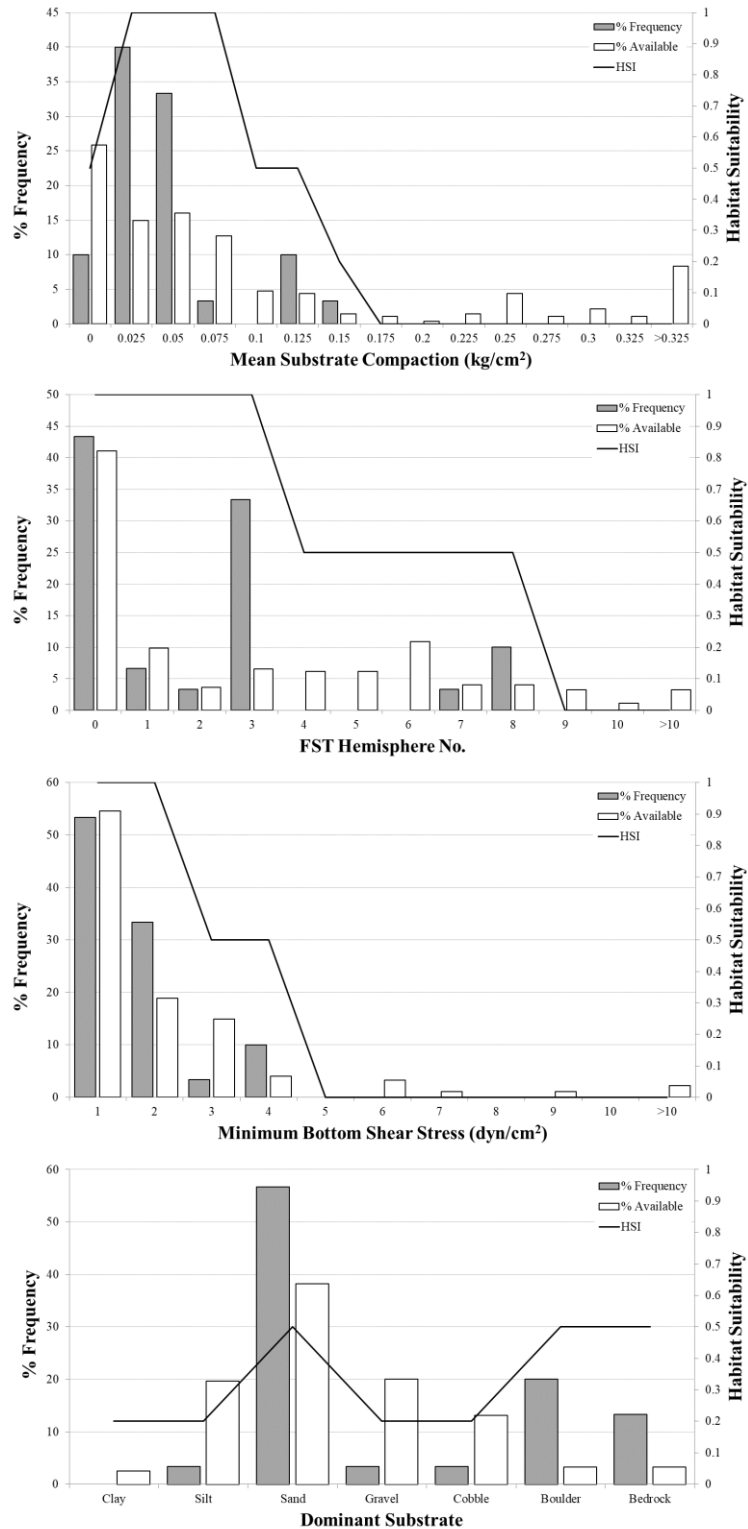


Figure 7. Percent frequency of occurrence (gray bars), percent frequency of habitats sampled (white bars), and habitat suitability values (black line) for lower Colorado River *C. petrina* (n = 30) in relation to mean substrate compaction (kg/cm²), FST hemisphere number, minimum bottom shear stress (dyn/cm²), and dominant substrate.

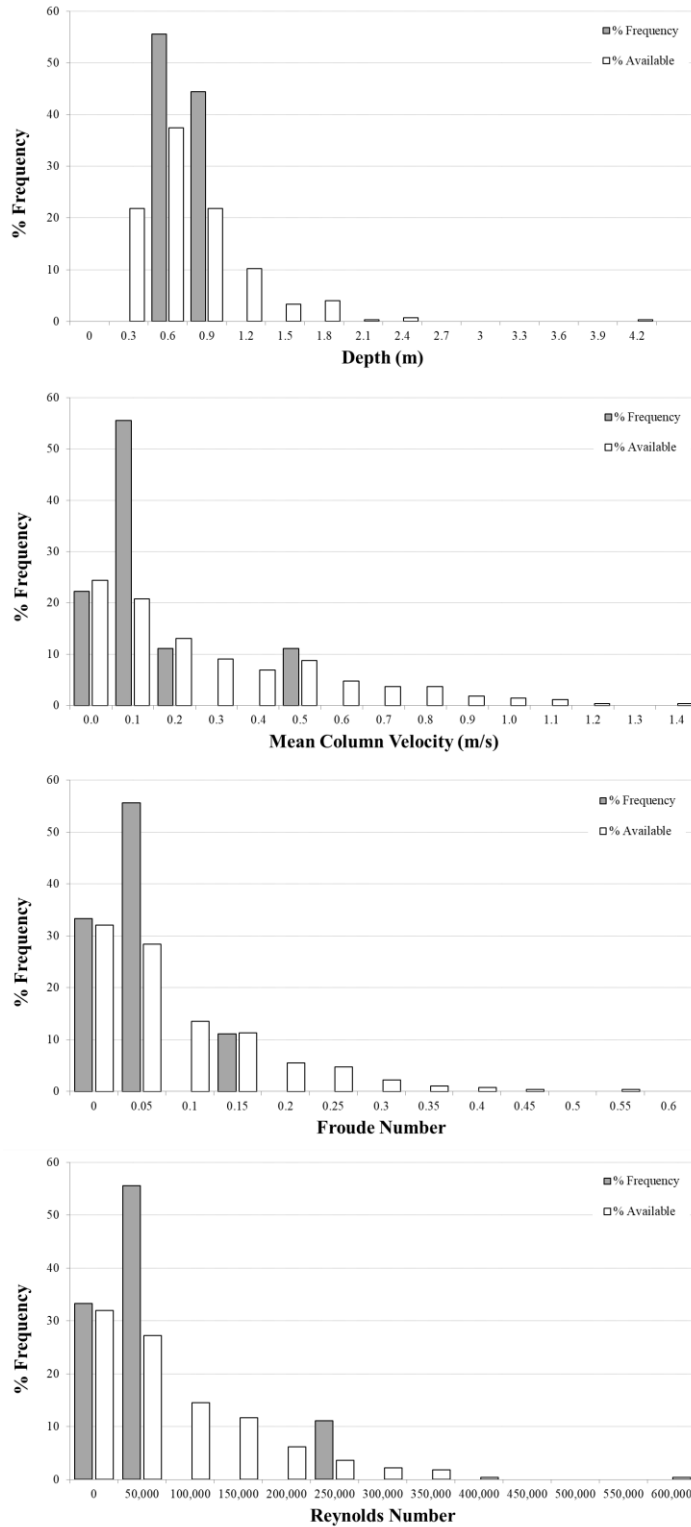


Figure 8. Percent frequency of occurrence (gray bars) and percent frequency of habitats sampled (white bars) for lower Colorado River *T. macodon* (n = 9) in relation to depth (m), mean column velocity (m/s), Froude number, and Reynolds number. HSC were not generated for *T. macodon* due to insufficient sample size.

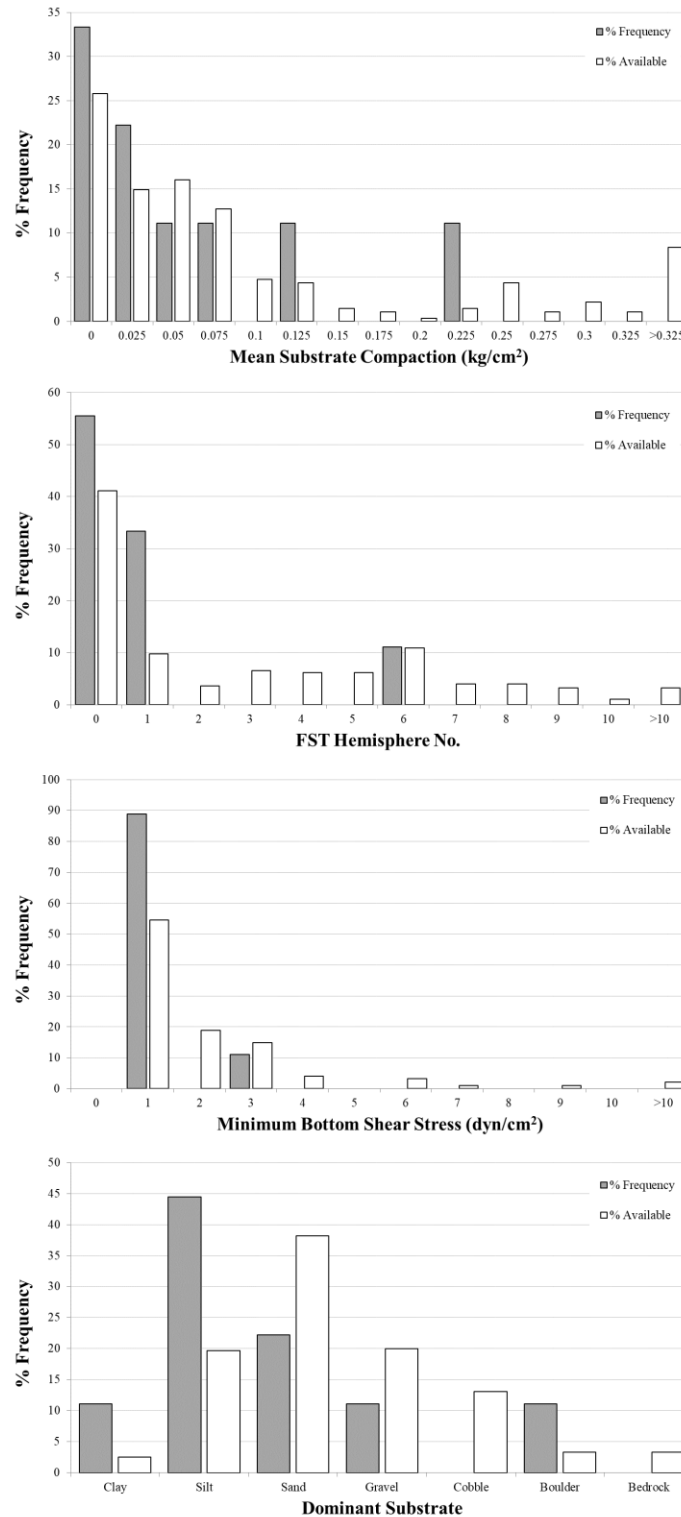


Figure 9. Percent frequency of occurrence (gray bars) and percent frequency of habitats sampled (white bars) for lower Colorado River *T. macrodon* (n = 9) in relation to mean substrate compaction (kg/cm²), FST hemisphere number, minimum bottom shear stress (dyn/cm²), and dominant substrate. HSC were not generated for *T. macodon* due to insufficient sample size.

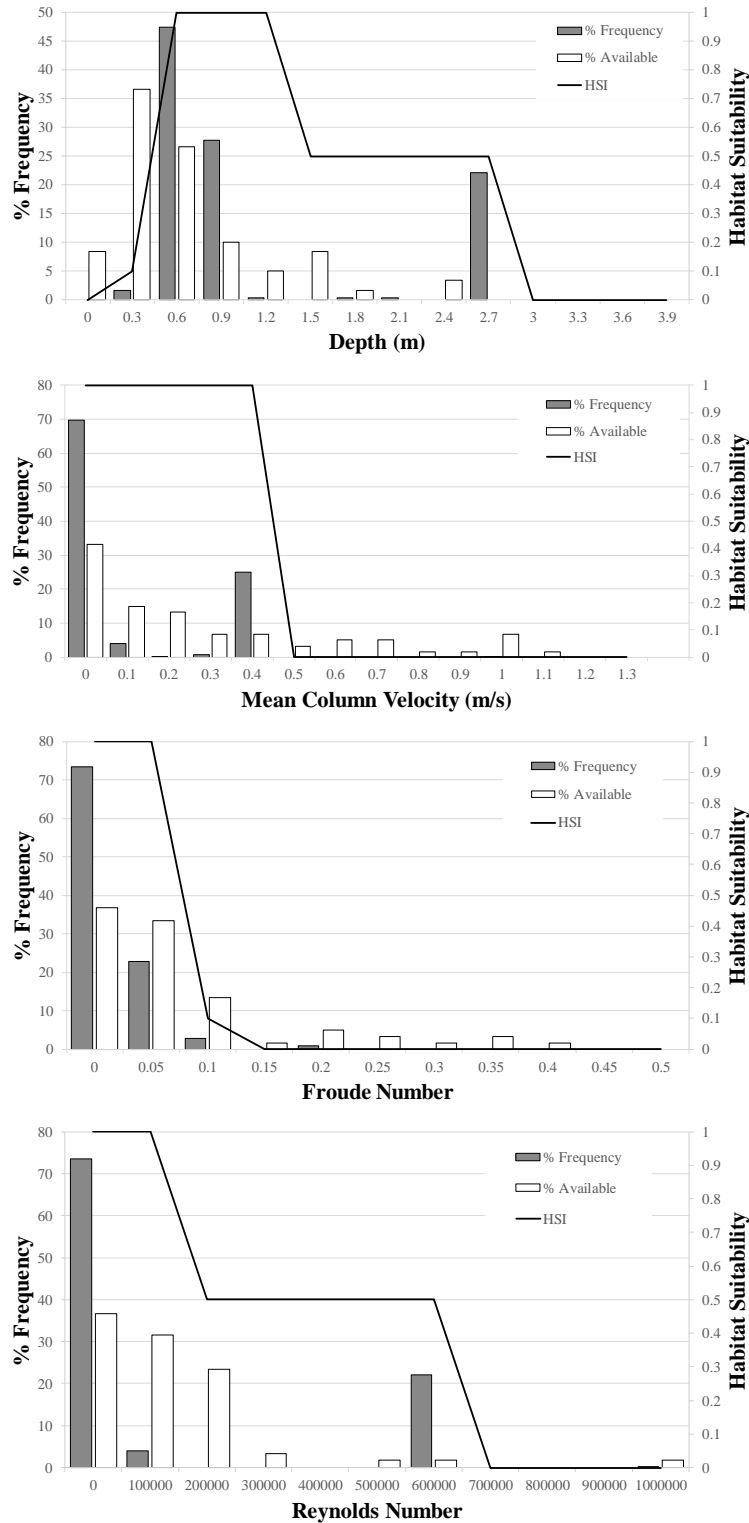


Figure 10. Percent frequency of occurrence (gray bars), percent frequency of habitats sampled (white bars), and habitat suitability values (black line) for Little River unionids ($n = 320$) in relation to depth (m), mean column velocity (m/s), Froude number, and Reynolds number.

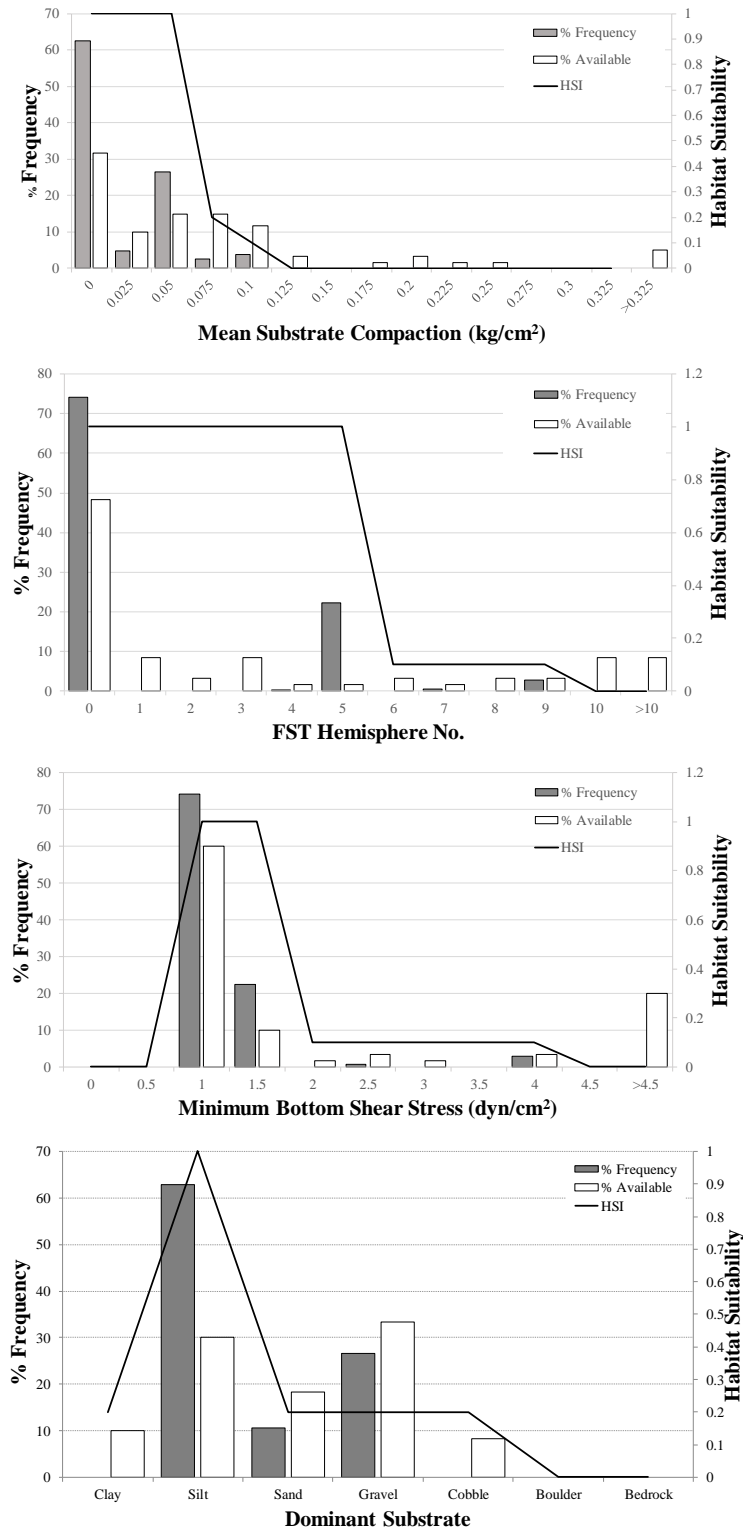


Figure 11. Percent frequency of occurrence (gray bars), percent frequency of habitats sampled (white bars), and habitat suitability values (black line) for Little River unionids (n = 320) in relation to mean substrate compaction (kg/cm²), FST hemisphere number, minimum bottom shear stress (dyn/cm²), and dominant substrate.

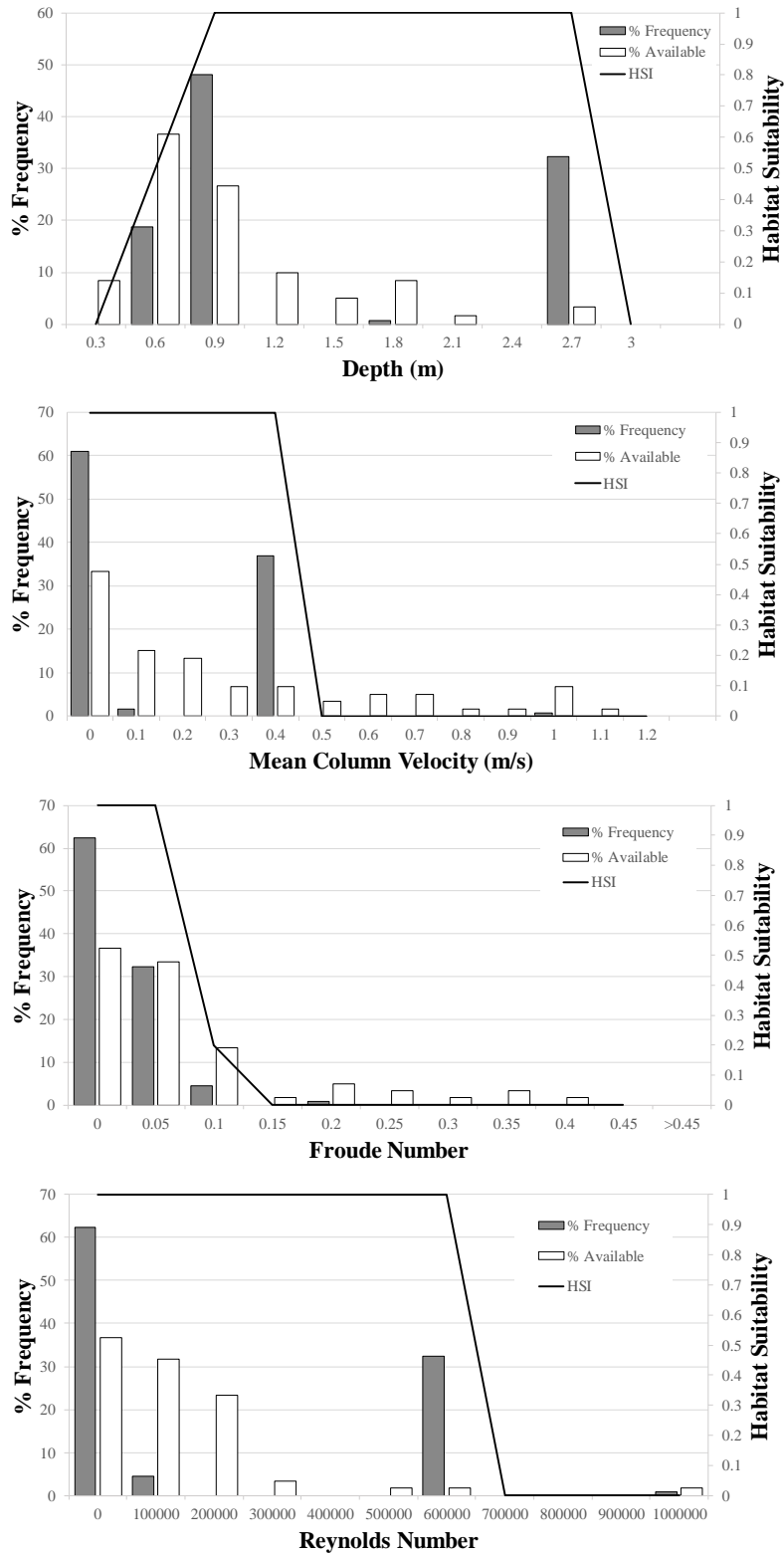


Figure 12. Percent frequency of occurrence (gray bars) and percent frequency of habitats sampled (white bars) for Little River *C. houstonensis* (n = 133) in relation to in relation to depth (m), mean column velocity (m/s), Froude number, and Reynolds number.

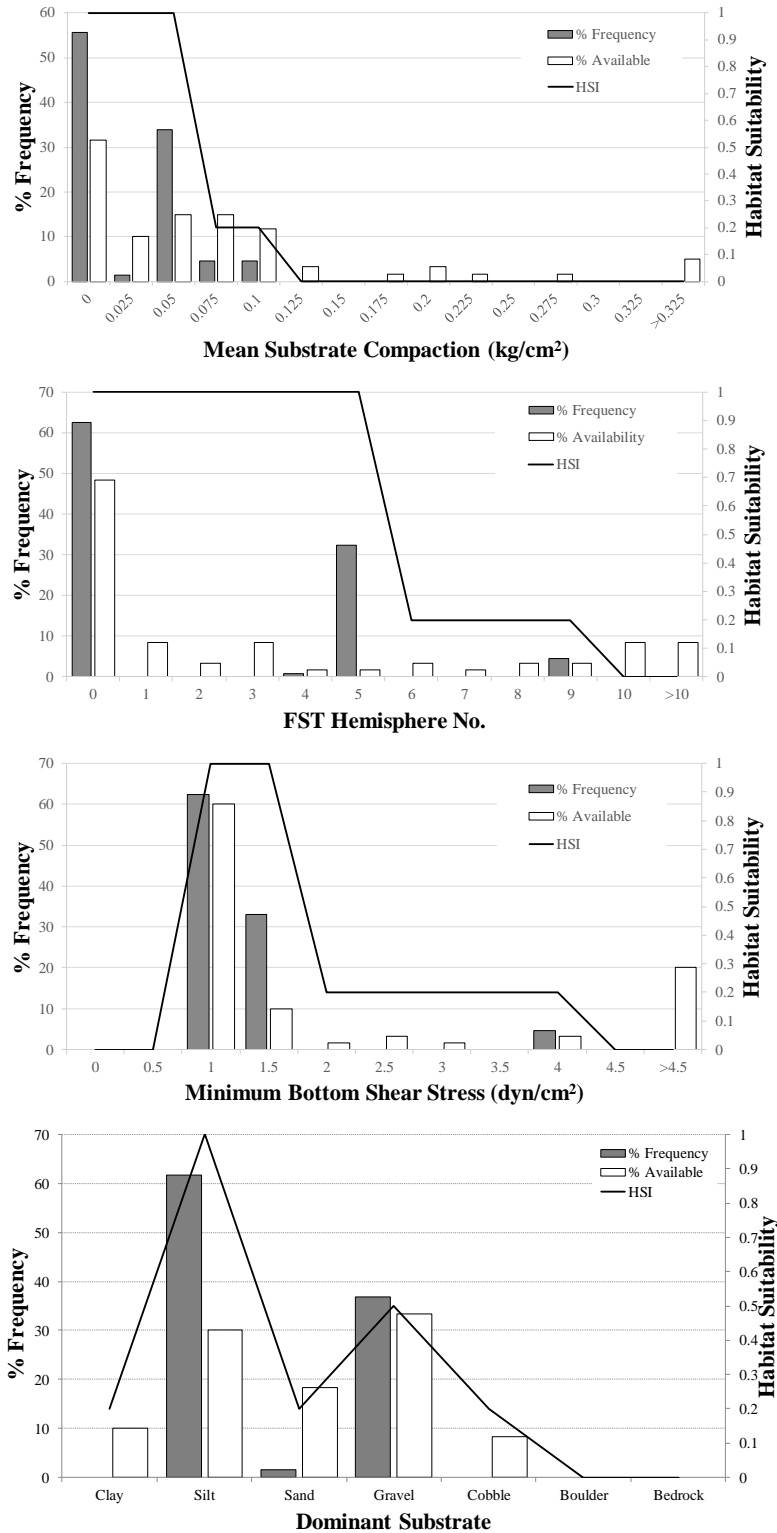


Figure 13. Percent frequency of occurrence (gray bars) and percent frequency of habitats sampled (white bars) for Little River *C. houstonensis* (n = 133) in relation to mean substrate compaction (kg/cm²), FST hemisphere number, minimum bottom shear stress (dyn/cm²), and dominant substrate.

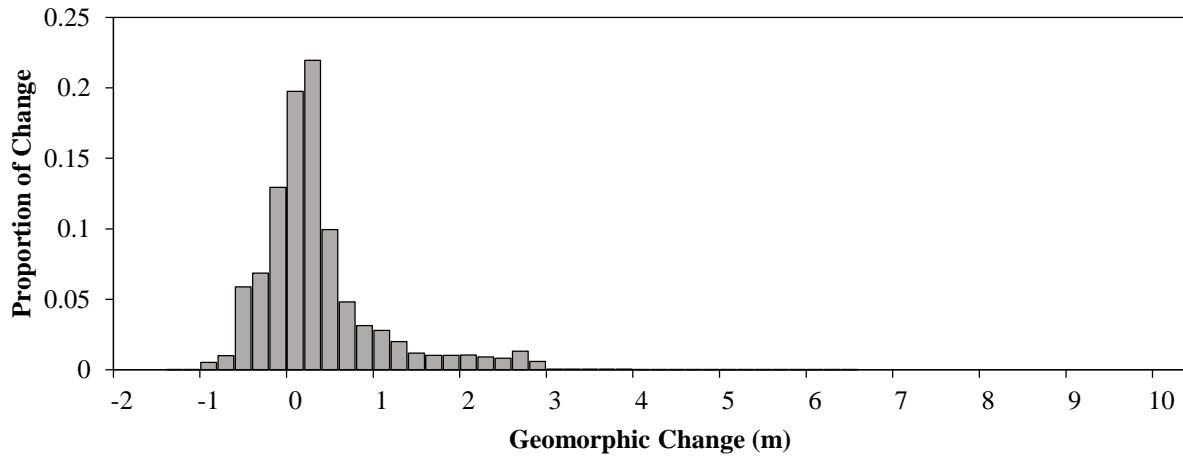


Figure 14. Histogram of changes in bed elevation between original model (2008) and updated model (2018) at the Altair site. Negative values represent deposition and positive values represent scour.

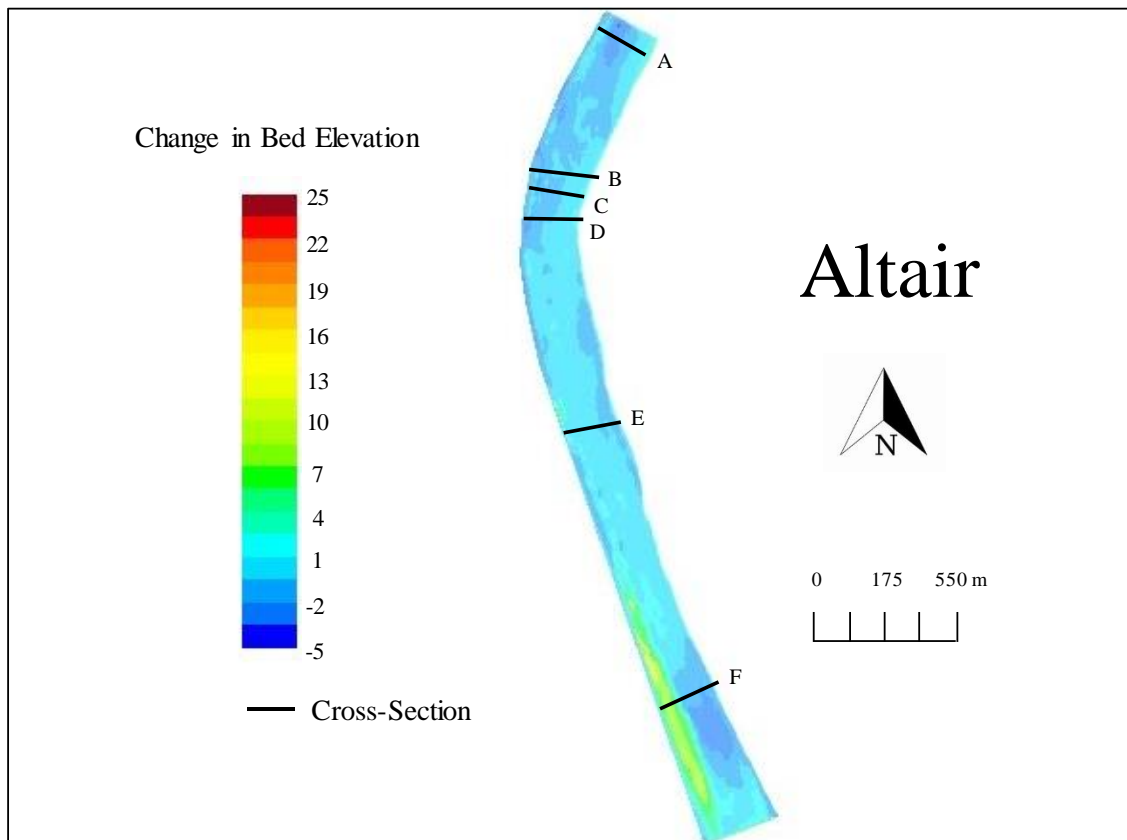


Figure 15. Map of change in bed elevation between original model (2008) and updated model (2018) at the Altair site. Negative values represent deposition and positive values represent scour.

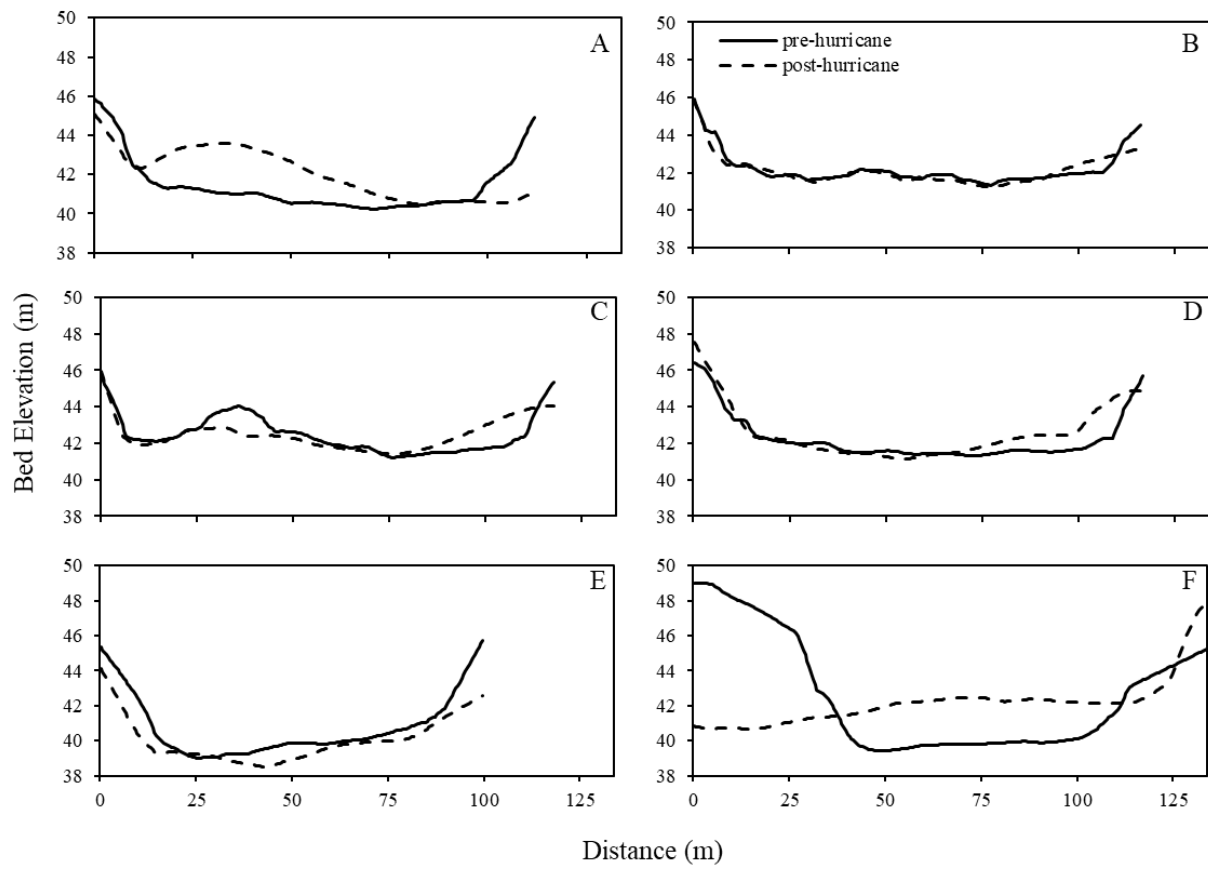


Figure 16. Cross-sections from the Altair site showing changes in bed elevation between the original model (pre-hurricane, 2008) and the updated model (post-hurricane, 2018). Cross-section locations are depicted in Figure 15.

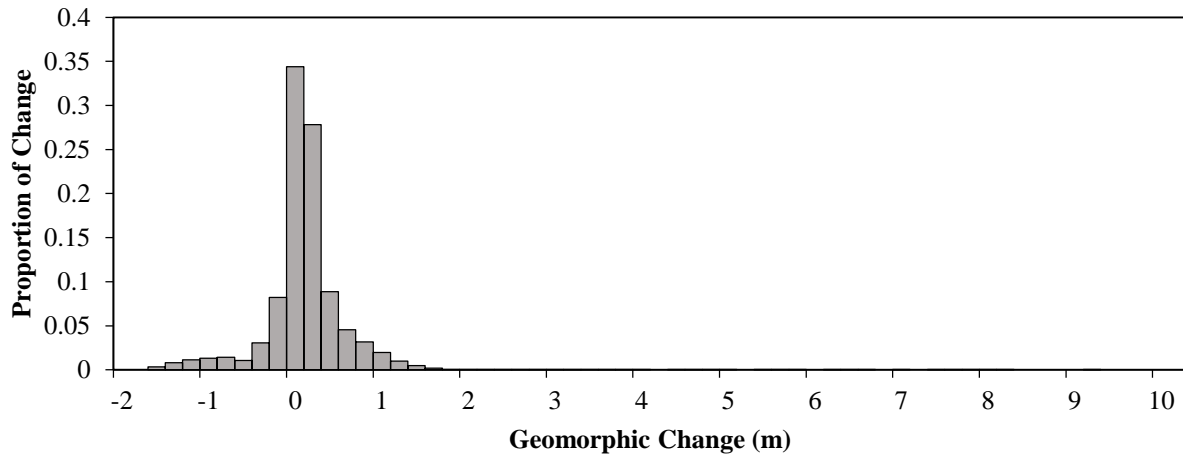


Figure 17. Histogram of changes in bed elevation between original model (2008) and updated model (2018) at the La Grange site. Negative values represent deposition and positive values represent scour.

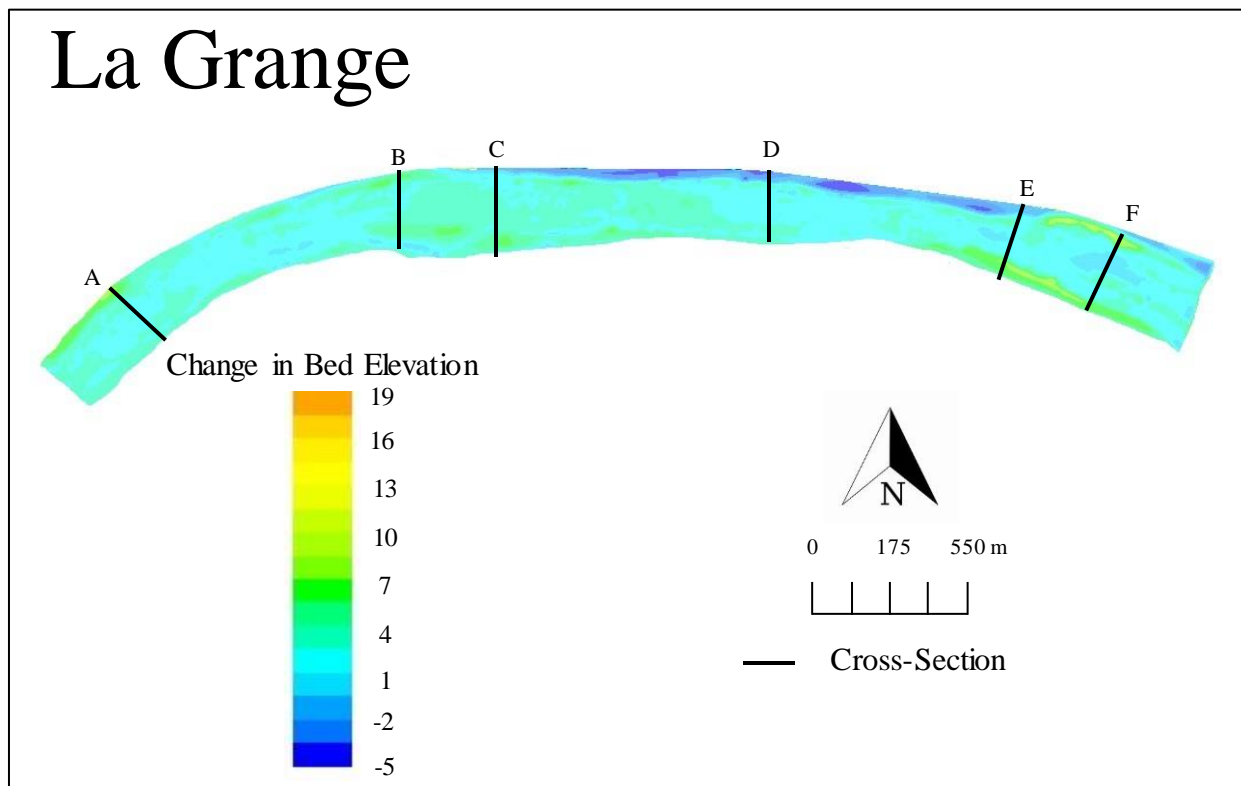


Figure 18. Map of change in bed elevation between original model (2008) and updated model (2018) at the La Grange site. Negative values represent deposition and positive values represent scour.

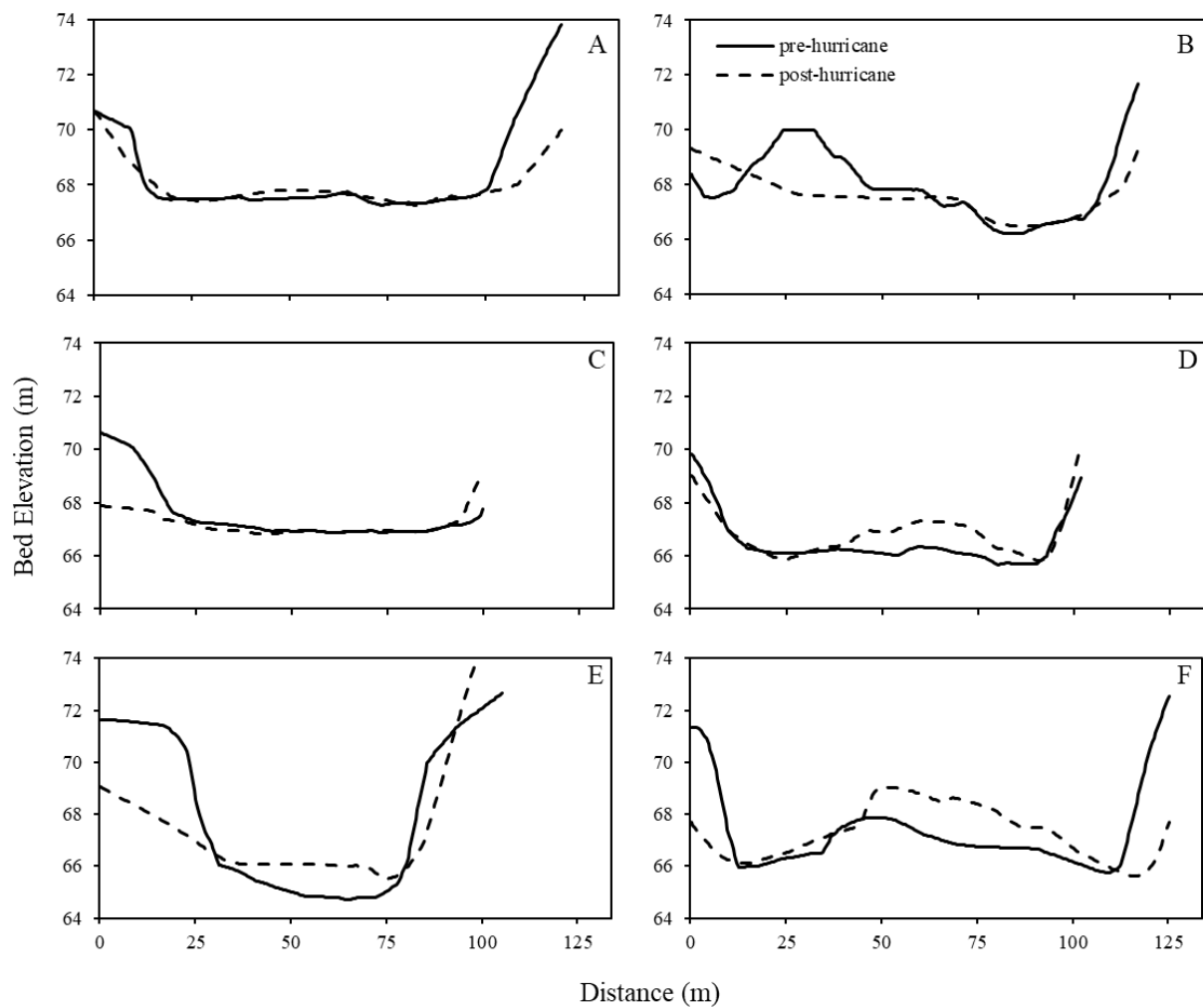


Figure 19. Cross-sections from the La Grange site showing changes in bed elevation between the original model (pre-hurricane, 2008) and the updated model (post-hurricane, 2018). Cross-section locations are depicted in Figure 18.



Figure 20. Map of persistent habitat at Altair.

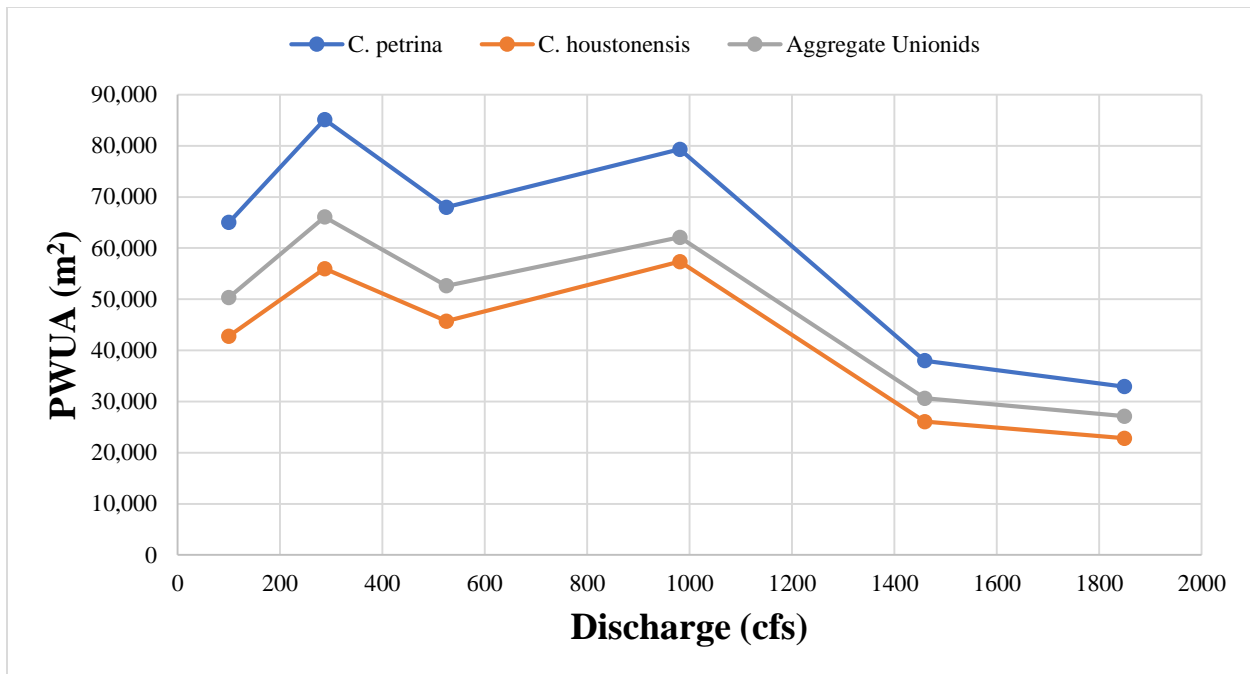


Figure 21. Persistent Weighted Usable Area (PWUA; m²) to discharge relationships for *C. petrina*, *C. houstonensis*, and aggregate unionids from the Altair study site.

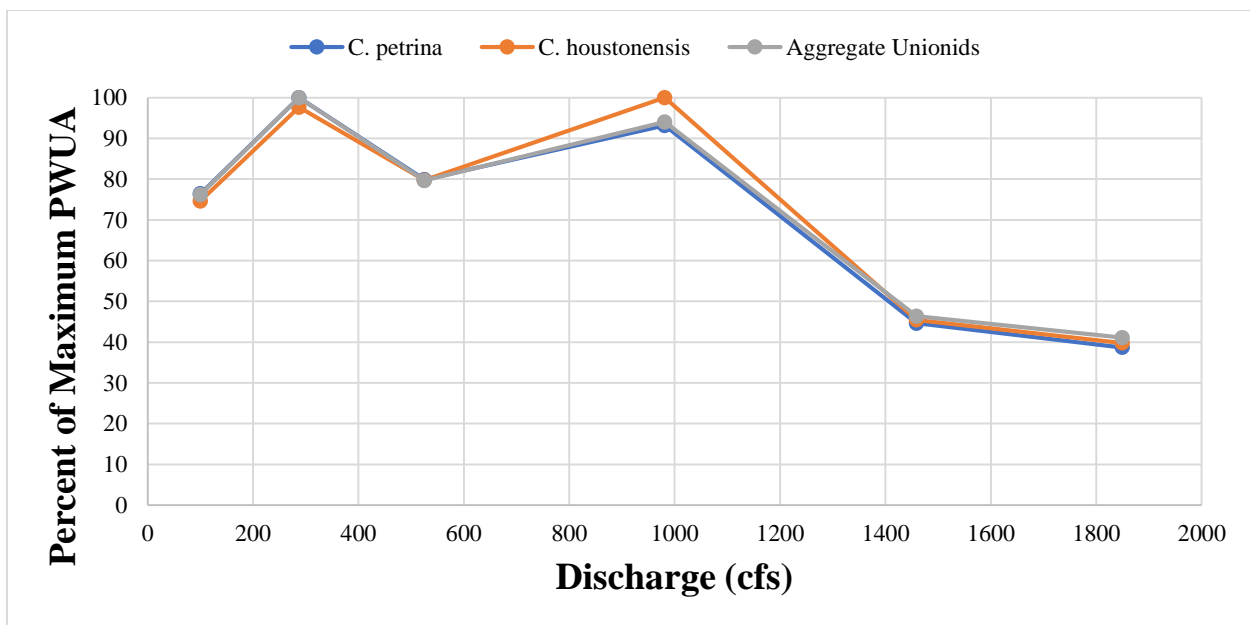


Figure 22. Percent of maximum PWUA to discharge relationships for *C. petrina*, *C. houstonensis*, and aggregate unionids from the Altair study site.



Figure 23. Map of persistent habitat at La Grange.

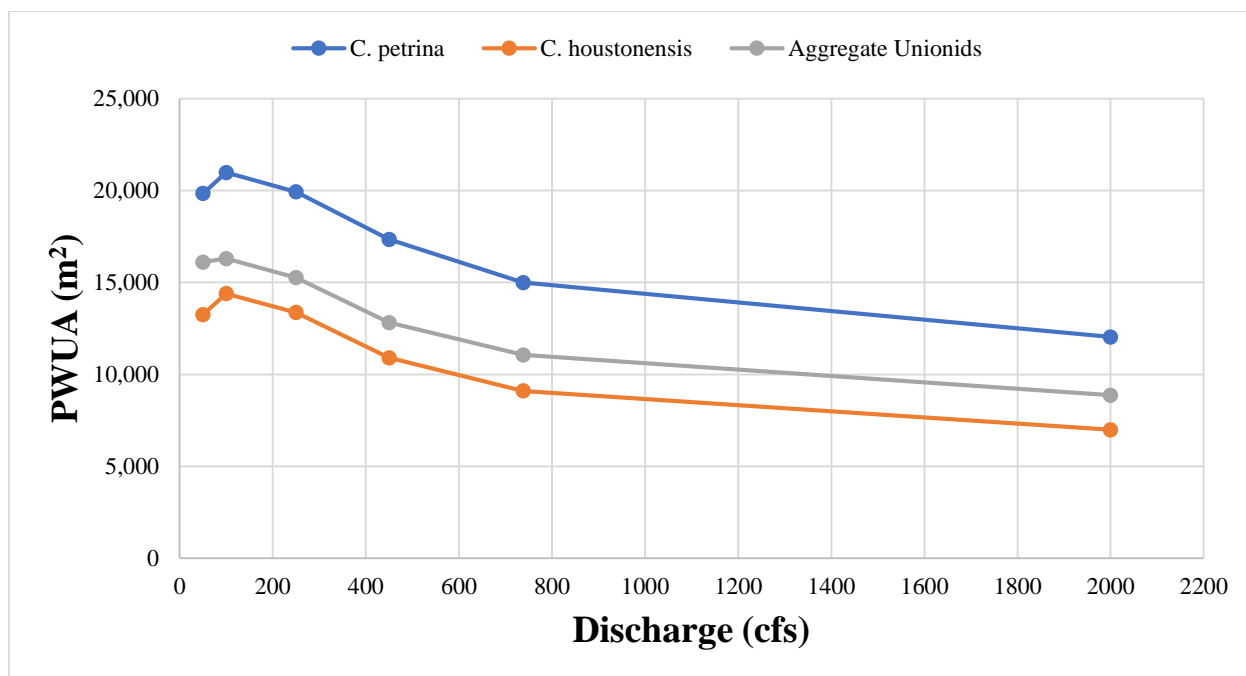


Figure 24. Persistent Weighted Usable Area (PWUA; m²) to discharge relationships for *C. petrina*, *C. houstonensis*, and aggregate unionids from the La Grange study site.

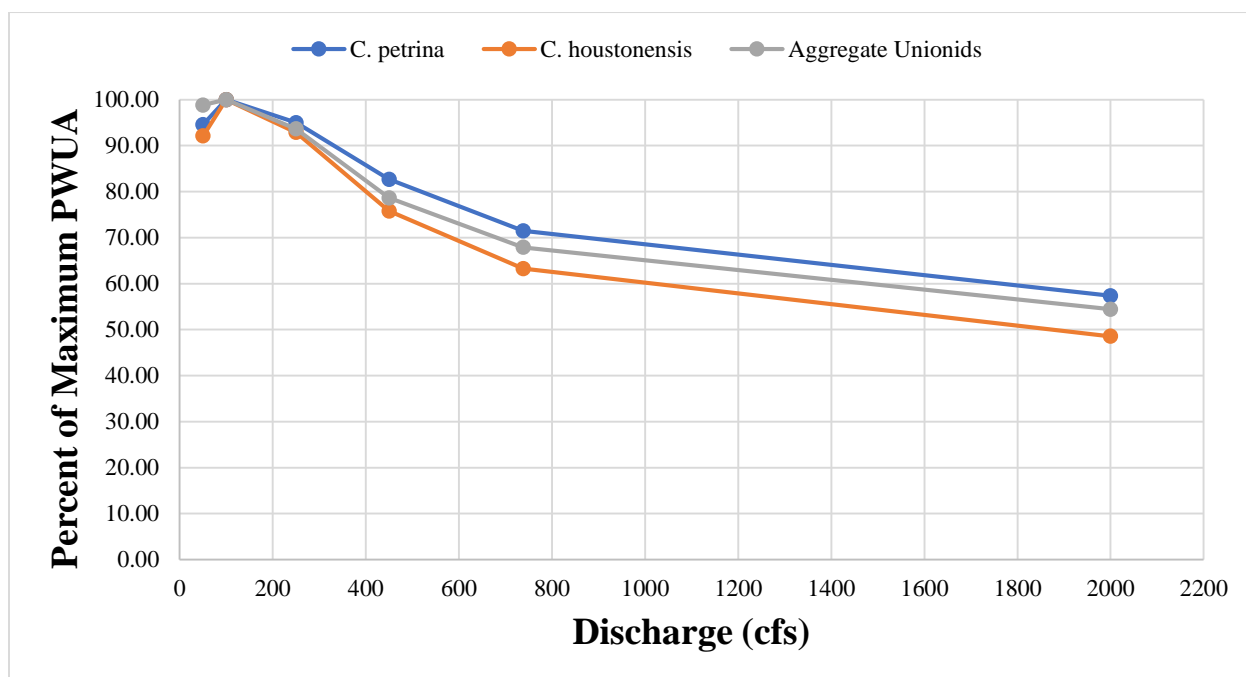


Figure 25. Percent of maximum PWUA to discharge relationships for *C. petrina*, *C. houstonensis*, and aggregate unionids from the La Grange study site.

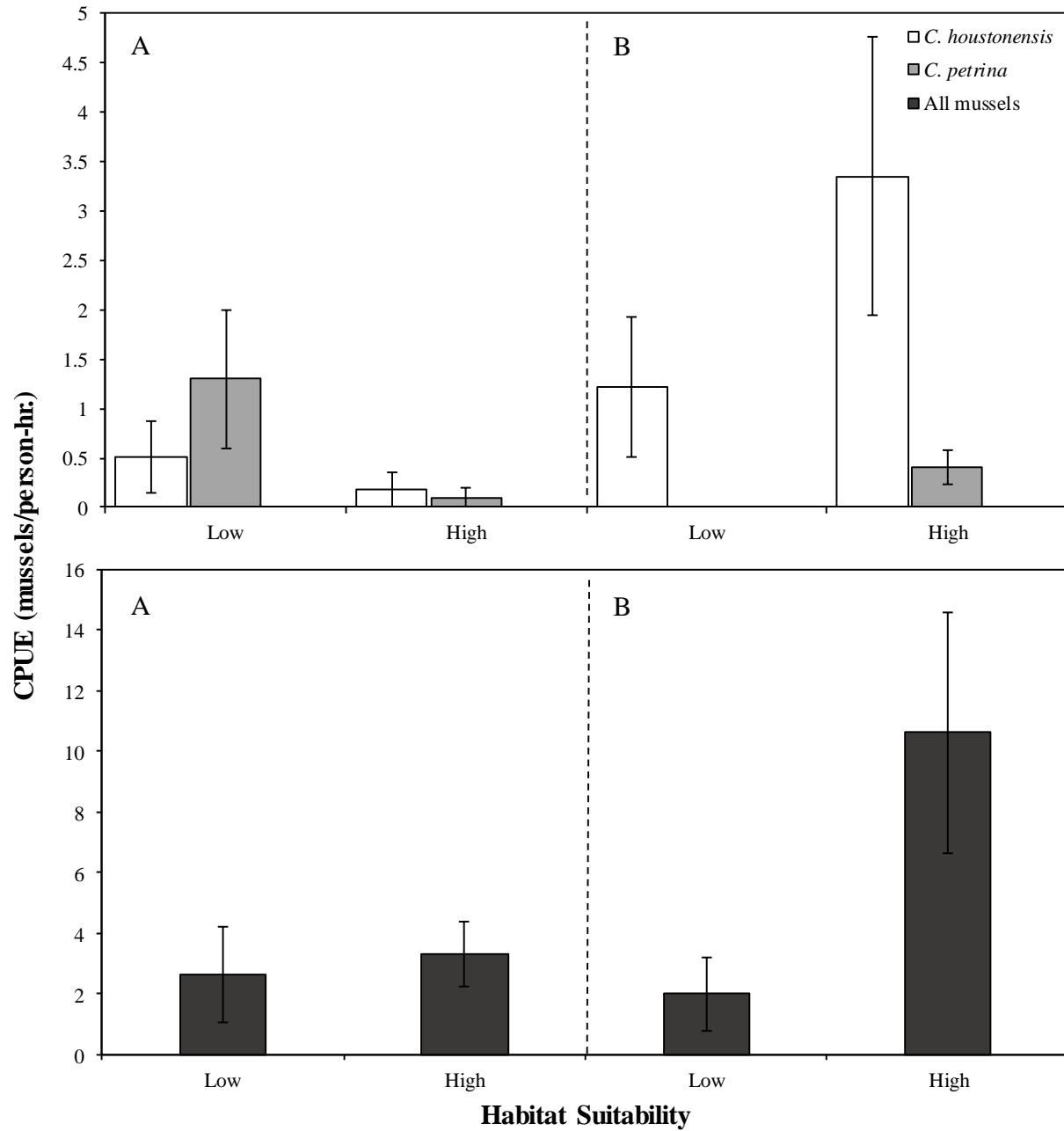


Figure 26. Mean catch-per-unit-effort (CPUE) of *C. houstonensis*, *C. petrina*, and aggregate mussels in low-quality (CSI<0.5) and high-quality (CSI>0.5) model-predicted habitat from non-persistent (A) and persistent (B) areas at the Altair site.

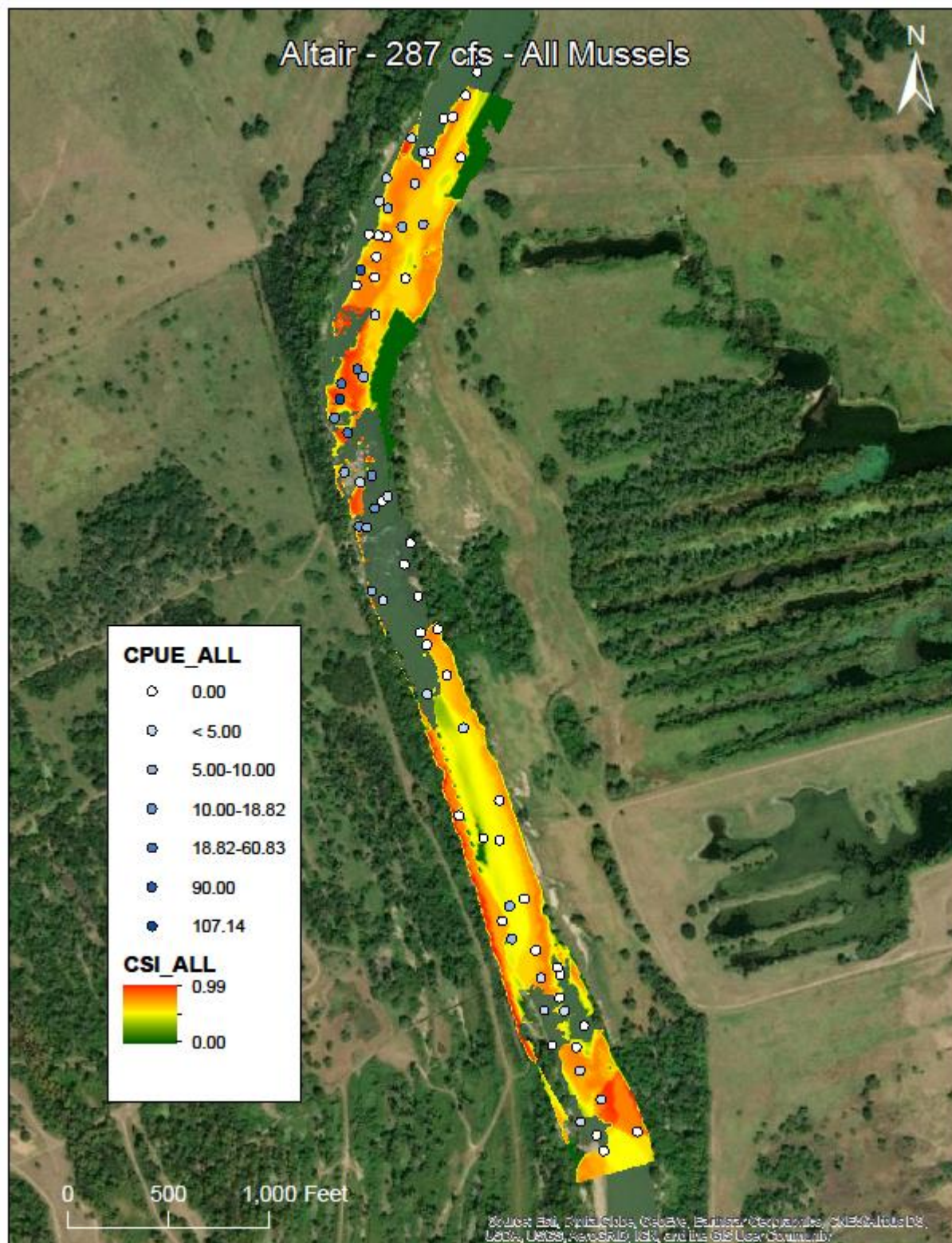


Figure 27. Model-predicted aggregate mussel Composite Suitability (CSI) in persistent habitats at the Altair site from the 287 cfs model run. Points represent aggregate mussel catch-per-unit-effort (CPUE) data from validation sampling efforts in summer 2018.

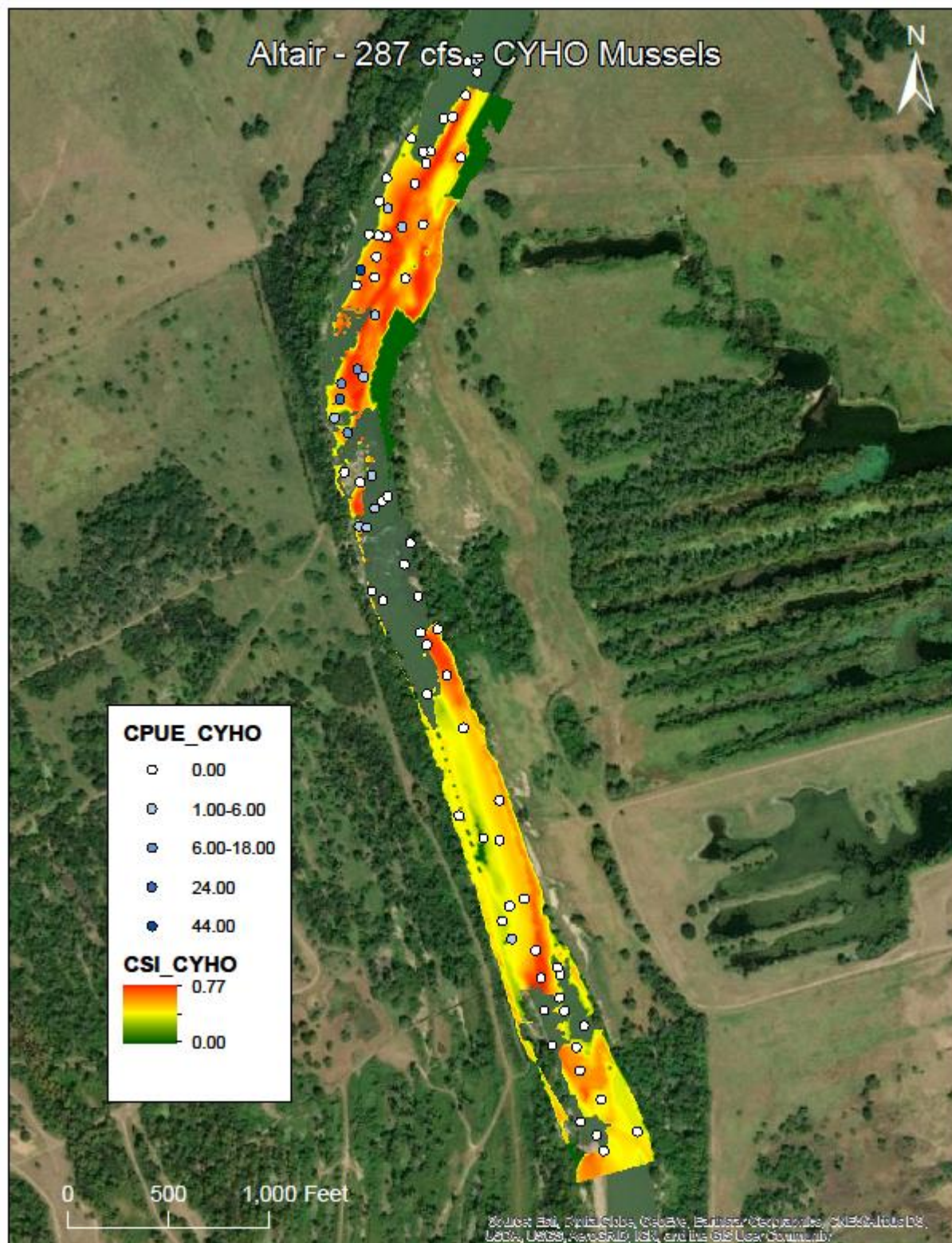


Figure 28. Model-predicted *C. houstonensis* Composite Suitability (CSI) in persistent habitats at the Altair site from the 287 cfs model run. Points represent *C. houstonensis* catch-per-unit-effort (CPUE) data from validation sampling efforts in summer 2018.

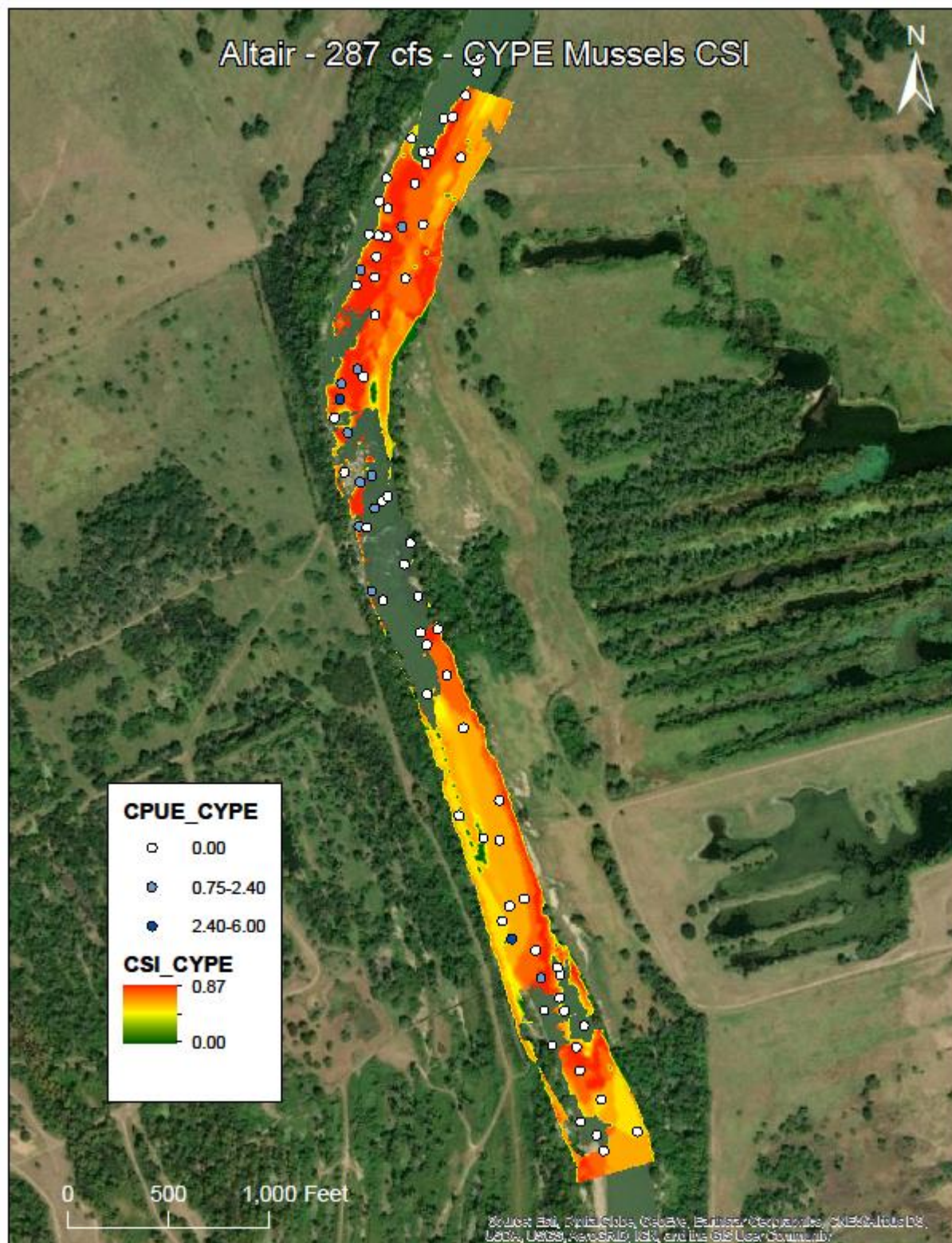


Figure 29. Model-predicted *C. petrina* Composite Suitability (CSI) in persistent habitats at the Altair site from the 287 cfs model run. Points represent *C. petrina* catch-per-unit-effort (CPUE) data from validation sampling efforts in summer 2018.

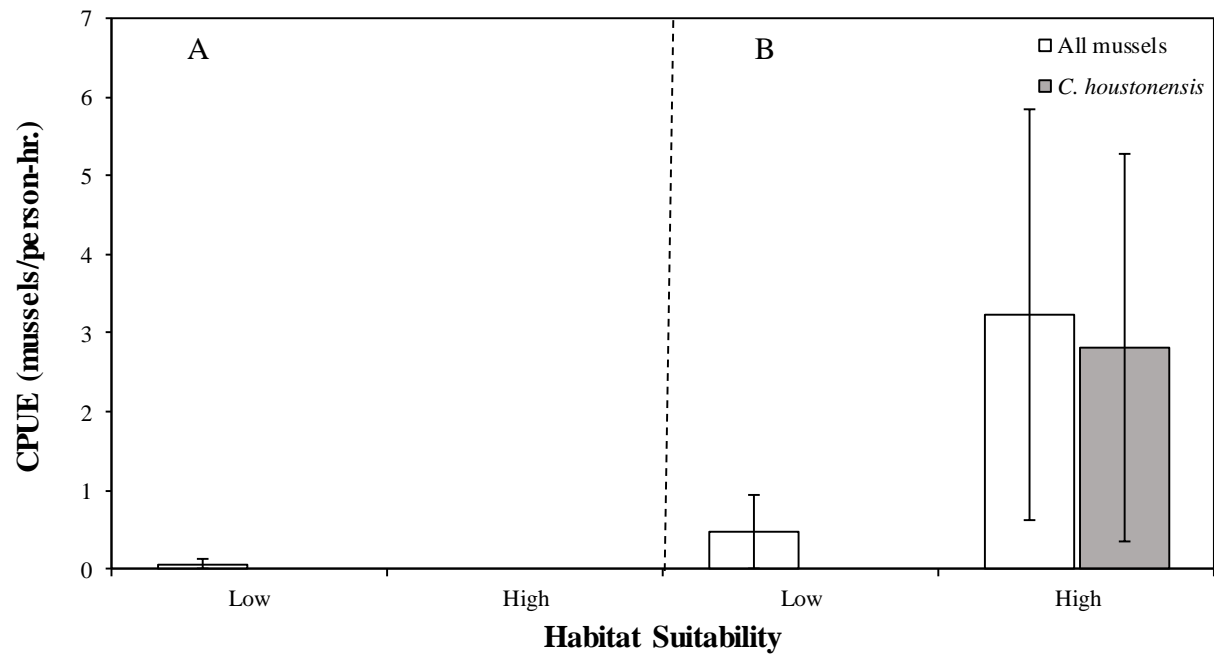


Figure 30. Mean catch-per-unit-effort (CPUE) of *C. houstonensis*, and aggregate mussels in low-quality (CSI<0.5) and high-quality (CSI>0.5) model-predicted habitat from non-persistent (A) and persistent (B) areas at the La Grange site.

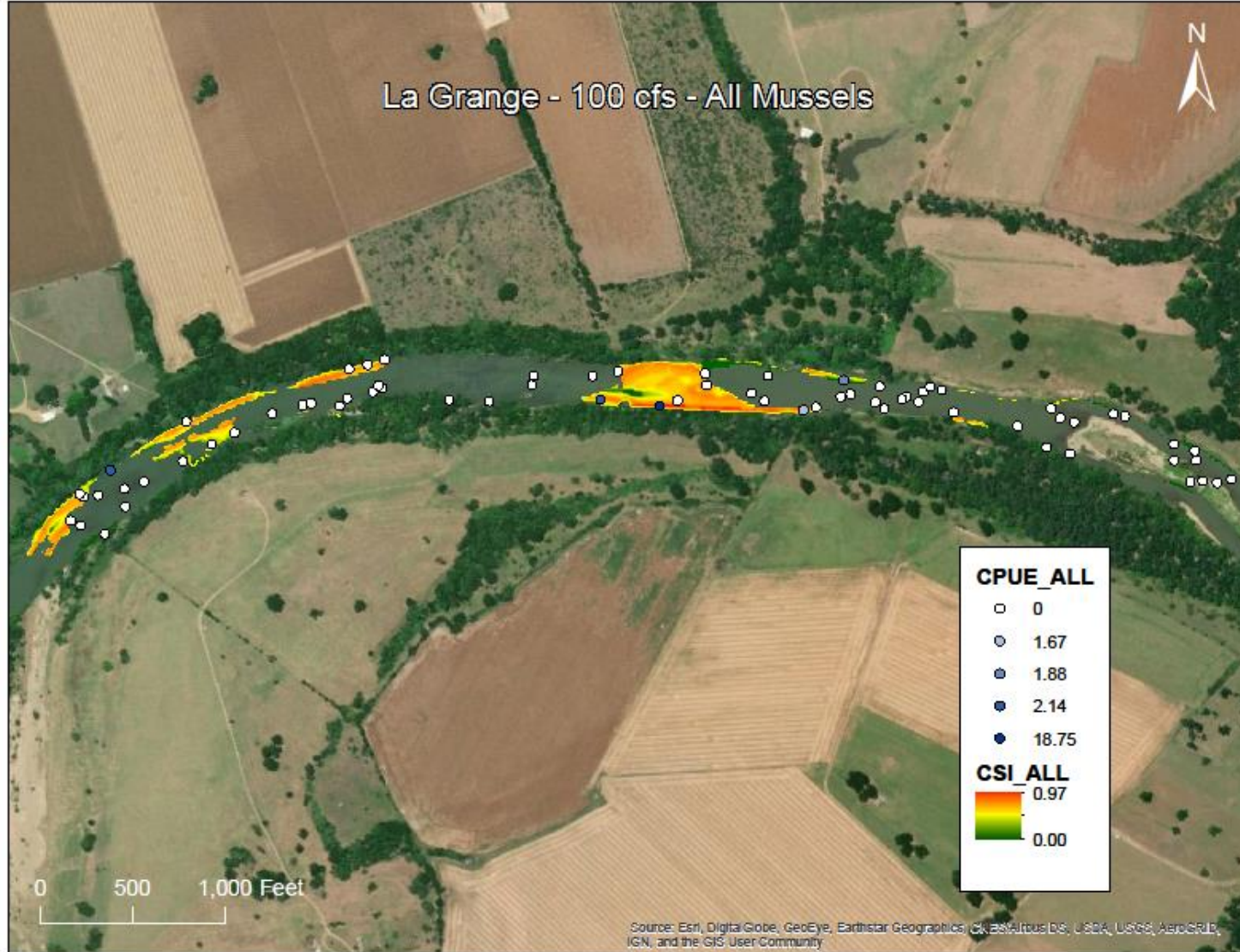


Figure 31. Model-predicted aggregate mussel Composite Suitability (CSI) in persistent habitats at the La Grange site from the 100 cfs model run. Points represent aggregate mussel catch-per-unit-effort (CPUE) data from validation sampling efforts in summer 2018.

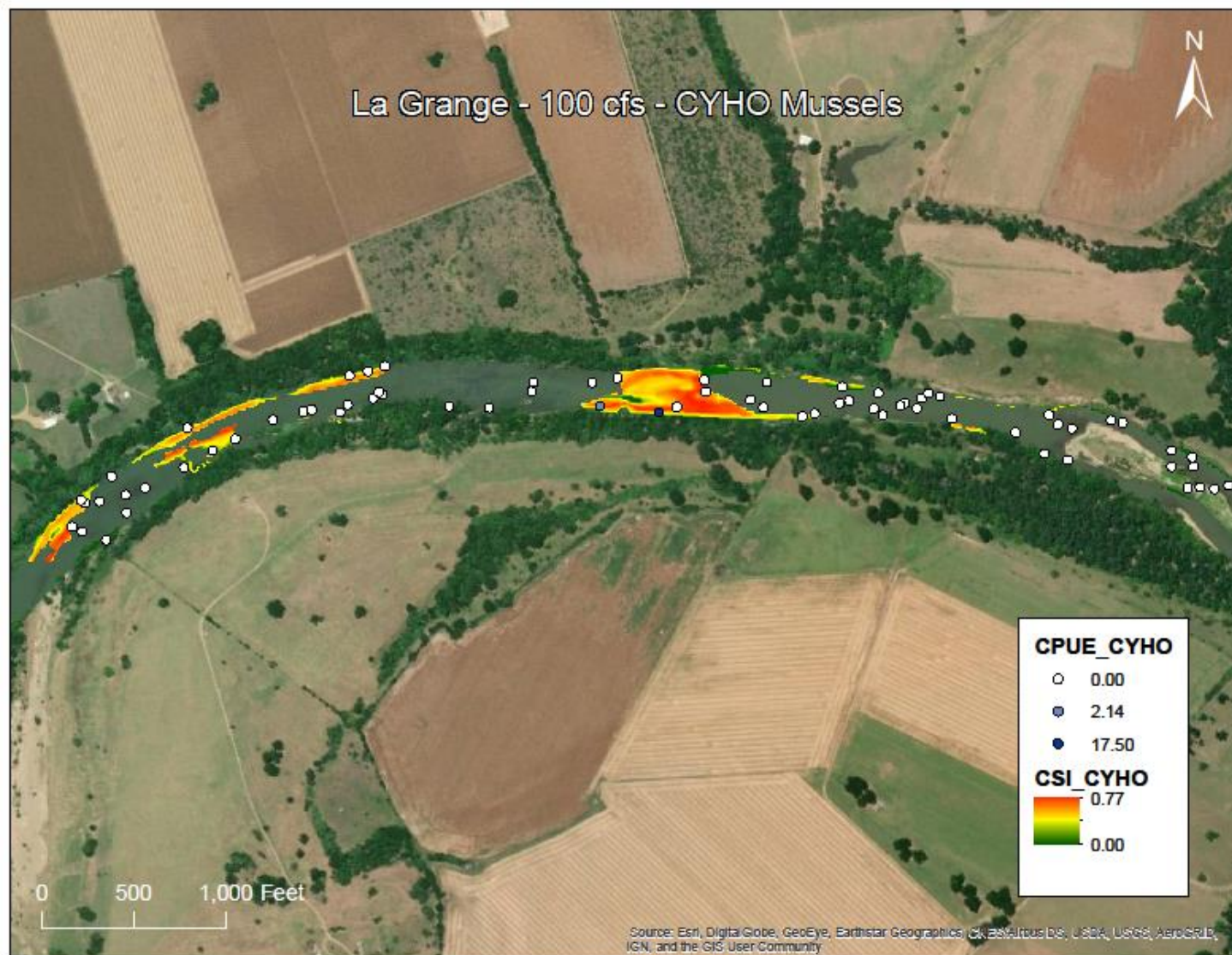


Figure 32. Model-predicted *C. houstonensis* Composite Suitability (CSI) in persistent habitats at the La Grange site from the 100 cfs model run. Points represent *C. houstonensis* catch-per-unit-effort (CPUE) data from validation sampling efforts in summer 2018.

References

- BIO-WEST, Inc. 2008. Lower Colorado River, Texas Instream Flow Guidelines. Colorado River Flow Relationships to Aquatic Habitat and State Threatened Species: Blue Sucker. Report prepared for Lower Colorado River Authority (LCRA) and San Antonio Water System (SAWS) Water Project.
- Bonner, T. H., E. L. Oborny, B. M. Littrell, J. A. Stoeckel, B. S. Helms, K. G. Ostrand, P. L. Duncan, and Jeff Conway. 2018. Multiple freshwater mussel species of the Brazos River, Colorado River, and Guadalupe River basins. Final Report to the Texas Comptroller of Public Accounts, February 28, 2018.
- Bovee, K. D. 1986. Development and evaluation of habitat suitability criteria for use in the Instream Flow Incremental Methodology. Instream Flow Information Paper 21. U.S. Fish and Wildlife Service Biol. Rep. 86(7). 235 pp.
- Gough, H. M., A. M. Hascho Landis, and J. A. Stoeckel. 2012. Behaviour and physiology are linked in responses of freshwater mussels to drought. *Freshwater Biology* 57:2356-2366.
- Layzer, J. B., and L. M. Madison. 1995. Microhabitat use by freshwater mussels and recommendations for determining their instream flow needs. *Regulated Rivers: Research and Management* 10:329-345.
- Maloney, K. O., W. A. Lewis, R. M. Bennett, and T. J. Waddle. 2012. Habitat persistence for sedentary organisms in managed rivers: the case for the federally endangered dwarf wedgemussel (*Alasmidonta heterodon*) in the Delaware River. *Freshwater Biology* 57:1315-1327.
- Newton, T. J., S. J. Ziglerand, and B. R. Gray. 2015. Mortality, movement and behavior of native mussels during a planned water-level drawdown in the Upper Mississippi River. *Freshwater Biology* 60. DOI: 10.1111/fwb.12461.
- Persinger, J. W., D. J. Orth, and A. W. Averett. 2010. Using habitat guilds to develop habitat suitability criteria for a warmwater stream fish assemblage. *River Research and Applications* (2010). DOI: 10.1002/rra.
- Poff, N. L., J. D. Allan, M. B. Bain, J. R. Karr, K. L. Prestegard, B. D. Richter, R. E. Sparks, and J. C. Stromberg. 1997. The Natural Flow Regime. *BioScience* 47:769-784.
- Randklev, C. R., M. Cordova, J. Groce, E. Tsakiris, and B. Sowards. 2014. Freshwater mussel (Family: Unionidae) data collection in the middle and lower Brazos River. Report submitted to Texas Parks and Wildlife (TPWD) as part of TPWD Contract No. 424520.
- Schwalb, A. N., and M. T. Pusch. 2007. Horizontal and vertical movement of unionid mussels in a lowland river. *The North American Benthological Society* 26:261-272.
- Statzner, B., F. Kohmann, and A. G. Hildrew. 1991. Calibration of FST-hemispheres against bottom shear stress in a laboratory flume. *Freshwater Biology* (1991) 26: 227-231.

- Steffler, P., and J. Blackburn. 2002. River2D hydraulic modeling program.
<http://www.river2d.ualberta.ca/>
- Strauss, R. E. 1979. Reliability estimates for Ivlev's electivity index, the forage ratio, and a proposed linear index of food selection. *Transactions of the American Fisheries Society* 108: 344-352.
- Stromberg, J. C., V. B. Beauchamp, M. D. Dixon, S. J. Lite, and C. Paradzick. 2007. Importance of low-flow and high-flow characteristics to restoration of riparian vegetation along rivers in arid southwestern United States. *Freshwater Biology* 52(4): 651-679.
- Texas Commission on Environmental Quality (TCEQ). 2012. Chapter 298 – Environmental Flow Standards for Surface Water; Subchapter D: Colorado and Lavaca Rivers, and Matagorda and Lavaca Bays. Effective August 30, 2012.
- Texas Instream Flow Program (TIFP). 2018. Instream flow study of the middle and lower Brazos River. June 15, 2018.
http://www.twdb.texas.gov/surfacewater/flows/instream/middle_lower_brazos/doc/BrazosRiverBasin_FinalRecommendationsReport_180615.pdf

Task 5: Captive Propagation

Principal Investigators: Ken Ostrand, Patricia Duncan, Jeff Conway

Addresses:

U.S. Fish and Wildlife Service, San Marcos Aquatic Resources Center, 500 E. McCarty Lane,
San Marcos TX 78666

U.S. Fish and Wildlife Service, Uvalde National Fish Hatchery, 754 County Road 203
Uvalde, TX 78801

U.S. Fish and Wildlife Service, Inks Dam National Fish Hatchery, 345 Clay Young Road
Burnet, Texas 78611

Email: Kenneth_Ostrand@fws.gov, patricia_duncan@fws.gov, jeff_conway@fws.gov

A.) March – Sept 2017: Texas fawnsfoot and false spike collection and transport to SMARC.

Adequate numbers of these species were not found during surveys in 2017. There are no suitable surrogate species because relatives are also rare and being considered for conservation status. Surveys for adequate numbers are ongoing.

B.) March – December 2017: glochidia extraction/fish infection for host fish determination.

Adequate numbers of Texas fawnsfoot were not found during surveys in 2018.

BIO-WEST, Inc. provided 2 gravid false spike to SMARC. These were used to infect shiners to determine practical host for captive propagation of false spike. SMARC will continue this work during 2019 if adequate numbers of false spike or Texas fawnsfoot are observed during surveys.